Intergovernmental Oceanographic Commission technical series

52

Cold water carbonate mounds and sediment transport on the Northeast Atlantic margin

Preliminary results of geological and geophysical investigations
during the TTR-7 cruise of *R/V Professor Logachev*
in co-operation with the CORSAIRES and ENAM 2 programmes
July-August, 1997

Editors: N.H. Kenyon
M.K. Ivanov
A.M. Akhmetzhanov

UNESCO 1998

SC-98/WS/53

For bibliographic purposes, this document should be cited as follows:
Cold water carbonate mounds and sediment transport on the Northeast Atlantic margin
IOC Technical Series No. 52, UNESCO 1998
(English)

Published in 1998
by the United Nations Educational,
Scientific and Cultural Organization
7, place de-Fontenoy, 75352 Paris 07 SP

Printed in UNESCO's Workshops

Printed in France

TABLE OF CONTENTS

ABSTRACT

The seventh Training-through-Research (TTR-7) international cruise of the R/V *Professor Logachev* was carried out in the northeast Atlantic in July – August 1997. As in previous years the cruise was conducted within the UNESCO/IOC "Floating University" Programme but this year in co-operation with the CORSAIRES and ENAM programmes of the European Commission. The expedition aimed to solve some outstanding problems in the field of geological processes on a passive continental margin and particularly to shed light on the nature and ecology of carbonate mounds recently discovered west off Ireland, which were thought to be due to hydrocarbons migrating upward. Modern analogues of hydrocarbon reservoirs were the other important objective of the cruise. A well developed system of tributary channels that runs from the margin south of Ireland to the Porcupine Abyssal Plain, and the potential area of sandy contourites lying to the west of the Faeroe Bank Channel were considered to be of interest as such analogues.

Comprehensive investigations resulted in the realisation that there are huge quantities of carbonate within cold water carbonate mounds. They are of enormous size (up to 400 m high, 5 km long) and have great diversity of shape. Over 150 mounds were mapped on just a small portion of the slopes of the Rockall Trough and Porcupine Seabight. Advances in understanding why carbonate mounds occur came from the biological, geochemical and sedimentological studies. The importance of fast flowing currents to the growth of cold water corals, the main growth builder of the mounds, was clearly demonstrated. Moulding of mounds by prevailing currents was also seen.

Contour currents are one of the main ways that slopes in the region are fashioned. In spite of the fact that sandy contourites are rarely recognised in studies of either ancient or modern sediments they were shown to be very significant in this part of the Atlantic. Sidescan sonar proved the most effective way to map the pathways of strong currents. By this method, a hitherto unknown, strong northward directed current was discovered in the Porcupine Seabight. Strong currents were also sweeping sands along the upper slope east of Rockall Bank and along the slope west of Porcupine Bank. Complex, sand filled channels shaped by the cold, salty overflow water from the Norwegian Sea were mapped in the Iceland Basin.

A new Tertiary igneous centre is believed to have been discovered at the foot of the Porcupine Bank.

The deep sea turbidite channel system in the Porcupine Seabight was shown to be inactive during the Holocene. (This is in contrast to the situation in nearby submarine canyons in the Bay of Biscay, which during the same period appear to have been the conduits for sands that have been brought to the shelf edge by tidal currents). Terraces had developed along the channel, probably by a slumping process.

ACKNOWLEDGEMENTS

Financial support for the seventh Training-through-Research cruise came from various sources among which were the CORSAIRES and ENAM-2 projects of the European Commission, the Intergovernmental Oceanographic Commission (IOC) of UNESCO, the Ministry of Science and Technology and the Ministry of Natural Resources of the Russian Federation. Additional support was provided by national funding institutions and universities in Belgium, Denmark, Ireland and the United Kingdom.

The cruise would not come to reality without the efforts of several people in different organisations acting in support of the Training-through-Research Programme. Credit should be given to Prof. Dr. I. F. Glumov (Ministry of Natural Resources of the Russian Federation), Dr. A. Suzyumov (UNESCO), and Dr. G. Kullenberg (Executive Secretary of IOC).

We gratefully appreciate assistance provided by C. van Bergen Henegouw of the Netherlands Institute for Sea Research for logistic support and Prof. Dr. V. T. Trofimov (Moscow State University) for administrative support. The port calls in Lisbon and Dublin were made possible with kind assistance of the administration of EXPO-98 (Lisbon, Portugal) and the Irish Marine Institute in Dublin, respectively.

The port call in Brest was made possible with the help of the CORSAIRES programme and IFREMER.

We also wish to thank the administration and staff of the Polar Marine Geological Exploration Expedition (St. Petersburg) for assistance with the cruise organisation. Captain A. Arutyunov and the skillful crew of the R/V *Professor Logachev* are thanked for the successful execution of the scientific programme of the cruise.

Finally we are very grateful to Rachel Cave (Southamptom Oceanography Centre) for her help with the report preparation.

INTRODUCTION

N. Kenyon and M. Ivanov

This paper is a report on the seventh annual expedition of the UNESCO/IOC Training-through-Research programme. Although known alternatively as the Floating University it has, in the past, confined its activities mainly to research into marine geology and geophysics. This year a significant biological element was added. The cruise was the first of the TTR ventures into the less hospitable weather of the North Atlantic, previous cruises having studied geological processes in the Mediterranean and Black Seas.

The idea behind the success of the Training-through-Research programme is to use the generous accommodation on the large research ships to train students by giving them the opportunity to take part in significant research. We have used the dedicated geological ships R/V *Gelendzhik*, operated by Yuzmorgeologiya Co. (Gelendzhik, Russian Federation) in 1991-1994, 1996, and the R/V *Professor Logachev*, operated by the Polar Marine Geological Exploration Expedition (St. Petersburg, Russian Federation) in 1995 and 1997. The funding has been ensured in each of the seven years of operation by making first rate scientific proposals and taking full use of the wide range of advanced equipment and the high standard of technical support provided on these ships. Longer term funds have come from the ESF and currently from UNESCO/IOC. Funds for the seventh cruise were from scientific sources such as the CORSAIRES and ENAM projects of the EC's MAST 3 programme. Russian, Irish, British and Danish universities and government organisations also contributed. Some funding was for the anticipated value of the science and some was for the training.

The seventh TTR cruise onboard the R/V *Professor Logachev* started from Dublin on 7th of July and the ship arrived in Aberdeen, the final port-call, on 14th of August (Fig. 1). The cruise was scheduled for two legs. The first one took place in the Porcupine Seabight and was mainly devoted to investigations of the enigmatic carbonate mounds whose origin was believed to be due to hydrocarbons migrating upward along faults (Hovland et al., 1994). Part of the time was spent studying an impressive deep sea channel system running across the eastern margin of the Seabight. The Leg terminated in Brest (France) on 24th of July for partial replacement of the cruise participants. Most of the cruise participants were able to take part in the Workshop on Core Processing organised by the CORSAIRES Project at IFREMER.

During the first half of the 2nd Leg the *Logachev* was working on both margins of the southern Rockall Trough, surveying areas of seabed mounds which were also known here from GLORIA long range sidescan sonar imagery and some available oil industry seismic data. Some of the mounds were found to be similar to those from Porcupine Seabight, others were of different, most likely volcanic, nature. The ship then sailed north to the Faeroe margin where cruise participants were able to look at the geological processes related to the Norwegian Sea Overflow Water spreading out to the Iceland basin from the Faeroe Bank channel.

The 51 scientists and students taking part this year were from both the main organising body, the UNESCO Centre for Marine Geology and Geophysics of the Moscow State University, and from 16 different universities in western Europe. The result is an unforgettable experience for many as they watch the slight, but hopefully significant, shift forward of the scientific frontiers in this frontier region of exploitation. The training benefit can, for some students, be immense. Some will find valuable material for use in theses and publish scientific papers in international journals. There is also scientific and cultural exchange that extends the bounds of the exchange programmes of the EC to reach the wider Europe, that rightly includes eastern Europe. This aspect of the programme is especially welcomed after the separate development that has occurred on either side of the Iron Curtain for most of the twentieth century. The benefits are maximised by having post cruise meetings, where progress in working up the data is discussed and the future programme is planned. This year the postcruise meeting was held at the University of Ghent, Belgium

The current report presents a considerable part of the data obtained during the cruise although the interpretation given is mainly preliminary and most of the analyses and advanced data processing will be done later. Comprehensive reports from other TTR cruises are available within the series of UNESCO Reports in Marine Science (Nos. 56, 62, 64, 67 and 68) and IOC Technical Series (No. 48). Scientific results of the cruise are partially presented in abstract books of the postcruise meeting

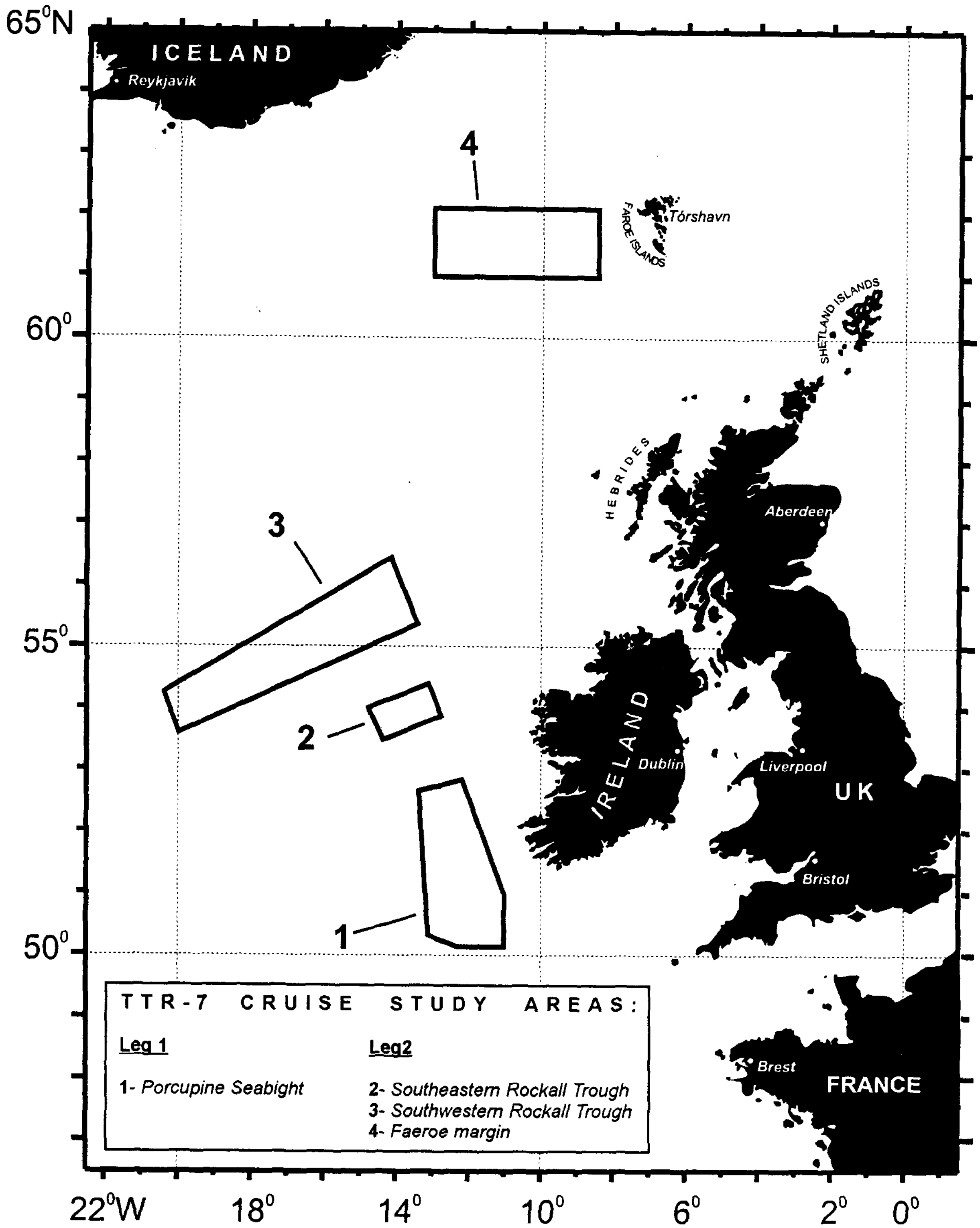

Fig. 1. Location map of the TTR-7 Cruise

published in UNESCO's *Marinf* report series (Nos. 91, 94, 99, 100) and in IOC Workshops Report series (Nos. 129, 143). So far there have been some 35 or so TTR papers published in international journals including a special issue of *Marine Geology*, on Mediterranean mud volcanoes.

List of the participants of the seventh Training-through-Research international cruise of the R/V *Professor Logachev* in the northeast Atlantic within the UNESCO/IOC "Floating University" Programme in co-operation with CORSAIRES and ENAM programmes

	Leg	
BELGIUM		
Rudy Swennen (University of Leuven)	1	
David van Rooij (University of Ghent)	1	
Sigrid Pillen (University of Ghent)	1	
Ben De Mol (University of Leuven)	1	
DENMARK		
Tove Nielsen (GEUS)		2
Tina Mikkelsen (University of Aarhus)		2
FRANCE		
Sebastien Zaragosi (IFREMER)	1	
Christine Degryse (University of Lille)	1	
IRELAND		
Angela McDonnell (University College Dublin)	1	
Andrew Wheeler (University College Cork)	1	
Robert Kennedy (Martin Ryan Institute, Galway)	1	
ITALY		
Adriano Mazzini (University of Genoa)		2
THE NETHERLANDS		
Jurgen Foeken (Free University of Amsterdam)		2
Max Horstink (Free University of Amsterdam)		2
Ewald Iking (Free University of Amsterdam)		2
Allard van der Molen (Free University of Amsterdam)		2
Ekaterina Ivanova (Free University of Amsterdam)		2
RUSSIA		
Alexander Arutyunov (PMGEE, St. Petersburg)	1	2
Yury Sokol (PMGEE, St. Petersburg)	1	2
Rafit Kalimullin (PMGEE, St. Petersburg)	1	2
Michail Savel'ev (PMGEE, St. Petersburg)	1	2
Alexey Krotov (PMGEE, St. Petersburg)	1	2
Alexander Shagin (PMGEE, St. Petersburg)	1	2
Michael Ivanov (PMGEE, St. Petersburg)	1	2

Skiridov Sergey (PMGEE, St. Petersburg)	1	2
Alexander Shohin (PMGEE, St. Petersburg)	1	2
Yury L'vov (PMGEE, St. Petersburg)	1	2
Vyacheslav Stetyukha (PMGEE, St. Petersburg)	1	2
Sergey Andreev (PMGEE, St. Petersburg)	1	2
Vadim Aleshin (PMGEE, St. Petersburg)	1	2
Yury Gemenchuk (PMGEE, St. Petersburg)	1	2
Sergey Novosotsky (PMGEE, St. Petersburg)	1	2
Vladimir Solov'ev (PMGEE, St. Petersburg)	1	2
Alexander Fedyukin (PMGEE, St. Petersburg)	1	2
Oleg Bespalov (PMGEE, St. Petersburg)	1	2
Igor Prytkov (PMGEE, St. Petersburg)	1	2
Vladimir Tsyganok (PMGEE, St. Petersburg)	1	2
Yury Krivov (PMGEE, St. Petersburg)	1	2
Gennady Dianov (PMGEE, St. Petersburg)	1	2
Igor Pavlov (PMGEE, St. Petersburg)	1	2
Andrey Kuryshev (PMGEE, St. Petersburg)	1	2
Igor Semenov (PMGEE, St. Petersburg)	1	2
Evgeny Matveev (PMGEE, St. Petersburg)	1	2
Yury Loktev (PMGEE, St. Petersburg)	1	2
El'vira Stetyukha (PMGEE, St. Petersburg)	1	2
Nataliya Silova (PMGEE, St. Petersburg)	1	2
Vera Sud'eva (PMGEE, St. Petersburg)	1	2
Tat'yana Vasil'eva (PMGEE, St. Petersburg)	1	2
Alevtina Lebed (PMGEE, St. Petersburg)	1	2
Nikolay Khot'ko (PMGEE, St. Petersburg)	1	2
Sergey Chernyaev (PMGEE, St. Petersburg)	1	2
Michail Bulavin (PMGEE, St. Petersburg)	1	2
Vyacheslav Ganin (PMGEE, St. Petersburg)	1	2
Alexandr Sergeev (PMGEE, St. Petersburg)	1	2
Alexander Machulin (PMGEE, St. Petersburg)	1	2
Evgeny Samsonov (PMGEE, St. Petersburg)	1	2
Valery Babanov (PMGEE, St. Petersburg)	1	2
Gennady Antipov (PMGEE, St. Petersburg)	1	2
Irina Antipova (PMGEE, St. Petersburg)	1	2
Victor Sheremet (PMGEE, St. Petersburg)	1	2
Boris Smirnov (PMGEE, St. Petersburg)	1	2
Valentin Konfetkin (PMGEE, St. Petersburg)	1	2
Alexandr Plakhotnik (PMGEE, St. Petersburg)	1	2
Sergey Luybimov (PMGEE, St. Petersburg)	1	2
Alexandr Ivanov (PMGEE, St. Petersburg)	1	2
Alexandr Marakulin (PMGEE, St. Petersburg)	1	2
Valery Gaynanov (Moscow State University)	1	2
Konstantin Spiridonov (PMGEE, St. Petersburg)	1	2
Sergey Buryak (Moscow State University)	1	2
Anna Volkonskaya (Moscow State University)	1	2
Olga Makhova (Moscow State University)	1	2
Kirill Epov (Moscow State University)	1	2
Petr Krinitsky (PMGEE, St. Petersburg)	1	2
Vyacheslav Gladush (PMGEE, St. Petersburg)	1	2
Igor Laletin (PMGEE, St. Petersburg)	1	2
Ekaterina Akenteva (Moscow State University)	1	2
Pavel Shashkin (Moscow State University)	1	2
Alexey Almendinger (Moscow State University)	1	2
Alexander Morozov (Moscow State University)	1	2

Yury Goremykin (PMGEE, St. Petersburg)	1	2
Anatoly Limonov (Moscow State University)	1	2
Oleg Krylov (Moscow State University)	1	2
Elena Kozlova (Moscow State University)	1	2
Andrey Akhmetzhanov (Moscow State University)	1	2
Alexander Sautkin (Moscow State University)	1	2
Leonid Mazurenko (Moscow State University)	1	2
Grigory Akhmanov (Moscow State University)	1	2
Irina Belenkaya (Moscow State University)	1	2
Yury Naumov (Moscow State University)	1	2
Alina Stadnitskaya (Moscow State University)	1	2
Anna Balashova (Moscow State University)	1	2
Anna Saprykina (Moscow State University)	1	2
UK		
Neil Kenyon (SOC)	1	2
Bryan Cronin (University of Aberdeen)	1	
Paulo Sumida (SOC)	1	
Nicholas Satur (University of Aberdeen)	1	
Rachel Cave (University of Wales, Bangor)		2
Justin Taylor (University of Wales, Aberystwyth)		2
John Wilson (Royal Holloway University)		2
Patrick Friend (SOC)		2
Christina Vina Herbon (SOC)		2

TECHNICAL REPORT

The present chapter does not include all the methods used during the TTR-7 cruise since some of them had been already described in previous reports of the Training Through Research expeditions (e.g. Woodside et al., 1997), including one on the R/V *Professor Logachev (*Ivanov et al., 1996). Although there were no new methods used some of the standard ones have been modified or improved. Description of these latest revisions can be found in this report. Positioning of the ship was done using GPS 4400.

I. Seismic data acquisition and processing

V. Gainanov and A. Volkonskaya

The seismic survey was executed using an "Enisey" pneumatic source (air-gun), a PSS-12 hydrophone streamer, and a 6-channel digital data acquisition and processing system of our own design.

"Enisey" pneumatic source (air-gun)

Working volume, *l*	**1.8**
Working pressure, *mPa*	**12**
Signal frequency range, *Hz*	**20-250**
First positive pulse amplitude at a distance of 1 m, *mPa*	**5.0**
Weight, *kg*	**45**

PSS-12 hydrophone streamer

Number of receiving sections	**2**
Number of empty sections	**6**
Number of depressor sections	**1**
Number of channels per receiving section	**6**
Number of hydrophones per channel	**15**
Type of hydrophones	**PDS-22**
Sensitivity of channels, *mV/Pa*	**350**
Length of receiving section, *m*	**50**
Length of empty section, *m*	**100**
Length of depressor section, *m*	**10**

Seismic profiling technology

The source and streamer were normally towed at an optimum depth of 4-5 m below the sea surface in order to obtain a better vertical resolution and signal-to-noise ratio. However, during rough sea conditions, when the noise level became significantly higher, the receiver was lowered to a depth of 10-15 m. This led to an essential decrease of the noise level but the signal's form deteriorated due to the increase of the signal's length, which, in turn, degraded the vertical resolution.

After testing the sensitivity and signal-to-noise ratio of all 12 channels of the PSS-12 streamer, the nearest 6 of them have been chosen for the data acquisition. Hence, the source-receiver spread was as follows:

- source-receiver distance (offset) for the first channel............ 350 m
- distance between receiving channels.......................................9.5 m.

The procedure of the digital data acquisition has been described in Woodside et al. (1997). The main parameters are listed below.

Data acquisition parameters

Amplifier coefficient, *dB*	**50**
Band-pass filter, *Hz*	**15-200**
Sampling period, *ms*	**1**
Trace length, *s*	**3000**
Shot interval, *s*	**10**

Digital data acquisition and processing software

The following software programmes were used during the cruise:

- **sw97_6.exe** -for 6-channel seismic data acquisition and real time processing;
- **readsum6.exe** -for putting in normal move-out corrections and 6-channel common shot point stack;
- **rwseis.exe** -for data processing (setting common delay, band-pass filtering, time-variable gain control, resampling);
- **prdec.exe** -for predictive deconvolution;
- **rwsefbmp.exe** -for output of data as a seismic time section on a plotter or Laser Jet printer or to convert data into BMP-format (for additional processing by image processing software);
- **MSP-soft** -for migration of seismic data.

The data processing software and some of the digital data acquisition hardware are the property of the Department of Seismometry and Geoacoustics, Geological Faculty, Moscow State University. The on-board processing included the following procedures:

- data reading;
- normal move-out corrections and common shot point stack;
- normalising the time sections to a single time (common delay);
- predictive deconvolution;
- band-pass filtering;
- migration (for some parts of profiles only);
- preparing data for output to print (gain regulation, horizontal and vertical scale regulation);
- data output to printer.

II. OKEAN and OREtech sidescan sonars and sonograph processing

E. Akentieva and P. Shashkin

Sidescan sonar produces acoustic images of the seafloor by transmitting regular pulses of sound out to the side of the sonar instrument and then displaying the backscattered echoes that return against time.

Two sidescan sonars were used during the cruise, OKEAN and OREtech. The OREtech is a high-resolution system which is able to insonify a swath of 2000 m (1000 m to either side) in the long-range mode (LR) and up to 500 m (250 m to either side) in the high resolution mode (HR). The OREtech system operates at 30 kHz. In LR mode, the vehicle is towed at about 130 m above the seafloor and in HR mode (100 kHz) at about 40-45 m. The OREtech system additionally provides the option to operate simultaneously with the acoustic short baseline underwater navigation system (SBS). Up-looking echosounder (EU) is merged with the transponder for possible operation with SBS. The EU pulse transmitted towards the vessel is received by the SBS receiver array. These navigation data are recorded and used for the processing of the OREtech data. The up-looking echosounder was also used to calibrate the pressure sensor which provides the determination of the distance from the vehicle to the water surface, in order to obtain more accurate measurements. The down-looking echosounder gives us the vehicle's altitude above the sea bottom. The OREtech vehicle also includes pitch, roll and heading sensors.

The OREtech system contains an acoustic subbottom profiler (SBP). The profiler uses a short 6 kHz pulse in order to give good resolution.

The OKEAN is a long-range sidescan sonar operating at a frequency of 9.5 kHz, which with its 10.2 km swath range and 6 knots towing speed, is well suited for surveying large deep-sea areas. However, the sonographs show fewer details than the OREtech images. The OKEAN vehicle is towed behind a ship at about 40-80 m below the sea surface. According to the waterdepth range in the study areas (600-1300 m), the pulse length was set to 1 s. Receiving time was set to 7 s.

Signals from the sidescan vehicle are recorded on a computer hard disk. The data are usually written as 11944 (for OREtech) and 4113 (for OKEAN) byte blocks. All processing stages of the OREtech and OKEAN data are generally the same. The first operation is the correction for a distortion of the image along the vehicle path caused by varying towing speed. Secondly, a time-variable gain (TVG) is applied to sonar data in order to make allowance for the drop-off of signal strength with increasing range and for the beam directivity configuration. The histogram of pixel values across a sonar track from an area with no seafloor features has been taken as a standard one ('test card'). OKEAN and OREtech data processing also requires a slant-range to ground-range correction. This uses the altitude of the vehicle, which is obtained from profiler records for the OREtech data, and is searched for manually using the first arrival in the OKEAN data. Line drop-outs, noise, and speckle are removed using 2D-filtering. Pitch sensor data are taken into account during the OREtech data processing. Once all processing has been done, data are geographically adjusted to obtain a mosaic.

OREtech profiler records also need to be corrected. The vehicle's height above the seabed varies during towing. The changes of the towing altitude can cause undulations in the subbottom profile even when the seafloor is flat. In order to shift the profiler record back to its correct position, the readings of the depth of the vehicle below the water surface, obtained by the pressure sensor, and data from the profiler, which give us the altitude of the vehicle above the seafloor, should be summed.

III. Underwater photo and television system

O. Krylov and A. Balashova

The photo and television system (FTA) is a towed construction with an open-frame shape, based on OREtech design. It contains deep-sea boxes with electronic equipment such as TV cameras, lights, flashes, external storage batteries from the 'Benthos' deep-sea photosystem as well as an echosounder and in-built navigational system ('Sygma'), which are attached to the frame.

FTA is used for the observation of sea floor surface features, sediment colour and bottom conditions. It is designed for surveys at water depths up to 6000 m. It is towed at 2-8 m above the sea floor. Video recording is carried out in both discrete and continuous modes, either together or separately. The continuous record is carried out by the highly sensitive colour TV camera CCS-5 and videorecorder BR-6200, which is installed in the electronic equipment box. The tape is VHS E180 or E240. The length of recording is up to 4 hours. The discrete recording is made by the TVC camera on compact VHS (c) tape EC-30, EC-45 or EC-60. Every pair of photos is correlated with the videotape at 3-second intervals. The regular period of interruption is from 3-4 to 20 seconds. The self-focusing lens can magnify target objects up to twelve times.

The stereophoto system 'Benthos' comprises two 337-model cameras, two 383-model flashes and 4 accumulator batteries. The angle of observation is 55° for each camera.

The echosounder is used to keep distance above the bottom. The best distance for shots is 4-5 m.

The FTA is towed by a KM-1-150 20 mm diameter cable with a maximum length of 10 km.

Specification and working parameters of the FTA OREtech

Stereophotosystem - 'Benthos'

Number of films	**2 x 1200 pictures**
Period	**3-20 seconds**
Light	**2 x 200 dg**

Videosystem (colour) VHS(c) -interrupted records

Recording time	**1200 x 3 seconds**
Light	**4 x 150 W**

TV system VHS -uninterrupted records

Recording time	**240 minutes**
Light	**150 W**

Echosounder	**200 kHz**
Underwater navigation system	**'Sigma'**
Operating depth	**6000 m**
Weight in air	**1000 kg**
Weight in water	**700 kg**

IV. Bottom sampling technique

G. Akhmanov, D. van Rooi, R. Kennedy, Yu. Naumov

Dredge

The dredging was carried out with a 75 cm diameter dredge with a length of 60 cm and wall thickness of 1.5 cm. The weight of the dredge is 200 kg and it is towed using a 250 kg depressor fixed on the cable at 1 m from the dredge. Teeth are present at the mouth of the dredge to scrape rocky surfaces. There is a net on the bottom for preventing the loss of small clasts. The dredge is towed by a winch with a 22 mm diameter cable. When the dredge reaches the sea floor, about 100m of cable is laid on the bottom and then the dredging is carried out, with the ship keeping a constant speed of 0.5 knots whilst the length of cable out is kept constant. Changes in tension of the cable ('bites') are noted during dredging, indicating the size of the bite and the time of the bite. The coordinates of the start and end points of the dredging trajectory are recorded with water depth, length of cable out, time, and ship position.

The ship's equipment for lowering-lifting operations during geological sampling consists of:

-an electro-hydraulic rotatable crane, with a 5 tonnes lifting limit;
-a single-arm davit, with 10 tonnes of lifting capacity;
-a single-drum electric winch, with 15 tonnes of tractive capacity, 0.2-2.0 m/s of lifting speed;
-a steel wire with diameter 22 mm;
-a depth meter.

Sampling stations were designated as TTR7-AT*XY*, where *X* refers to the sequential number of the station (from 1), and *Y* indicates sampling method: *G* -when gravity corers were used, *D* -for dredging sites, *B* – for box corer, *K*-kasten-corer-like sampler, and *Gr*-for TV-controlled grab sampling stations.

Gravity core specification

The gravity core used has a length of 6 m and weighs of approximately 800 kg (Fig. 2). The outer diameter is 146 mm, the inner diameter 133 mm. The corer was put in the water with help of two cranes, one with a capacity of 0.8 tonnes and the other of 3 tonnes. The maximum water depth that can be reached is over 5000 m. When the gravity core is retrieved onto the deck, it is laid on its side and the core catcher is removed (A). Then the plastic liner inside is removed and put on the specially prepared wooden holder, where it is firmly held in place by ropes and manpower while other people (approximately 5 persons) push the cored sediment out with an extruder (B). On the other side of the liner, a team is standing by to cut the extruded sediment into sections of about 60 cm. Then the core section is laid in a half tube of fiberglass with top-bottom labelled plastic sheets underlying the section. Sections are brought to the geological lab where they are cut in halves using a wire 'cheese cutter' and knives (C). After labelling, one half is brought to the photo box where the core description is made (D). After sampling for biostratigraphy and smear slide analyses (from the inner part of the core), this part is cut into two halves again (i.e. quarters of the core) each of those is wrapped in plastic and paper for transport to MSU and CORSAIRES (Brest, Gent, Leuven or Kiel) (E) for the carbonate mound targets and to the Southampton Oceanography Centre (UK) for the turbidite targets. The other half is also cut into halves to be used by two geochemistry teams (the methods and aim of their work is explained in the geochemistry section). As soon as their work is done, the remaining core is subsampled again for additional sedimentological and mineralogical purposes (F).

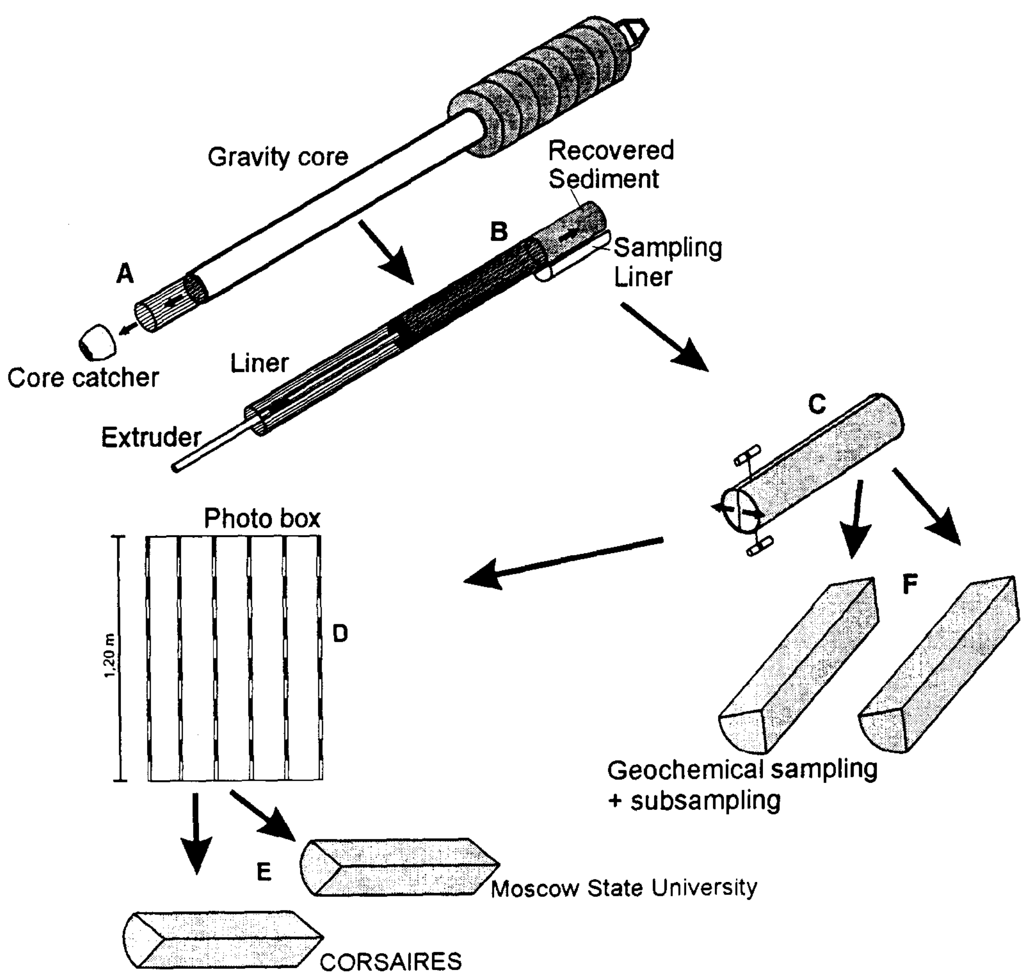

Fig. 2. Principles of gravity core operations and subsampling strategy

Box corer

The dimensions of the box corer are 50 x 50 x 50 cm. It is able to obtain undisturbed samples from the sea floor, weighing approximately 185 kg. Only the upper sediment layer can be recovered. Lowering and retrieving operations are undertaken using a hydraulic A-shaped frame with a lifting capacity of 12 tonnes, a single drum winch with tractive capacity for half the wire of 15 tonnes, and a speed of deployment and retrieval of 0.2-2.0 metres per second, by hydraulic crane. The samples obtained by box corer can then be used for sedimentological description, pore water extraction and other studies.

TV Grab sampler

The GTVD-2 TV-controlled grab sampler system was designed by PREUSSAG Meerestechnik AG (Germany) in 1988 for marine operations in depths of up to 6000m. Primarily designed for sampling of bedrock fragments greater than one tonne from the seafloor it has been later used by PMGEE to sample sulphides from black smokers on mid-ocean ridges in the Atlantic and Pacific oceans. During the TTR-7 cruise it was used to sample carbonate build-ups in the Porcupine Seabight and Rockall Trough. The grab system consists of two principal parts: the grab module and onboard control unit with a monitor and a videotape recorder.

The grab module is fitted with a monochrome TV camera and four floodlights which allow selection of the sampling site by the operator. Two-storage lead-acid batteries (12V, 230Ah) provide an autonomous power supply to the system. Six hydraulic arms, tipped by hard wearing steel, form an onion shaped hollow body when closed. To perform closing, each arm is equipped with its own hydraulic cylinder.

The operator-controlled onboard unit transmits high frequency signals to the grab via a co-axial cable. An electronic box on the grab decodes the signals and converts them into instructions for the hydraulic arms, floodlights and TV camera. The TV signals from the grab are transmitted to the ship via the same cable. Video signals (VHS) from the grab cameras are recorded onboard. Using the manual control system, operation of all the functions of the grab, including repeated opening and closing of the arms, are monitored in real time. The grab may be operated in an automatic mode, in which closing of the grab is triggered when the grab touches the bottom.

Operations of the grab sampler are performed at very low vessel speeds. The grab is positioned very precisely relative to the vessel using the Sigma 1000 underwater navigation system (Limonov et al., 1996). The specifications of the GTVD-2 grab sampler are listed below:

Total dimensions *Closed* *Open*	**(diameter/ height)** *2.85/ 2.64m* *1.90/ 2.70m*
Weight *in air* *in water*	 *3.2 tons* *2.8 tons*
Volume of the hollow body formed by the closed arms	*1.1m³*
Pressure at grab arms	*200 bar*
Maximum grab pressure	*29 kN*
Depth of operation	*up to 6000m*

V. Geochemical sampling

B. De Mol, A. Stadnitskaya, R. Swennen, I. Belenkaya, and R. Cave

Various studies report on the relationship between seeping methane gas, carbonate genesis and diagenesis. If methane migrates to more oxic zones, it will be converted to bicarbonate and carbon dioxide and these components can act as the base for carbonate precipitation if a Ca-source is available. In such processes the source and the genesis of the methane, its migration mechanism and the associated precipitation are usually poorly understood. There is still a lack of thorough knowledge about the effect of gas-seeps on the geochemical and biological environment and on sediment diagenesis at or near the seafloor.

On seismic-profiles and sidescan sonar lines (e.g. Hovland et al., 1994; R/V *Belgica* cruise report, 1997) several mounds and pockmarks have been observed at water-depths of more than 600m, in the northern part of the Porcupine Basin. These knolls (Hovland et al., 1994) and similar structures in other areas (Henrich et al., 1996; Hovland and Thomson, 1997) have been explained so far by migration of methane gas along tectonic faults from underlying gas-charged layers.

Until now a detailed sedimentological and geochemical investigation of these structures has not been carried out. The sedimentological research of the on-mound and surrounding sediments should allow characterisation of the different mound-components (Fig. 3). Based on the data gathered it should be possible to distinguish whether the mounds are pure biological features dominated by bacteria, corals, etc. or whether they consist of inorganic structures (e.g. clay-diapirs).

Geochemical research (especially stable isotopes) allows inferences on whether methane seeps play a present-day role in mound formation. It will help to deduce whether gas leaks create a chemical environment which is suitable for deep-sea coral growth, for minerals to precipitate during diagenesis and to cause alteration of components. These processes might exert a stabilizing effect on the mound structure. It is also important to characterise geochemically the deep-sea corals. This can provide information on their growth conditions and maybe they can be used as a kind of geological archive, just like tropical corals. For this type of research it is important to isotopically date these corals.

Special attention will also be focused on the role that bacteria play in these knolls and whether they are involved in mineral precipitation and diagenesis.

Sampling procedure

B. De Mol

Sampling was carried out using syringes with a cut tip. Syringes of 60 ml were washed in distilled water before being used. In the most important cores with respect to our objectives we took samples every 20 cm. When the sediments were too hard to be sampled by syringes a 2 cm piece of sediment was cut every 20 cm with a knife. Subsequently the samples inside the syringes and the cut samples were put in special well sample bags and immediately frozen in liquid nitrogen or in a freezer at approximately -15 °C. The nitrogen-frozen samples were collected for subsequent geochemical analysis, especially for analysis of porewater and gas composition. These analyses will be carried out in the laboratories of GEOMAR (Kiel, Germany) and of University of Leuven (Belgium). A second sample for bacteriological research was taken using syringes of 5ml with a cut tip. These samples will be analysed by Prof. Swings (University of Gent, Belgium). The main objective is to investigate whether bacteria have an influence on the actual mound formation and stabilisation.

After the most urgent analyses (gas and pore water) have been carried out, the sediment will be analysed using petrographical techniques (classical microscopy, CL, SEM, TEM). This will allow characterisation of the different components, the degree of diagenesis and alteration, possible cementation structures and hopefully phenomena testifying to the interaction between bacteria and mineral phases. This research will be carried out at the University of Leuven.

Geochemical analysis will be performed on both macro (bulk sediments) and micro components. A special objective during this research phase will focus on possible signatures which relate to the influence of gas, fluid and bacterially mediated processes. X-ray diffraction measurements will be carried out to illustrate the variation in mineralogy downcore and also the variation according to geological setting, while X-ray fluorescence should give an overall view on the chemical composition of the samples (major and trace elements). Results of both X-ray techniques may also contain information about diagenetic processes such as recrystallization, alteration and so on. Rare element analysis (analysed by ICP-MS) will give some information about input and origin of terrestrial components and microprobe and ICP-MS analysis will be carried out to analyse micro-components.

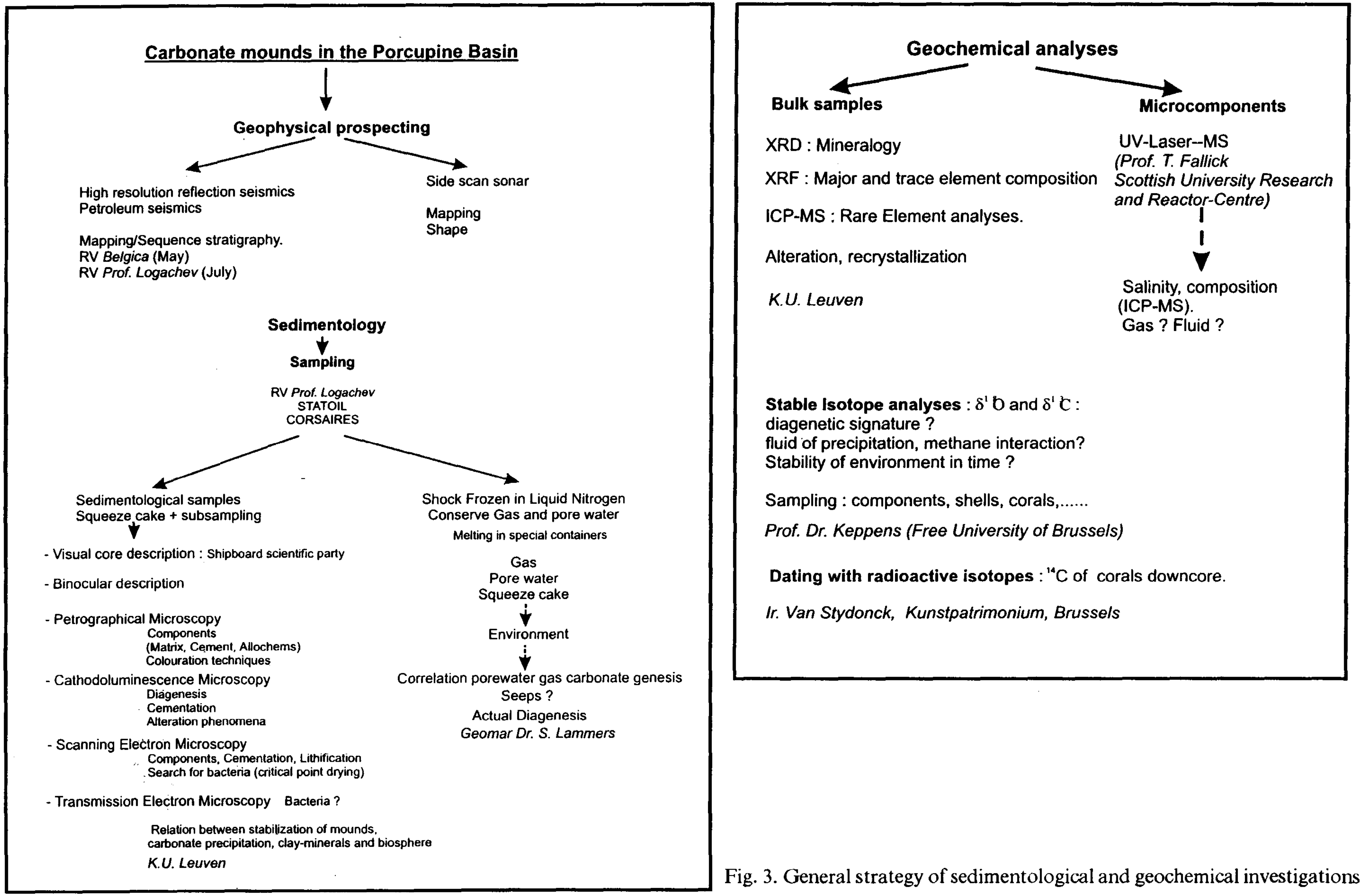

Fig. 3. General strategy of sedimentological and geochemical investigations

Furthermore, stable isotope analyses $\delta^{13}C$ and $\delta^{18}O$ of macro and micro samples will provide information on whether methane mediated processes affected precipitation and diagenesis. The micro isotope analyses will be carried out with an UV-laser-MS in collaboration with Prof. A. Fallick (Scottish University Research and Reactor Centre, East Kilbride). Additionally the stable isotope signature of corals might give us information on variation through time. For this research absolute dating by ^{14}C technique will be performed.

Gas analysis

A. Stadnitskaya

The sampling for subsequent hydrocarbon gas analysis was made using a syringe with a cut tip. Samples of 40 cm^3 were taken from all different lithological intervals of the cores or at the same intervals as described above, wherever possible.

For Total Organic Carbon (TOC), fluorescent analyses, and bituminological investigation, 100g of wet sediment were sampled from the same intervals as for the gas analysis.For isotopic $\delta^{13}C$ (CH_4) analysis, 0.5 kg of sediment was taken from the upper, middle and lower parts of each core.

A standard gas sampling method was applied. The degassing was accomplished according to the head-space analysis, adapted for shipboard conditions (Bol'shakov and Egorov, 1987). The principles of this method are as follows: known quantity of sediment is placed into a glass jar of 119 cm^3 in volume with screwed cover rubber gasket; the sediment is then flooded with distilled water leaving a small part of the jar volume free; the hermetically sealed jar is shaken so that the sediment is mixed with water, liberating the pore-gas until the phase equilibrium is established, in accordance with Henry's law. The jars were shaken three times during 24 hours following sampling, each for three minutes. Subsequently the gas phase was transferred into glass jars filled with saturated NaCl solution and stored in a freezer at approximately -12 °C.

Pore water analysis

I. Belen'kaya

pH and Eh values were measured in situ with platinum and Cl-silver electrodes using an Ion-meter device immediately after core retrieval on the deck. The pH probe was calibrated prior to each measurement with pH 7 and pH 10 standard buffers. For pore water analysis, 50-100g of sediment were sampled according to variations in lithology along the core. Subsequently water from the samples was squeezed into polyethylene bags using titanium press-forms under a pressure of 100-150 Pa. The water samples were then sealed and frozen at a temperature of -4°C.

Porewater sampling

R. Swennen

Sediment moisture has been taken with the use of "Rhizon soil moisture samplers (SMS)" linked by (two females) luer connectors to plastic luer lock syringes of 10 ml. The advantages of using this sampling device are:

- small diameter: 2.5 mm
- no ion-exchange capacity
- delivered by one manufacturer as one system (produced by Rhizosphere Research products, Dolderstraat 62, NL-6706 JG Waganingen, The Netherlands (Fax +31-317-422415; e-mail: meijboom@ab.dlo.nl) distributed by Eikelkamp B.V., P.O.B. 4, NL-6987 ZG Giesbeek, The Netherlands (fax: +31-313-632167))
- relatively low cost

A standard Rhizon SMS (Fig. 4) consists of a 10 cm long porous polymer which is connected to a 10 cm long PVC tube and a "luer-lock (LL-) connector" (male). Every sampler is pre-packed with a protecting cap. The porous material (+5 cm of the PVC-tube) is strengthened with a 15 cm R/VS-wire. This R/VS-wire is connected to the end of the porous polymer tube. The sampler, strengthened by the R/VS-wire, can be placed within a sediment sample without disturbing the latter. Sampling the pore-water is achieved by creating a vacuum by using the piston of the syringe and blocking the created vacuum with a wooden retainer at 11 ml. By doing so a driving force for the pore-water extraction is achieved. Pore-water yield, in the most porous samples, was about 0.5 ml/min.

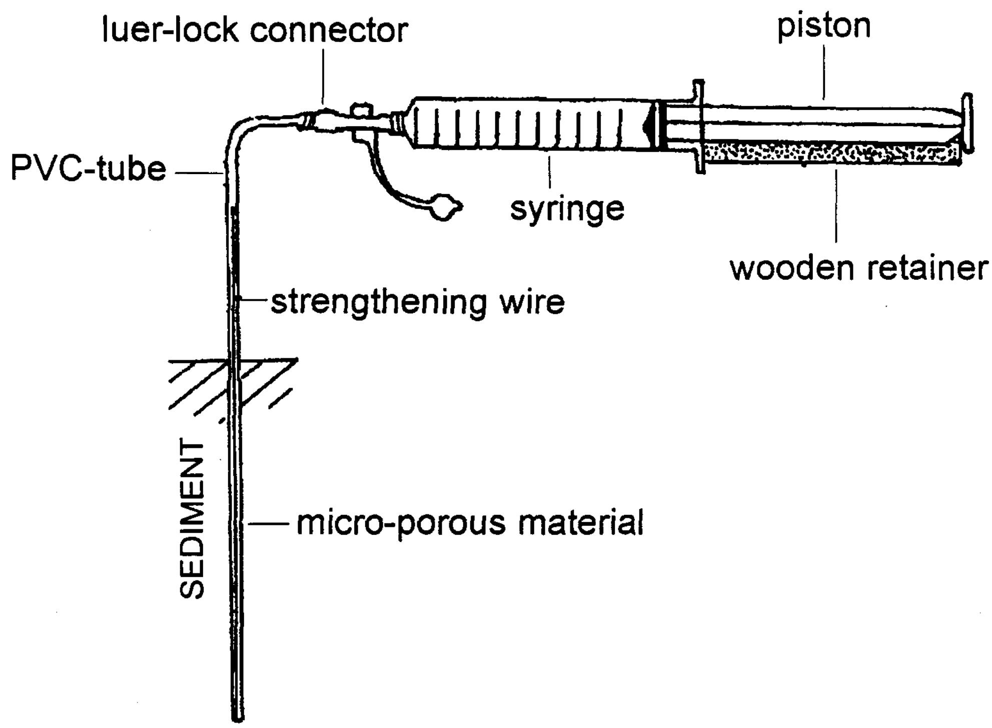

Fig. 4. Schematic of Rhizon sediment moisture sampler

Geochemical Sampling, Leg 2

R. Cave

Sub-surface and surface sediments in all ocean basins contain, in various proportions, Fe and Mn oxyhydroxides, Pb, Sr and REE. In most cases, layers enriched in these elements result from depositional and post-depositional processes including diagenesis. Such processes are affected by the physical and chemical parameters of the overlying water column, as well as sediment provenance and mass accumulation rates. Fe-Mn rich oxyhydroxides also form a major component of metalliferous sediments found near active mid-ocean ridges, and in sediments overlying basaltic basement in ocean basins down to at least Palaeocene age. These are believed to be derived as a result of hydrothermal activity. Pb in these sediments is derived both from basaltic and seawater sources, while REE and Sr enrichment in hydrothermally influenced sediments results from scavenging of REE from seawater by plume particles.

Results from ICP-MS analyses of REE and other elements to be carried out on samples from cores obtained in the NE Atlantic during TTR-7 will be used in comparative studies with recent pelagic sediments from areas influenced by hydrothermal activity, in order to try to quantify the respective influences of diagenesis and hydrothermal activity on the availability of these elements in marine sediments.

The applied sampling strategy was as follows. Core subsampling was carried out using a 60 ml syringe with a cut tip. Where sediments had a large proportion of coral debris, samples were cut out with a plastic spatula. The syringe was rinsed with distilled water between samples. Samples were taken on the basis of colour/apparent lithology changes downcore, as this combination was taken to best represent changes in diagenetic conditions within the core. Samples were put into zip-lock bags and refrigerated at 4°C for later analysis onshore (to be carried out at Southampton Oceanography Centre). Where coring was unsuccessful, but some surface sediment was obtained, a small sample of this was taken.

Pore water samples were taken from cores AT49G, AT56G, AT69G, AT71G and AT73G, using Rhizon soil-moisture samples kindly provided by Dr. Rudy Swennen. Samples were generally taken from the topmost layer, and from the one beneath, with corresponding core samples. Sampling averaged 10 minutes for each syringe (10 ml), though there was some variation. One sample produced only 3 ml of fluid, and it was found on removal of the syringe that the PVC proboscis had broken half way along its length. After sampling, the proboscis was removed and each syringe capped, bagged and refrigerated at 4°C.

Some rocks and corals were recovered with yellow coating, probably iron oxide, and others with a black coating, believed to be manganese oxide. Samples of these were taken and refrigerated for future analysis. The black-coated samples were recovered from deep water (> 2000m) and apparently from the seabed surface. The yellow coated samples came from a site AT 51Gr in shallower water (600-700 m) and were buried in the sediment. Samples of the sediment surrounding these pieces were also taken.

VI. Sampling of benthos

P. Sumida and R. Kennedy

Faunal samples were taken only at stations where carbonate mounds were thought to be present. Stations AT4D and AT8D were dredge samples up the slope of Large Mounds (LM) LM3 and LM2 respectively. Stations AT15GR and AT24GR were TV grab samples from the crests of a mound (LM3) and a Barrier Mound (BM) respectively. The TV Grab allows a previous observation and choice of the site to be sampled, giving an idea of the structure and distribution of the benthic megafauna. Benthos was manually picked from the outer tangle of the dredge. The sediment in the dredge and the top 20 cm of the grab was then sieved on a 1 mm mesh and visible macrofauna was collected. Both live and dead corals were collected to examine the fauna living on and in the coral. All fauna collected was fixed in 10% neutrally buffered seawater formalin, and later identified using a stereo microscope to the lowest possible taxonomic level. Where possible the feeding mode of the various taxa was noted. Line drawings of some of the more common taxa were made.

SCIENTIFIC REPORT

I. PORCUPINE SEABIGHT (Leg I)

I.1. Objectives and geological setting

N. Kenyon and M. Ivanov

Objectives

The objectives of the first leg of the 7th TTR were:

1. Deep-water carbonate mounds (north Porcupine Seabight and Celtic Margin of the Porcupine Seabight)
2. Deep-water turbidite channels, the Gollum channel system (Celtic margin of the Porcupine Seabight)
3. Slope stability (Biscay margin of the Celtic Sea)

These TTR objectives were planned to be met by the following surveys:

1. A reconnaissance of the eastern and northern margins of the Porcupine Sea Bight, based on OKEAN-long-range sidescan sonar records and seismics. For this purpose two adjacent tracks were generated. The aim was to collect information on the upper reaches of the Gollum channel system, on the presence of "barrier-type" mounds and on the seismo-stratigraphic expression of the upper sedimentary sequences in this area;

2. detailed investigation of mound structures described by Hovland et al. (1994) in the northern part of the Porcupine Sea Bight and the small mound structures discovered by the R/V *Belgica* cruise to north-west of the large mound structures. Furthermore attention was paid to the recently discovered "barrier-type" mounds in the eastern part of the Porcupine Seabight. This was achieved by surveys with the OREtech medium to high resolution 30/100 kHz deep-towed sidescan sonar over several of the mound sites. Furthermore, gravity coring of the periphery, the moat, the flank and the crest of these carbonate mounds should provide information on their setting and uppermost structure. Underwater TV/video survey was expected to gain additional and detailed information on the seafloor processes taking place in the areas of mound occurrence. Important information on the mound composition would be contained in bottom samples retrieved by the Preussag TV-controlled grab sampler. Particular attention was paid to biological investigation of these bottom samples.

3. detailed investigation of the central part of the Gollum channel system by the OREtech medium to high resolution 30/100 kHz deep-towed sidescan sonar, profiling and gravity coring of different sedimentary sub-environments (levees, terraces, channel, etc.);

4. detailed investigation of some possible instability features on the Biscay margin were planned but not carried out, as permission to work arrived too late.

Surveys 1, 2 and 4 were of particular interest to the CORSAIRES partner, while representatives from SOC, UC Cork and U Aberdeen were additionally interested in survey 3.

Physiography of the Porcupine Seabight

N. Kenyon and P. Hunter

The Porcupine Seabight sits on the map rather like a pear that has had a bite taken out of the wide part and then been placed upright on a table such that the bite, the exit to the deep Atlantic, is on the left hand side. Bathymetric charts of the Porcupine Seabight were lacking in detail prior to the map made by the Institute of Oceanographic Sciences, UK (Hunter and Kenyon, 1984). This improved greatly on the previous charts that had been prepared by Brenot and Berthois (1962) from much more limited data.

The technique for making the map was a novel one. It has been shown that it is better to make some assumptions about geological processes when contouring from scattered soundings (Laughton, 1986). There are usually benefits over maps that are contoured by computers. However it is still possible to make errors because ones assumptions may be wrong. An example of this is seen on the maps of the canyoned margin of the bay of Biscay (e.g. Roberts et al., 1979), which assume that unless there is evidence to the contrary, the canyons run down the line of greatest gradient. However the more recently available swath mapping techniques have shown that the canyons can be fault guided and run oblique to the greatest slope (Kenyon et al., 1978; Sibuet et al., 1984). The basic sounding sheets were compiled from all the data that had been supplied to IOS as a part of the GEBCO deep-sea mapping programme. In order to connect up the contours in the best way to depict the true shape of the ground, sidescan sonar data were analysed for relief features and the interpretation overlaid on the sounding sheets. Contours can then be drawn that are a great improvement on what would otherwise be drawn on the basis of soundings and assumption of process alone. Features on the sidescan sonar that are due to those small scale roughness contrasts that are not associated with relief, were not used. The resulting map has proven to be generally correct within the area where sidescan sonar was available. The sidescan sonar data were obtained with both the long-range GLORIA system from cruises in 1977 and 1981 and from medium range, 36 kHz hull mounted, sidescan sonar used on the same cruises. The range of the GLORIA data is about 20 km and the data obtained cover the eastern slope and the Gollum Channel. The range of the hull mounted sidescan sonar system was 2.5 km to each side but in deeper water much of the record is taken up by the water column. However useful narrow beam profiles and narrow strips of sidescan sonar could be obtained with this equipment and it could be operated with little loss in data quality at ships cruising speeds of 12 knots.

The basin is about 350 km long and is open to the deep ocean in the south west through a constricted gap. The Irish shelf and the Celtic Sea are to the east, the Goban Spur to the south, the Porcupine Abyssal Plain (about 4700 m deep) and the Porcupine Bank to the west and the less than 300 m deep Slyne Ridge to the north. The basin margins are at their steepest (> 2.7°) where the Gollum Channel system is located, west of the Celtic Sea shelf edge. Overall gradients are greater than 1° here but are generally less than 2 degrees. These lower gradients are less than those for the slopes of the Bay of Biscay and the Rockall Trough. The basin floor lies between about 2000 and 3000 m.

The Gollum Channel system is one of the very few lengthy, leveed channel systems known from the NW European margin. It is named after a particularly unpleasant creature in J.R.R. Tolkien's book "Lord of the Rings", the more heroic and positive places, tribes and characters having been used for other features on the margin here. It is a striking looking tributary system with low sinuosity and narrow, steep sided channels. The heads of the channels are in depths of about 300m. They do not form steep walled amphitheatre shaped canyon heads like those in the Bay of Biscay (Kenyon et al., 1978). The widths remain fairly constant from top to bottom of the system. The deepest and widest slope channels are in the north. The gradient is greatest on the slope, decreasing to a minimum between 2300 m and 2500 m where a few meanders are found. Below 2500 m the gradient and the height of the walls increase. This implies that the channel has cut down through the steeper slope at the mouth of the Porcupine Seabight and has not yet reached an equilibrium grade. The levees are low, but can be seen on the bathymetric chart and appear to be higher on the right hand side. All profiles across the lower reaches of the channels show terraces. There is a sharp bend to the left at the mouth of the channel which is probably guided by older, more resistant rocks. There are rugged areas of probable outcrop near the mouth of the Seabight.

North of the Gollum Channel system there are two broad deeps cut into the slope. They are about 20 km and 25 km long, 10 km wide and up to 400 m deep. There appear to be accumulations of sediment at their foot. As there are no open channels at the base it is assumed that they are old slide scars.

The narrow linear deeps to the north of the two broad deeps include the closed deeps and the down slope trending deeps, described in the section on the OKEAN line. These are either partly filled channels or the site of erosion by gas seepage.

On the high resolution sidescan sonar data belonging to SOC there are iceberg ploughmarks. This is their southernmost occurrence recorded in the NE Atlantic. In water deeper than the ploughmarks there are small sand waves, recorded down to a depth of 550 m. The occurrence of sand waves at these depths has been a mystery that is starting to unravel as a result of this cruise.

The presence of carbonate mounds on the eastern and northern slopes of the Seabight was not suspected until the paper by Hovland et al. (1994) and the R/V *Belgica* cruise of 1997. The 1981 RRS *Discovery* cruise had mapped two mounds, one is on the bathymetry map and the other was too low, where crossed, to be on the map.

The western margin of the Seabight increases in steepness to the south. There is a pronounced outward bulge in the contours that lie in the north, the reasons for which are not yet known.

Brief Geological History of the Porcupine Basin

A. McDonnell

The Porcupine Basin is one of the largest offshore Irish basins and lies approximately 150 km to the southwest of Ireland. It is a Mesozoic to Cenozoic basin, which is elongate in a north-south direction and displays a roughly symmetrical cross section. Water depths in the present day basin vary from 300 m in the north to over 2000 m in the south. As a consequence of this southerly deepening most exploration wells to date have been concentrated in the northern shallower part of the basin. The Basin is bounded to the north and west by Precambrian to Lower Palaeozoic basement highs and is bounded to the east by the Irish Continental shelf. The history of the Porcupine Basin is described in terms of pre-rift (Devonian-Permian), syn-rift (Triassic-Jurassic) and post-rift (Cretaceous-Tertiary) phases of basin evolution (Croker and Shannon, 1987).

Pre-Rift

The Pre-rift succession in the basin contains Devonian, Carboniferous and Permian deposits. The Devonian appears to be sparsely preserved, being encountered in only a few wells where it records the interfingering of continental fluvial deposits and nearshore marine strata. It is interpreted to represent a series of transgressions and regressions. These fluctuations continued through to the Carboniferous where a thick deltaic succession is preserved. Thick coarsening upward sandstone units are capped by coals deposited in a marshy delta top environment. The coals act as a potential gas source rock in the basin while the deltaics hold limited reservoir potential. The overlying Permian succession is dominantly continental, dominated by shales but also containing evaporites and is interpreted to represent continental playa lake deposition. The Permian and Carboniferous are only locally preserved and are thought to have been deposited in a series of north-east south-west oriented sub-basins which exploited an underlying Caledonian trend (Shannon, 1991).

Syn-Rift

The syn-rift phase of basin evolution contains strata of Triassic and Jurassic age. The Triassic is preserved locally in sub-basins and an oscillating nearshore environment of deposition is interpreted. It was deposited during an initial rift phase marking the break up of Pangea. The main phase of rifting occurred during the Mid to Late Jurassic during which time the basin developed its present day north-south orientation, oblique to both Caledonian and Variscan trends. The north-south trend is thought to be a response to extensional stresses in the nearby evolving North Atlantic Ocean.

A marine transgression marks the Lower Jurassic while in the Middle Jurassic an ancient shoreline is interpreted to have existed in the centre of the basin, separating marine deposition to the south from continental deposition to the north. During this time, in the north of the basin braided stream deposits were laid down, grading upwards into finer sediments of meandering river channels. Active rifting took place in the Late Jurassic accompanied by a regional sea level rise. Upstanding areas were submerged as the sea transgressed northwards and a range of lithologies and facies were developed throughout the basin reflecting syn-rift deposition. Depositional environments range from estuarine, tidal channel and beach deposits to fluvial and lacustrine deposits in the west. In the basin centre a submarine fan complex was developed. Rifting waned during the early part of the Cretaceous and a major unconformity marks the Jurassic-Cretaceous boundary.

The Jurassic contains the greatest potential in the basin for oil rich source rocks and also contains considerable reservoir quality sandstones, with a range of potential plays both structural and stratigraphic, present.

Post-Rift

A period of thermal subsidence followed rifting, with sediments of Cretaceous age onlapping and infilling the topography. The Cretaceous consists of a deepening marine environment although deposition is interrupted by a minor rift episode of Aptian-Albian age. A deltaic complex was developed in the basin at this time. In the Upper Cretaceous a major rise in sea level occurred which resulted in chalk deposition. At the base of the Tertiary however, a relative fall in sea level marked the end of carbonate deposition.

Palaeocene and Eocene times record the shedding of clastics into the basin in the form of submarine fans from the western and eastern basin margins while a delta complex prograded from the north. Relative sea level rose throughout the Upper Tertiary and quieter water marine strata were deposited interrupted occasionally by channeling. There has been relatively little study carried out dealing with the Pleistocene and Holocene history of the basin however during this time sediments were likely to have been sourced from the Irish continental shelf to the east. Present deposition in the basin dominantly comprises quiet water deep marine mud although a deep sea channel system (Gollum System) is developed in the south of the basin, sourced from the eastern margin. A number of mounded features are also evident which have been interpreted by Hovland et al. (1994) as carbonate mounds possibly initiated by gas seeps to the surface.

I.2. Seismic profiling data

A. McDonnell, O. Krylov, A. Limonov

General description of collected seismic lines and preliminary seismic stratigraphy of the area

Seismic profiling was carried out in the Porcupine Basin (Porcupine Seabight) from the 9th until the 11th July 1997. Twelve profiles (PSAT-1 to PSAT-12) were taken with a ship speed of approximately 6 knots and recording time of 3.0 sec. The profiles have a total length of 567 km. In terms of location (Fig. 5) profiles PSAT-1 to PSAT-3 define a NW-SE line along the continental slope on the southeastern margin of the Porcupine Basin. Profiles PSAT-5, 6 and 8 were run parallel and westwards of the northwestern section of profile PSAT-3. These lines were spaced about 9 km apart to provide overlapping of the OKEAN sonographs. Profiles PSAT-4, 7 and 9 are short connecting sections. PSAT-10, 11 and 12 were shot parallel and approximately 9 km westwards of PSAT-3, 2 and 1 but don't extend as far south, stopping short of the Gollum Channel zone.

The profiled seismic section can be divided into 3 main seismo-stratigraphic sequences resting on a highly irregular, buried topography representing acoustic basement which may be Cretaceous to Lower Tertiary in age. A number of sub-sequences can also be identified. The upper sequence is tentatively correlated with Base Miocene to Holocene deposits, while the middle sequence is inferred to be Upper Oligocene in age. The lower sequence is suggested to comprise Oligocene strata. Information from Hovland et al. (1994) was used to aid in dating these deposits. The slope of the margin becomes progressively steeper from north to south, with line PSAT-1 intersecting the steepest section of the slope, which is incised by canyons and gullies. This slope change may be of some importance, as there appears to be a relationship between slope gradient and style of deposition.

Seismic line PSAT-01

Line PSAT-01 (117 km long) is located at the southeastern corner of the study area and is characterised by very variable and irregular sea floor relief. The distinctive topography is primarily created by a large channel system, which is transected by the profile. Bathymetry maps display the channels extending from the eastern margin of the Seabight out into deeper water areas in the west. Six main channels are crossed. The channels have flat bottoms and some are flanked by terraces and levees.

Inspection of the section allows three main sequences (S1-3) to be identified (Fig. 6). S1 is the oldest sequence and displays very low amplitude reflectors which were affected by signal attenuation. S2 shows moderate amplitude events while S3, the youngest package, displays a moderate to high amplitude character. The sequences rest on an acoustic basement, which defines a very irregular, locally faulted, topography highlighted by a very high amplitude upper boundary. Internally the basement displays a much weaker, dominantly transparent character, but in the upper part locally continuous stronger events are seen, suggesting sediment stratification. The basement is quite shallow in the most southern and the most northern parts of PSAT-01 where it is at a depth of approx. 0.5 s (TWTT). In the intervening section, a distance of approx. 85 km, the basement is much deeper reaching 1.5 s (TWTT) at its deepest. It is in this basal low that the thickest accumulation of sediment occurs, infilling and levelling off topography. The Gollum Channel system exploits this region suggesting an underlying basement control on location of the system.

S1 onlaps and infills this buried topography. It comprises low amplitude, laterally continuous events. The upper boundary of the sequence is undulatory in nature and is defined by the lowermost continuous reflector of a package of moderate to high amplitude events. S1 makes up very large-scale (12 km diameter approx.) mound features (Fig. 7), which appear to be composed of at least three depositional sub-sequences. A dominantly concordant contact exists between these sub-sequences, but locally marginal truncation of underlying reflectors is evident. These packages appear to build up directly on top of each other, reaching a crestal height of 500 ms and thinning laterally. All three sub-sequences display the same low amplitude character. The palaeolows between these mounds are onlapped and infilled by sediments with very low amplitude continuous reflectors similar to the mounds themselves. The infilling strata can also be subdivided into different depositional units, although they generally demonstrate the same internal pattern suggesting there was little variation in

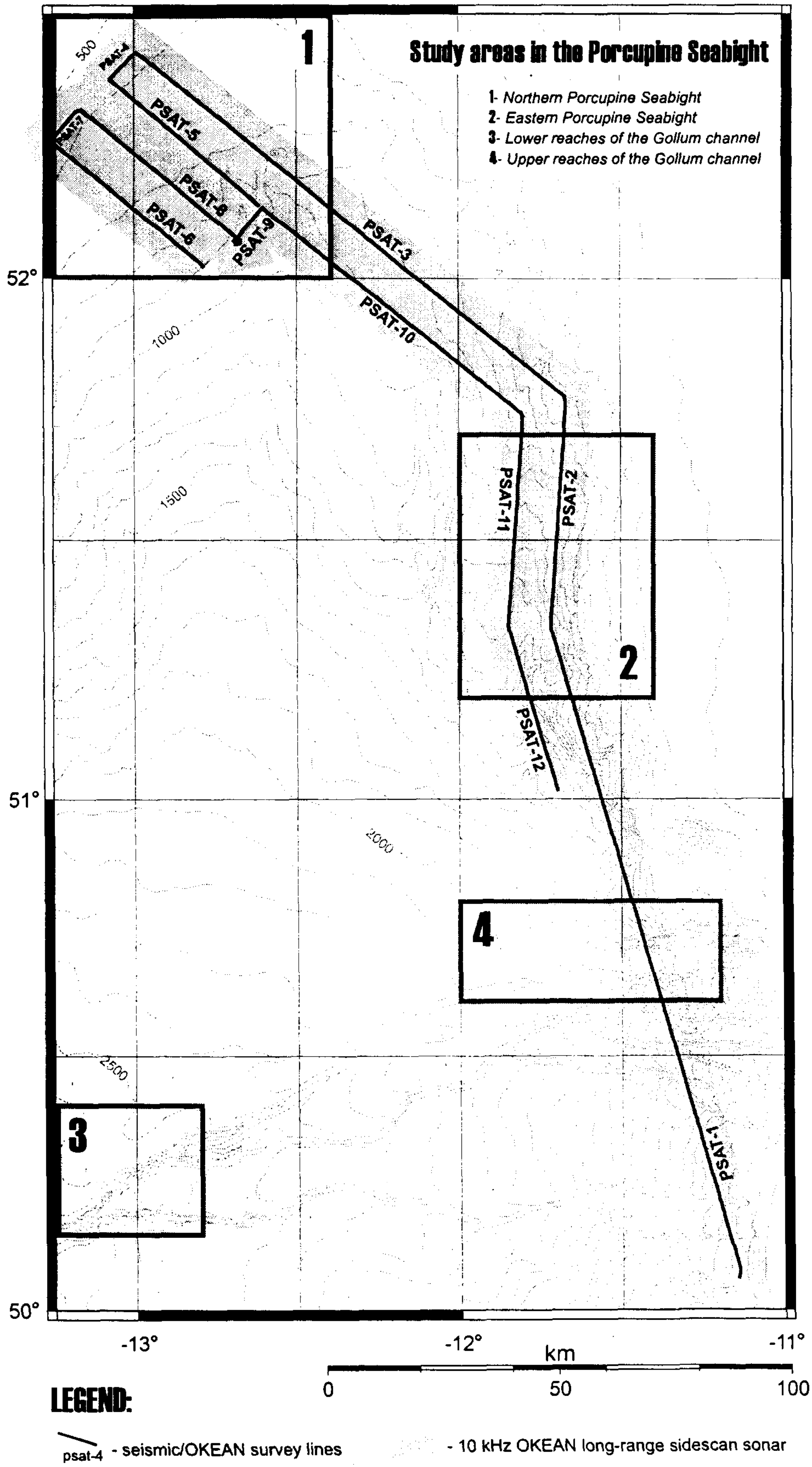

Fig. 5. Seismic tracks and study areas in the Porcupine Seabight

the type of sediments infilling the lows. Externally, Sequence S1 displays great thickness variations laterally as it infills the underlying topography, reaching a maximum thickness of up to 0.1 s TWTT.

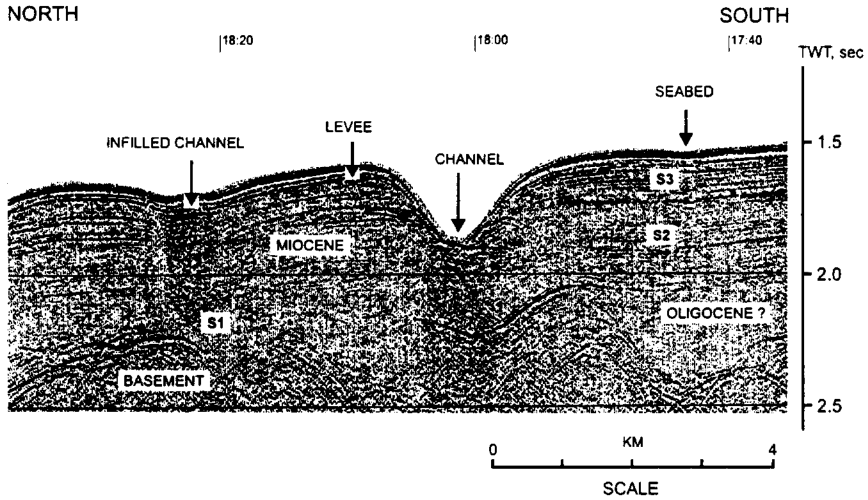

Fig. 6. Section from line PSAT-1 showing sequences S1-S3 on faulted basement topography

S2 and S3 are both moderate to high amplitude packages which generally show flat, parallel events and also display the initiation of the channel features which exist to the present day. S2 displays moderate to high amplitude, parallel, continuous reflectors with minor internal discontinuities. It rests with general conformity on Sequence S1 but is locally erosive. Externally the geometry is sheet-like, with thickness varying laterally. Sequence S2 is thinnest on the basement high to the south (200 ms TWTT) and thickens northwards along the line PSAT-01, reaching approx. 500 ms in certain areas. S2 appears to thin and onlap onto a large buried slope feature between time marks 0:0 -1:20 (Fig. 8). A prograding package is evident at the edge of the palaeoslope. Internally the slope package contains flat parallel reflectors with the amplitude increasing towards the top.

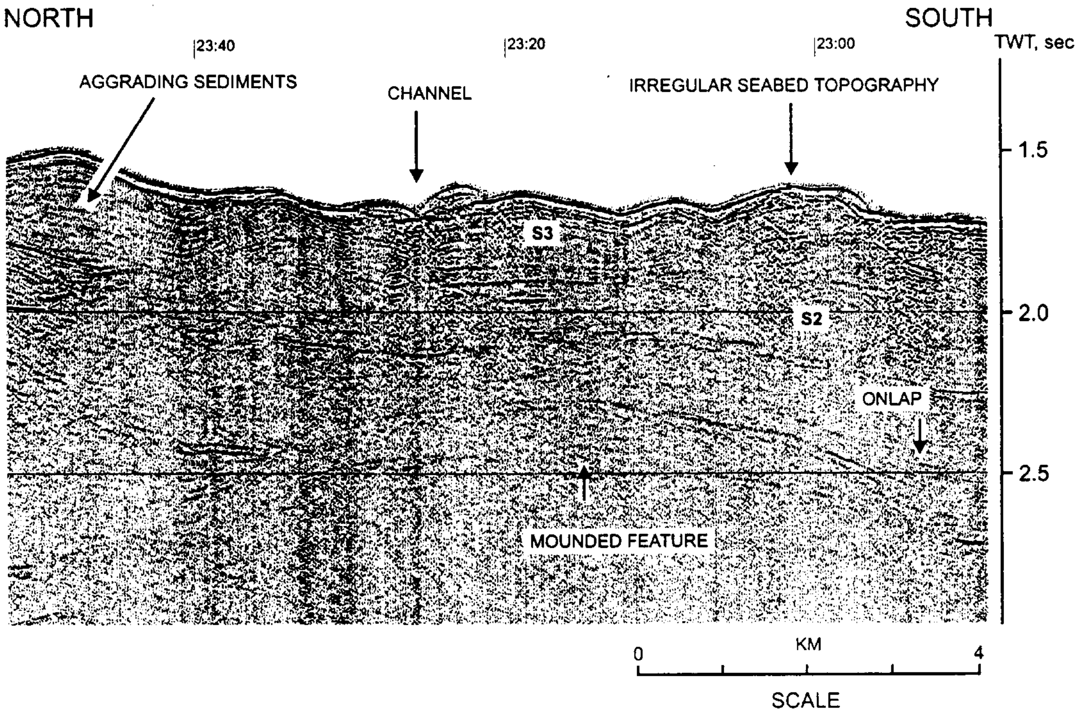

Fig. 7. PSAT-1. Example of one of three large mound features present in S1, possibly Oligocene in age

The Gollum Channel system seems to have initiated during the early deposition of Sequence S2. Internally the channels display a high amplitude seismic signature with a sequence of infills present. Occasional very high amplitude continuous events are seen in the channels and this high impedence contrast may have been created by coarse channel lags. Many of the channels show vertically aggrading convex upward reflectors at the channel edges, which are interpreted as levee features.

Sequence S3 comprises the youngest deposits and its lower boundary is defined by the basal reflector in a package of high amplitude events. Internally, the sequence shows higher amplitude events than Sequence S2, with a flat-parallel geometry dominating. Externally, the sequence is the thinnest (200 ms) in the south of the line and thickens to the north (350 ms). Channelling continued throughout deposition of this Sequence and the sea bed displays a very irregular topography created by the channel system and its associated levees. Some channels have been completely infilled. Figure 9 illustrates a section across one of the largest channels in the area (time mark 22:20), and at least three different phases of channel fill are evident. The most recent fill thins to the north where the channel bank is the steepest. It is suggested that this variable thickness may be a function of current activity, with the current concentrated along the northern side of the channel, while a bar feature simultaneously developed on the southern side of the channel. Moving further north along the line, the sequence appears to aggrade upwards and onlap a large positive mound feature rising above the seafloor (Fig. 8) (23:40 -0:20) which is located directly above the palaeoslope onlapped by sequence S2. The strata onlap the base of the steep southern slope of this feature, with slight evidence for moating evident. This pattern may represent sediment drift or contourite type deposition. The large mounded feature is interpreted to be laterally equivalent to Sequence S3; the internal reflectors are less continuous than elsewhere in the Sequence with some evidence for events dipping to the south. A slight angular unconformity is present in the upper section of this mound feature with parallel-flat events truncating underlying tilted structures.

Seismic line PSAT-02

The line PSAT-02 (43 km) crosses the uppermost part of the continental slope of Ireland northwest of PSAT-01. In this line, the basement is very near the surface and the sediment thickness reaches only 250 ms. As a consequence, only Sequences S2 and S3 are present. The sea bed topography differs from that in PSAT-01, being much smoother, with gentle undulations. An irregularly mounded region with a number of smaller peaks (Fig. 10) is evident between 4:40 and 4:10. A slight velocity pull up effect is observed below this mounded region implying that the mounds have a higher acoustic velocity than surrounding sediments, suggesting that it may be a carbonate build up. There is no evidence for faulting seen beneath the mound, however acoustic basement is near the surface. Internally, the seismic pattern is very chaotic although continuous events can be correlated beneath the mound. There is no moat evident surrounding the high. Slightly to the southeast, at 3:40 approx., a smaller topographic high can be seen with a similar internal character. At the southern end of line 02, the sediment begins to thicken as the basement progressively deepens.

Seismic line PSAT-03 (115 km)

There are three seismic sequences in this line also, which can be approximately correlated with the previous ones. At the southern end of the line the basement becomes deeper and a very thick sediment pile, 1.0-1.5 s, is accumulated in the low. This is similar to the thickness observed in PSAT-01. The uppermost sequence is 460-520 ms thick, and there are two distinct parts to the package. This is roughly equivalent to S3. The first lowermost part is represented by short chaotic reflectors (time marks 16:40-17:20, 1:30-2:10). An erosional base truncating underlying flat parallel reflectors is evident beneath this chaotic zone (Fig. 11). The chaotic reflectors pass into more parallel flat reflectors to the north. The second part consists of very flat, continuous, moderate amplitude events (time marks 18:40-19:20). The chaotic zone may represent a period of slumping in the basin. It is unlikely to represent a buried carbonate 'reef' type feature due to its very large extent and the fact that there is no velocity anomaly observed beneath the chaotic zone. The second two sequences in this section have a lower amplitude, locally transparent in character but the upper part of Sequence 2 displays a zone of flat, stronger events. It is these stronger events which are eroded by the chaotic sequence in the overlying sequence. Sequence 2 is not more than 200 ms thick. Sequence 1 displays

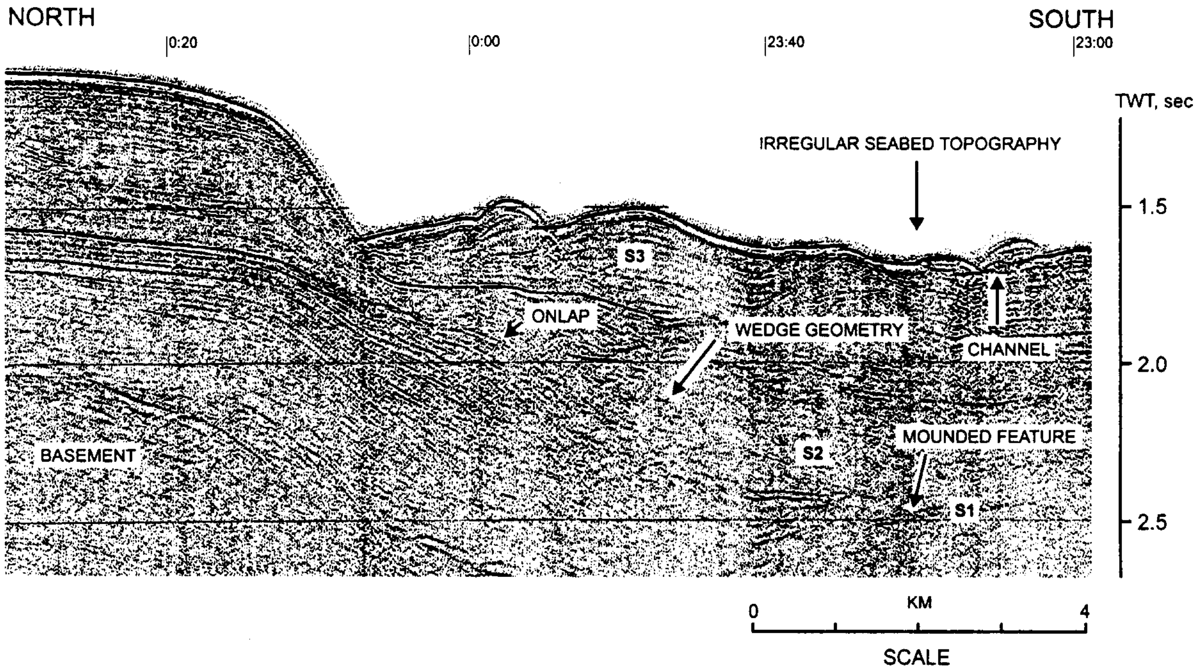

Fig. 8. Northern end of line PSAT-1 showing onlap of S2 onto a large topographic high

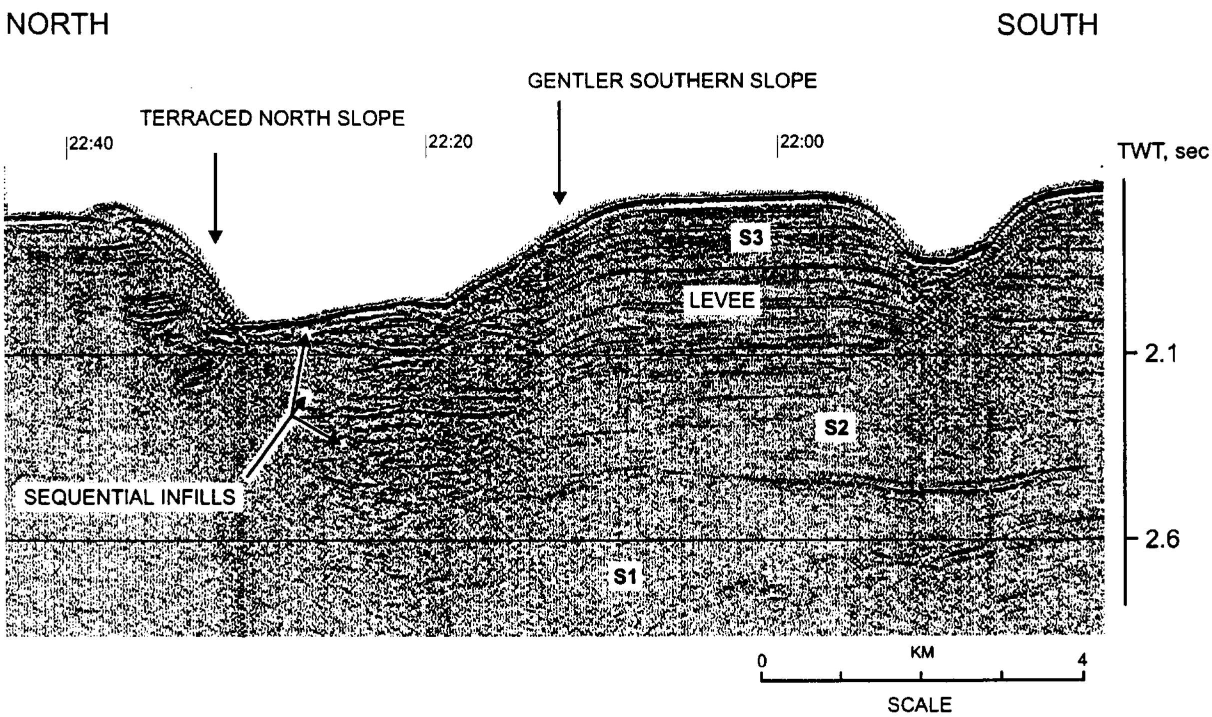

Fig. 9. PSAT-1 crossing a deep-sea channel and levee system. Bathymetry map shows the channel is sourced from the east and runs westward into a deeper basinal setting. A number of channel infills are seen

very low amplitude, and in the north of the section its character is masked but it is seen in the south between the time marks 1:00-2:10. The internal character of this sequence is different to the equivalent section in the south (PSAT-01): there is no mounding developed and the horizons are much flatter and more parallel (Fig. 12).

At the seabed surface, a mounded feature with a very high relief, chaotic internal seismic reflector configuration and irregular terraced edges can be seen. A moat is present to the south of this feature but there is no such low to the north. Velocity pull up is evident beneath the mound feature (Fig. 11). Overall sediment deposition was quieter and more uniform in this region of the survey area then further to the south where the underlying basement was much more irregular and the basin margin was steeper.

Seismic line PSAT-04

PSAT-04 is a very short section (6 km). It is a perpendicular line running in a northeast-southwest direction connecting PSAT-03 to PSAT-05. The line displays very flat, parallel, moderate to high amplitude reflectors throughout the entire section, with little or no disturbance.

Seismic line PSAT-05

Lying parallel to PSAT-03 this line is characterised by the same overall subsurface architecture. A lowermost thick low amplitude sequence with amplitude increasing towards the top is locally truncated by a second sequence consisting of a zone of chaotic internal pattern overlain by a shallower zone with flatter events. Laterally, the chaotic seismic reflection character changes into more parallel-bedded events. The sea bed topography is different however in line 05, as there is no mound evident, instead there are two small dips in the topography bordering a slightly uplifted structure (1:20-1:30).

Seismic lines PSAT-06-08

Bathymetry data show these lines running down the basin slope. The seismic sections exhibit the same internal acoustic pattern and sequences as were seen in lines PSAT-03 and 05, although the sequences are thicker. The sea bed topography is quite smooth and slightly undulatory and a large mound is evident on line 08, displaying the same chaotic internal character as the mound feature seen on line 03. The two mounds are not connected though, as is seen from the intervening line and also sonar data confirm that these are separate features.

Seismic line PSAT-10

This line displays the same character and geometry as PSAT-03, although the packages are thicker, with sediment thickening towards the north. The sediments are about 350 ms thick on the marginal high compared with 250 ms on line 03. The basement is slightly deeper on line 10. The seabed also is smoother and flatter on this section than on 03, with fewer depressions present.

Seismic line PSAT-11

Line 11 runs parallel with line 02 and demonstrates a similar basement high (time marks 10:40-13:40) overlain by thin sedimentary cover although the sediments are slightly thicker than in line 02. The seafloor topography is smoother than on line 02 and no mounds are observed. At the southern end of the line, Sequence S2 comprises a southward-thickening wedge of strata, similar to that on line 02, however the wedge shape is much better developed in this line. The internal reflectors dip uniformly to the south towards the basinal zone. An unconformity is present higher in the section which may be Pleistocene in age (Fig. 13).

Seismic line PSAT-12

Line 12 lies parallel with line 01 but doesn't extend as far south. The basement is not as evident in this region. The reflectors in Sequence 2 appear to bend down towards the south creating a slope-like feature similar to that seen on line 01. At the base of these bending strata is a chaotic looking package. The sea floor topography in line 12 is less varied than in line 01.

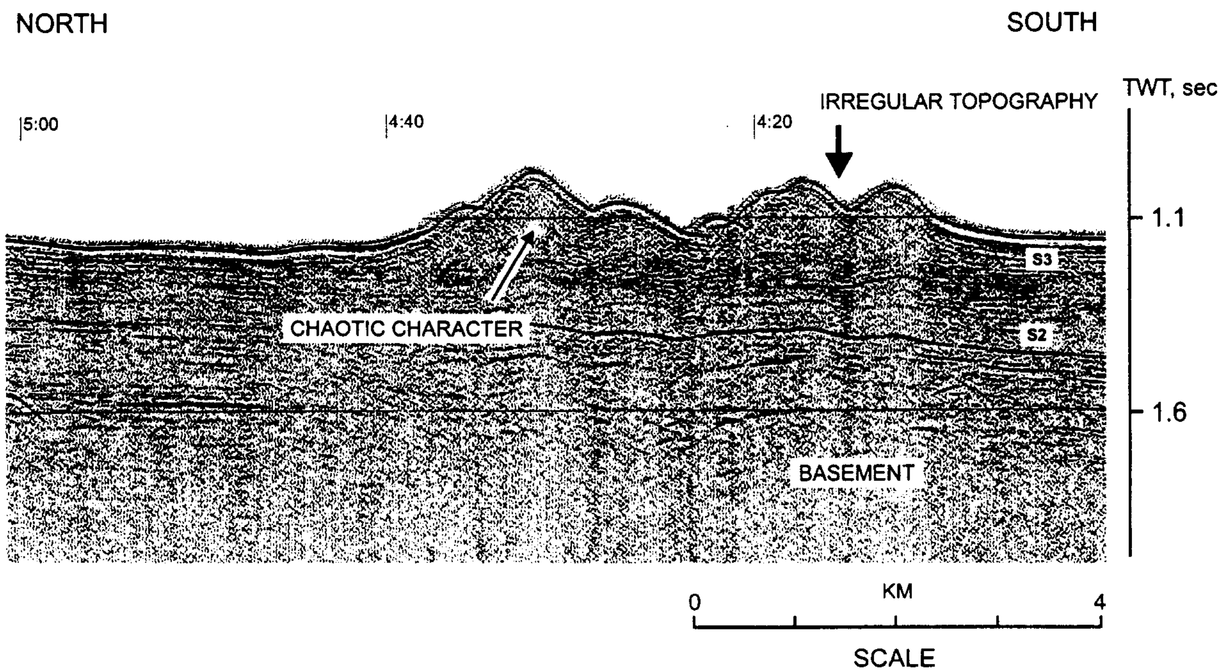

Fig. 10. PSAT-2 displaying an irregular mound on the seafloor. The internal character is chaotic in nature but does not mask underlying events

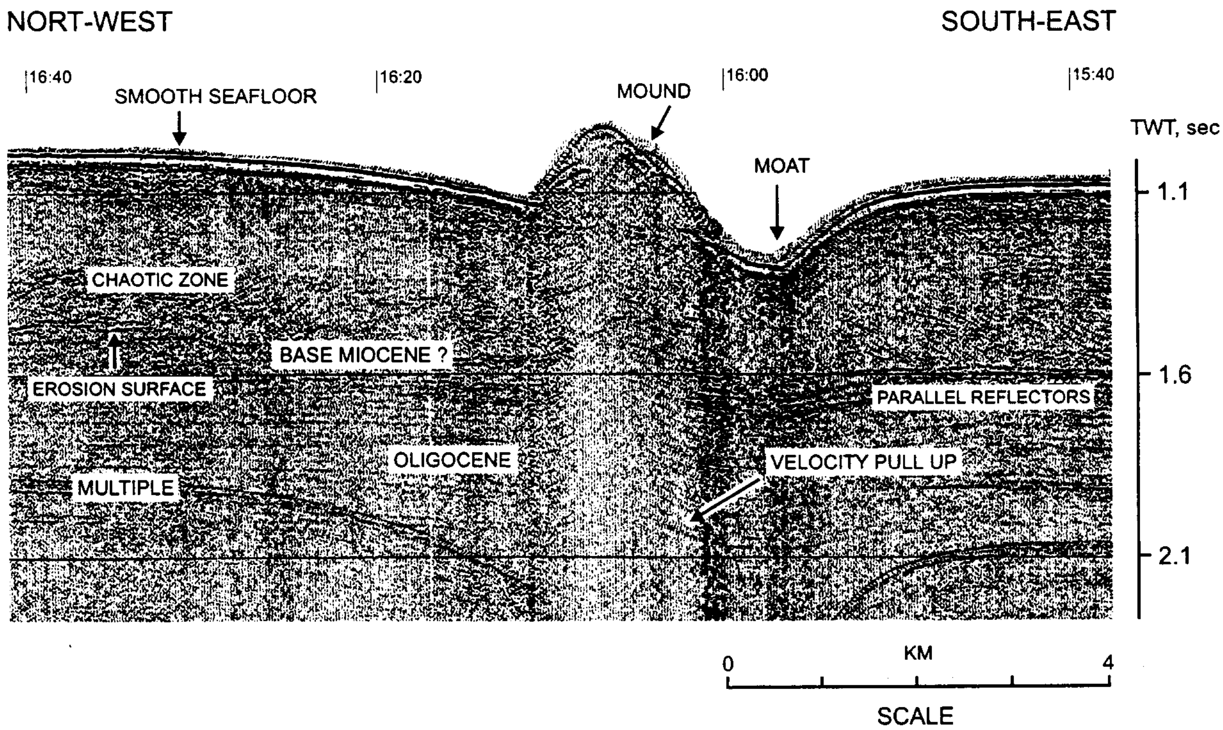

Fig. 11. PSAT-3. The mound in this diagram lies in the northern Seabight area. A distinctive chaotic internal character is evident and velocity pull up effect can be seen beneath the knoll, suggesting a high internal velocity. The mound is moated to the south, possibly due to current action. A package displaying a disturbed character and erosive base can be seen lower in the section

Summary

Three main sequences are identified. The sediments appear to have been preferentially deposited in palaeolows in topography probably created by faulting. There is subsequent onlap and infill of these lows, eventually levelling the topography. During the Latest Oligocene and Early Miocene times, channelling developed which was sourced from the eastern margin and extended out into the basin, with the main channel activity in the southern region. A strong unconformity at the base of S3 is suggested to be related to a global sea level fall at that time. This strong unconformity may also be related to a tectonic inversion event which occurred in the Celtic Sea area at the end of the Oligocene (Rowell, 1995). Strong erosion occurred, possibly in the Pleistocene times related to the glaciation. Using data from coring analysis (see sedimentology section) it is suggested that many of the carbonate mound features were killed off during the glacial Pleistocene, probably by unfavourable water circulation. They were subsequently buried under a blanket of clay sediments, however the largest of the mounds survived and continue to develop to the present day.

The slope of the margin appears to have influenced the depositional style of the sequences with a much more irregular geometry seen in the southeastern part of the area where the slope is steepest. More uniform deposition occurred in the northern part where a much gentler slope exists.

Conclusions

- Three main sequences are identified in the area. The sequences are tentatively dated as Oligocene (S1), Upper Oligocene (S2) and Miocene to recent (S3).

- Sequence S1 is characterised by very low amplitude reflectors which display a large scale buried mounded topography in the southern lines. The corresponding sediments subsequently onlap and infill the palaeolows between these mounds. In the northern section S1 displays a more uniform flat-bedded nature.

- Sequence S2 includes moderate amplitude reflectors with a dominantly uniform flat bedded character but it locally aggrades against a large mound feature in the south. In the north the equivalent sequence is also quite uniform in nature. Channels are developed in the south.

- Sequence S3 is composed of moderate to high amplitude reflectors, which are heavily channelised in the south but much less so in the north. Large mound features are present on the seafloor or in the shallow subsurface, which are interpreted as carbonate (coral) build-ups. These are dominantly present in the north. There is no evidence for such features in the southeastern region where the environment may not be suitable for coral growth. Factors influencing this zonation may include increased sediment input in the south east due to the channelling, and water currents may also be unsuitable in this region. A strong erosional event is evident at the base of the equivalent sequence in the north, where a chaotic seismic character is also shown. This is tentatively interpreted as a slumped zone. It is interesting to note that many of the interpreted carbonate build-ups are located above this chaotic zone.

- The underlying basement appears to influence deposition, with the Gollum Channel system exploiting the region underlain by a basement low. Thinner sedimentary cover is accumulated on the basement highs while more of sediments accumulate in the lows.

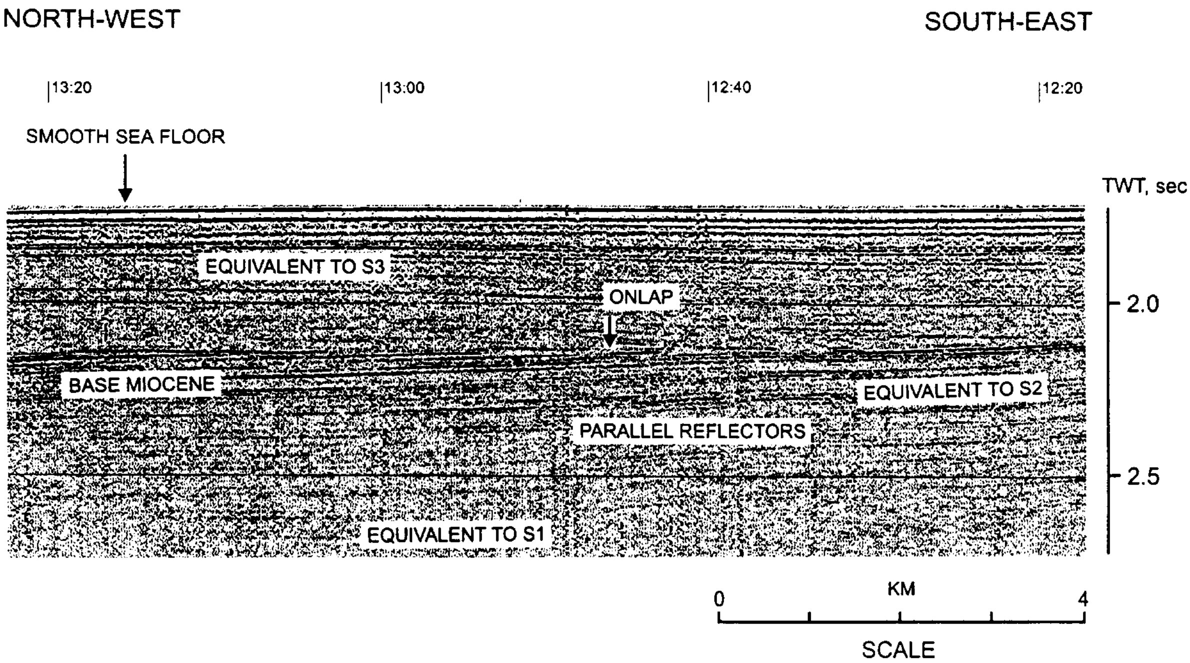

Fig. 12. PSAT-3 showing typical character of the succession in the northeast area. The reflectors are much more uniform and parallel bedded and there is no evidence for mounding or seafloor channeling

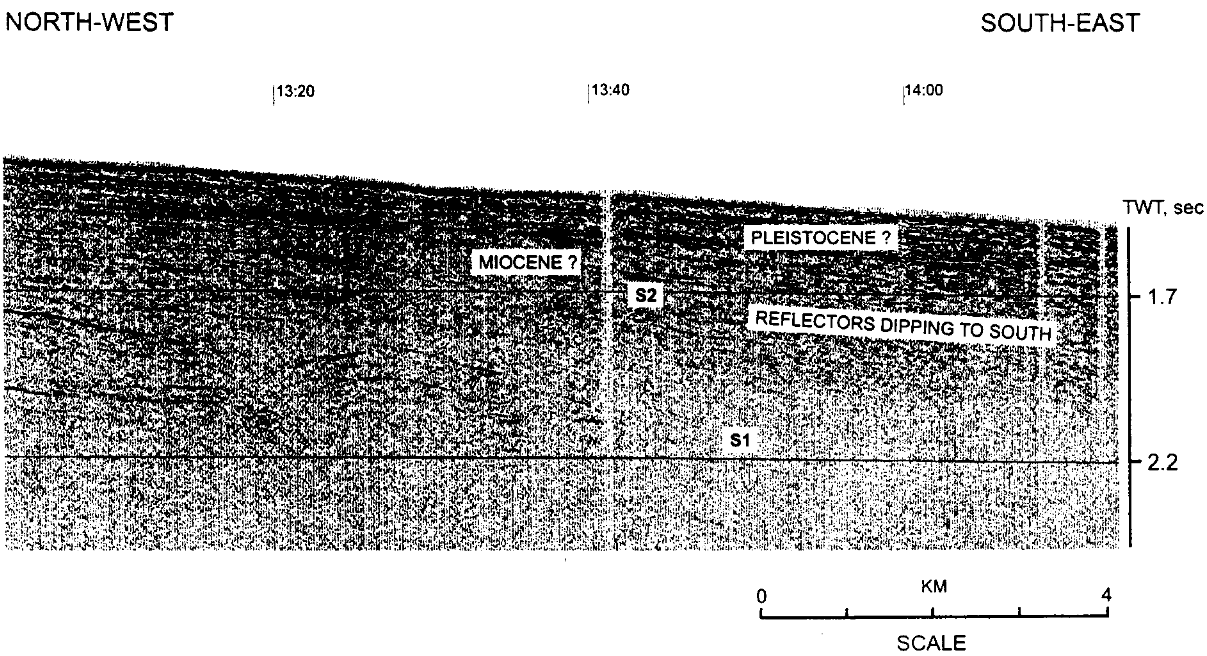

Fig. 13. Typical character of PSAT-11, with an unconformity present in the uppermost part of the section, possibly Pleistocene in age. The seafloor has a smooth topography

I.3. Long-range sidescan sonar data

N. Kenyon and A. Akhmetzhanov

Northern mound province on OKEAN and GLORIA sidescan sonars

A mosaic was made that gave complete cover with the 9.5 kHz OKEAN sidescan sonar of an area of about 4200 km^2. It covers the greater part of the area of upstanding mounds described by Hovland et al. (1994) and part of the area of buried mounds mapped from seismic on the R/V *Belgica* cruise. A mosaic of the same area with the 6 kHz GLORIA system was made in 1996 (McGrane et al., 1997). There is little backscatter variation on the OKEAN or GLORIA mosaics, apart from isolated features that are shown from profiles to be mounds. The two large closed deeps or "blind valleys", up to 150 m deep, that are shown in Fig. 3 of Hovland et al. (1994), were not readily identified on OKEAN although seen in part by GLORIA, which for some unknown reason was also able to image a small 40 m deep from the NW of the area mapped by Hovland et al. (1994), Fig. 3.

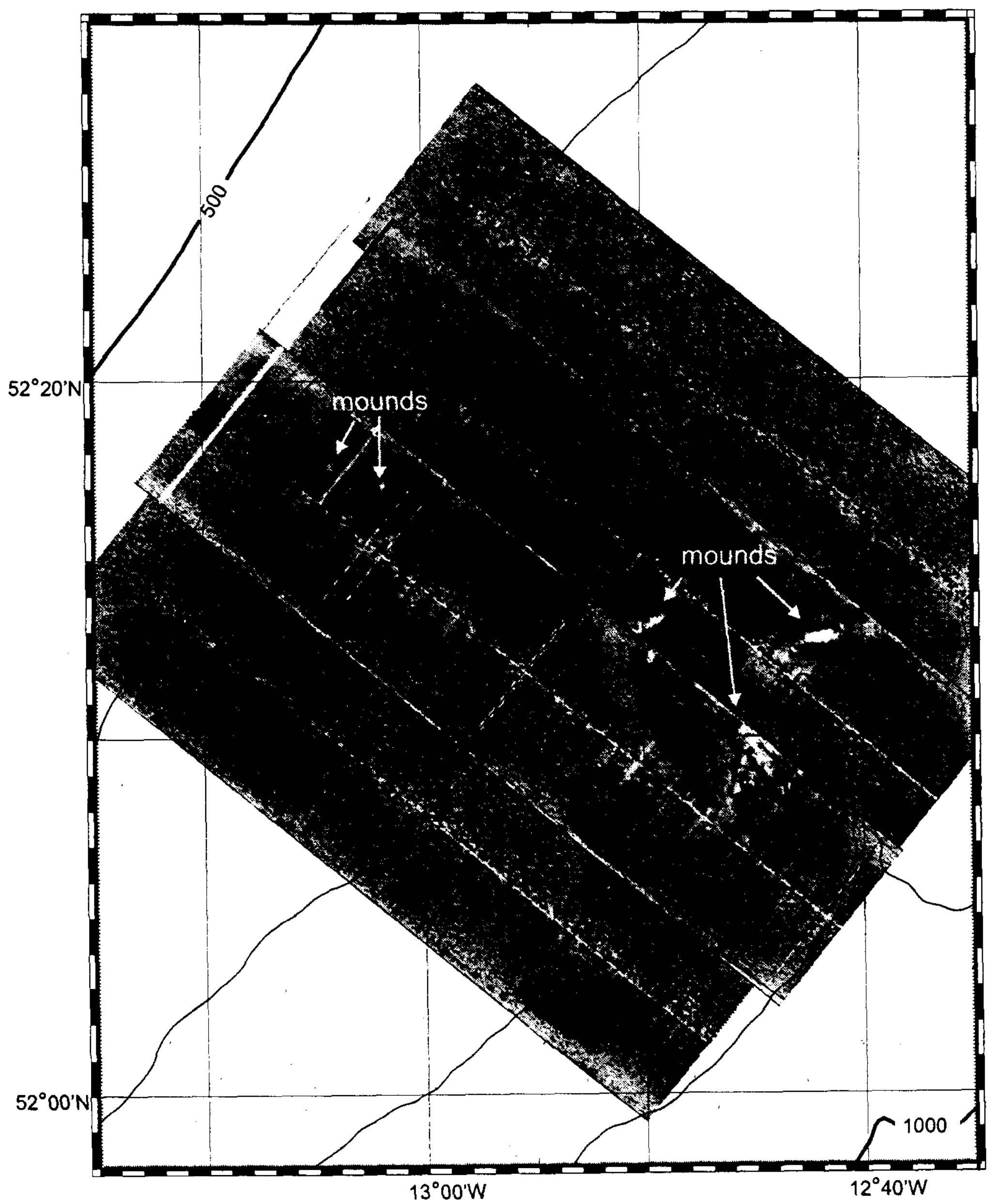

Fig. 14. Fragment of OKEAN mosaic showing carbonate mounds in the northern Porcupine Seabight

Approximately 12 mounds are mapped by OKEAN and a similar number by GLORIA (Fig. 14). Generally the mounds have medium to high backscatter compared with the low backscatter of the background. Normally they are visible on the OKEAN records mainly due to their relief expression and perhaps no lithological information can be derived from the image. Although rather scattered they are concentrated in two main locations. One of them is situated within an area of the closed deeps and they appear to be arranged along the NW-SE direction which is coaxial with the deep axis. The mapped mounds show great variation in shape as they do on the three OREtech profiles. Some are subcircular and others are elongate or compound, having both elongate and circular elements (as seen on complex mound 3 on OREtech line 3). The few isolated elongate mounds are oriented west-east. Their size is normally about 1 km in diameter. In some cases the longer axis of elongated ones reaches up to 2 km. The largest of the mounds seen on the OKEAN mosaic has a particularly complex shape which probably resulted from conjunction of several elongated build-ups (Fig. 15).

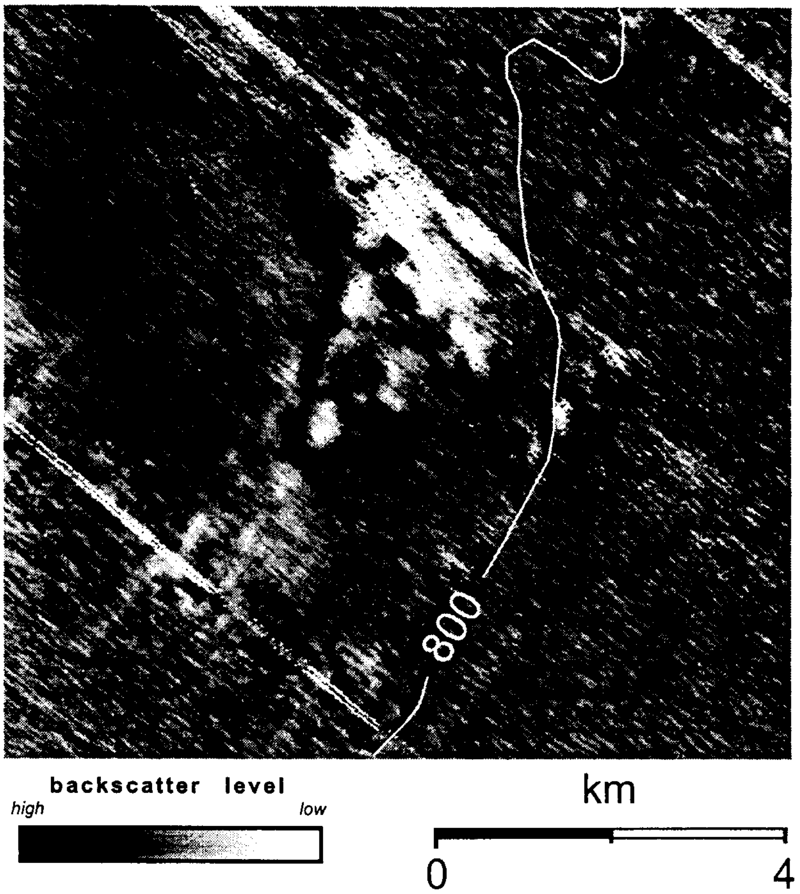

Fig. 15. Blow-up of the OKEAN mosaic: complex carbonate mound

There are a few other mounds located 5-6 km north-west of closed deeps location. These mounds all seem to be subcircular and of about 200-300 m in diameter (the seismic profiles from the R/V *Belgica* cruise showed these mounds to be of similar size to the upstanding mounds but to be largely or entirely buried).

A comparison was made with the distribution of mounds mapped by different techniques and equipment. The area chosen is that mapped from seismic lines by Hovland et al. (1994), Fig. 3. This was compared with maps made by 30 kHz OREtech sidescan, by 9.5 kHz OKEAN sidescan and by 6.5 kHz GLORIA sidescan. The latter data are from the R/V *Siren* cruise of 1996. Predictably the sidescan sonars produce the best plan view maps with the best data usually coming from the OREtech with its higher resolution sidescan. However both GLORIA and OKEAN were able to map a large complex mound which is shown on Fig. 3 of Hovland et al. (1994) as several closely spaced isometric mounds. It is located at 52°08.2'N 12°44.5'W (Fig. 15). Other than that there are no new mounds from this area.

The lower frequency sidescan systems are able to penetrate into the uppermost sediments by up to a few tens of metres in the most favourable materials, uniform fine grained, soupy mud. However no shallow buried mounds were detected by this method.

OKEAN and GLORIA on the eastern Porcupine margin

The eastern slope of the Porcupine Seabight has been surveyed by both the 9.5 kHz OKEAN (this cruise) and by the 6.5 kHz GLORIA sidescan sonars. The GLORIA cruises were RRS *Discovery* 87 and 123. They have been briefly reported on in Kenyon et al. (1978) and Kenyon (1987) although some useful data from these cruises remains undescribed.

Gollum Channels

OKEAN line PSAT-01 crossed the upper part of the Gollum Channel system but showed no new information that had not been seen on the GLORIA survey of the entire system. OKEAN imagery displays a pattern of linear, west-east directed features with higher level of acoustic backscatter. The pattern corresponds to the narrow tributary channels with widths of up to 1 km and coalescing down slope, which are confirmed to be relatively straight and, from the seismic profile, to be steep sided and fairly flat floored. Backscatter variations defining channels are likely to be caused by accumulation of coarse material and by stronger acoustic return from channel walls. The best seen channels were observed between time marks 18:30 and 19:00, where according to the available bathymetry several tributaries come to a junction point. Bathymetry shows that erosion is not as pronounced at these places as at others. This could suggest a quite recent origin for the observed tributaries although the backscatter pattern shows that they have been the most active conduits of coarse material in recent times. The channels increase in size to the north. Further description of the Gollum Channels can be found elsewhere in this report.

Gollum Channels to northern mound province

OKEAN lines PSAT-02 and PSAT-11 together with their northern extensions, PSAT-03 and PSAT-10, give coverage of most of the mid slope. This part of the slope west of Ireland has complex physiography and sedimentation processes. Very little work has been published about it apart from some seismic analysis and some benthic biology (e.g. Rice et al., 1991). The long-range sidescan data have been analysed in terms of acoustic facies and the facies then attributed to geological features and/or processes. Acoustic facies/features recognised are:

1. Step-like features
2. Linear deeps (blind valleys)
3. Mounds
4. Possible sand bodies

Step-like features

These are seen on line PSAT-01 between time marks 21:30 and 1:00, running almost along slope. The are likely to be positive, step-like features expressed on the sonograph as sinuous bands of high backscatter suggesting the presence of steps on the seafloor with height of several tens of meters. At some places (22:10) they are disturbed by downslope running channels. The origin of these features is not clear. They could be terraces worked out by bottom currents and in some places they seem to be arranged into an en echelon pattern suggesting the presence of several generations. According to another interpretation strong acoustic return might be caused by the headwall of slump bodies propagating downslope. The first interpretation seems to be more plausible since further north these terraces could be correlated with linear deeps which are probably of an erosive nature.

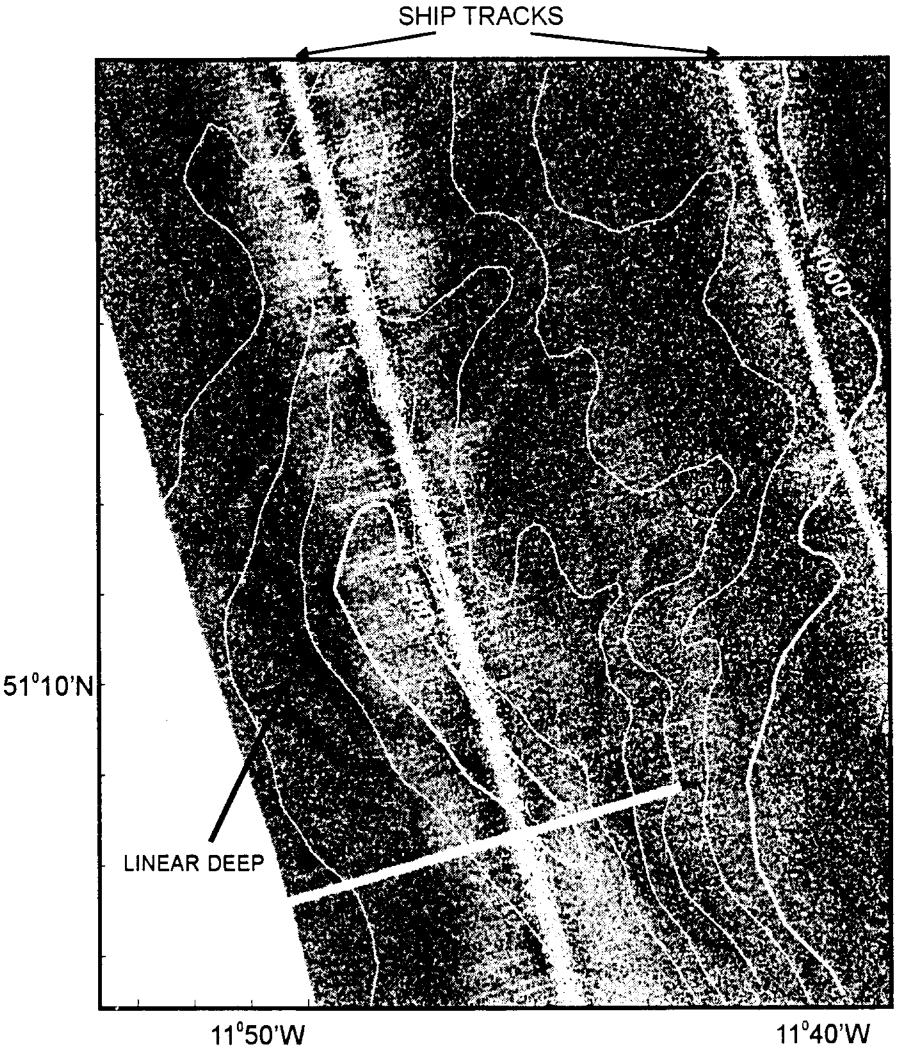

Fig. 16. Fragment of OKEAN mosaic displaying one of the linear deeps. Bathymetry from GEBCO'97

Linear deeps

Two separate systems of closed linear deeps are recognised. Both run very obliquely down slope and along slope. They are mapped from the GLORIA data and one is remapped from the OKEAN (PSAT-12). The depth below their surroundings is up to 200 metres and it has been shown by the bathymetric map (Hunter and Kenyon, 1984) that they are closed, and that they do not run down slope like channels that are maintained by turbidity currents. The deeps have faintly seen straight, parallel margins and weakly backscattering floors and sides. The main trends are NNE-SSW and NW-SE. They are believed to form a class with the linear deeps reported from further north in Fig. 3 of Hovland et al. (1994). Their origin is not known though it is suggested here that they are oriented along fault lines. They may be kept open by currents (along slope or down slope) or by seepage, or both. If seepage is responsible then their formation is probably similar to that proposed for pockmarks (Hovland and Judd, 1988).

There are also some down slope, NE-SW trending, linear channels. They have shallow profiles. The best seen are crossed at 09:50 and 10:45 on PSAT-03 (Fig. 16). There are some small strongly backscattering spots associated with the channels.

Mounds

These were first reported from the 1997 *Belgica* cruise although there is an unreported mound that was crossed by RRS *Discovery* cruise 123 at 50°34.2N 12°2.8W. This is a moated and subcircular mound that is less than 100m high and thus does not appear on the bathymetry map, which has a 100m contour interval. It is at the edge of a "blind valley" in 1200m of water, which is deeper than reported carbonate mounds.

Approximately nineteen relatively highly backscattering linear or subcircular features are seen on the OKEAN lines (Fig. 17). Most are on line PSAT-02 and have been confirmed by OREtech lines. Most are linear and trend NE-SW but one trends NW-SE. The seismic profiles confirm that they are acoustically transparent ridges upstanding above the layered slope sediments. The greatest length is 1.5 km. They are presumed to be carbonate mounds similar to those in Hovland et al. (1994) and may be oriented predominately along reactivated Hercynian fault trends. The backscatter level variations are mainly caused by topography of the mounds with higher acoustic return from slopes facing the tow-fish whereas the opposite slopes are normally shadowed.

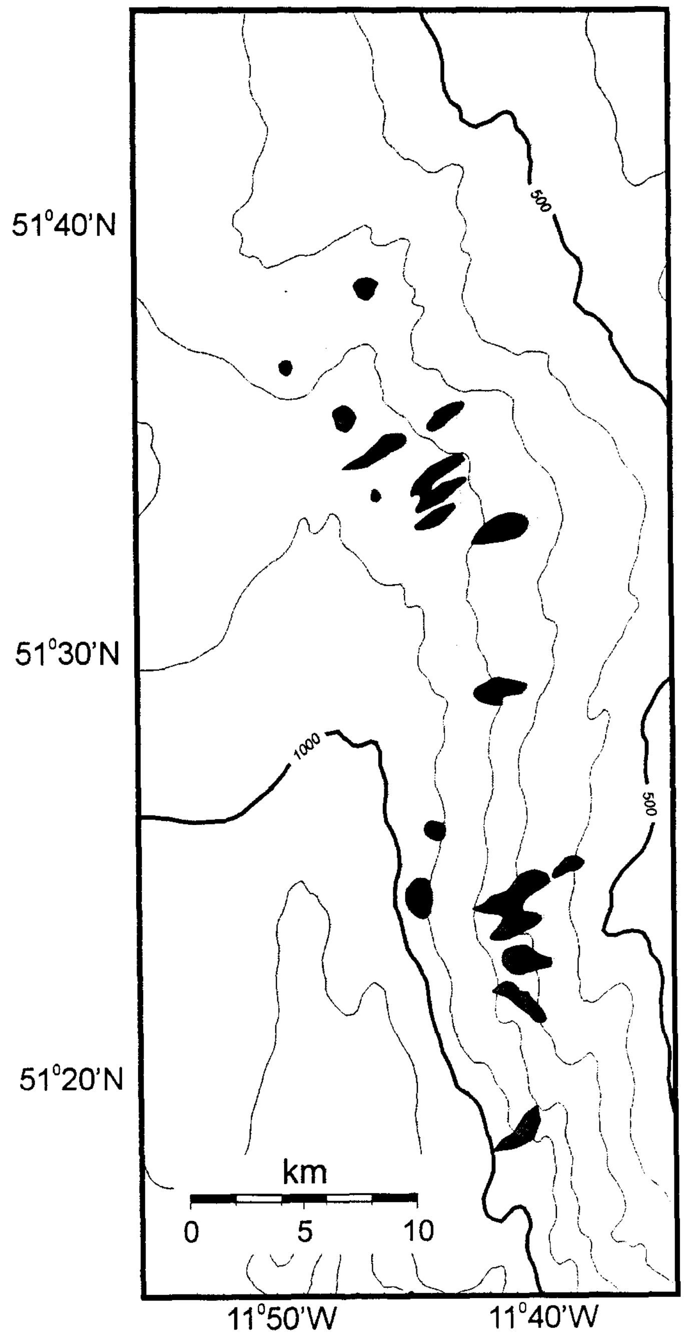

Fig. 17. Sketch map of carbonate mound distribution in the eastern Porcupine Seabight based on the OKEAN mosaic

Possible sand bodies

Rather irregularly shaped and sized patches of weak backscatter are interpreted as sands moving across the slope from data seen on the 3 OREtech profiles. The extensive low backscattering area is at the northern end of PSAT-02 and PSAT-11 with a possible extension onto PSAT-03 as far as perhaps 11:00 hrs. It associated with a band of strong acoustic backscatter seen on the line PSAT-11 between timemarks 10:30 and 11:30 (Fig. 18). According to bathymetry this strongly reflective area coincides with an elongated elevation expressed in the seafloor relief. That is likely to mark an area of recent erosion or non-deposition due to the presence of bottom current which may lead to accumulation of coarse sandy or gravelly material. Thus, the low backscattering area could be an extensive contourite sand sheet being accumulated or transported at appropriate hydrodynamic conditions. However to justify it ground-truthing is needed.

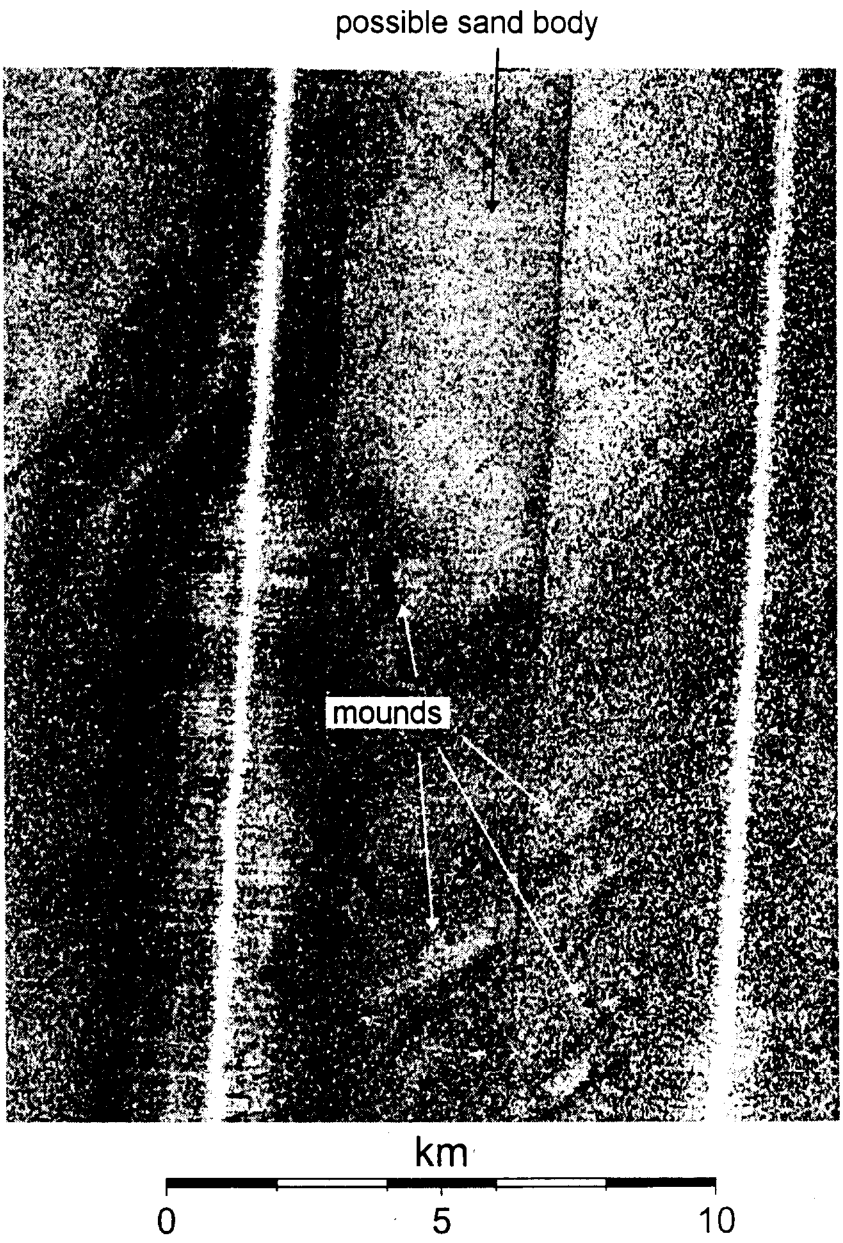

Fig. 18. Fragment of OKEAN mosaic from eastern Porcupine Seabight. Low backscattering area at the northernmost part is interpreted as an extensive contourite sand sheet. Several elongated mounds are also seen

I.4. OREtech sidescan sonar data

THE NORTHERN PORCUPINE SEABIGHT

A. Wheeler, C. Degryse, A. Limonov, and N. Kenyon

3 OREtech deep-tow 30 kHz sidescan sonar and 6.5 kHz profiler (Fig. 19) provide detailed imaging of mound structures, most of which were also cored. This provided both detailed mapping and additional data relating to mound shape, topography and acoustic properties largely dependent on surface roughness and sediment type. The integration of OREtech data and the coring information allows the interpretation to be made regarding the structure and evolution of the mounds. Profile lines show the surface topography immediately underneath the deep-tow fish and limited subsurface reflective properties.

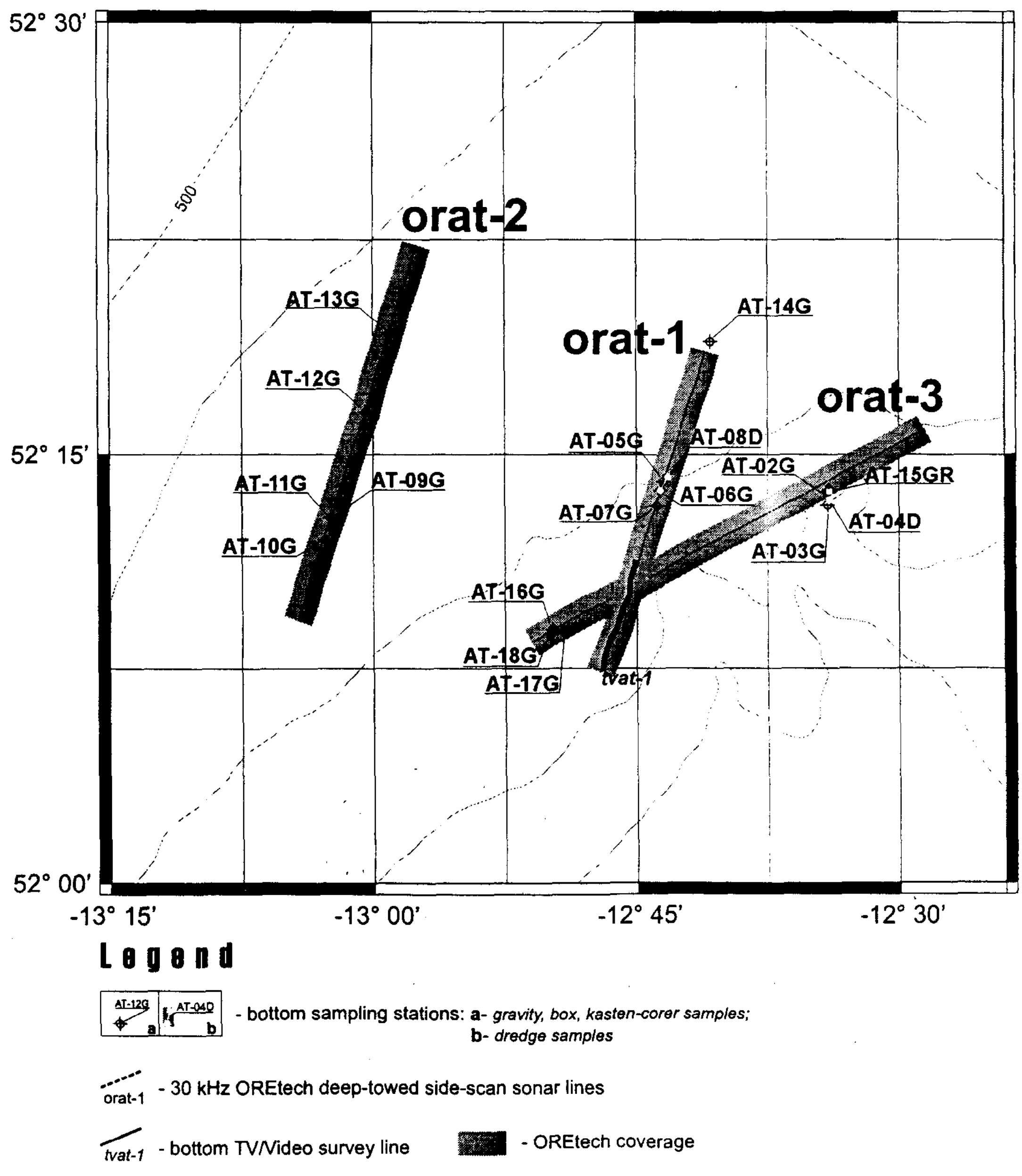

Fig. 19. Location of OREtech lines and bottom sampling stations in the northern Porcupine Seabight

General description of OREtech lines

A general description of the OREtech lines is given below. As the most important features on the lines are the mounds they have been described separately after the general descriptions. Table 1 summarises some technical information on OREtech lines run in this area. Seabed profiles with well-expressed mounds are shown in Fig. 20.

Line	Date	Time, GMT		Northern end		Southern end		Water Depth, *m*			Length, *km*
		Start	End	Latitude	Longitude	Latitude	Longitude	Northern end	Southern end	Maximum variation	
ORAT1	11.07.97	15.01	21.50	52°18.52N	12°40.96W	52°07.60N	12°46.79W	700	931	264	22.4
ORAT2	12-03.97	22.43	06.32	52°09.06N	13°04.34W	52°23.52N	12°56.86W	623	723	100	28.4
ORAT3	14.07.97	02.01	09.06	52°08.27N	12°51.17W	52°15.79N	12°28.47W	784	808	100	29.4

Table 1. Specification of OREtech lines in the northern Porcupine Seabight

ORAT-1

The start of the sidescan sonar image reveals a uniform intermediate backscatter intensity believed to be a pelagic facies or fine contourite facies. The profiler record shows that this facies has a slight dip (10 m per 1 km) before Large Mound 2 (see description in separate section below) is encountered. South of this mound, uniform facies is again encountered, gently dipping by about 50 m over a distance of about 6 km. A zone of high backscatter is encountered on the eastern side of the sonograph at 18:40. The zone covers an area of approximately 750x500 m and is revealed as another mound in OKEAN line PSAT-5. The uniform facies is interrupted by Large Mound 4 (see below), about 6 km south of Large Mound 2. The southern end of the image displays a return to the uniform facies for 3 km distance. The subbottom profile shows layered undisturbed sediments.

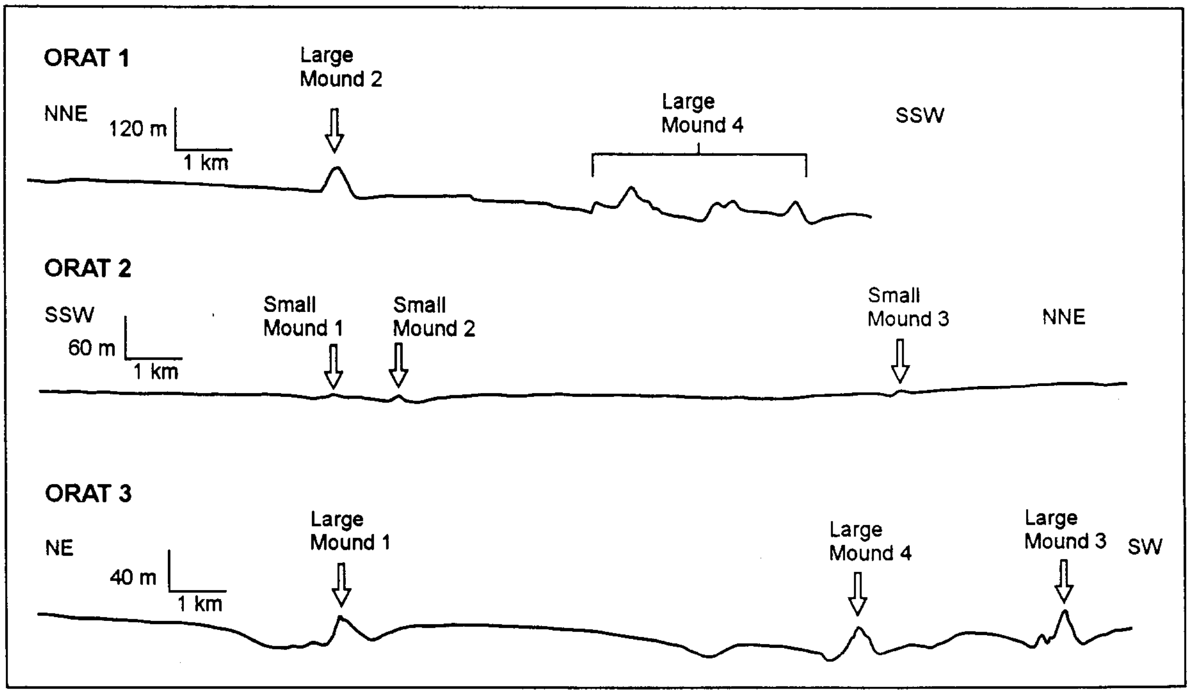

Fig. 20. Seabottom topography along OREtech lines in the northern Porcupine Seabight

ORAT-2

The backscatter pattern is rather uniform along the line. The intermediately backscattering seafloor, covered by stratified sediments, in some places has south-north oriented bands of slightly enhanced or reduced backscatter intensity which do not affect the subbottom layering. This pattern is only interrupted by three small mounds surrounded by moats (see below). Away from the mounds, the penetration on the profiler varies between 10 and 30 m.

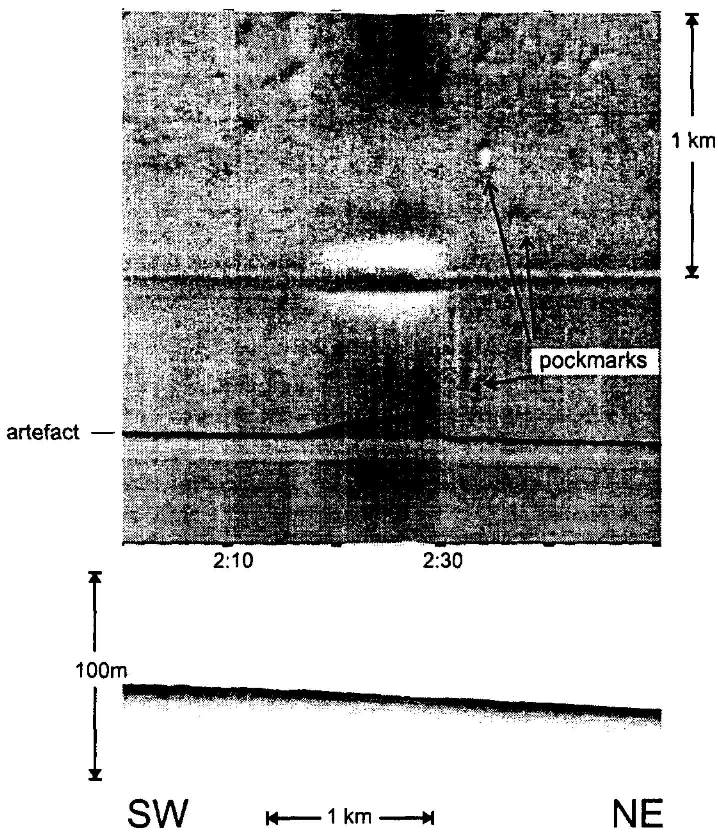

Fig. 21. Possible pockmarks identified on the ORAT-3 line

ORAT-3

This profile crosses ORAT-1 at the location of Large Mound 4. In the NE end of the line, the sonograph has uniform facies of intermediate backscatter with numerous circular depressions of stronger backscatter (Fig. 21). These features are from a few tens of metres to 100 m across and are randomly distributed in this area. They are interpreted as pockmarks suggesting gas seepage in this area of the seafloor, although no acoustic anomalies are observed on the profiler record. The pelagic facies with pockmarks is followed by a uniform facies of intermediate backscatter till 03:40, where Large Mound 1 (see below) is encountered. The profile shows that the seabed drops by 80 m with an increasing gradient towards the moated mound. The rest of the line has intermediate backscatter intensity with slight variations.

The profile shows that between the three mounds the seabed is broadly domed, with the exception of a steep depression at 06:20, which is poorly visible on the sonograph but marks the head of a large deep linear depression on the bathymetry map.

On this OREtech line, the seabed mounds are obviously situated within linear topographic lows which probably guide bottom currents.

Description of mounds

Three types of mounds are identified on the OREtech lines: large multiple ridge-shaped mounds, a large conical mound, and small conical mounds.

Large Mound 1

This is a sinuous ridge mound covering an area of about 2 km^2 (Fig. 22). The length of the ridge is ca. 2.2 km and the width is ca. 1 km. The ridge is sinuous trending NE-SW. The ridge reaches a height of ca. 70 m along the profile line which does not go over the crest of the ridge. This is probably only half of the maximum height of the mound. The mound generates a high backscatter intensity probably caused by surface roughness, and this interpretation is supported by the presence of small shadows on the crest of the ridge. High backscatter intensity is also observed at the base of the mound. The mound is surrounded by a moat structure which is also shown in a seismic line in Hovland et al. (1994). The sidescan image also generates a high backscatter intensity for the moat although the intensity is less than for the mound itself. The high backscatter intensity is possibly due to coarse coral particles and dropstones.

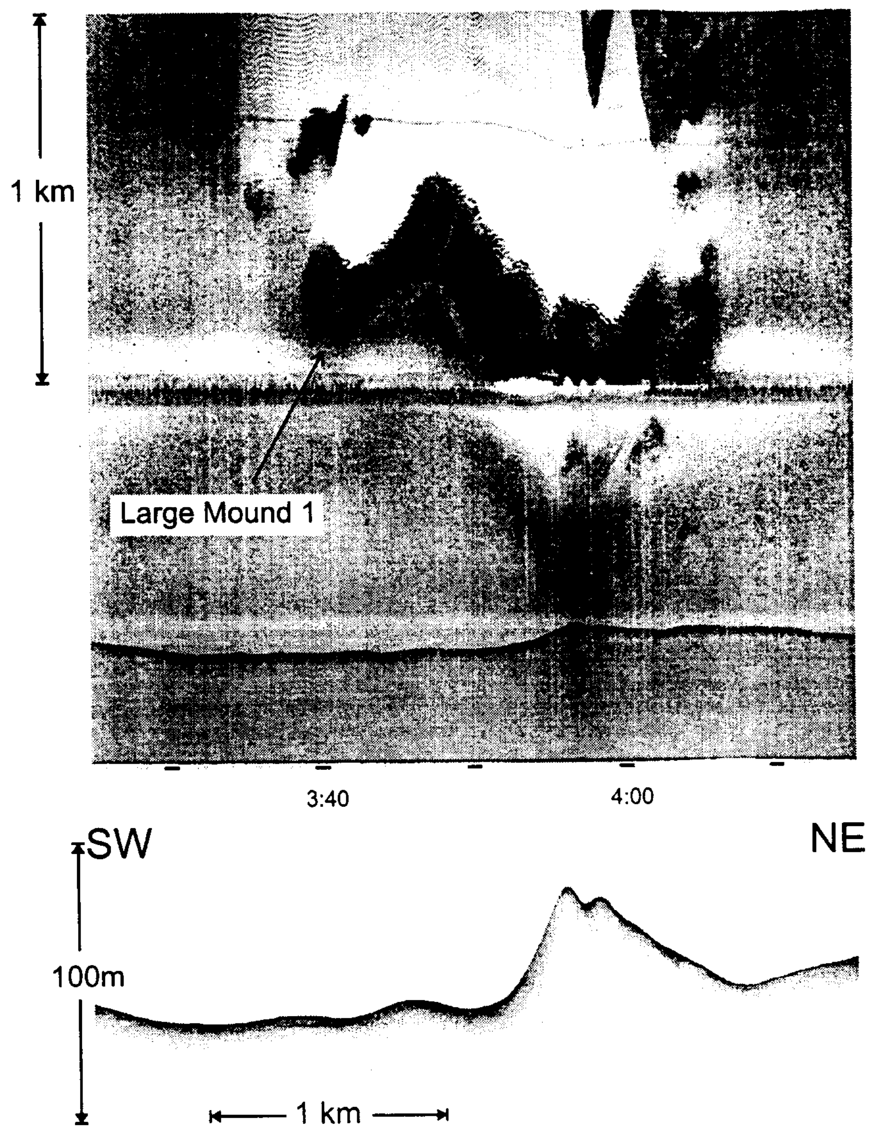

Fig. 22. OREtech imagery and 6 kHz profiler record across Large Mound 1

Large Mound 2

This mound is conical in cross-section and has a diameter of ca. 2 km (Fig. 23). The OREtech line passes directly over its top, allowing us to accurately calculate the height of the feature (150 m). The mound shows high backscatter at the crest, although there seems to be an interference effect near the summit due to the proximity of the feature and the deep-tow fish. The very oblique grazing angle results in large acoustic shadows covering most of the mound slopes. Nevertheless, it is possible to infer that the backscatter intensity on the sides of the mound is also high, becoming higher at the foot of the mound, in the moat. The moat is more pronounced down the regional slope to the south-southwest. The depth of the moat is about 15 m.

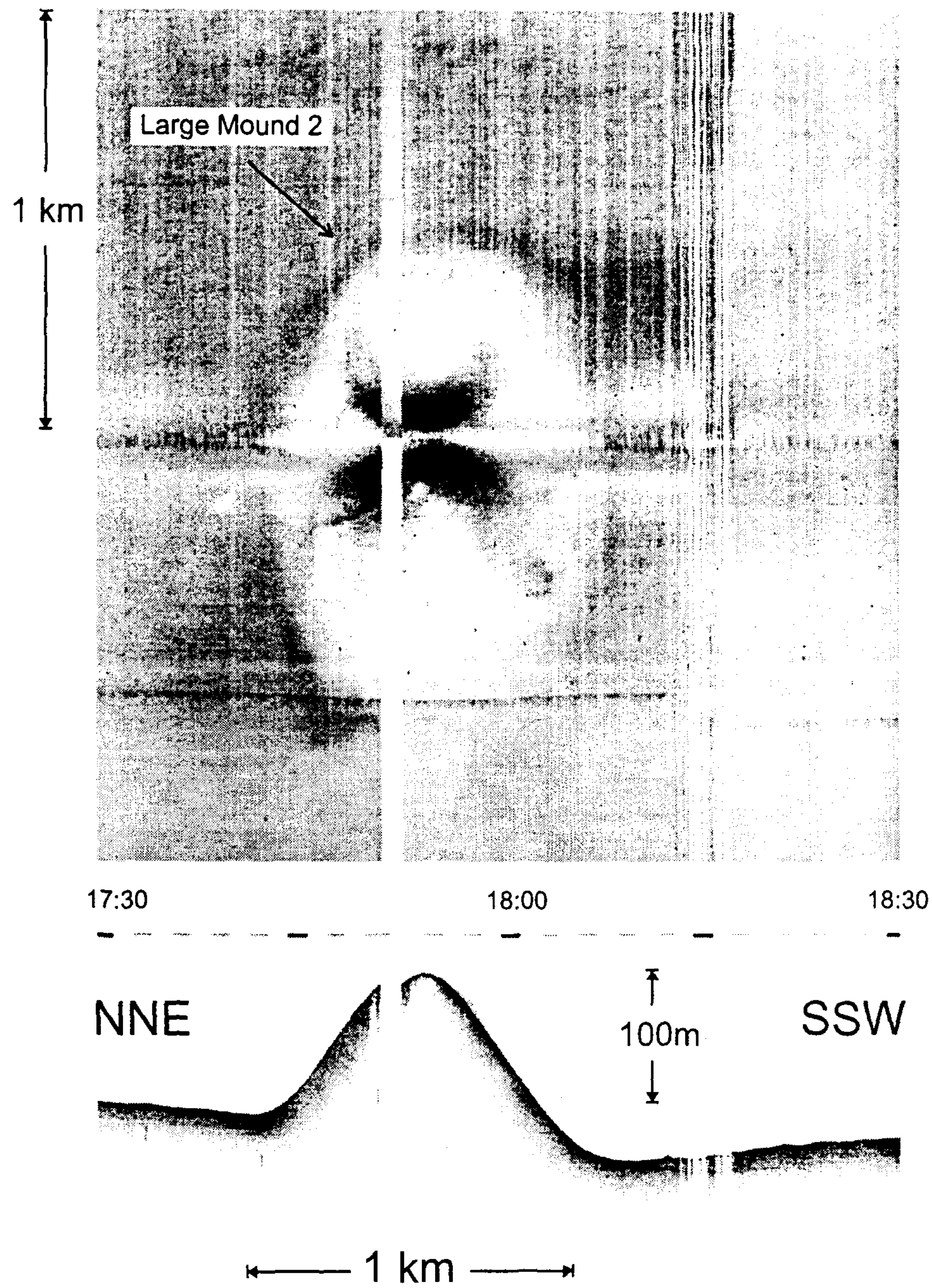

Fig. 23. OREtech imagery and 6 kHz profiler record across Large Mound 2

Large Mound 3

The sidescan sonar image of Large Mound 3 (Fig. 24) reveals a multiple ridged structure orientated NW-SE. The extent of the composite mound calculated from plan view is ca. 1.5 km^2. The length of the longest ridge is about 1.7 km and the maximum width is 1 km. The height of the largest mound defined from the profile directly under the deep-tow fish is ca. 80 m. However, this may not represent the maximum height that the mound reaches. The mound is composed of a minimum of three subparallel ridge structures that trend NW-SE. The most southwestermost ridge increases in elevation resulting in a shadow near its northern end. This northeasternmost ridge is the largest and is of a more irregular shape. The backscatter intensity is highest on the crest of the mound and at the base of the mound. The small shadows generated along the crest of the ridges may be due to individual cold water coral colonies. The mound is surrounded by a moat feature which also possesses an enhanced backscatter intensity.

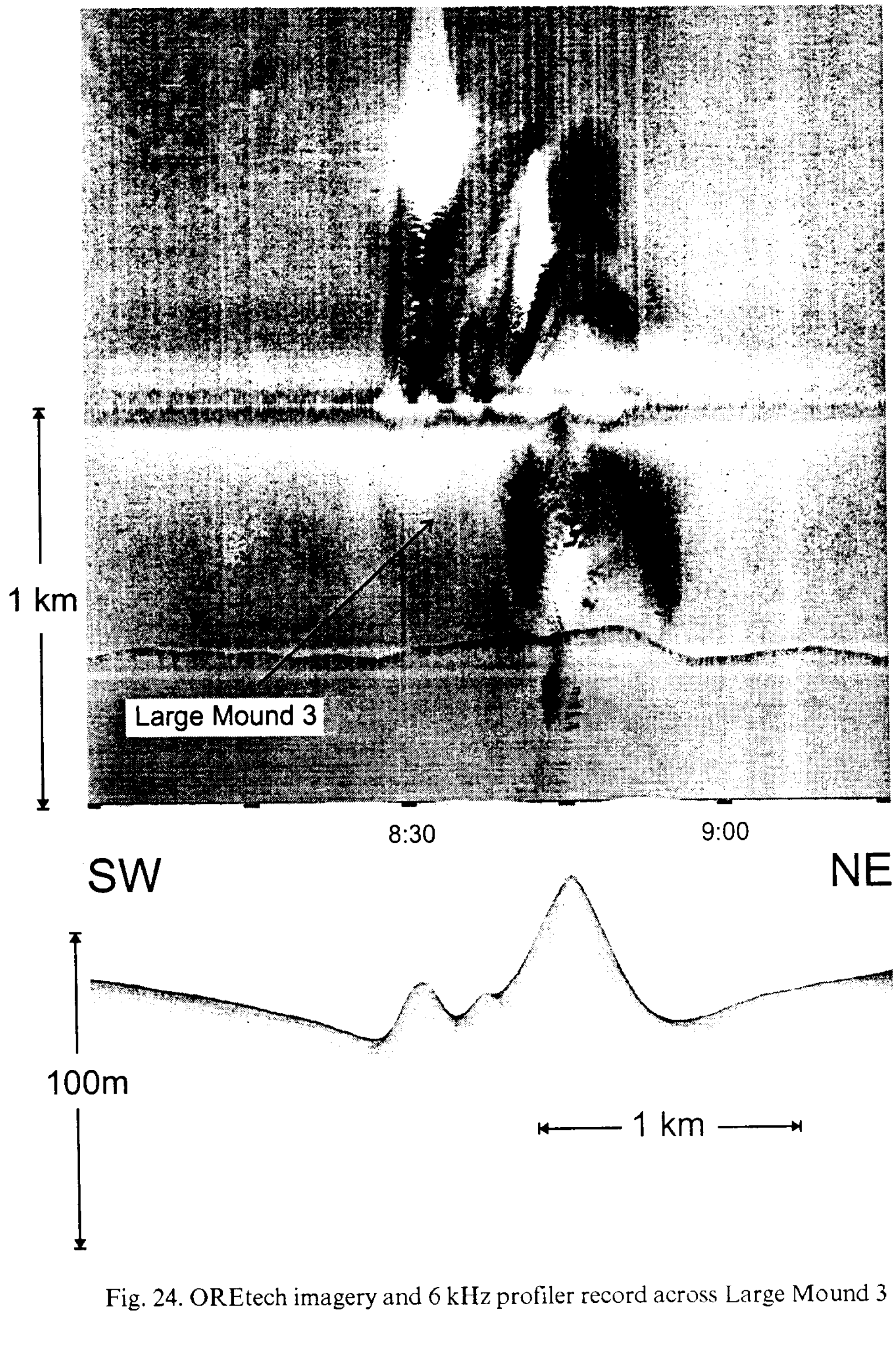

Fig. 24. OREtech imagery and 6 kHz profiler record across Large Mound 3

Large Mound 4

This is the largest of the mounds that was imaged (Figs. 25, 26), covering an area of ca. 5.5 km^2 and is a multiple sinuously ridged structure. The length of the longest ridge is about 4 km and the maximum width is about 1 km. It has a pattern resembling lobes and clefts. A minimum of twelve segments have been identified. The profile allows us to calculate the height of the structure as in excess of 120 m.

The sidescan sonar image shows high intensity backscatter on the ridge flanks. This is mostly a function of steepness of the ridge slope facing the tow-fish. Higher backscatter intensity is observed towards the base of the slope comparable with the other mounds. Moat-like features also exist at the base of the structure and are visible on the profile. These also have a slightly higher backscatter which is probably a function of grain-size.

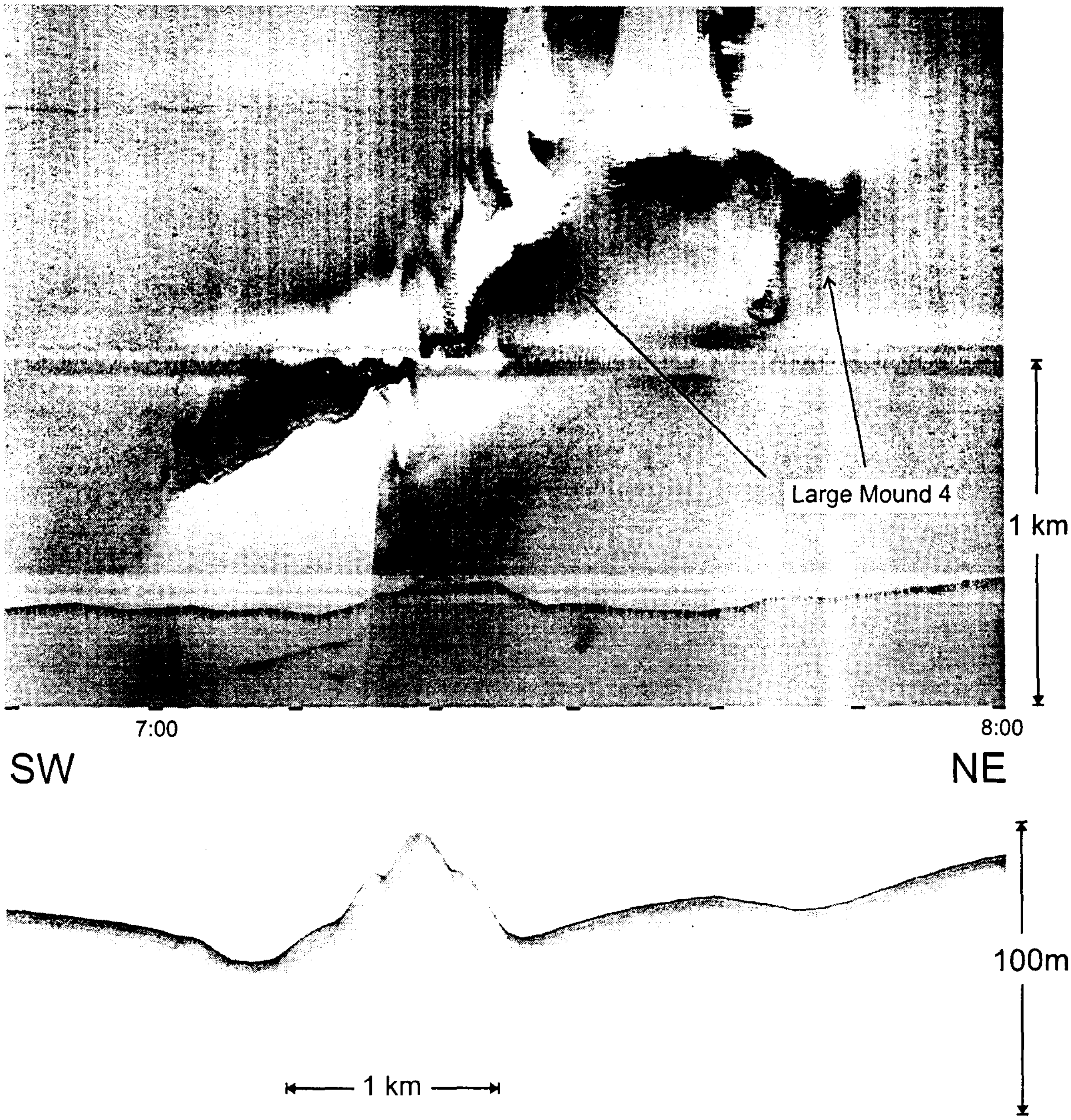

Fig. 25. OREtech imagery and 6 kHz profiler record across Large Mound 4

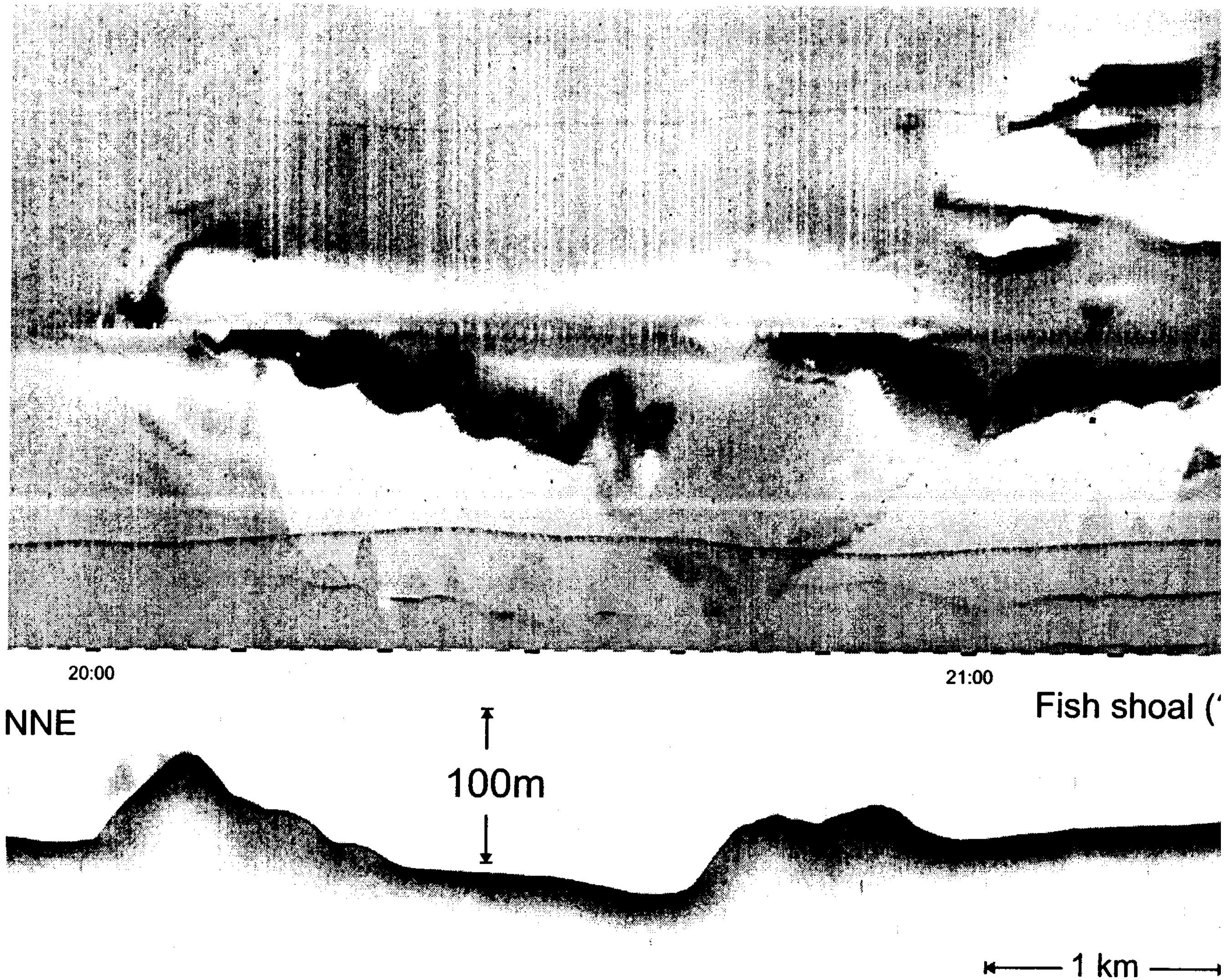

Fig. 26. Large Mound 4 on the ORAT-3 sonograph and 6 kHz profiler record

Small mounds

The small mounds are of a low relief, being less than 20 m high and have an approximate diameter of 200 m (Fig. 27). They are also surrounded by a topographic low interpreted as a moat feature. They are circular in plan view and generate a high backscatter image. This is best seen on Small Mound 1 where the imaging is near vertical and only a small shadow is produced. The top of Small Mound 2 also generates a high backscatter image and casts a small shadow. Small mound 3 is not illustrated in the report but shows the same characteristics.

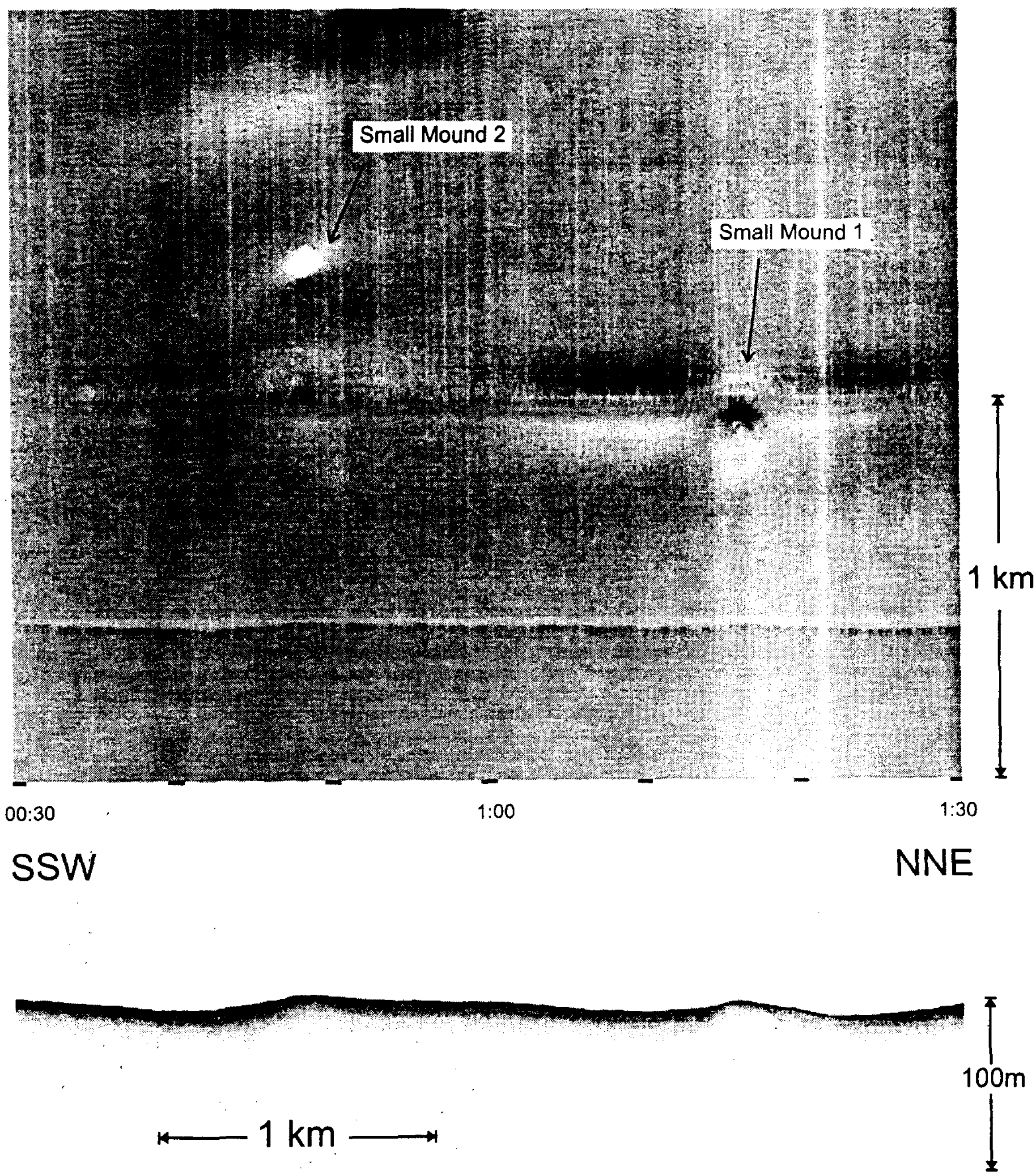

Fig. 27. Small Mounds 1 and 2 seen on ORAT-2 sonograph and subbottom profiler record

THE EASTERN PORCUPINE SEABIGHT

OREtech lines 5 and 8 and lines 4 and 9 respectively were run parallel to each other and about 2 km apart on the eastern Porcupine Seabight margin to allow mosaic construction (Fig. 28). The first two lines are in parallel with seismic line PSAT-2 and cross a group of carbonate mounds discovered during this cruise. Southerly lines ORAT-4 and 9 run from E to W over an area of the so called "Belgica reefs", discovered during the R/V *Belgica* cruise (1997) and supposed to be of a barrier type. The main peculiarities of the seafloor are described below from individual sonographs and profiles, and the general view is provided from the mosaic analysis.

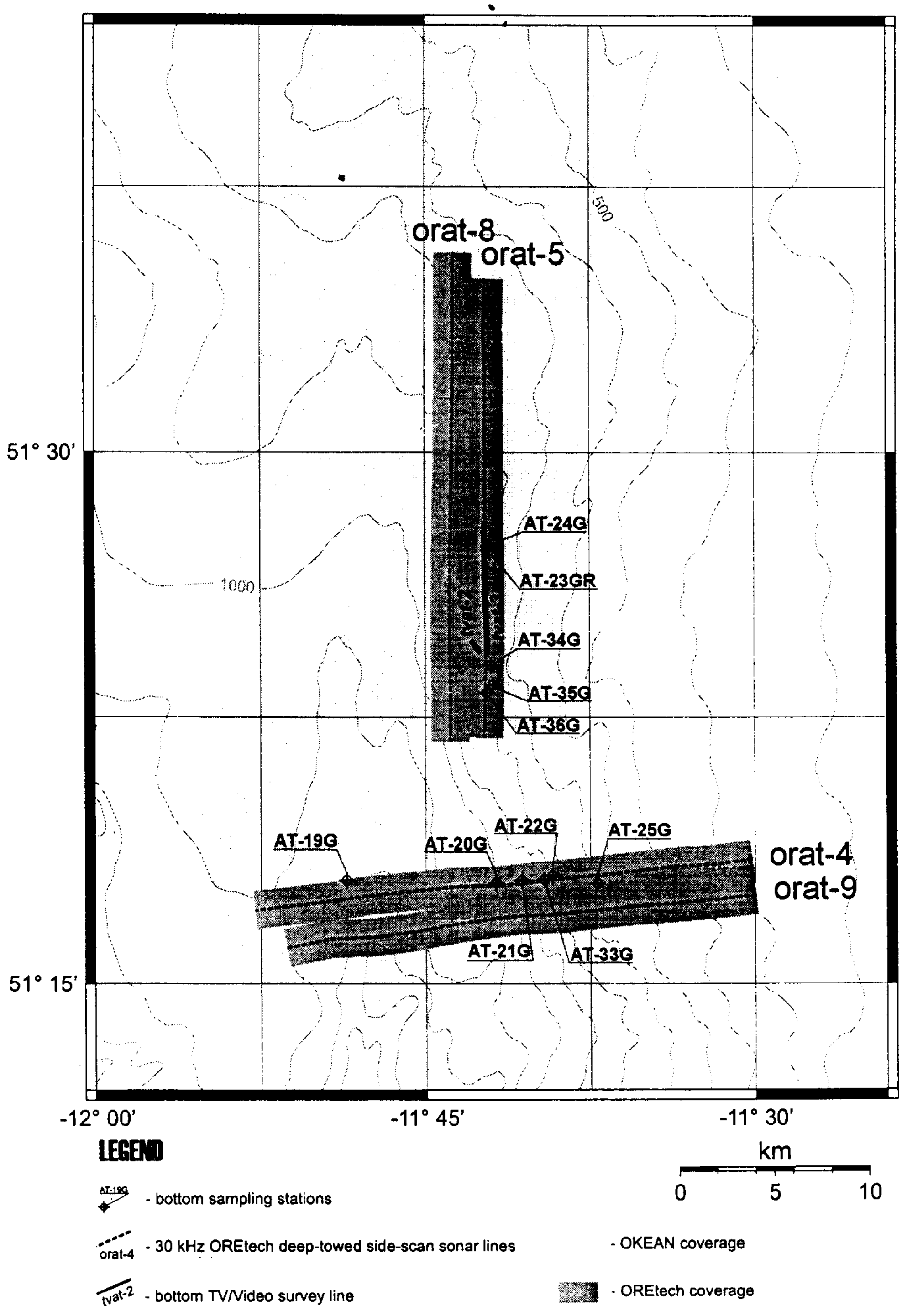

Fig. 28. Location of OREtech lines and bottom sampling stations, eastern Porcupine Seabight

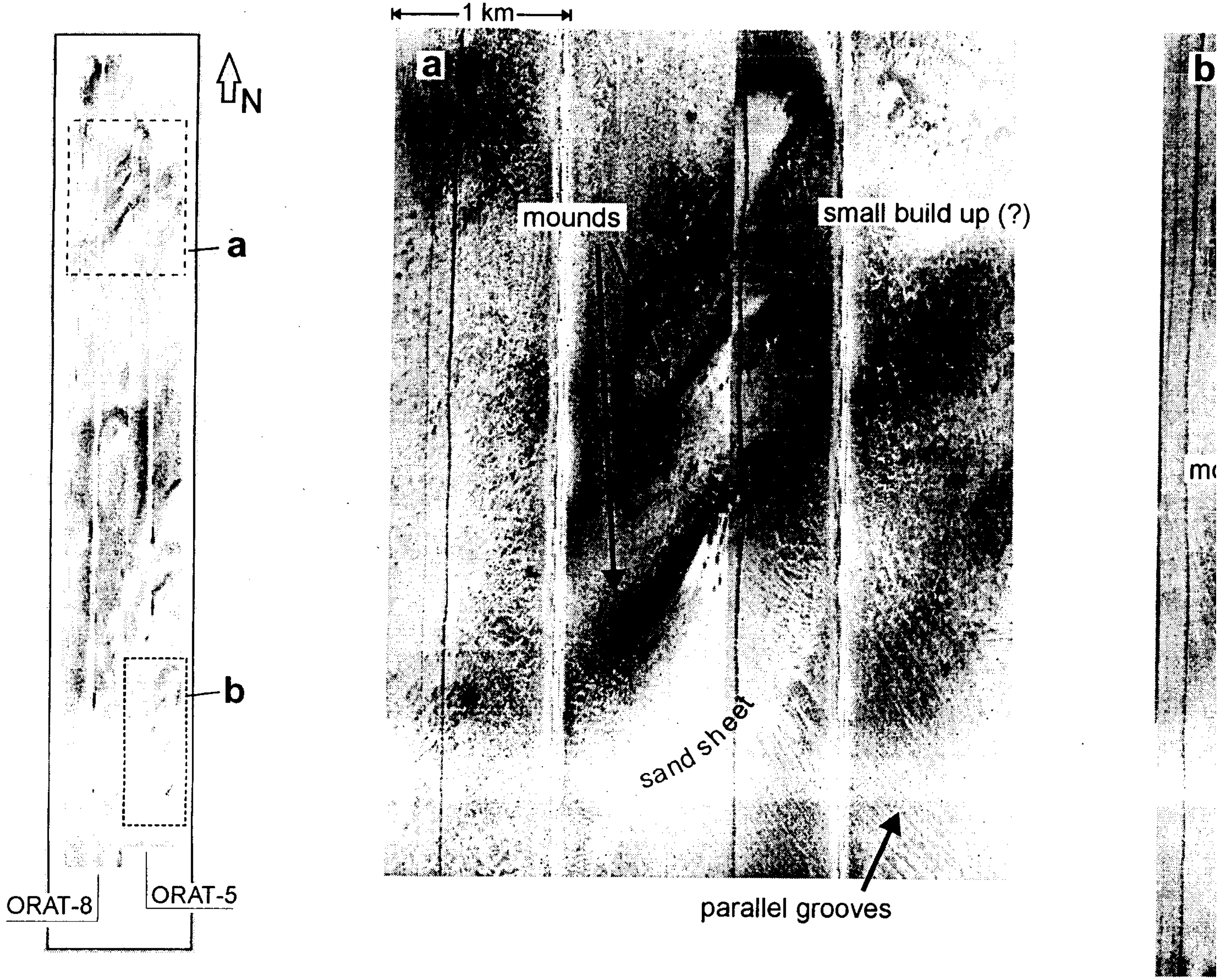

Fig. 29. Fragments of OREtech mosaic showing carbonate mounds and associated bottom features in the eastern Porc

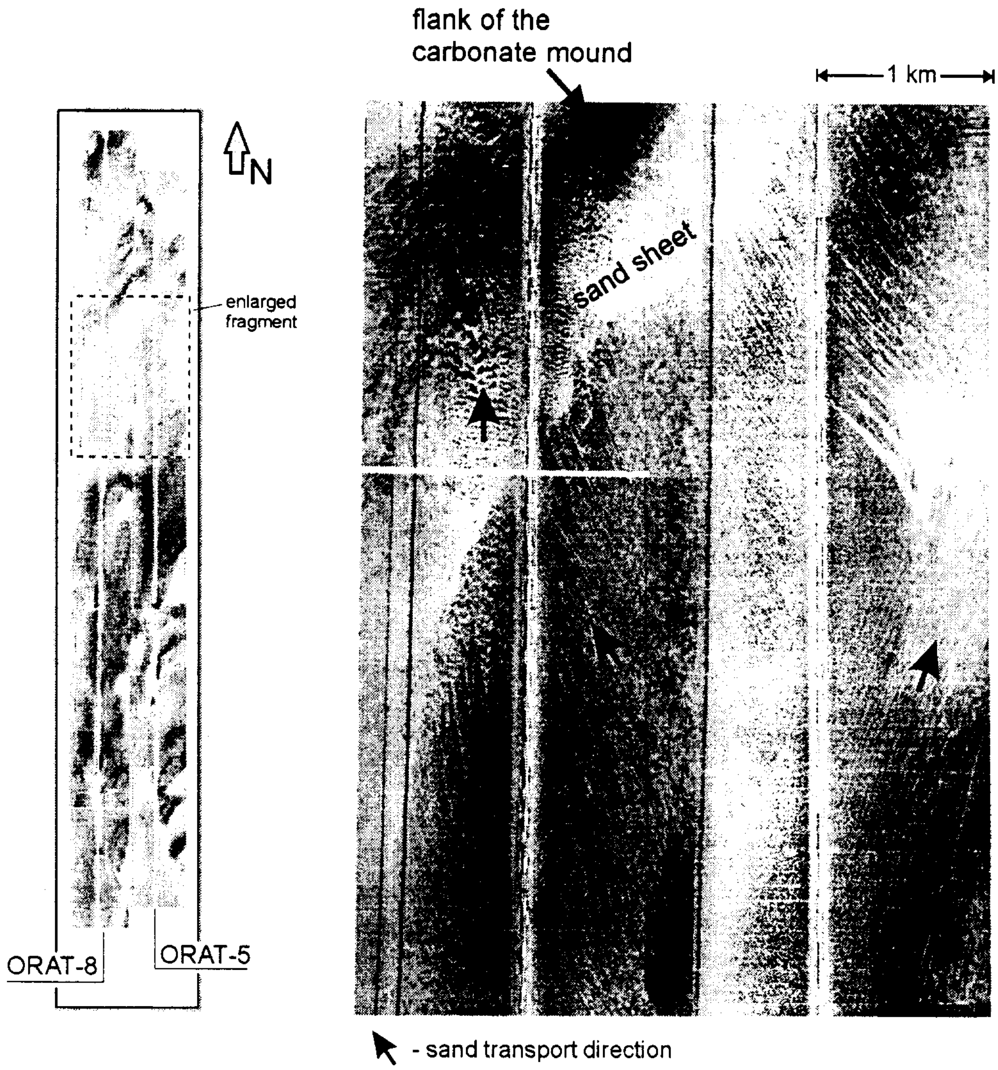

Fig. 30. Criss-cross bottom striation observed on the lines ORAT-5 and ORAT-8

ORAT-5/8

At least 10 large and 5 small mounds can be distinguished on the sonographs. Most of the large mounds are ridges elongated in a NNE-SSW direction and arranged en echelon. This is especially well seen in the northern segments of both lines and in the southern third of line ORAT-5 (Fig. 29). The ridges may have inherited the Hercynian trends although evidence for faulting is not observed in the corresponding seismic section. Despite the general high level of the seafloor backscatter, the mounds are notable for still stronger backscatter. The observed length of these features varies between 2 and more than 4 km, and the width is between 500 m and 1 km. The maximum recorded height reaches 150 m for the largest of the ridge where it is crossed by profile ORAT-5 (00:50). Moats are not typical of these mounds, and only two of them demonstrate their presence on the northern sides. The moats are marked by even stronger backscatter than that for the mounds.

The small mounds are more circular and are from 150 to 500 m across. They are chaotically distributed between the larger ones. None of them was crossed by the profiles, hence their height remains unknown.

There are a large number of very small isometric features with positive topography observed in many areas of the sonographs. Their diameter is a few tens of metres. Judging from the combination of strong backscatter on their sides facing the tow-fish and deep shadows on opposite sides, these features have a high, steep relief. They could be big ice-rafted rock blocks but more likely they are small carbonate build-ups because they are mainly spread around large mounds (Fig. 29).

Another peculiar feature of these OREtech lines is the presence of traces of strong bottom currents that go round the mounds roughly in a south-north direction, following the depth contours. The currents striate the seafloor, and variably-scaled ripple marks, normally crossing the striation, are clearly visible in some places, particularly between the mounds. Some parts of the current swept seafloor are marked by very weak backscatter suggesting the presence of a thicker and homogeneous sand layer. In sonograph ORAT-5 (22:35-23:15) (Fig. 30) there are two systems of striation. The main one, described above, is obliquely overprinted by more rough system. It is not excluded that this second system could be a result of trawling activity. The currents strongly erode the seafloor: the truncation of subbottom layers is obvious in the profile record from ORAT-5 (23:40-00:00) (Fig. 31).

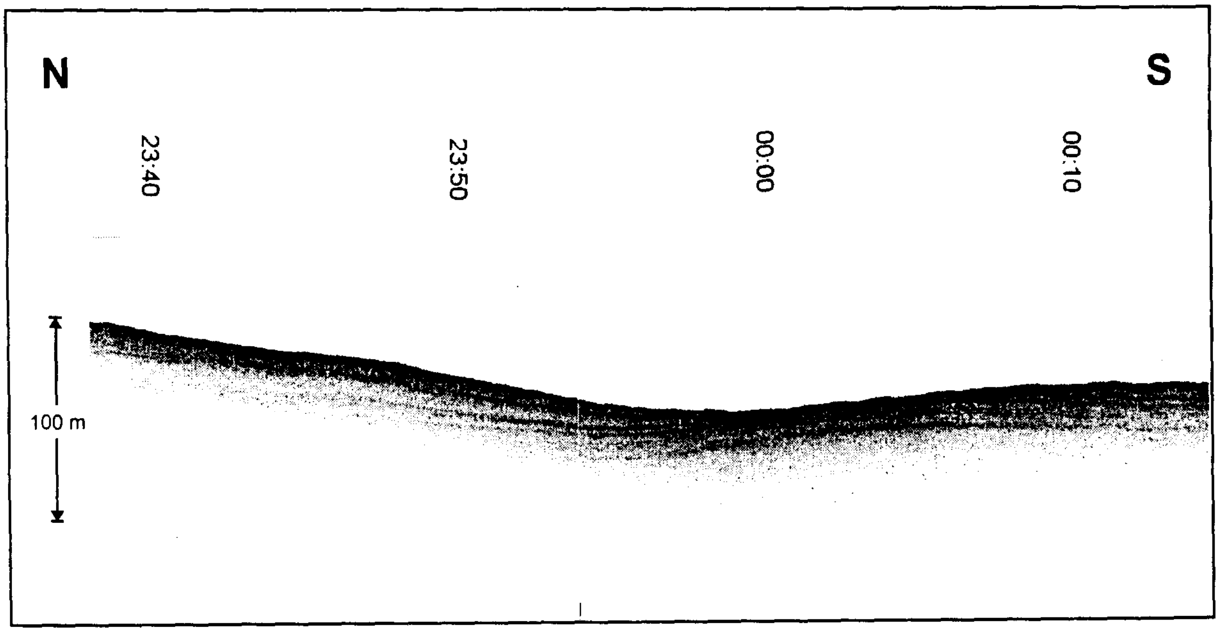

Fig. 31. Truncation of beds observed on the subbotom profiler record along line ORAT-5

ORAT-4/9

The "Belgica reefs" appeared to be almost completely buried under layered sediments that are well imaged in the profile records and create a moderate backscatter level on the sonographs. The subbottom layers are also truncated in some places by the same current system as described above, although the current pathways are not so pronounced as in the ORAT-5/8 mosaic. In this instance the currents are directed almost normally to the OREtech lines, again along the isobaths. The continental slope on the profile records has a terrace-like cross-section with the buried "reefs" being normally associated with the terrace scarps. The relief lows at the base of these "terraces" are marked by bands of weak backscatter which are interpreted as belts of sand (Fig. 32). They are usually covered by small-scale sand waves.

A few patches with strong backscatter, up to 200 m across, may correspond to the shallowest subbottom position of the tops of the "reefs". The correlation of the patches between the lines is impossible, this being so, we failed to define the trend of these features from the OREtech images. However, OKEAN sonograph PSAT-1 shows the only NE-SW lineation which can be taken as general for these features.

Some unexplained specific features are noted for these OREtech lines. On line ORAT-9, the eastern end of the line (as far as 01:40) has fields of a weakly backscattering seafloor. The fields have

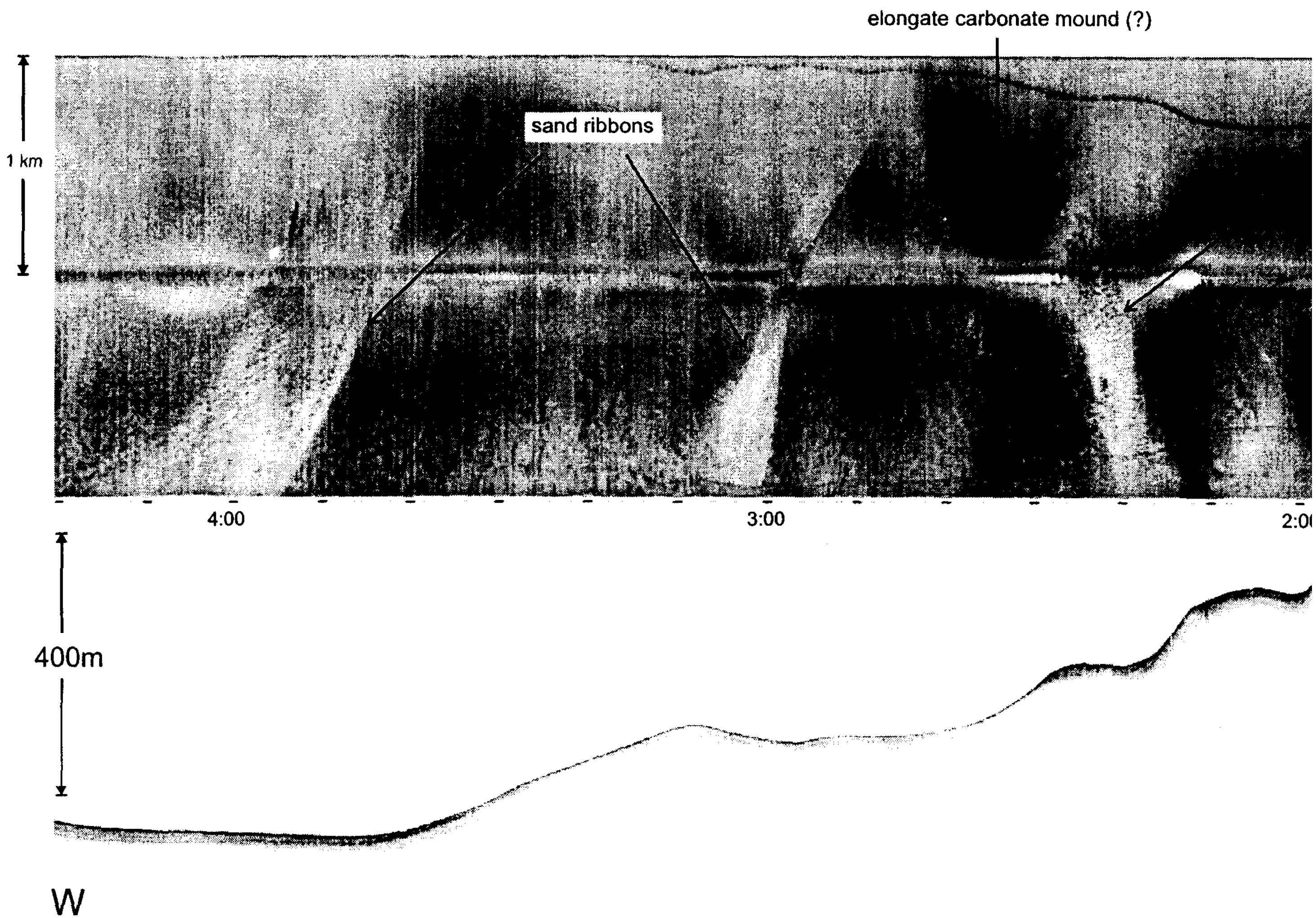

Fig. 32. Bands of weak backscatter seen on the ORAT-4 sonograph and interpreted as ribbons of sand

an irregular, wavy plan shape and can be thought to be sand sheets. Following the line westwards these fields transform into discrete small (within 100 m across) spots with low backscatter, which have no regular distribution and are mostly accompanied by ripple marks. The detailed analysis of the sonograph showed that only two of them reveal any relief: one spot is topographically positive and the other is negative. The nature of these features is not clear.

The next peculiarity is the presence of a very strong reflector in the subbottom profile record in line ORAT-9 between 02:00 and 06:30. The reflector occurs at a subbottom depth of about 8-9 m from time marks 02:00 to 03:00 and further westwards it approaches the seafloor. That part of ORAT-9 sonograph where this reflector crops out on the seafloor is clearly distinguished by stronger backscatter than the rest of the image.

Discussion of the features in the OREtech lines from the northern and eastern Porcupine Seabight

The mounds described in the Porcupine Seabight are surrounded by seafloor areas covered by soft sediments. No "basement" on which the mounds developed is inferred from the data above although there probably many ice rafted boulders that may be focal points for coral growth. Morphologically, the mounds can be subdivided into several types: large conical, more or less isometric in plan shape; large elongate, consisting of several conjugate ridges; large individual ridges; and small conical mounds which are normally buried by hemipelagic or fine contourite sediments. Two additional types can be provisionally distinguished for the eastern margin of the Seabight: "barrier reefs" ("Belgica reefs") and very small (~ n x10 m across) isolated build-ups. It is supposed that all these types represent different stages and variations of the mound evolution. General evolution of large, complex, ridge-shaped mounds can be viewed as a growth of individual small mounds progressively coalescing with each other along linear zones defined by different seabed conditions. These conditions are as follows:

(1) Seafloor morphology. Some of the described mounds are associated with prominent seafloor features, such as gentle valleys (the northern Porcupine Seabight) or scarps on the seabed ("barrier reefs" in the eastern Porcupine Seabight). However the valleys are to some extent created by the effect of the growing mound as an obstacle in the field of the current.

(2) Bottom currents. The mounds in the eastern Porcupine Seabight are evidently associated with strong bottom currents that left their traces on the seafloor in the form of "comet marks", striations, and sand waves. It is thought that the currents favourably affect the coral growth, supplying them with nutrients. Although no current bedforms were noted for the northern Porcupine Seabight, the location of the mounds in the seafloor depressions and characteristic contourite signature on the seismic profiles suggests that they are also influenced by currents guided by those depressions.

The bottom currents are directed along the depth contours, thus they belong to contour type, that is in accordance with the general water circulation pattern in this region of the North Atlantic (New et al., 1996).

The origin of the closed linear deeps, away from the current induced moating effect of the mounds, is a problem remaining to be resolved.

THE SOUTHERN PORCUPINE SEABIGHT: GOLLUM CHANNEL SYSTEM

N. Kenyon, B. Cronin, A. Wheeler, N. Satur, and S. Zaragosi

Channel morphology

ORAT-6

ORAT-6 is an ENE-WSW -trending, 15-km OREtech line running obliquely across the levees, terraces, channel walls, and channel floor of a central section of the northeast-southwest trending Gollum Channel (Fig. 33). The general morphology shows a steeply incised thalweg channel, 300 m deep and 1000 m wide in the centre of a 5 km wide valley with terraced margins and flanked

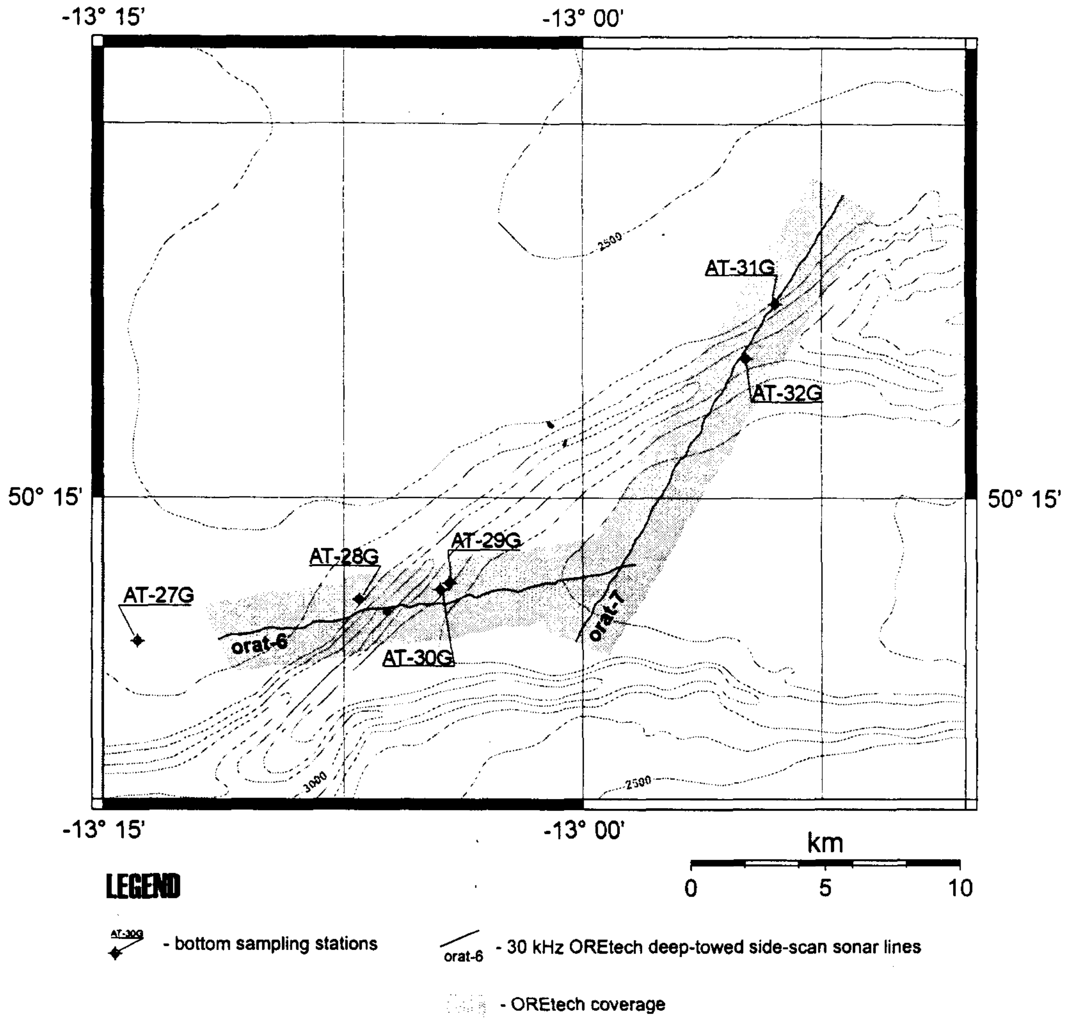

Fig. 33. Location of OREtech lines and bottom sampling stations in the lower reaches of the Gollum channel system

by a laterally extensive levee/overbank system. Terraces are backed by a series of scalloped-shaped scars (Fig. 34).

Channel.

The OREtech profiler shows the channel floor to be very flat with concave upward surfaces at the base of the channel wall. These are interpreted to be sediment accumulations slumped in from the channel walls. There are no parallel, strong reflectors imaged by the profiler on the channel floor. This may indicate the absence of significant thickness of hemipelagic sediment within the channel. The sidescan sonar images show the floor of the channel to have moderate backscatter with only small variability. There are some small-scale features on the floor that could be erosional surfaces.

The channel walls are very steep, only changing in gradient at the channel floor, represented by the concave upward features described above. The western channel wall has a distinctive top with a very abrupt change in slope, whereas the eastern wall has a more gradational change in slope from the steep channel walls to the terrace on the flank.

Both channel walls show the development of a series of narrow gullies incised into the wall. This is particularly well imaged on the eastern wall (Fig. 34). At this location, small slump scars can be seen with the transported sediment having a rough, irregular texture and moderate to high backscatter.

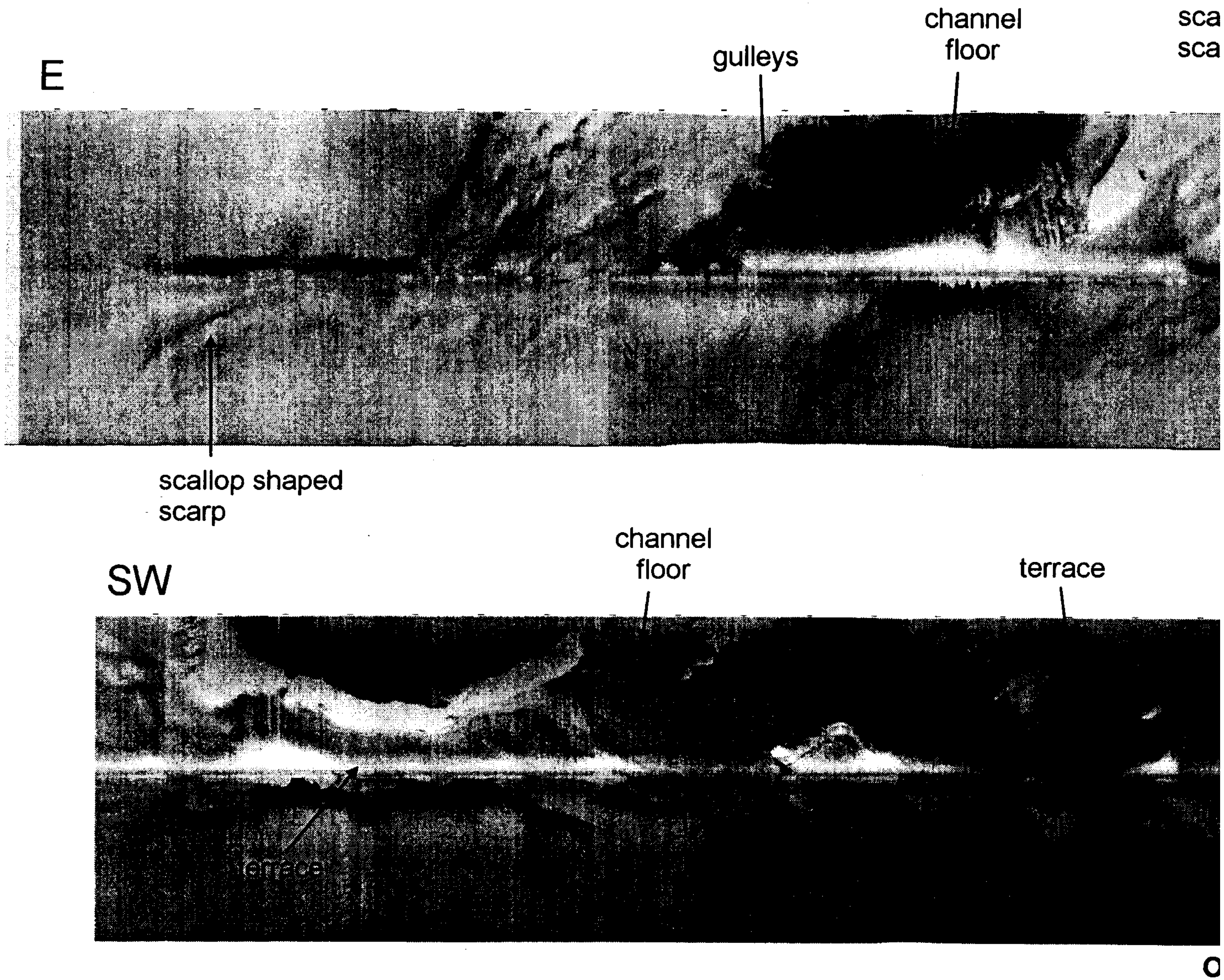

Fig. 34. OREtech lines running across Gollum channel

Terraces.

The profiler record shows the western terrace to have a steeper profile than the eastern terrace. Also the depth of the eastern terrace is at 2250 m in comparison to 2620 m for the western side. The terraces have an irregular topography over which with a drape of approximately 10 m of parallel-bedded sediment has been removed. They have a moderate backscatter on the sidescan sonar record. A series of ridge-like features can be seen on these terraces. These are interpreted to be a result of small-scale, normal faulting with downthrow towards the channel. The faulting is believed to be rotational and shallow seated. The back edge of the terraces is imaged as a steep, continuous, curved slope with relief of approximately 50 m. On the east side of the channel, a ridge feature can be seen to be truncated by the terrace. This helps in eliminating these ridge-like features as erosional. The overall cross-sectional morphology of the channel from these lower reaches up to the eastern Porcupine Seabight slope has a slightly asymmetric "steerhead" geometry.

Overbank areas.

Outside of the terraces are relatively flat areas with parallel-bedded sediments greater than 50 m in thickness. The western flank of the channel appears to be slightly inclined away from the channel indicating some low levee type build up of overbanking turbidity currents. Figure 35 summarises the main features of the Gollum Channel observed along ORAT-6 line.

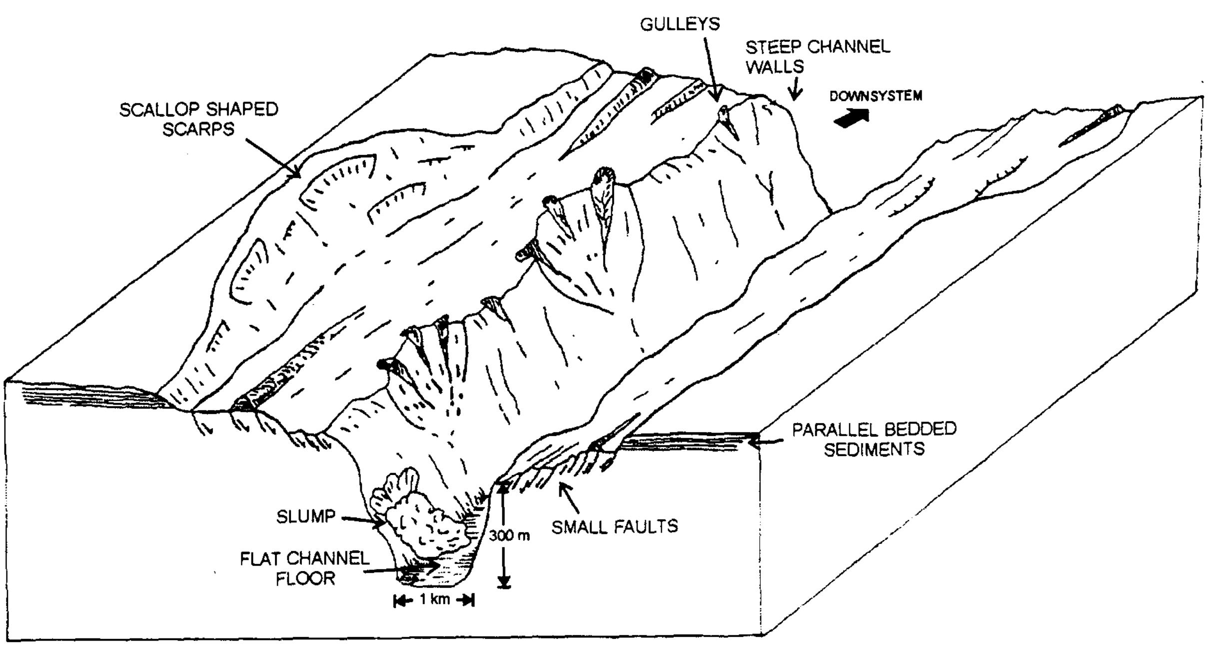

Fig. 35. Schematic block-diagram of Gollum channel

ORAT-7

OREtech line 7 trends SW-NE to the north of ORAT-6 (Fig. 33). It shows the joining of one tributary channel into the main channel. On the flanks of the channels, several terraces, similar to those on ORAT-6, can be identified (Fig. 34).

Channels.

The channels are here seen to be slightly sinuous with the floors within the steerhead cross-section, being 1 km in width and flat. The east-west -trending floor of the main channel is 2800 m in depth and has moderate-high backscatter. The N-S -trending, 2850 m deep, floor of the tributary channel has a similar backscatter on the right side of the floor, but on the east side, a wedge of low backscatter sediment can be identified. It is interpreted that this wedge is sediment that has slumped in from the channel walls, or is a sand bar-type feature on the inside of a channel meander.

There are two ridges that extend into the channel. The ridge on the west side of the channel appears to influence the deposition and/or erosion of sediment on the channel floor. This can be seen on the sidescan sonar record in the form of a triangular feature extending towards the floor from this ridge. Linear patterns in the main channel, down system of the ridge on the east side can be observed and may be a result of its influence on the flow in the channel.

The steep channel walls are between 250 and 300 m in height, which is almost the same as those seen on ORAT-6. The crests of the channel walls are rounded, gradually passing into flat terraced areas. There appears to be some gullies on the channel walls, but less extensively developed than those seen down system on ORAT-6, with no evidence for slumping or sliding of sediment onto the channel floor.

The terraces and channel overbank areas are similiar to those on ORAT-6

I.5. Bottom sampling results

R. Swennen, B. Cronin, M. Ivanov, E. Kozlova, A.J. Wheeler, A. Akhmetzhanov, A. Sautkin, D. Van Rooij, S. Zaragosi, L. Mazurenko, C. Degryse, P. Sumida, N. Satur, R. Kennedy, G. Akhmanov, I. Belen'kaya, S. Pillen, Yu. Naumov, A. Stadnitskaya, B. de Mol, A. Balashova, A. Saprykina

Introduction

Three areas were sampled. The first area, the northern Porcupine Seabight, was sampled using gravity corer, dredge, and grab-sampler. The objective was to recover material from the crest, flanks, moat, and surroundings of a series of possible carbonate mounds which had previously been discovered only by seismic and. The mounds were thought to have grown on sites of gas seepage (Hovland et al., 1994), and the sampling strategy, supported by a large geochemical and biological effort onboard, was to test this hypothesis.

The second area, on the east, or the Celtic Sea, margin of the Porcupine Seabight, was sampled using gravity corer and grab-sampler. Some peculiar linear, perhaps barrier, mounds had previously been discovered during the R/V *Belgica* cruise (1997), and the objectives were to sample them in a similar fashion to the first area.

The third area, in the south of the Porcupine Seabight, was sampled using gravity corer. The area had been mapped using GLORIA data, and locally swath bathymetry data were also available. This area contained the impressive and large Gollum Channel System, which drains from east to west. OREtech profiles across the proximal and middle reaches of the channel were to be ground-truthed by gravity cores, to test the activity of turbidity currents in the most recent past. A total of 40 gravity cores were collected using the procedure outlined in Technical Report. Later in the leg, the plastic liner used in the corer became stressed and eventually unusable, so coring operations and removal of the core from the barrel of the corer were carried out without it. This did not in any way affect coring operations and certainly did not reduce sediment recovery at all.

Total sediment recovery in this leg was ca. 102 m. Technical information on coring sites is given in Table 2. The cores are described individually below in the order in which they were retrieved (Figs. 36-68). Brief preliminary interpretation of the cores according to the three target areas follows this section. Areas 1 and 2 (carbonate mound section) are short because the focus of the sampling was geochemical, stratigraphic, and biological and not lithological. A section on the interpretation of the turbidite channel area follows this sampling section, which combines data from the OREtech survey, the seismic and OKEAN data from the upper reaches of the channel system, and is supplemented with data from the previous GLORIA survey.

TEST CORE

Core TTR7-AT-1G (Fig. 36)

Hemipelagic core. Upper 0.28 cm are medium-coarse foraminiferal sand with shell fragments, one fragment of coral (at 0.12 m) and rare (<2 cm diameter) black, angular dropstones. A half pecten was found isolated at 20 cm. Unusually, this was found inverted, and it was shown that the half-shell would immediately flip to convex down if allowed to settle naturally in water. Its position may indicate bottom reworking, although no lamination or other evidence for current activity can be seen. Next interval (0.28-0.45 cm) is bioturbated silty mud, olive-green in colour. Bioturbated cavities are filled with foraminiferal sand. The rest of the core is olive-green clay. Millimetric broken shell fragments and forams are scattered and rare.

Core No.	*Date*	*Time (GMT)*	*Latitude*	*Longitude*	*Cable Length, m*	*Depth, m*	*Recovery, cm*
TTR7-AT-1G	9.7.97	10.21	49°54.98' N	11°15.03' W	575	580	376.5
TTR7-AT-2G	11.7.97	04.48	52°13.66' N	12°33.96' W	795	793	392
TTR7-AT-3G	11.7.97	05.57	52°13.16' N	12°34.03' W	925	840	369
TTR7-AT-4D	11.7.97	10.15 to 10.29	52°13.52' N to 52°13.35' N	12°33.90' W to 12°33.95' W	845 to 850	822 to 886	N/A
TTR7-AT-5G	12.7.97	12.25	52°13.99' N	12°43.38' W	623	637	60.5
TTR7-AT-6G	12.7.97	13.23	52°13.67' N	12°43.56' W	790	790	247
TTR7-AT-7G	12.7.97	14.15	52°13.13' N	12°43.78' W	782	774	370
TTR7-AT-8D	12.7.97	14.55 to 15.42	52°13.68' N to 52°14.14' N	12°43.54' W to 12°43.18' W	795	789	N/A
TTR7-AT-9G	13.7.97	11.31	52°12.73' N	13°02.38' W	700	706	361
TTR7-AT-10G	13.7.97	12.28	52°11.94' N	13°02.74' W	699	696	393.5
TTR7-AT-11G	13.7.97	13.23	52°12.72' N	13°02.46' W	707	703	388.5
TTR7-AT-12G	13.7.97	14.54	52°16.40' N	13°00.42' W	700	675	403.5
TTR7-AT-13G	13.7.97	16.31	52°19.19' N	12°59.07' W	660	651	388.5
TTR7-AT-14G	13.7.97	11.22	52°18.88' N	12°40.70' W	630	624	145
TTR7-AT-15Gr	13.7.97	22.34	52°13.60' N	12°34.05' W	811	794	1.5 tonne
TTR7-AT-16G	14.7.97	12.05	52°08.80' N	12°19.80' W	700	691	389
TTR7-AT-17G	14.7.97	12.56	52°08.72' N	12°49.15' W	745	737	126
TTR7-AT-18G	14.7.97	13.46	52°08.65' N	12°49.89' W	791	786	198
TTR7-AT-19G	16.7.97	09.42	51°17.88' N	11°48.59' W	1176	1177	366
TTR7-AT-20G	16.7.97	11.26	51°17.82' N	11°41.78' W	1007	1008	275
TTR7-AT-21G	16.7.97	12.16	51°17.88' N	11°40.59' W	900	896	361
TTR7-AT-22G	16.7.97	13.42	51°17.90' N	11°39.57' W	798	798	349.5
TTR7-AT-23G	16.7.97	17.29	51°27.28' N	11°42.08' W	686	700	326
TTR7-AT-24Gr	17.7.97	14.14	51°27.19' N	11°42.05' W	730	736	<1.5 tonnes
TTR7-AT-25G	17.7.97	16.36	51°17.79' N	11°37.15' W	685	686	281
TTR7-AT-26G	17.7.97	17.56	51°17.66' N	11°39.75' W	790	810	366
TTR7-AT-27G	18.7.97	16.19	50°12.14' N	13°13.92' W	2686	2675	345
TTR7-AT-28G	18.7.97	18.00	50°12.98' N	13°07.03' W	2696	2690	334
TTR7-AT-29G	18.7.97	19.21	50°13.30' N	13°04.22' W	3019	3025	344.5
TTR7-AT-30G	18.7.97	21.45	50°13.17' N	13°04.48' W	3033	3035	331.5
TTR7-AT-31G	19.7.97	13.39	50°18.87' N	12°53.97' W	2850	2840	351.5
TTR7-AT-32G	19.7.97	15.13	50°17.79' N	12°54.87' W	2885	2885	27
TTR7-AT-33G	21.7.97	12.20	51°18.00' N	11°39.19' W	731	744	328
TTR7-AT-34G	21.7.97	14.05	51°23.92' N	11°41.98' W	783	785	0
TTR7-AT-35G	21.7.97	14.38	51°23.37' N	11°41.89' W	772	774	328
TTR7-AT-36G	21.7.97	15.32	51°23.14' N	11°42.17' W	828	830	339
TTR7-AT-37G	21.7.97	22.04	50°45.31' N	11°17.58' W	745	740	0
TTR7-AT-38G	21.7.97	23.17	50°43.80' N	11°14.16' W	983	980	0
TTR7-AT-39G	21.7.97	00.43	50°40.81' N	11°14.90' W	1002	985	197.5
TTR7-AT-40G	28.07.97	10.20	50°37.16' N	11°54.34' W	2164	2160	308

Table 2. General information on the cores sampled in the Porcupine Seabight

Core No.	*Target feature*	*Comments*
TTR7-AT-1G	Pelagic mud,	Test core; core liner breaks in two
TTR7-AT-2G	Large mound 1	Carbonate mound core
TTR7-AT-3G	Large mound 1	In moat to the south of the carbonate mound
TTR7-AT-4D	Large mound 1	The upper flank of the same carbonate mound.
TTR7-AT-5G	Large mound 2	Taken on the crest of the carbonate mound 2, on the same transect as AT6G/7G/8D
TTR7-AT-6G	Large mound 2	Taken in a moat south-southwest of the carbonate mound 2
TTR7-AT-7G	Large mound 2	Taken further south-southwest, outside the moat of the carbonate mound 2
TTR7-AT-8D	Large mound 2	Taken from the lower slope of the carbonate mound 2
TTR7-AT-9G	Small mound 1	This core was taken from the southeastern slope of a low relief structure (small mound 1), being positioned on the basis of the unprocessed ORAT-2 sonograph
TTR7-AT-10G	Small mound 2	The core was taken to the southeast of another low-relief mound (small mound 2) from the same OREtech line
TTR7-AT-11G	Small mound 1	The core was taken slightly over 100 m to the west of AT9G, as a small positioning error led to uncertainty whether that core had hit the crest of the mounded structure
TTR7-AT-12G	Pelagic mud	This core was taken on a flat area of seafloor with a layered sequence seen on the subbottom profiler record
TTR7-AT-13G	Small mound 3	This core was taken near the base of another low relief structure further north-northeastwards along line ORAT2, as another test to see if the mounds could be penetrated to reach the mounded, and presumably buried, structure
TTR7-AT-14G	Small mound 4	The core was recovered about 3 km northeastwards from the start point of ORAT1 where a low-relief mound was defined from OKEAN data and echosounder record
TTR7-AT-15GR	Large mound 1	Taken on the crest of carbonate mound structure 1 for biology samples
TTR7-AT-16G	Large mound 3	Taken on the crest of large carbonate mound 3
TTR7-AT-17G	large mound 3	Core taken on the flank of large carbonate mound 3
TTR7-AT-18G	large mound 3	Flank target - to test the uniform aspect of flank facies
TTR7-AT-19G	Barrier mound	Core taken in slightly mounded area at the base of series of terraces
TTR7-AT-20G	Barrier mound	On the lower "terrace" slope - an attempt to penetrate presumably outcropping reef
TTR7-AT-21G	Barrier mound	Second attempt at a presumed exposure of carbonate material on the sea floor, the steeper of the two slopes targeted on the 'barrier reef'
TTR7-AT-22G	Barrier mound	An attempt to retrieve reefal material at the terrace edge upslope of Site AT21G
TTR7-AT-23G	Barrier mound	An attempt to sample the summit of one of the mounds of this group
TTR7-AT-24Gr	Barrier mound	The top of another carbonate mound about 1 km south of Site AT23G
TTR7-AT-25G	Barrier mound	Core taken from a strongly backscattering spot at the edge of the upper "terrace"
TTR7-AT-26G	Barrier mound	On the "terrace" edge, about 500 m SSE of Site AT22G
TTR7-AT-27G	Gollum Channel Levee	Core to the west of the Gollum Channel, on a flat, stratified and low backscattering part of the levee
TTR7-AT-28G	Gollum Channel Terrace	Core taken from a terrace on the northwestern side of the Gollum Channel
TTR7-AT-29G	Gollum Channel Thalweg	Core taken from the edge (eastern flank of thalweg) of the Gollum Channel. This was targeted at the deep thalweg but the narrowness of the conduit in this reach and the length of the cable frustrated our attempts to hit the thalweg.
TTR7-AT-30G	Gollum Channel Thalweg	The same geomorphologic position as for the previous one but about 750 m to the southwest. It was also targeted at the deep thalweg
TTR7-AT-31G	Gollum Channel Thalweg	Core taken from the northern flank of the Gollum Channel, downstream of the confluence of two main tributary valleys of this channel system. We had aimed at the thalweg but missed again
TTR7-AT-32G	Gollum Channel Thalweg	Core taken from the Gollum Channel. This was the only core to hit the thalweg of the channel. Sand was seen falling from the core catcher into the sea during recovery. Fine sand was found at the base of the core.
TTR7-AT-33G	Carbonate Mound	The last attempt to recover corals from a presumably outcropping top of the "reef"
TTR7-AT-34G	Crest of carbonate mound	From the crest of one of the newly discovered mounds observed in PSAT-02
TTR7-AT-35G	Carbonate Mound	Crest of a slightly southerly carbonate mound arranged en-echelon to the previous one. Direct hit
TTR7-AT-36G	Carbonate Mound	Field of barchan-shaped bedforms near the en-echelon carbonate mounds
TTR7-AT-37G	Gollum Channel head	Northern flank of Gollum Channel head
TTR7-AT-38G	Gollum Channel head	Thalweg of the main Gollum Channel head
TTR7-AT-39G	Gollum Channel head	Levee on the southern side of the main Gollum Channel head
TTR7-AT-40G	Gollum Channel middle reaches	This was the first core taken in Leg 2. The aim of coring was to complete the investigation (begun in Leg 1) into recent sediment transport activity in the canyon system feeding the Porcupine abyssal plain. The core was taken approximately 1 km NNE of the thalweg, in the upper reaches of the Gollum Channel (here 3.7 km in width)

Table 2. General information on the cores sampled in the Porcupine Seabight *(continuation)*

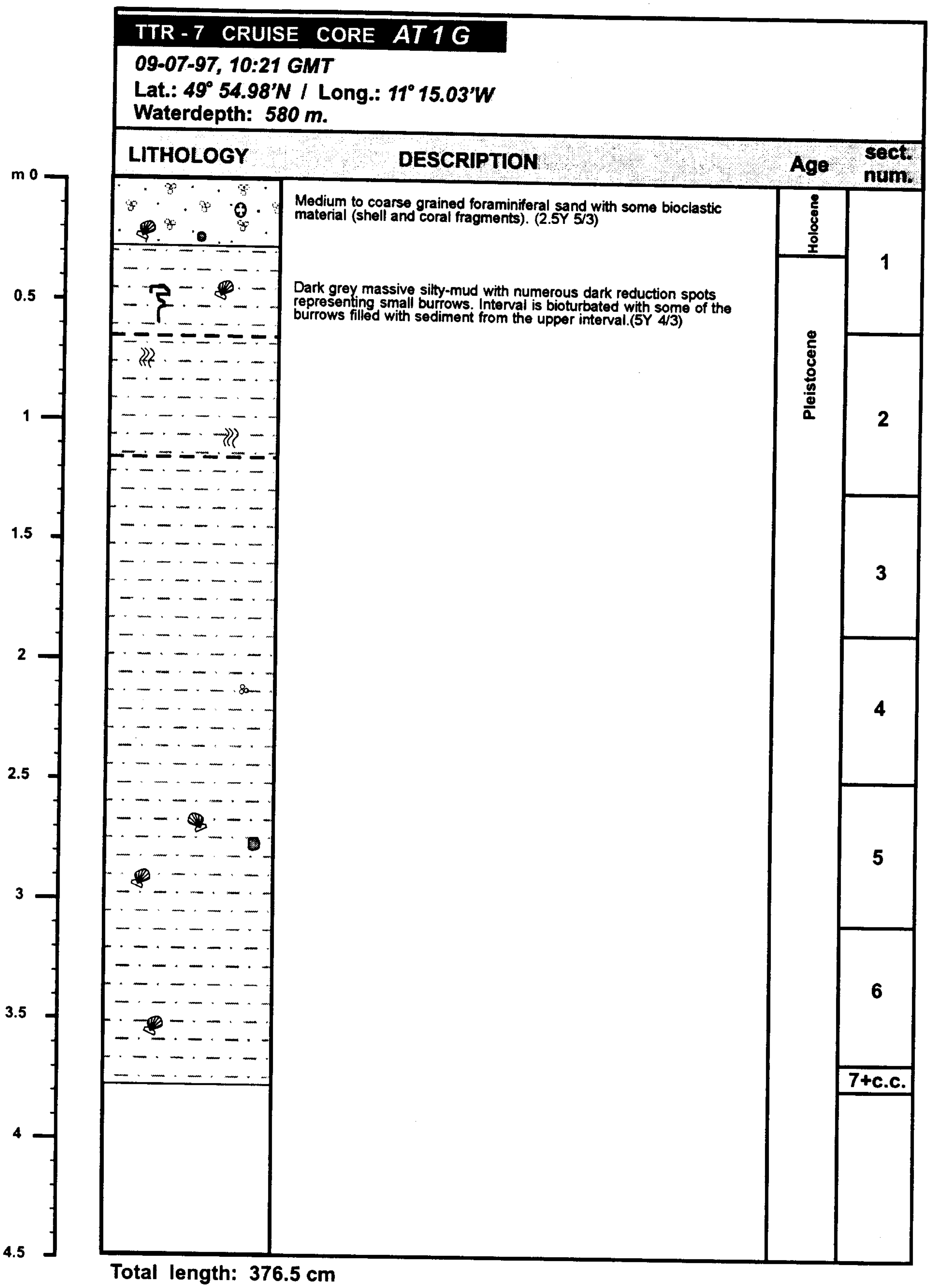

Fig. 36. Core log AT-1G

NORTHERN PORCUPINE SEABIGHT

Large carbonate mound 1

Core TTR7-AT-2G (Fig. 37)

Live and dead corals in foraminiferal ooze. The core comprises two major packages: (i) alternating bands of foraminiferal grey/olive marls with low densities of broken corals and (ii) densely-packed branched coral horizons. The densely-packed intervals (70-100%) occur at 0-23, 23-47, 99-107, 129-140, 161-176, 197-211 cm. A sand layer composed of broken corals is found at 123-129 cm. Some dropstones were recovered (e.g. at 85 cm), but they are not as common as in later cores. The lower section (289-392 cm) comprises light-grey massive marl with carbonate crust fragments, and broken white coral fragments with dark-grey carbonate mud fills, up to 1.5 cm in diameter. Other faunal fragments identified include live corals in the upper 0-23 cm, crab fragments, gastropods and echinoderms. Most of the core is bioturbated, and this is seen as black reduction spots.

Core TTR7-AT-3G (Fig. 38)

This core comprises two main packages with only subtle visual differences. (i) The upper section (0-180 cm) consists of olive-grey foraminiferal sands and marls which fine downsection through more silty foraminiferal marls. Bioturbation, in the form of reduction spots, is very common. Larger burrows, filled with coarser material, are found between 143 and 174 cm. Lenses of finer marly material also occur (e.g. 65-86 cm). Shell fragments and other bioclastic material are found throughout this package. Bivalves were found at 70, 72, and 87 cm, and one 3-cm coral branch at 101 cm. One dropstone was recorded at 153 cm. (ii) The lower package (180-369 cm) comprises structureless mud with occasional dropstones (e.g. 181, 220 and 295 cm). The core is richer in forams (from 236 cm) and reduction spots associated with bioturbation, down the core. Between 296 and 369 cm the core is typified by massive mud apart from thin bioclastic and foraminiferal layers (sometimes with intact corals and bivalves) at 326, 347, and 352 cm.

Dredge TTR7-AT-4D

This sample was taken to collect as much biological material as possible from the structure. The top of the dredge contained carbonate ooze from the first point of contact with the seafloor. A range of biological samples, including echinoids, corals, and sea urchins, were collected. These are described in the biology section below.

Large carbonate mound 2

Core TTR7-AT-5G (Fig. 39)

Coral core. The core incorporates a hard carbonate crust (0-6 cm) over coarse sand with >80% debris. The debris included forams, bryozoans, Balaonoides fragments (a crustacean, also found in dredge AT4D), broken corals and other material. The rest of the core comprises grey silty foraminiferal marl with white spots and a patchy, mottled pattern. The 6-35 cm interval was dry and the 35-60.5 cm interval was wet. A brown gastropod was seen at 58 cm.

Core TTR7-AT-6G (Fig. 40)

Moat core. The core comprises interbedded grey marls and thin sandy foraminiferal and bioclastic debris layers. The marls vary in colour from olive-grey, to olive-green to greyish-brown. The are commonly strongly bioturbated but otherwise structureless. Shell fragments were found at 43, 52, 82, 108, 112, and 113 cm, and several coral fragments were found (e.g. at 207 cm). Clinkers were found in some burrows (e.g. 21 cm). Dropstones were also common in this core at 72, 94, 96, 99, 113 cm (up to 7 cm in diameter), and 127 cm. The marls get siltier downsection. Rare reduction spots were

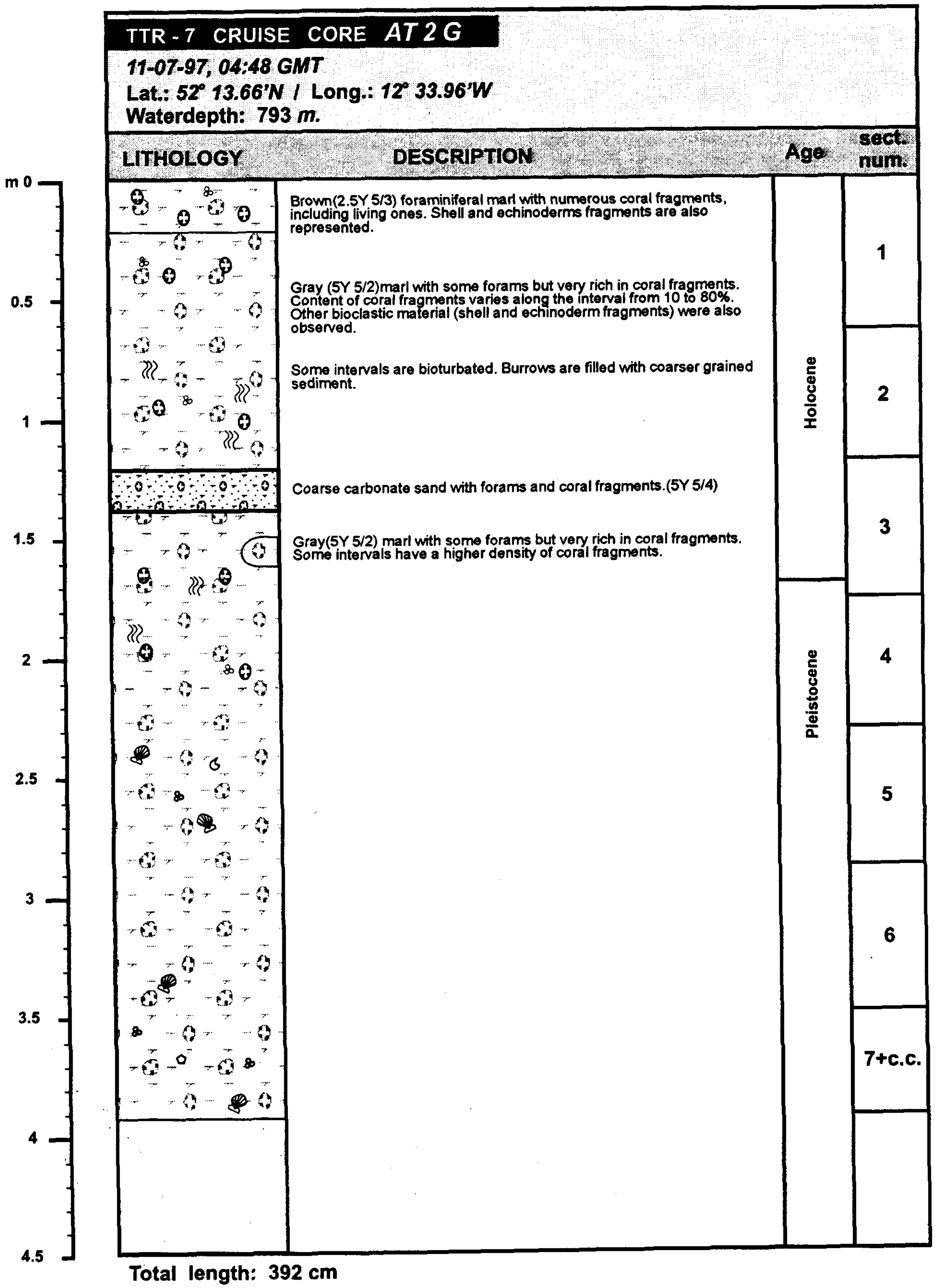

Fig. 37. Core log AT-2G

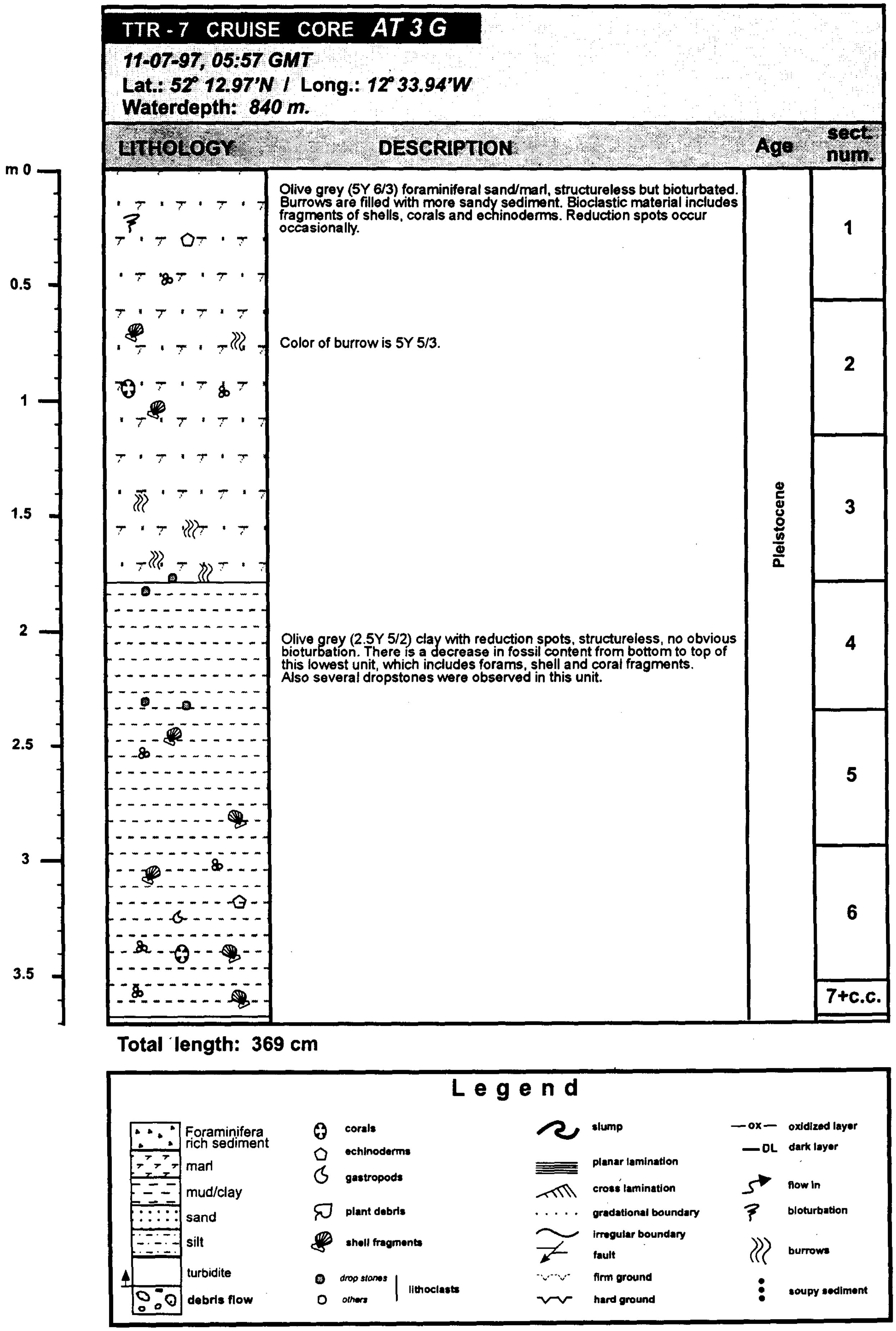

Fig. 38. Core log AT-3G

also seen. The coarser intervals were found at 0-12, 102-104 (which could be a horizontal burrow) and 183-195 cm. They comprise coarse-grained forams with a terrigenous admixture, some pebbles, and shell fragments.

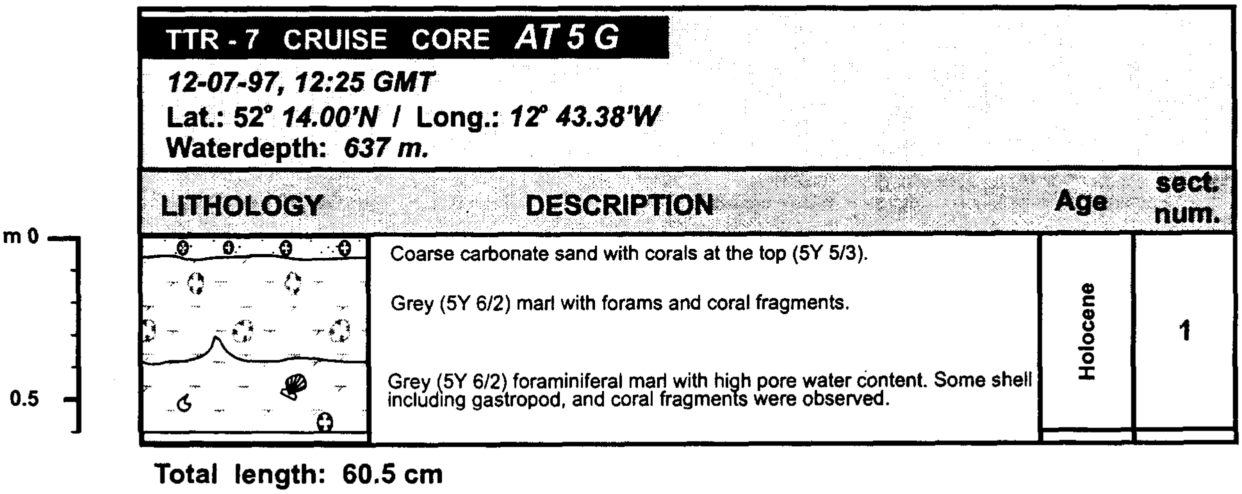

Fig. 39. Core log AT-5G

Core TTR7-AT-7G (Fig. 41)

Pelagic core. This core comprises olive-grey/greyish-brown, silty, structureless, foraminiferal marls. Locally very strong bioturbation mixes lithic fragments and other coarse material. Reduction spots are scattered through most sections. The most vigourous bioturbation is seen at 301-316 cm. Occasional shell fragments occur associated with these spots. Only one dropstone was encountered, at 16 cm. The dropstone layers found in AT6G are not present in this core.

Dredge TTR7-AT-8D.

Similar results to AT4D. The biological samples collected are described in the biology section below.

Although small mounds on the O.R.E.tech sonograph and profiles appeared to be completely buried under hemipelagic sediments, we checked also the opportunity to recover bioclastic sediments from them. The results are described below.

Small mound 1

Core TTR7-AT-9G (Fig. 42)

Bioturbated pelagic core. This core comprises greyish-brown to dark greyish-brown, bioturbated, massive marls with rare black spots. The marl is more silty downsection, due to an increase in coarser forams. Large vertical and oblique burrows are seen at 62-104 cm and filled with softer, lighter clay (from the section above). Other burrows (e.g., at 118 cm) are filled with coarse sandy material, which is rich in forams and shell debris. The rest of the section (120-361 cm) is massive silty marl with local but rare black spots and some shell fragments.

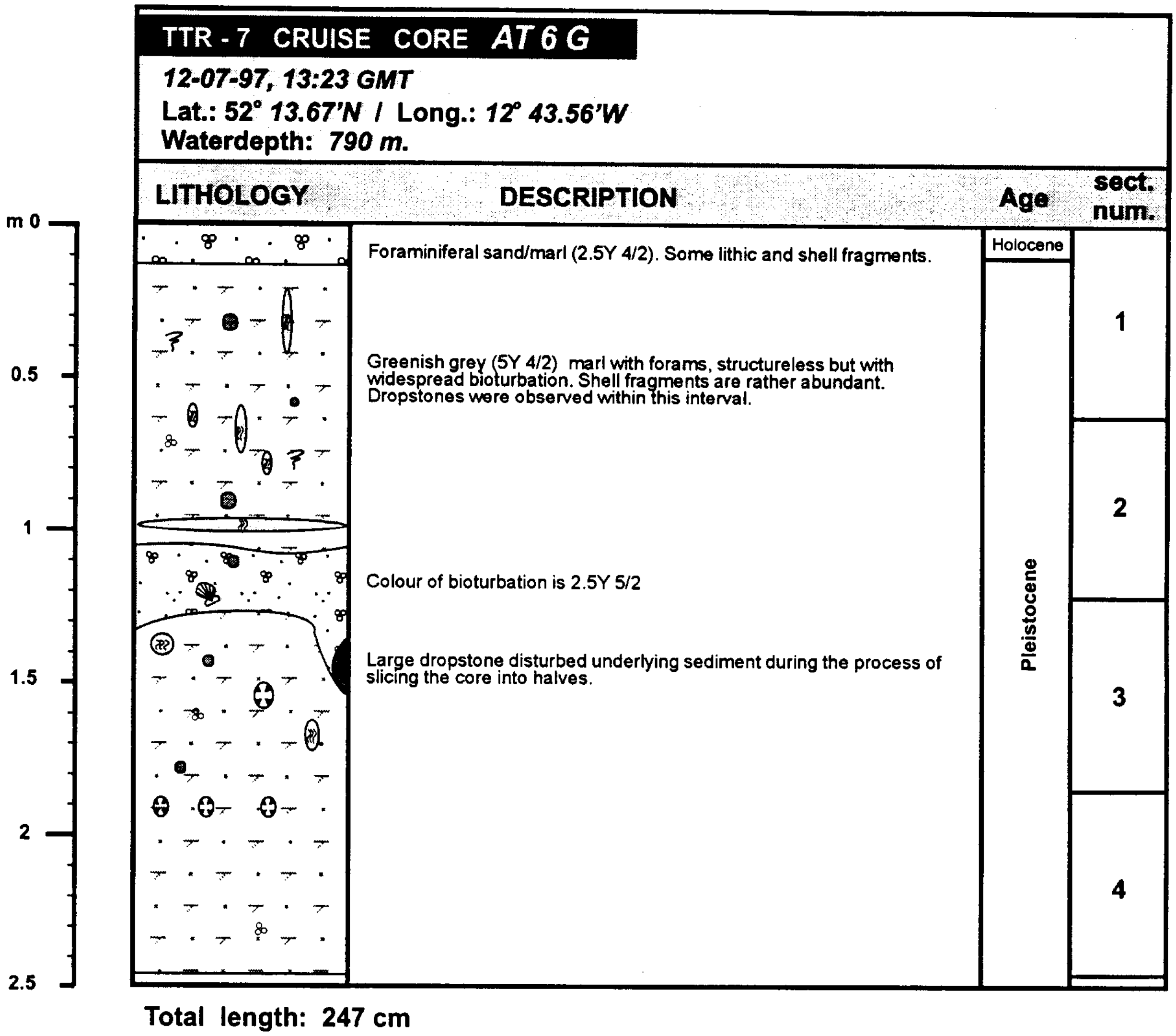

Fig. 40. Core log AT-6G

Small mound 2

Core TTR7-AT-10G (Fig. 43)

Pelagic core. The core retrieved greyish-brown to very dark-grey bioturbated, silty, foraminiferal marls. Burrowing is common as in the last core. Very large burrows were seen between 75 and 137 cm, filled with foraminiferal sand, the largest of which has a diameter of 5 cm. Reduction spots are again associated with the bioturbation. Some of the burrows are filled with dark-grey, soupy clay and others with an admixture of bioclastic debris. Shell fragments and larger forams are scattered through the remaining section, becoming coarser towards the base.

Small mound 1

Core TTR7-AT-11G (Fig. 44)

Bioturbated pelagic core. This core is very similar to the last two. The upper 10 cm comprises light olive brown, water-rich, soupy clay. The rest of the core comprises olive-grey to greyish-brown, silty marls. These are bioturbated throughout and become coarser and siltier downsection with a corresponding increase in bioclastic fragments, intact bivalves, larger foram tests and reduction spots. A zone of particularly intense burrowing is recognised between 73 and 145 cm. These burrows are

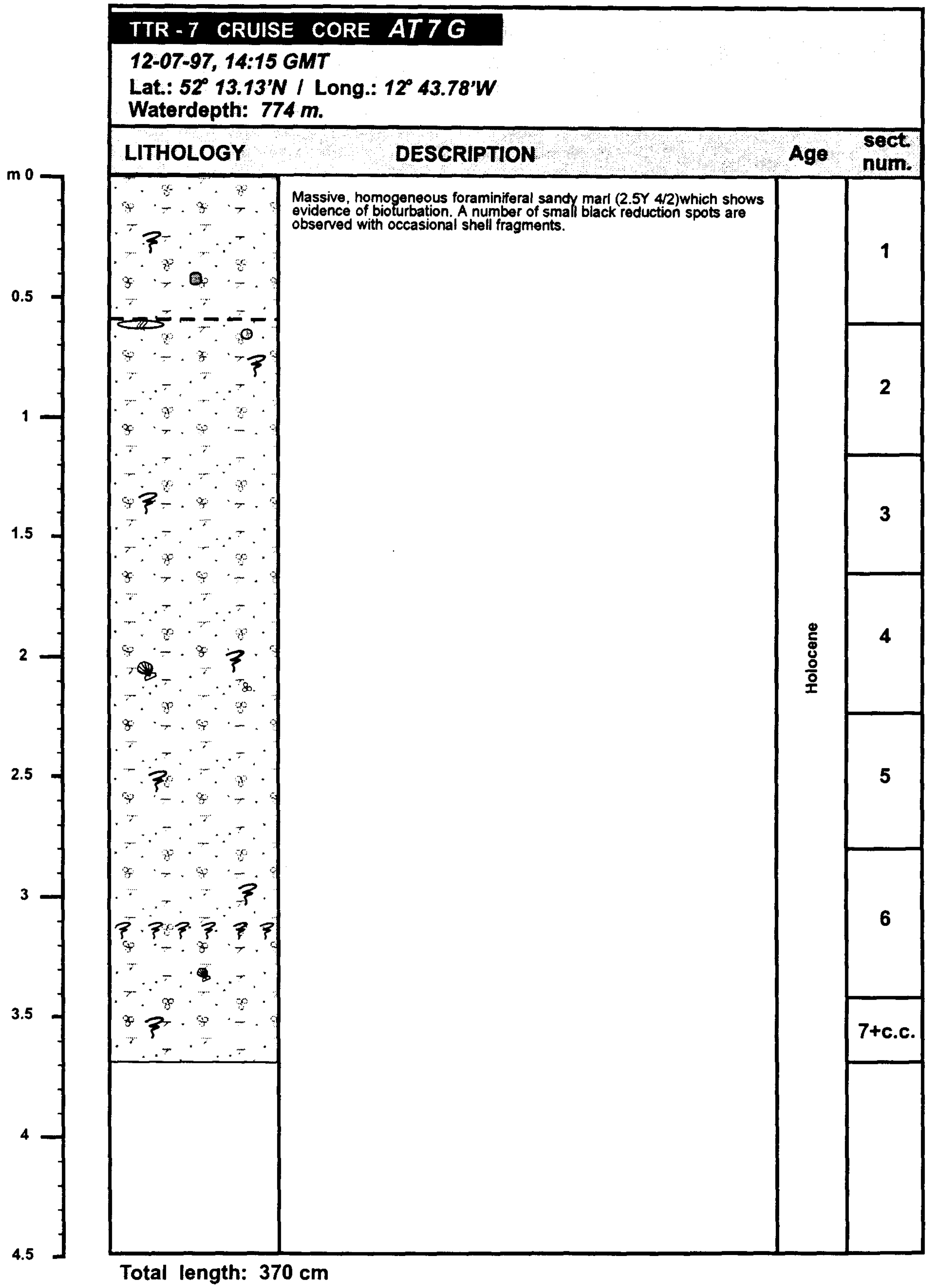

Fig. 41. Core log AT-7G

patchy and irregular features and contain less foraminiferal sand than the last two cores. 2 cm in diameter bivalve was found at 103 cm. One unbroken coral (*Lophelia*) was found at 148 cm. The rest of the core is bioturbated but without the larger burrows typical of the upper section (except 267-272 cm). A layer of shell fragments is found at 241 cm, and very common scattered shell fragments with reduction spots are observed from 297-388.5 cm.

Background pelagic sediments

Core TTR7-AT-12G (Fig. 45)

Bioturbated pelagic core. The core comprises greyish-brown, massive, bioturbated marls with occasional dropstones, burrows and bioclastic material. The core becomes coarser with forams and bioclasts downsection. The upper 2 cm comprise soupy, olive-brown, water-rich marl with high concentrations of foraminifers, and one intact tube of polychaeta. A single echinoderm spine was found at 22 cm. The intensely bioturbated and burrowed interval is again present between 28 and 80 cm. Here silt mixed with mud and coarser shelly material are found in the lighter patchy areas, with reduction spots common. The lower part of section 2 (80.5-105.5 cm) comprises dark mud under the burrowed interval which coarsens downwards, contains a 3.5 x 1.0 cm dropstone at 88 cm, and is increasingly bioturbated towards the base. The interval from 56 to 218.5 cm includes bioturbated greyish-brown marls with some small burrows filled with forams, and dark spots scattered throughout. Burrows become larger towards the base of this unit. The rest of the core (218.5-403.5 cm) shows silty marls with shell fragments, reduction spots, small dropstones (e.g. 258.5 cm) and occasional intact gastropods (e.g. 258 cm). One patch of extremely intensive bioturbation, associated with colour change and mixing of finer material, is observed between 304.5 and 314.5 cm.

Small mound 3

Core TTR7-AT-13G (Fig. 46)

Pelagic core. The core comprises bioturbated greyish-brown to olive-grey foraminiferal silty marls which coarsen downsection, interbedded with some sandy foraminiferal bands. The upper section (0-13 cm) is made up of a soupy greyish-brown sandy marl. From 13 to 83 cm is a bioturbated marl interval with increase in amount of burrows down towards its base. Reduction spots and lithic fragments in burrows are common. The 83-88 cm interval is represented by a planar laminated foraminiferal coarse sand with bioclastic fragments, and laminae correspond to grain-size changes (traction?). The 88-246 cm interval comprises bioturbated grey marls which coarsen and increase in burrowing downsection. Intense burrowing and well-developed vertical systems, which includes a branched network towards its base, are found between 114 and 173 cm. One gastropod was found at 146 cm. This unit appears to correlate with previous cores. The 246-287.5 cm interval comprises grey-brown marls which have an increased proportion of shell fragments, larger forams, reduction spots (manganese precipitates?), and other identifiable bioclastic debris [e.g. bivalve at 249 cm; scaphopod (a type of gastropod) at 271 cm]. The rest of the core comprises dark greyish-brown silty mud with less bioclastic fragments, some sand-filled burrows (342.5 and 347.5 cm), and common reduction spots. Forams were not visible in the lower section (345.5-388.5 cm).

Small mound 4

Core TTR7-AT-14G (Fig. 47)

Coral core. Bands of dead coral concentrations interbedded with olive-grey silty foraminiferal mud with intact and broken coral fragments. The first interval (0-80 cm) comprises ~80% of branching corals with some silt and coral fragments, and a black dropstone (2 cm in diameter) at 21 cm. Silty foraminiferal marl with occasional fragments is found at 80-90 cm. A second band of 80% of branching corals is observed from 90 to 93 cm, with clay and silt matrix. Interval 93-105 cm is silty foraminiferal marl with occasional fragments, and interval 105-112 cm contains up to 80% of

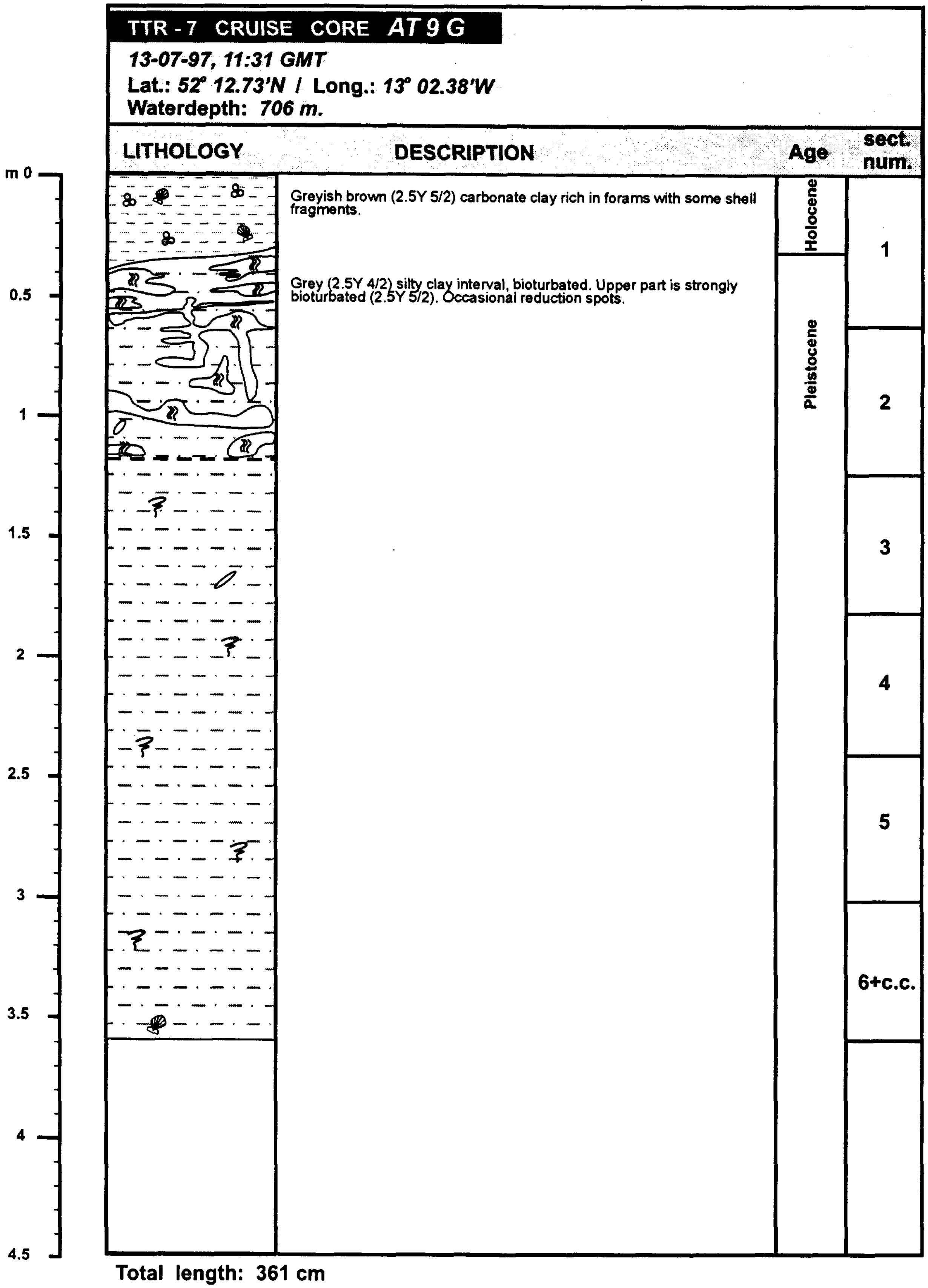

Fig. 42. Core log AT-9G

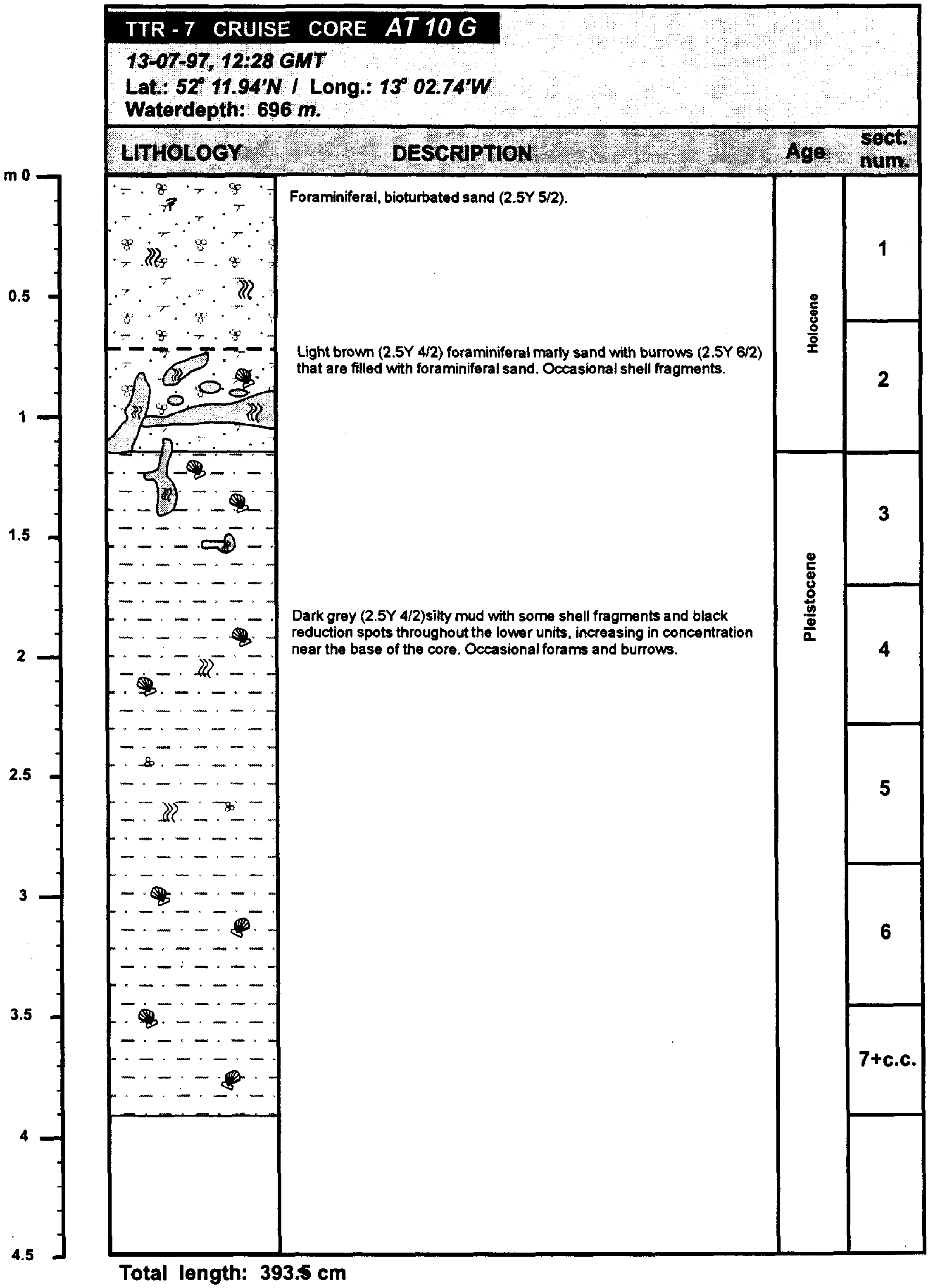

Fig. 43. Core log AT-10G

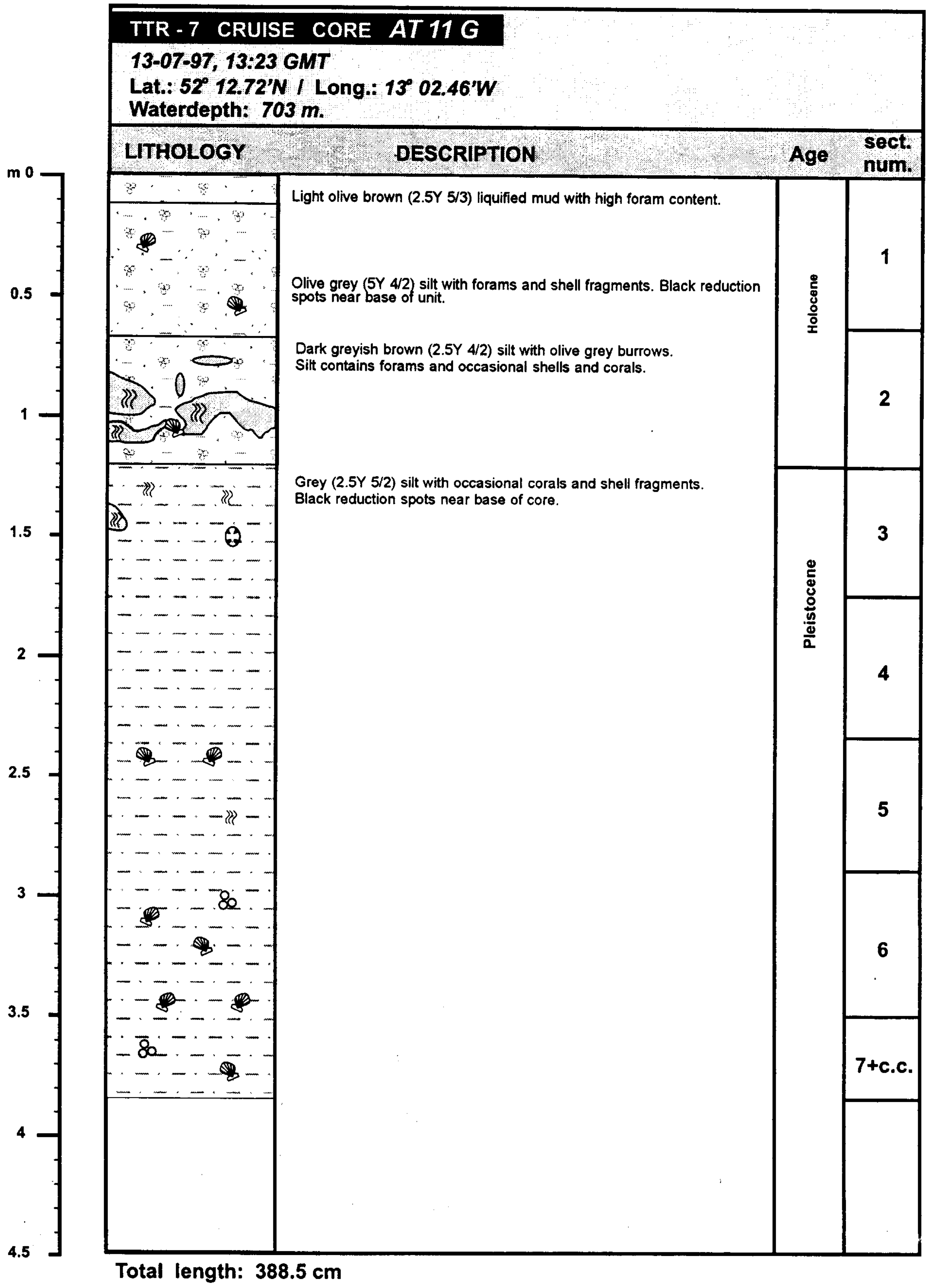

Fig. 44. Core log AT-11G

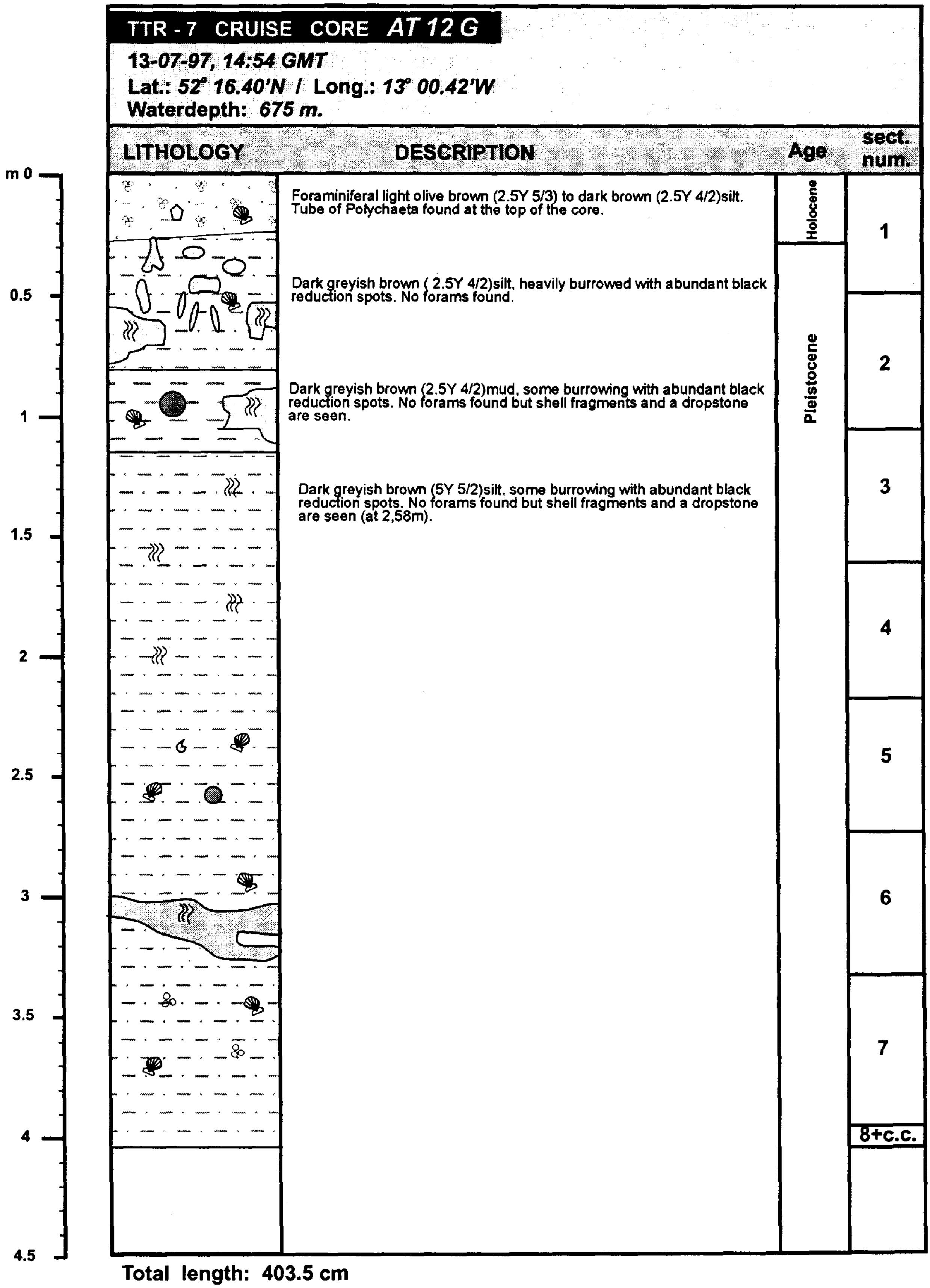

Fig. 45. Core log AT-12G

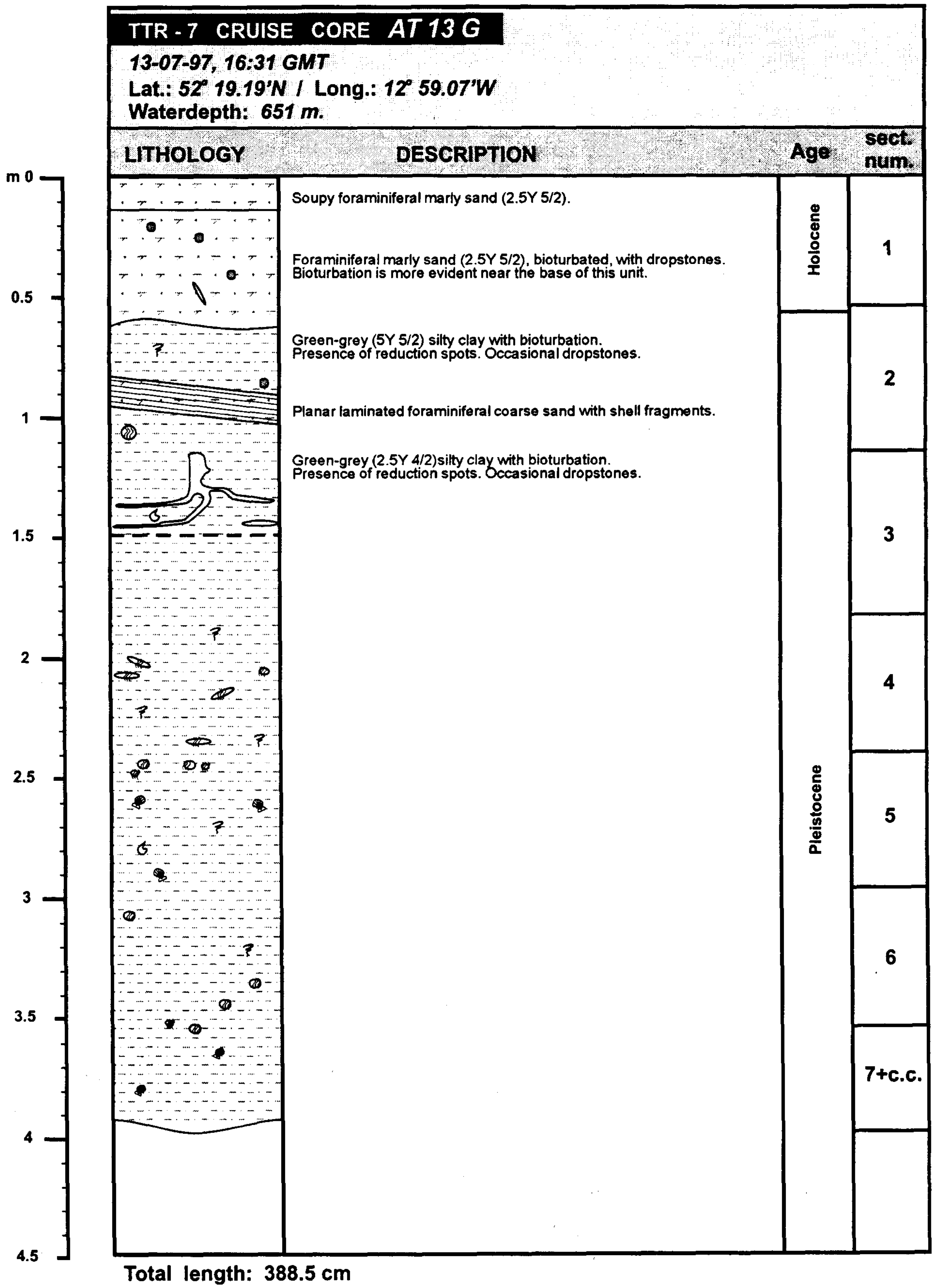

Fig. 46. Core log AT-13G

branching corals in a silty clay matrix. Interval 112-120 cm is silty clay with forams, and interval 120-145 cm is olive-grey clay with about 50% of corals.

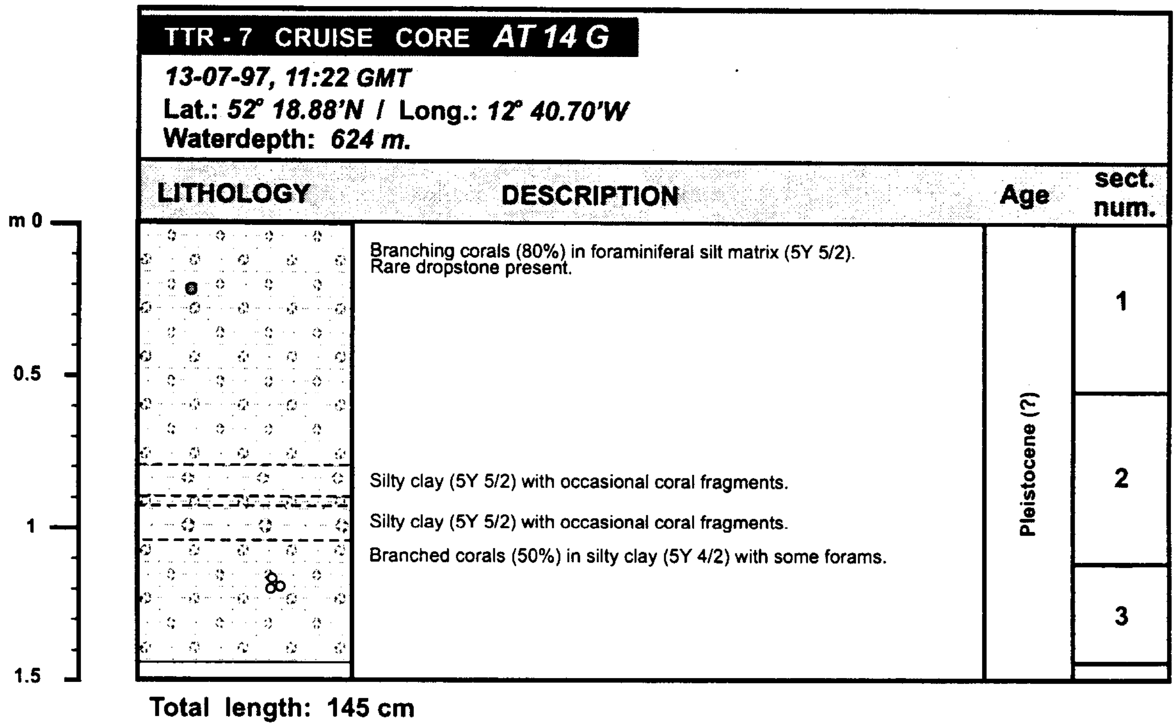

Fig. 47. Core log AT-14G

Large carbonate mound 1

TV-Grab TTR7-AT-15Gr

Large carbonate mound 3

Core TTR7-AT-16G (Fig. 48)

Mixed core with corals and bioturbated pelagic sections. The upper interval (0-3 cm) comprises light brown foraminiferal sandy marl with occasional corals. Intervals 3-15 and 30-89 cm include light olive-brown silty marl. Intervals 15-30 and 89-111 cm consist of coarse, grey to greyish-brown, massive, clast-supported sands with angular coral and other bioclastic fragments. One large (1 cm in diameter) coral was found at 106 cm. Interval 111-205 cm is made up of strongly bioturbated marl with admixture of forams, shell and coral fragments, associated with colour changes, mottling and strong burrowing. Some of the burrows are filled with grey, soupy material. The lowest interval (206-389 cm) comprises greyish-brown to dark and light grey marls which coarsen (foram content) downwards to silty foraminiferal marl. Scattered 'hard black spots' (most likely MnO_2 or pyrite), scattered coral fragments (238, 331, 342, and 344-384 cm), reduction spots, 2-cm diameter gastropods (338 cm), and horizons of shell fragments (297-299 and 325-330 cm), including brachiopods (some in life position) are found in this interval.

Core TTR7-AT-17G (Fig. 49)

Coral core. The core includes alternating light grey and grey foraminiferal marls with coral fragments interbedded with dense bands of unbroken branched corals. The upper interval (0-11 cm) comprises

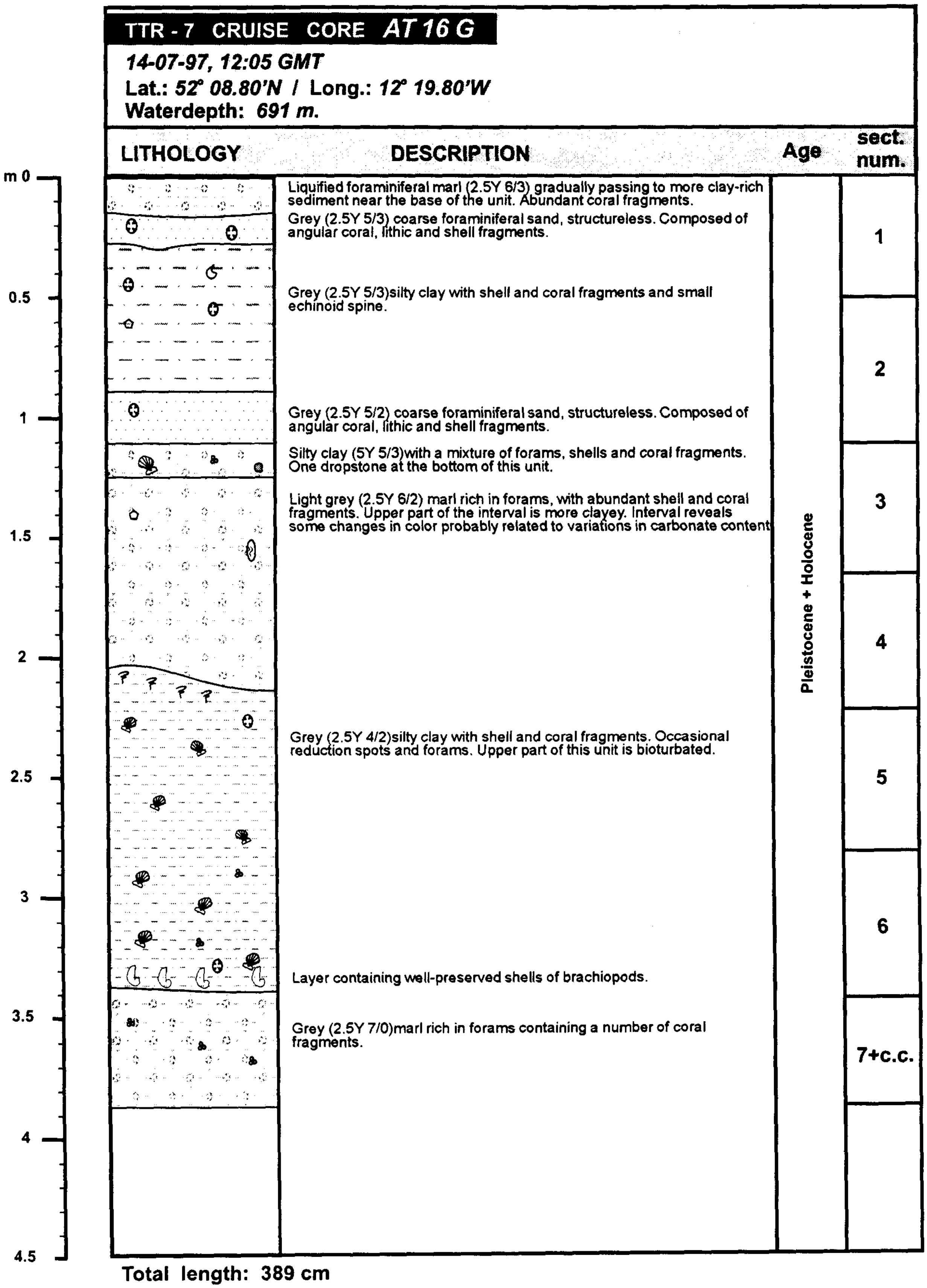

Fig. 48. Core log AT-16G

a pelagic drape of coarse foraminiferal sand with coral fragments up to 5 cm long. Interval 11-42.5 cm consists of light grey marls with shell and coral fragments (less than in the upper layer), which decrease in quantity and size towards the base. Interval 42.5-66 cm includes grey clay with no forams (?) and local broken coral heads. Silt content increases towards the base where a coral density is about 20%. Interval 66-94 cm is grey silty foraminiferal marls with a coral density of about 40%. Interval 94-108 cm comprises grey silty foraminiferal marl with a coral density of about 20%, and interval 108-126 cm is the same lithology but with a broken coral density of about 40%. Bioclastic fragments appear towards the base of the section.

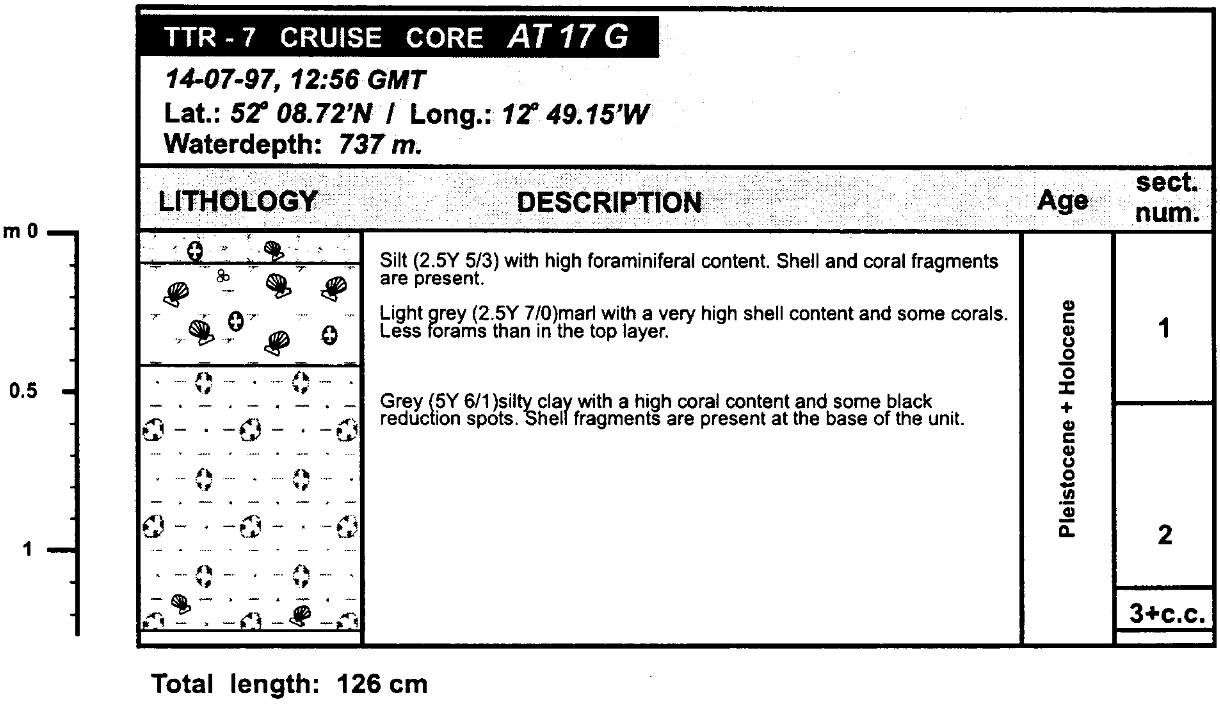

Fig. 49. Core log AT-17G

Core TTR7-AT-18G (Fig. 50)

Bioturbated pelagic core with coral fragments and unusual yellow staining. Interval 0-11 cm comprises dark greyish-brown, medium grained, foraminiferal sand with some small pebbles (dropstones up to 1 cm in diameter) and many shell and other bioclastic debris. Interval 11-24 cm is made up of dark greyish-brown silty mud which fine downwards to clay and contain three 2 cm in diameter black and grey dropstones. Shell and coral fragments are found at the base. Interval 24-58 cm represents the section with yellow staining (olive-yellow, light yellowish-brown, light grey-white), with vigorous bioturbation which we interpret as having been oxidised. The yellow patches have a blue-grey 'halo' around the edges. Bivalves of 1.5-cm diameter are also found scattered through this interval. Interval 58-198 cm comprises bioturbated silty marls with no shell fragments in the upper part, and both shell fragments and echinoderm spines come in at 154 cm.

EASTERN PORCUPINE SEABIGHT

Suspected barrier reef mounds

Core TTR7-AT-19G (Fig. 51)

Pelagic core. Upper interval (0-5 cm) comprises light olive-grey foraminiferal sand with silt. Interval 5-91 cm is a grey bioturbated silty clay with some reduction spots (millimetre scale). Interval 91-120

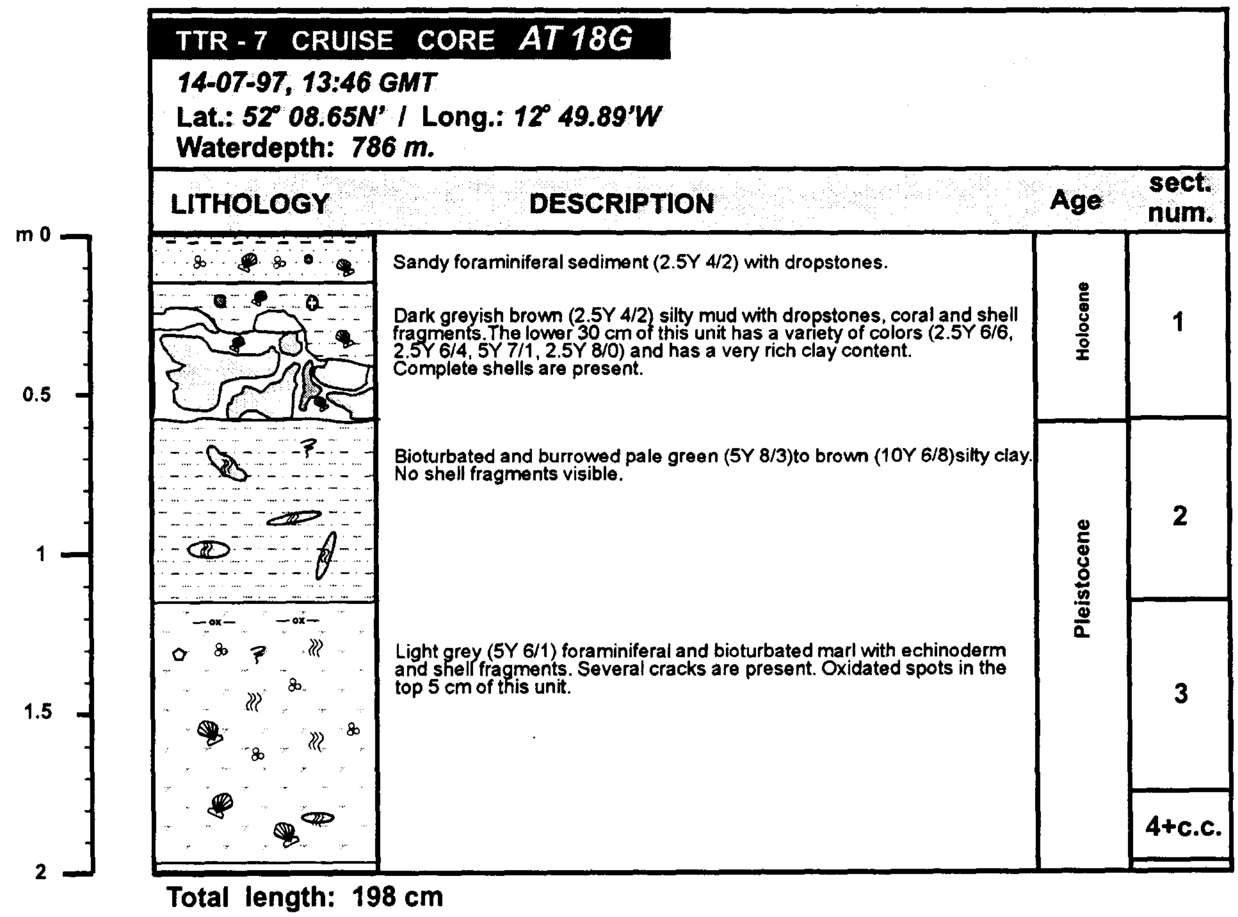

Fig. 50. Core log AT-18G

cm is a grey bioturbated clay with reduction spots. Interval 120-148 cm contains a series of horizontal burrows (*Zoophycos*?), five in total, in the same background grey bioturbated silty clay with reduction spots. Burrows initially looked like laminations. The interval between 148 and 288 cm includes dark greyish-brown silty marl and clay with no obvious bioturbation, though some black spots are seen - most likely representing pyrite. One small shell fragment is encountered at 217 cm. Interval 288-366 cm is more bioturbated dark greyish-brown clay, locally silty, with millimetric reduction spots and locally millimetric shell fragments occur.

Core TTR7-AT-20G (Fig. 52)

Pelagic core. Upper interval (0-4 cm) comprises olive-brown foraminiferal sandy mud. Interval 4-275 cm is a dark greyish-brown to greyish-brown mud with some bioturbation and minute reduction spots scattered through the section (pyrite). Rock fragments are found (33, 72, and 140 cm). Scattered shell fragments are observed through most of the core and become common towards the lower parts of the section. Burrows are also common, particularly between 124 and 275 cm. Burrows are filled with sandy sediment, the best example was seen at 188 cm.

Core TTR7-AT-21G (Fig. 53)

Pelagic core. Interval 0-13 cm includes the usual light olive-brown soupy sandy clay with abundant forams. Interval 13-39 cm comprises grey silty clay with subtle bioturbation marked by a mottled pattern, due to the presence of reduction spots. The interval 39-94 cm continues with the same grey marly clay but burrows are more common and filled with reduced material. One bivalve was found at

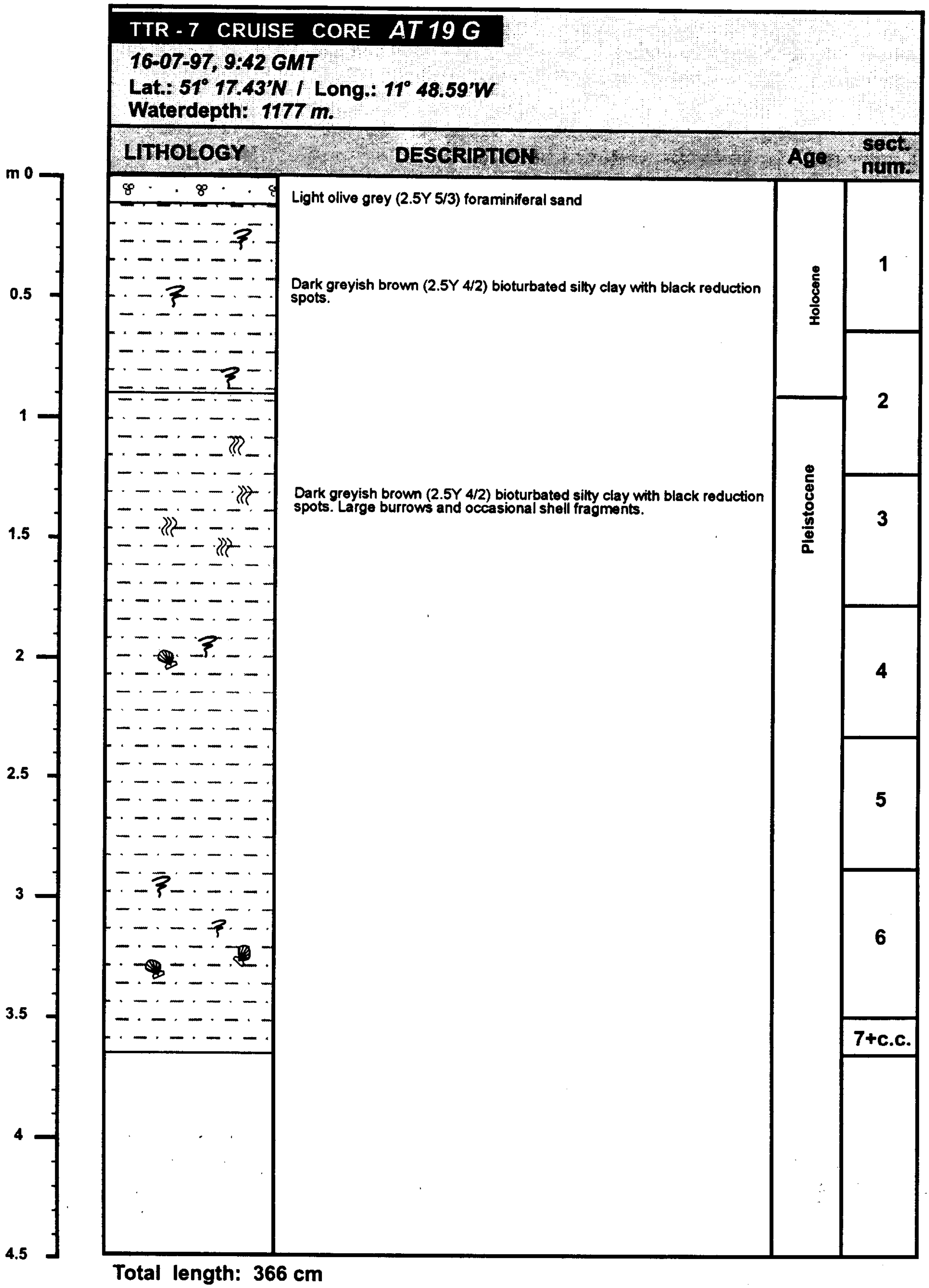

Fig. 51. Core log AT-19G

92 cm. Interval 94-247 cm is grey silty clay with rare burrows and scattered reduction spots. Interval 247-361 cm is bioturbated dark greyish-brown silty clay with various amounts of burrowing and reduction spot mottling. One dropstone was recognized at 262 cm. Shell debris and an increase in reduction spots are observed in the lower 60 cm of section.

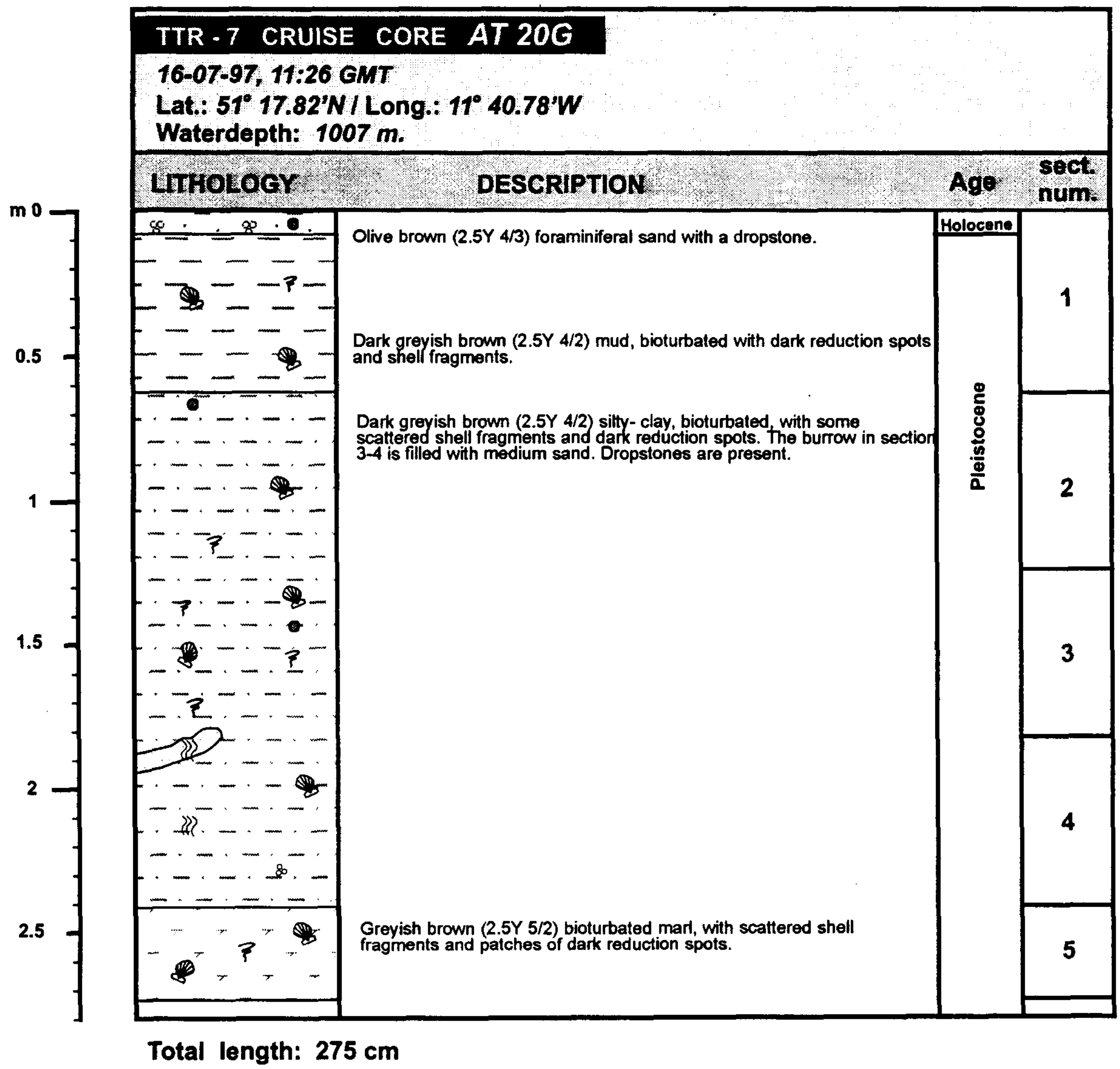

Fig. 52. Core log AT-20G

Core TTR7-AT-22G (Fig. 54)

Pelagic core. Brown silty clay with varying amounts of bioturbation, burrowing, dropstones, dark spots, and bioclastic fragments. Dropstones are found at 22 and 168 cm. A gastropod is found at 199 and a coral fragment at 265 cm. Shell fragments are observed in larger quantities between 298.5 and 349.5 cm.

A group of large ridge-shaped carbonate mounds north of "barrier reefs"

Core TTR7-AT-23G (Fig. 55)

Coral/pelagic core. Upper interval (0-13 cm) comprises a foraminiferal light olive-brown, soupy sand. One well-rounded 1-cm diameter dropstone is found at 10 cm, and the unit is also full of coral

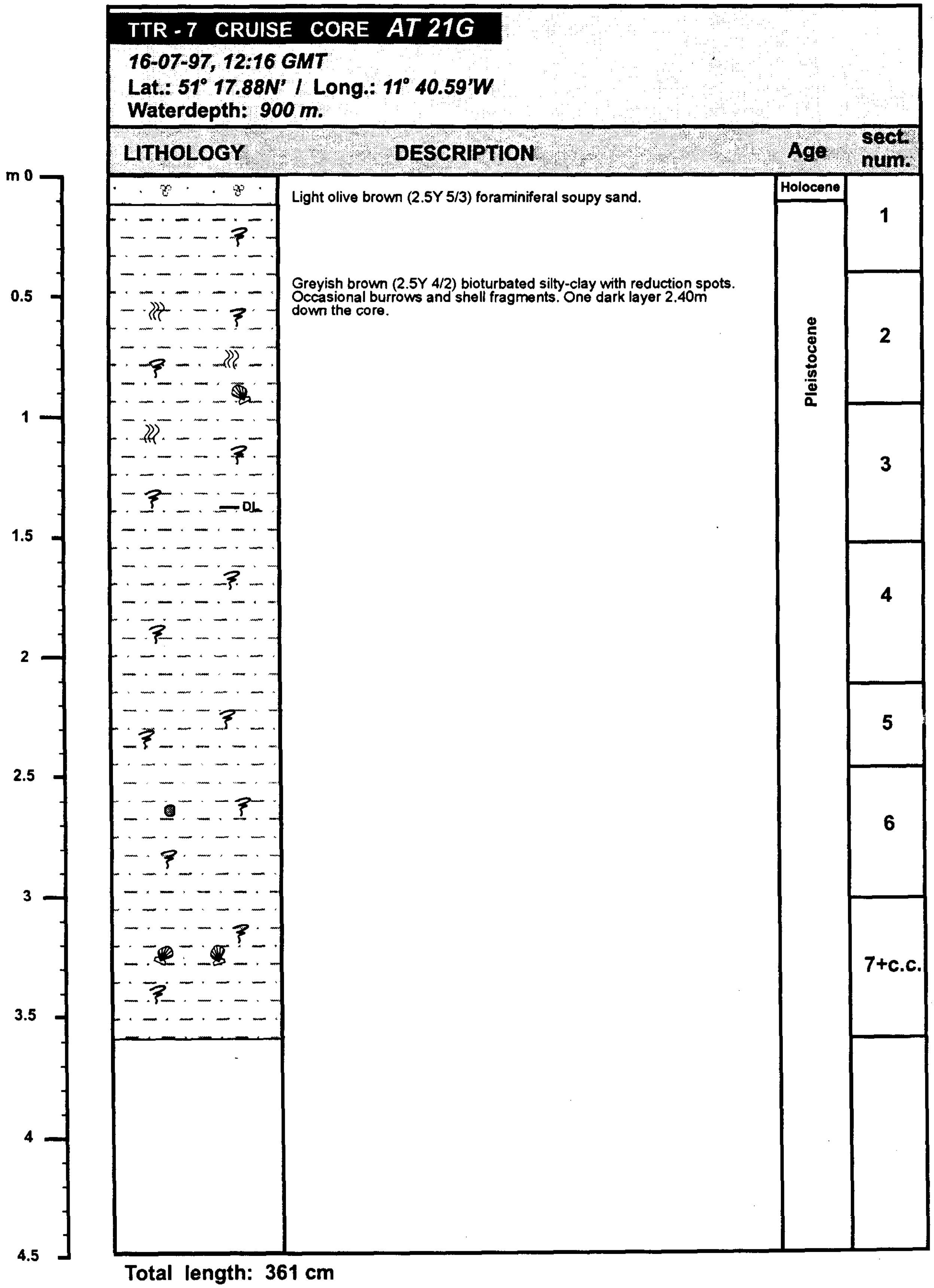

Fig. 53. Core log AT-21G

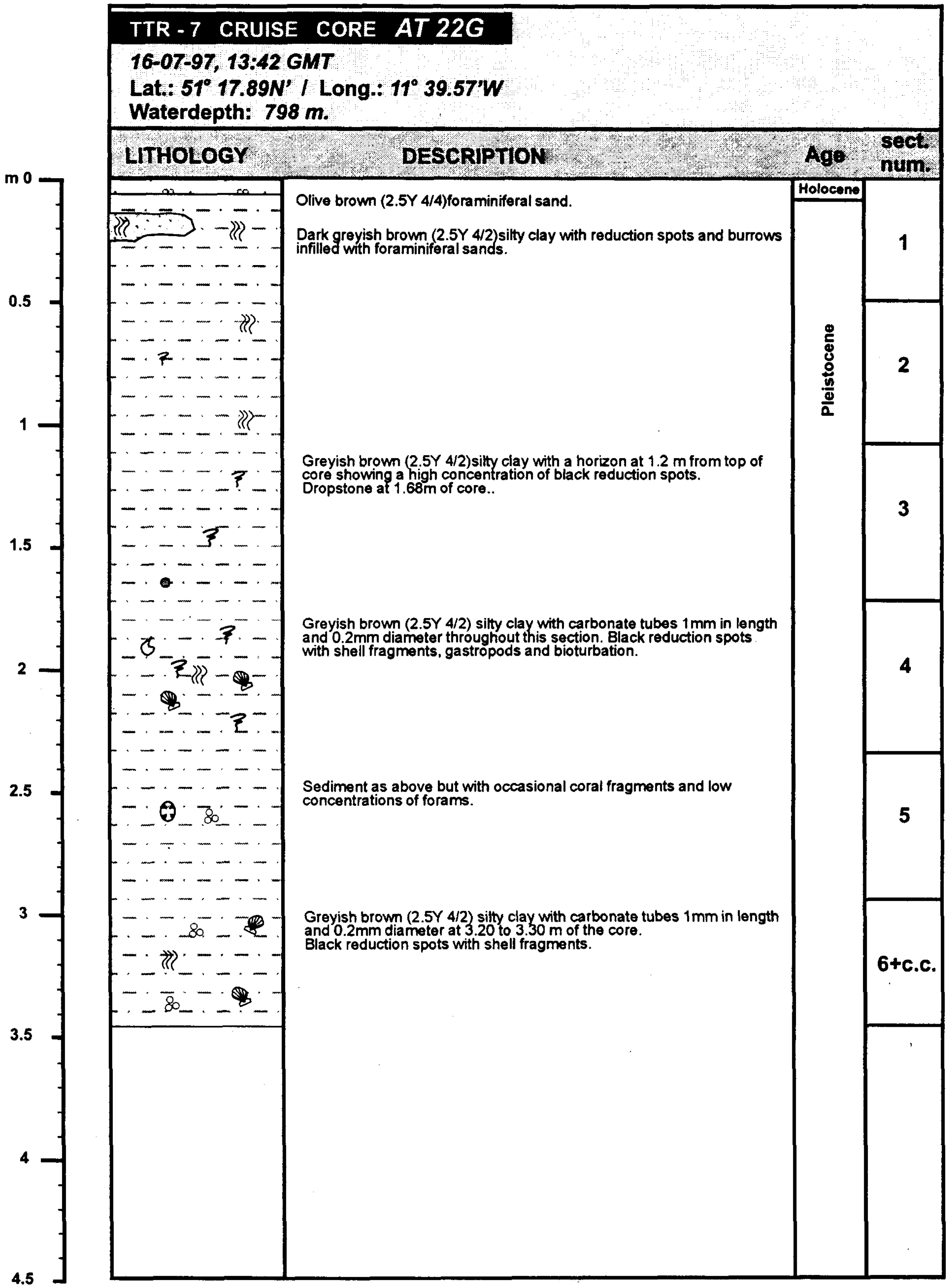

Total length: 349.5 cm

Fig. 54. Core log AT-22G

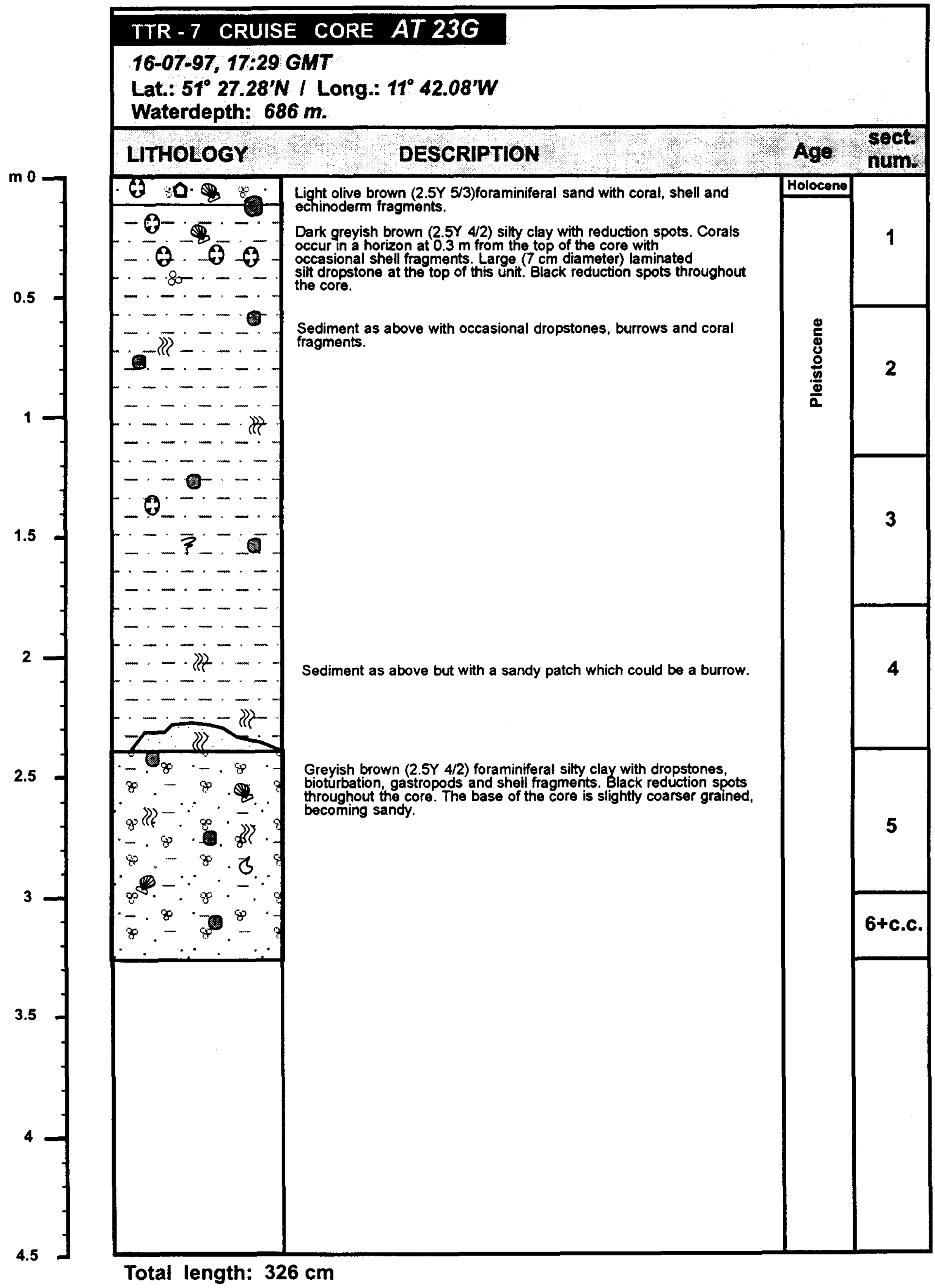

Fig. 55. Core log AT-23G

fragments, small shell fragments and echinoderm spines. A large (7 cm diameter) dropstone (siltstone) is found at 13 cm. Interval 13-235 cm includes dark greyish-brown, greyish-brown to olive-grey silty marl which is locally bioturbated and burrowed. Coral fragments are found at the very top of the unit (15-17 cm), other corals are found at one horizon (30-35 cm), and a solitary coral head at 155 cm. There is a slight increase in foram content and grain size from 35 cm. Some complete bivalves are present (e.g. at 15 cm). Burrows and reduction spots are found scattered through the section. A dropstone is encountered at 126 cm. Interval 235-239 cm comprises a greyish-brown sandy marl. Interval 239-326 cm consists of dark greyish-brown, foraminiferal, bioclast-rich silty clay. Two large dropstones are observed at 239 and 282 cm, and one smaller dropstone of schist (?) at 310 cm. A gastropod is found at 286.5 cm (<1 cm diameter). Reduction spots and some burrowing are also scattered through the section. Grain-size increases from silty mud to medium sand from 313 to 326 cm. One interesting, lighter coloured horizon (reduced?) is found at 314 cm.

Core TTR7-AT-24Gr.

Coral sample. Beige foraminiferal sand about 2 cm thick with many *Madrepora* fragments. They consist almost entirely of a dead assemblage. Only very exceptionally, some living species were collected. Maximum height of *Madrepora* colonies was 20 cm but most of the fragments consisted of single branched pieces less than 2 cm long. Several pieces displayed a ruby-brown colour. Furthermore, echinoid species, crinoids and heavily altered *Lophelia* pieces are present. This sandy layer is underlain by a grey (2.5Y4/2) clayey silt to silty clay without any macroscopic structures. This layer is at least 50 cm thick.

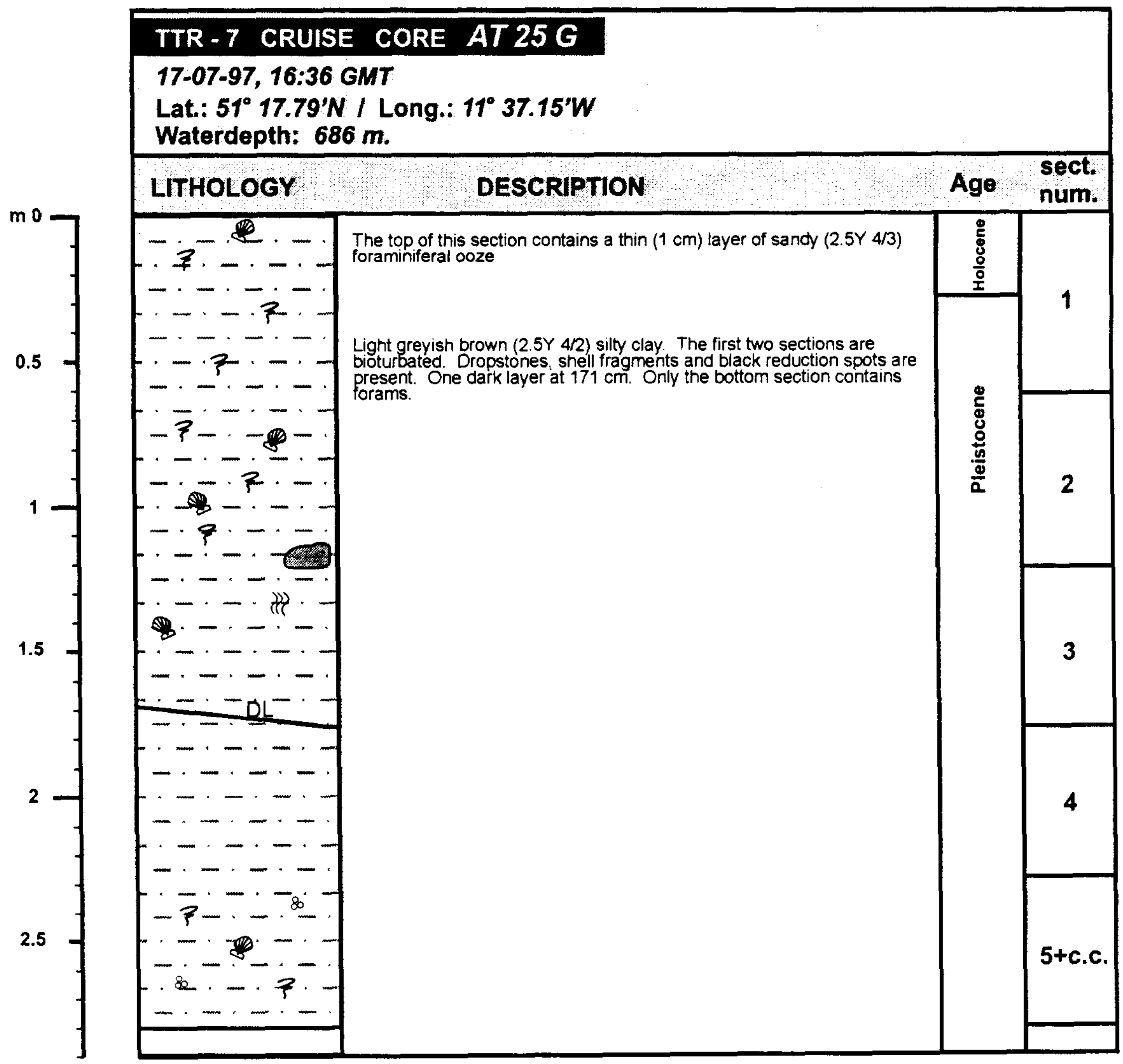

Total length: 281 cm

Fig. 56. Core log AT-25G

Return to the "barrier reefs"

Core TTR7-AT-25G (Fig. 56)

Pelagic core. Dark greyish-brown, massive, structureless clay. The upper section (0-1 cm) comprises an olive-brown, sandy, foraminiferal drape which also includes shell fragments and lithic fragments. The rest of the section shows clays with reduction spots, millimetric and larger shell fragments, one large (9-cm diameter) dropstone at 114.5 cm, bioturbation and burrows with coarser fills throughout, and a dark organic layer at 172 cm. Becomes more silty towards the base.

Core TTR7-AT-26G (Fig. 57)

Pelagic core. The upper 0-3 cm comprises an olive-brown sandy interval with forams and bioclastic (and lithic?) fragments. The rest of the core consists of dark greyish-brown clays which become siltier down section. Dropstones are found at 44 cm (shale fragment), 214 cm (1-mm diameter, quartz), and 214 cm (1-mm diameter, black-coloured). Bioturbation varies in intensity through the core, and shell fragments are rarer.

SOUTHERN PORCUPINE SEABIGHT: GOLLUM CHANNEL SYSTEM

Middle reaches

Core TTR7-AT-27G (Fig. 58)

Pelagic core. The upper section (0-14 cm) comprises light brown soupy foraminiferal, bioturbated marl. The rest of the core is represented by interbedded light grey to grey marls and dark grey clays with local silty clays. The marls are usually bioturbated with scattered reduction spots. Green tinges or layers are present at 18-20 and 111 cm. Bioturbation is most intense between 72 and 87 cm, where horizontal burrows are seen. Two horizontal burrows are observed at 98 and 103 cm. Sections lower down have slightly less bioturbation. Shell fragments increase downcore, as does the foram content. One silty clay layer occurs at 107-114 cm, with one small dropstone and some coarse sand mixed in. Two other small dropstones (0.3 cm) are found at 286 cm, associated with a burrow.

Core TTR7-AT-28G (Fig. 59)

Pelagic core. This core consists of three main packages. The uppersection (0-47 cm bsf) includes light brown foraminiferal marl (0-13cm) overlying light brownish-grey foraminiferal marl. This unit is heavily bioturbated and oxidized. Towards the base, forams are concentrated in burrows, and a layer of green mineralization occurs at 15 cm depth. The second section (47-124 cm) consists of dark greenish-brown bioturbated silty clays with foraminifera and abundant *Zoophycos* burrows. A small layer with high ice-rafted debris (IRD) content is present at 89 cm depth. The third section (124-334 cm) comprises a grey silty clay with reduction spots. A dropstone is found at 232 cm, and a layer of dropstones and high IRD content is found between 269 and 280 cm. A layer of green mineralization is found at 320 cm depth.

Core TTR7-AT-29G (Fig. 60)

Pelagic core with turbidites. This core can be divided into three main packages. The upper section (0-58 cm depth) consists of an oxidized pale-brown, bioturbated marl with foraminifera infilling burrows (0-13 cm) overlying a light grey, bioturbated marl (13-58 cm) with foraminifera and layers of green mineralization at 28, 31, 42, and 50-54 cm depth. The second section (58-159 cm) includes a light olive-grey marl with foraminifera and a dropstone at 92 cm depth. Below 159 cm, is a bioturbated grey silty clay with reduction spots and numerous turbidites. The turbidites usually consist of a foraminiferal sand with an erosive base fining up into mud and are usually approximately 10 cm thick.

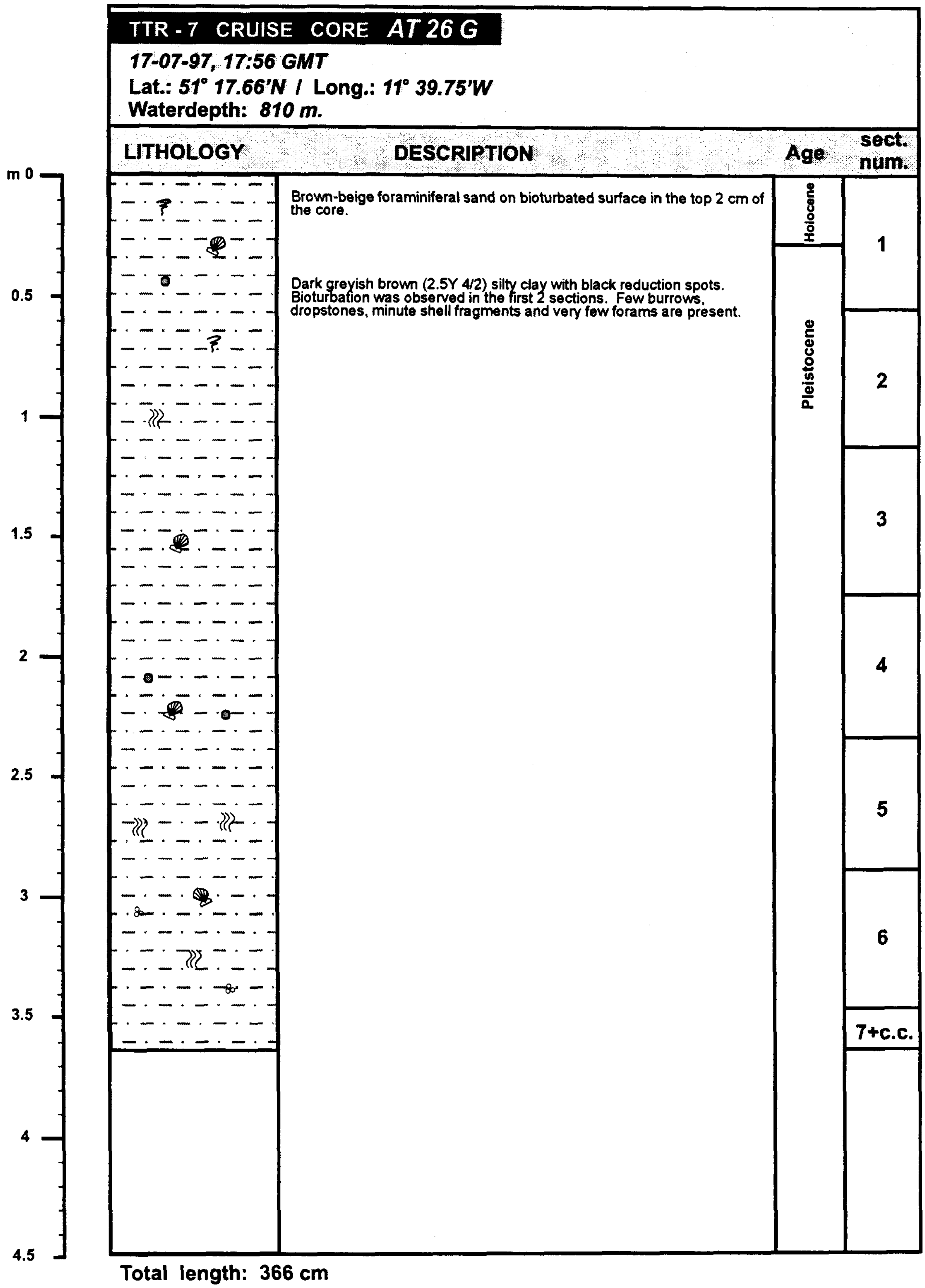

Fig. 57. Core log AT-26G

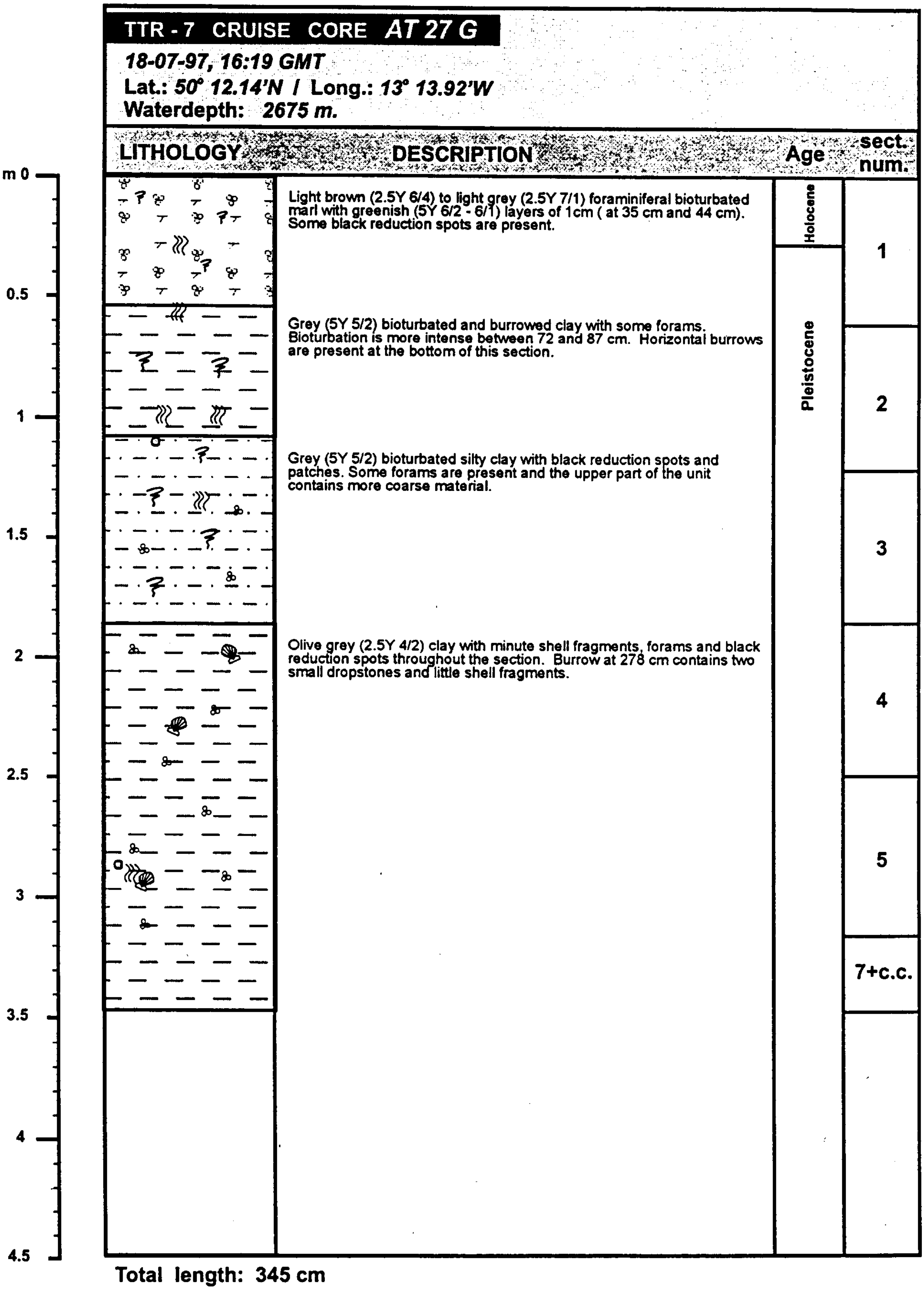

Fig. 58. Core log AT-27G

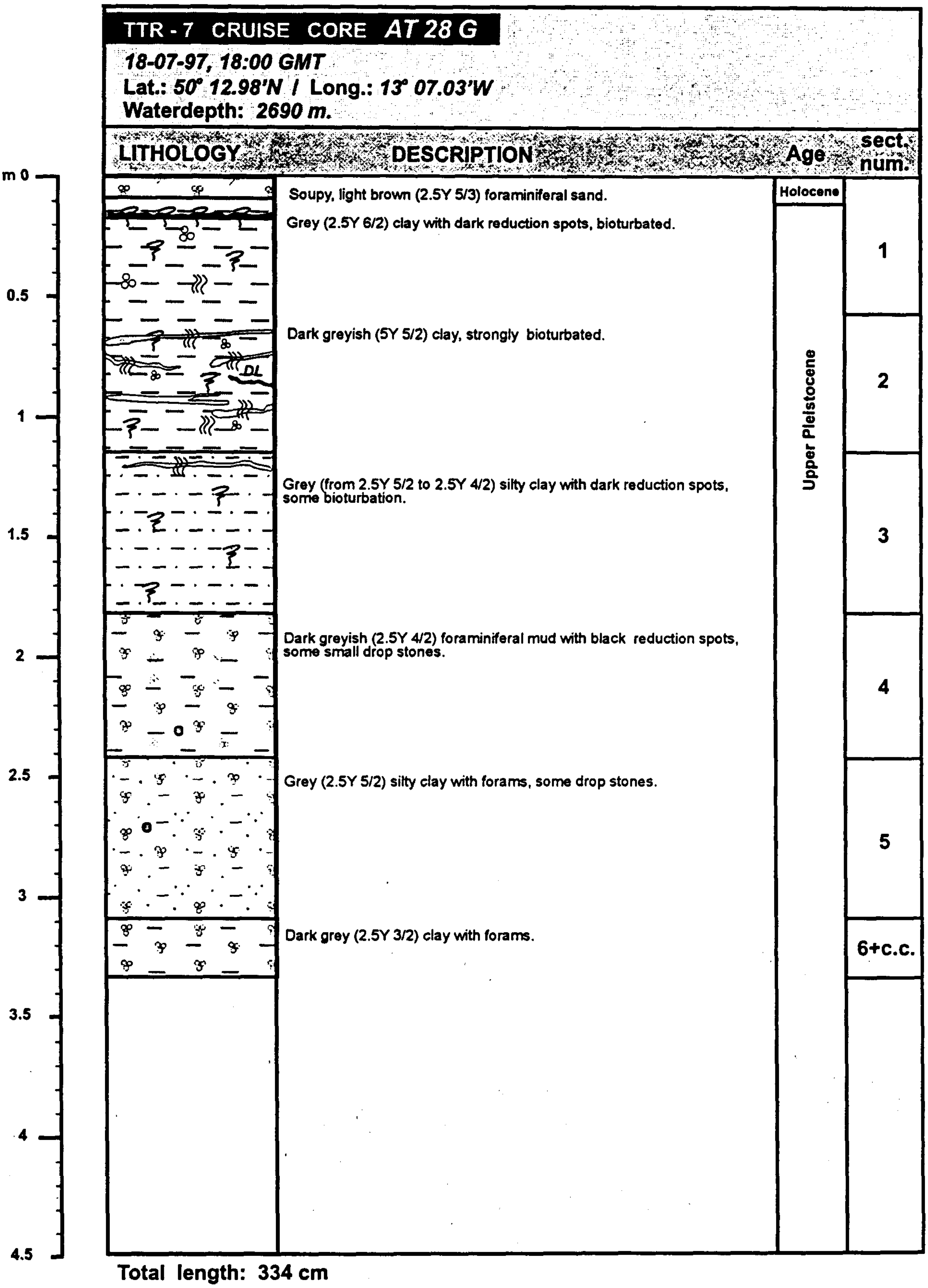

Fig. 59. Core log AT-28G

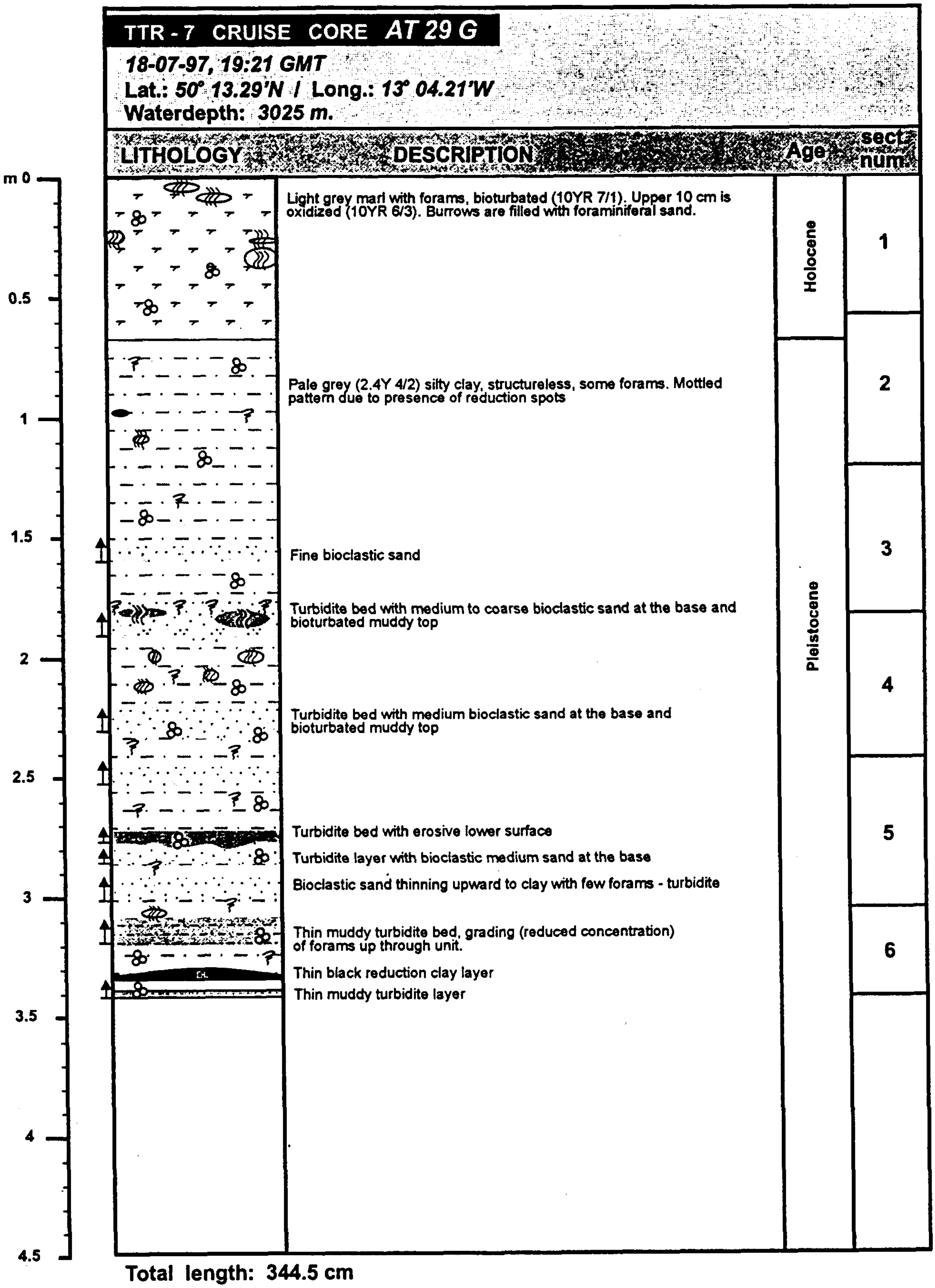

Fig. 60. Core log AT-29G

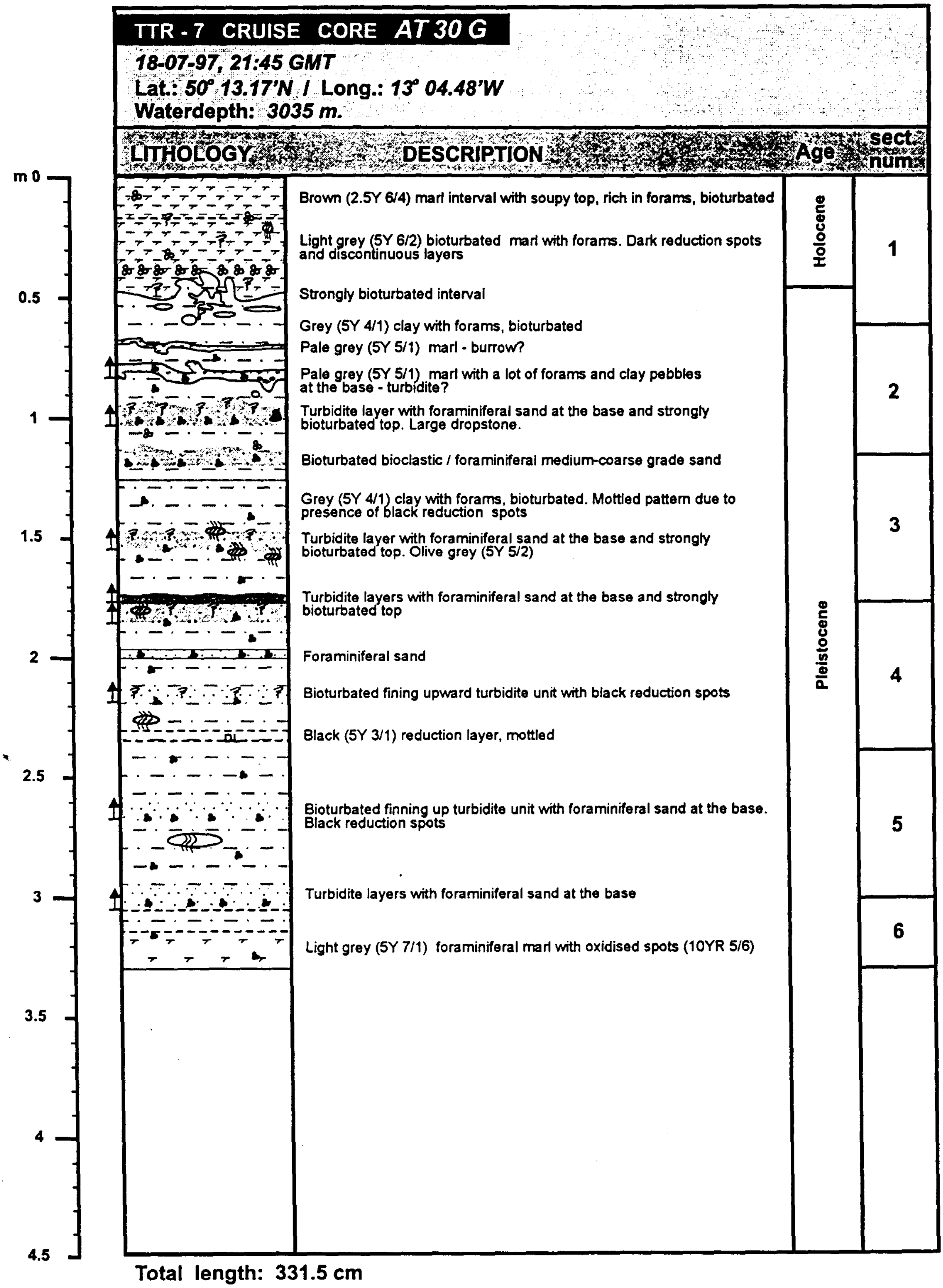

Fig. 61. Core log AT-30G

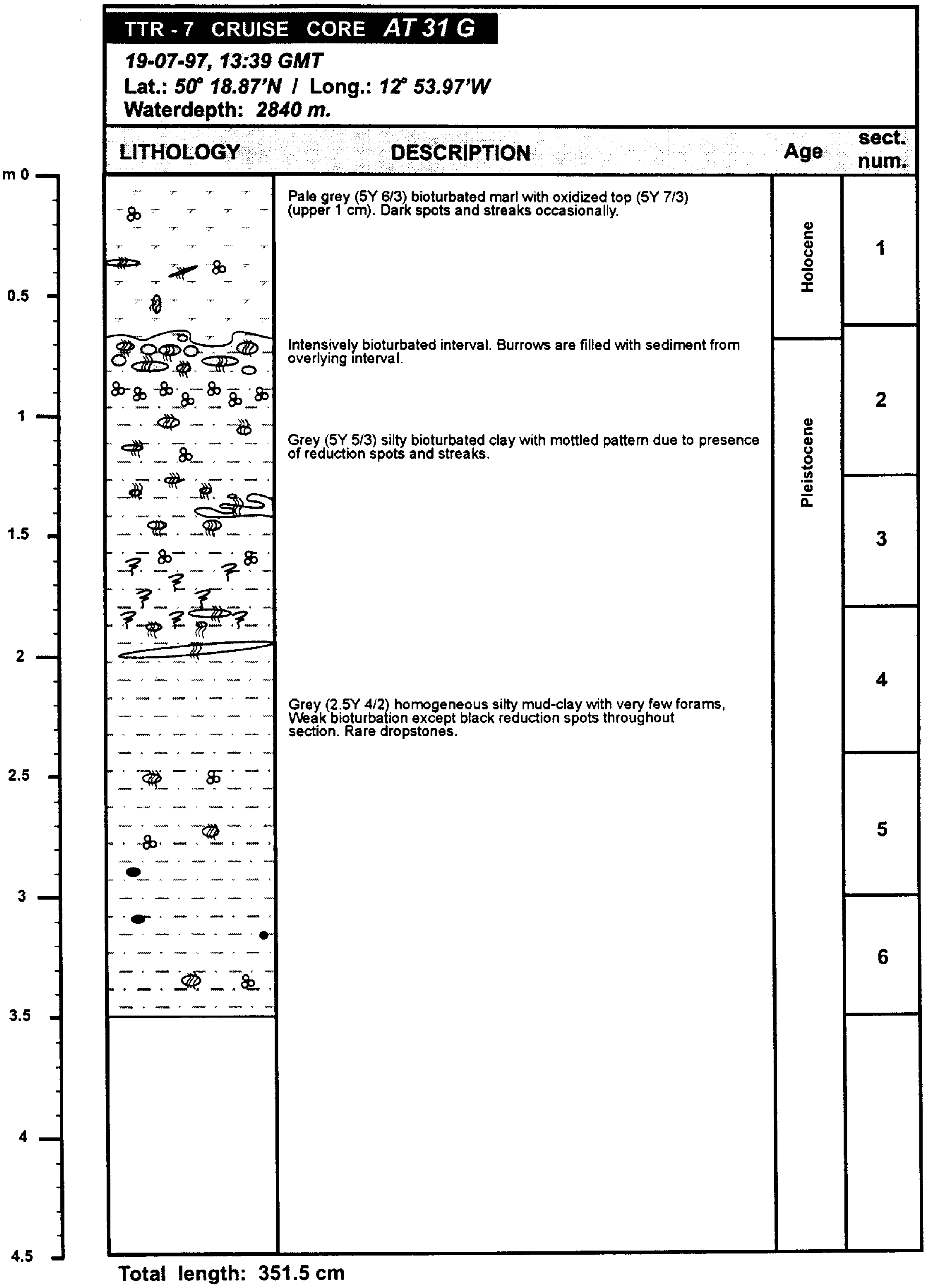

Fig. 62. Core log AT-31G

The bases of turbidites occur at 183, 194, 233, 255, 279, 288, 303, 321, 324, and 344 cm depth. Black reduced layers occur at 291 and 336 cm.

Core TTR7-AT-30G (Fig. 61)

Pelagic core with turbidites. This core consists of four main packages. The upper oxidized section (0-48 cm) is made up of a bioturbated brown foraminiferal marl overlying a grey bioturbated marl with foraminifera. A layer of green mineralization occurs at 24 cm, and a layer of foraminiferal sand occurs at 40 cm. The second section includes a grey bioturbated silty clay with turbidites. The turbidites consist of foraminiferal sands with erosive bases fining upwards into mud which is bioturbated at the tops. The average thickness of the turbidites is 10 cm. Turbidite bases occur at 102, 119, and 155 cm. A layer of green mineralization exists at 68 cm, and a thin layer with high IRD content is observed at 134 cm. The third section (160-307 cm) represents a grey silty clay with bioturbation, reduction spots, and turbidite units. Turbidites are comparable with those occurring higher up the core. Turbidites are approximately 10 cm thick and are found at 155, 179, 187, 219, and 261 cm depth. A black reduced layer is encountered at 236 cm. The fourth section (307-331 cm depth) consists of an oxidized light grey foraminiferal marl.

Core TTR7-AT-31G (Fig. 62)

Pelagic core. This core includes three main packages. The upper section (0-58 cm) consists of pale-grey bioturbated marl with occasional reduction spots. The second section (58-155 cm) comprises bioturbated dark clayey marl which is intensely bioturbated between 66 and 92 cm. The third section (155-351 cm depth) is olive grey silty clay with reduction spots. Green mineralization layers are abundant at the top of the section (156, 159, 161, 167, 170, 172 and 178 cm) and dropstones occur at 291 and 321 cm depth.

Core TTR7-AT-32G (Fig. 63)

Pelagic core. This core consists of pale-brown oxidized foraminiferal marl overlying grey foraminiferal marl. Grains of fine sand were found at the base of this marl.

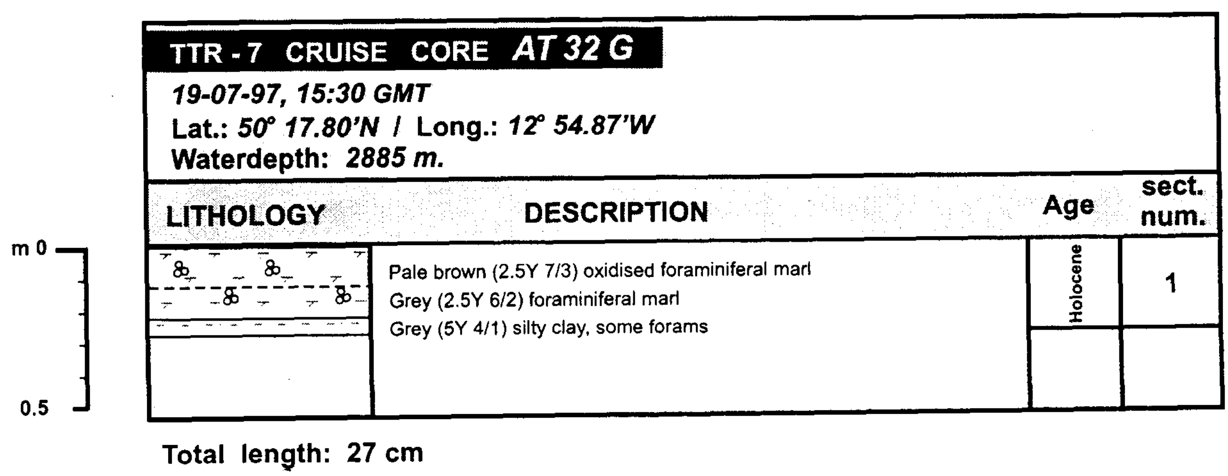

Fig. 63. Core log AT-32G

RETURN TO THE EASTERN PORCUPINE SEABIGHT

"Barrier reefs"

Core TTR7-AT-33G (Fig. 64)

Pelagic core. Thin brown soupy Holocene drape with forams (0-3cm). The rest of the core comprises greyish-brown, silty clays and marls with reduction spots, bioturbation and scattered fragments of shell and other bioclastic debris. One echinoid spine base was found at 84 cm.

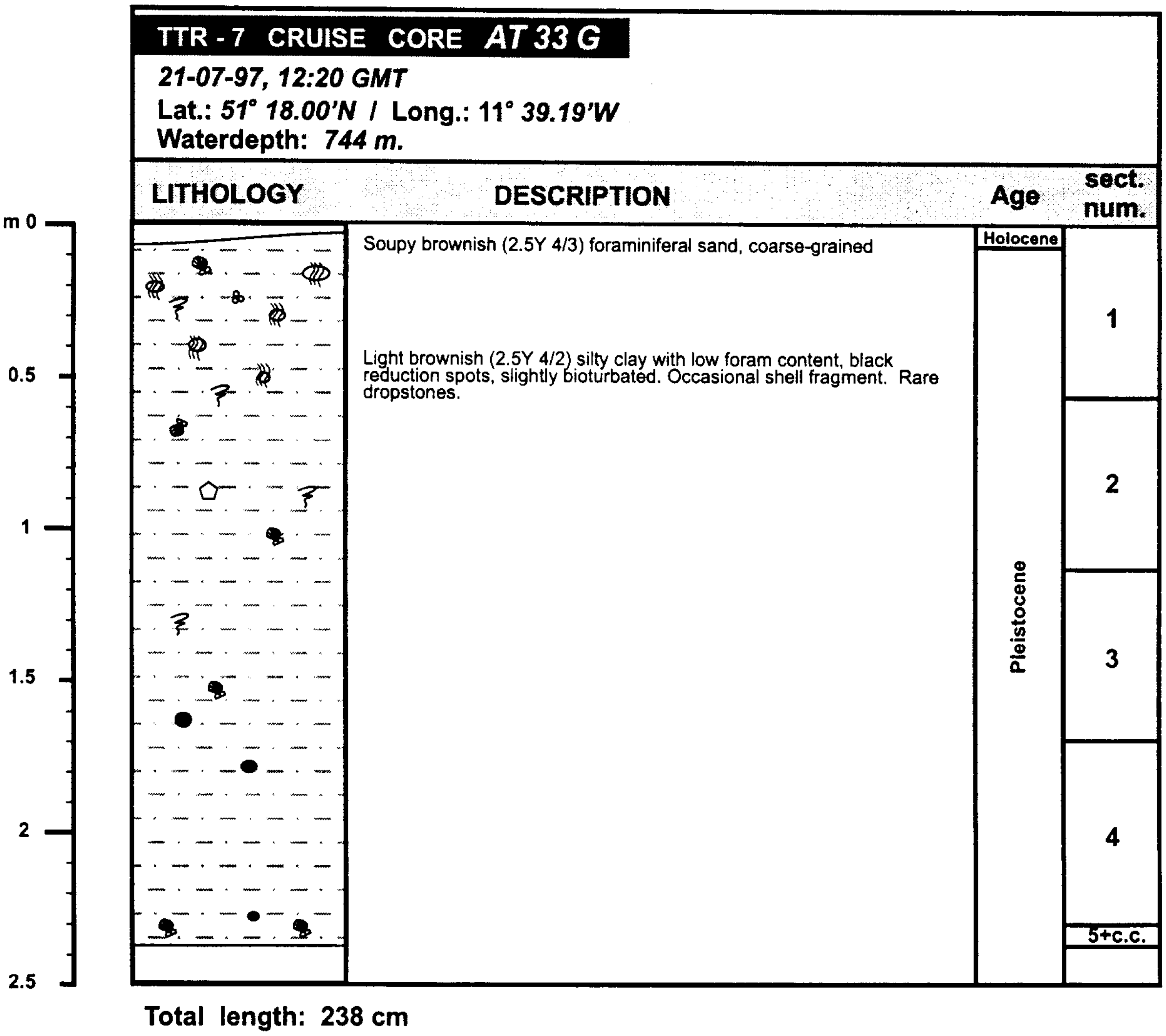

Fig. 64. Core log AT-33G

Core TTR7-AT-34G

No recovery. Core catcher contained a handful of dead, broken *Madrepora* corals. Also, and most importantly perhaps, we recovered some coarse sand. Under the handlens, this consists of ~40% transparent quartz, ~20% milky-white quartz, ~20% lithic fragments (black or green-grey in colour, probably dropstone material) which were very similar to those found in the grab samples, and ~20% bioclastic fragments (mainly shell fragments). No forams were found.

Core TTR7-AT-35G (Fig. 65)

Coral core. The core comprises three intervals. The 0-21 cm interval is a greyish-brown marl with corals, coral fragments, and dropstones up to 1.5 cm in diameter. The 21-72 cm interval is light grey to grey marl with corals, coral fragments and dropstones. A very large dropstone occurs at 61.5 cm (6 cm in diameter). The upper and lower boundaries are sharp but highly irregular (diagenetic fronts) marked by colour changes alone. The rest of the core, with a few exceptional patches, comprises lighter grey marl with corals, coral fragments, and other bioclastic debris. This is typical carbonate mound facies without interbedding of coral masses with muddier intervals.

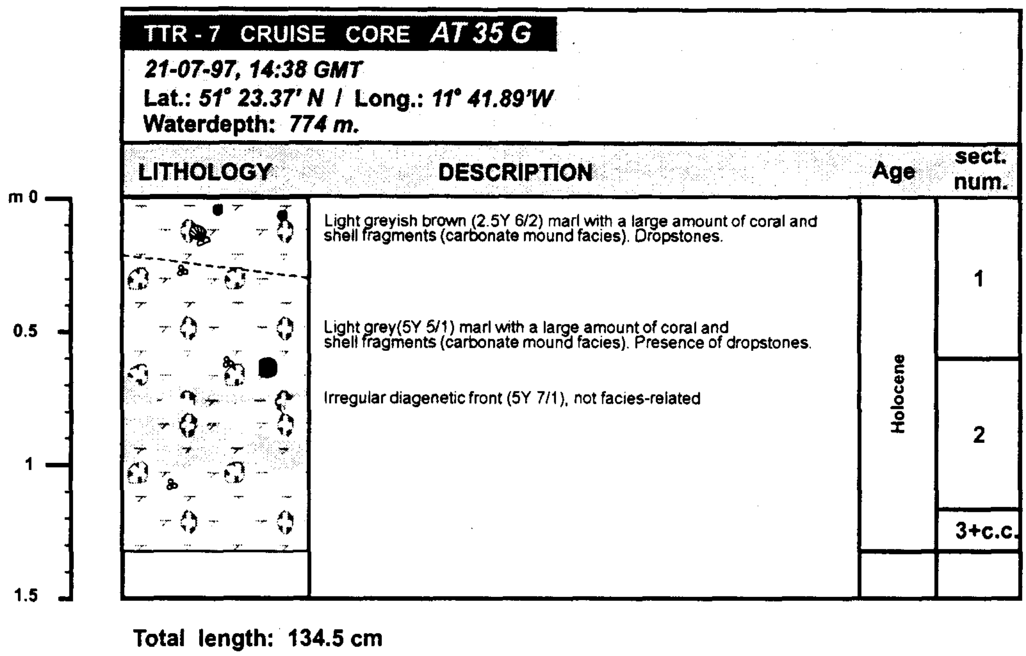

Fig. 65. Core log AT-35G

Core TTR7-AT-36G (Fig. 66)

Pelagic core with sand drape at the seafloor. The core is thought to have missed any of the main dunes seen on ORAT5. The upper 2 cm comprises coarse olive-brown sand which is also oxidized. No Holocene marl is present. The core was recovered with the seafloor intact, and a *Polychaete* cast was present on the upper surface. The rest of the core includes dark grey silty clay, mildly bioturbated, with scattered reduction spots, some broken shell detritus (e.g. at 181 cm). A charcoal dropstone was found at 308 cm. Scattered millimetric shell debris and forams become more common towards the base of the core.

RETURN TO THE SOUTHERN PORCUPINE SEABIGHT

Gollum Channel head

Core TTR7-AT-37G

No recovery. Traces of sand. No mud is present. Two attempts were made at this site.

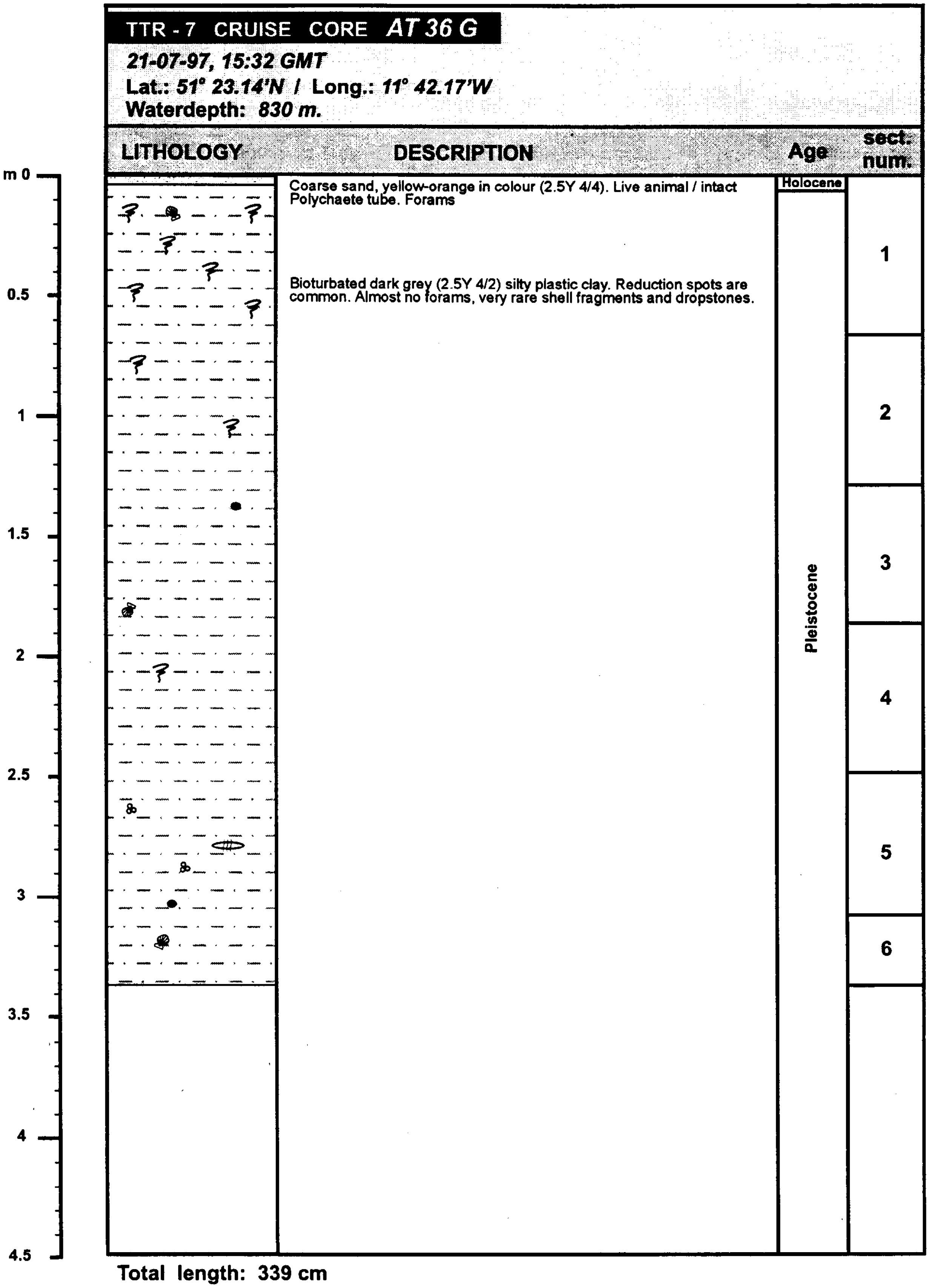

Fig. 66. Core log AT-36G

Core TTR7-AT-38G

No recovery. Sand in the core-catcher. No mud recovered.

Core TTR7-AT-39G (Fig. 67)

Pelagic core with a drape of gravelly sand at the top of the first section.

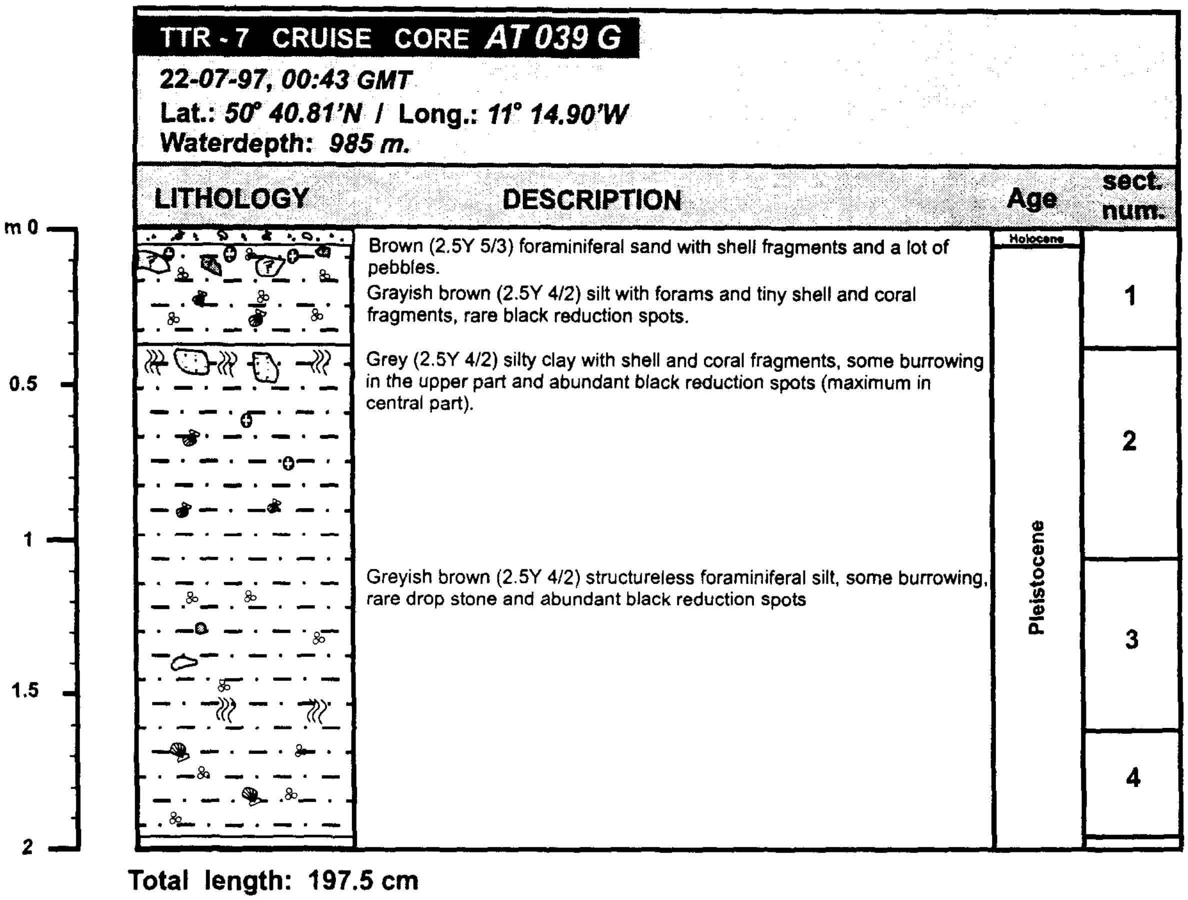

Fig. 67. Core log AT-39G

Core TTR7-AT-40G (Fig. 68)

The core comprised three units, here named A (unconsolidated Holocene pelagic sediment), B (Pleistocene hemipelagite) and C (debris flow deposit). The top 6 cm of the core (Unit A) comprised a light-brown, soupy foraminiferal ooze. From 6 cm -51 cm below core-top, the composition was largely a structureless, homogenous light-grey mud/clay (Unit B) with some recent bioturbation structures. From 51 cm below core-top, Unit C had been heavily bioturbated, but was now infilled with material from Unit B. Below this area of bioturbation, there was a dark-grey clay clast of 15 cm in length, with a width at least as wide as the core (14 cm). Wavy internal laminae were present in the clast, running at an oblique angle to other laminae present in the core. The clast itself was bioturbated, and now infilled with sediment from Unit B. Bioturbation continued from below the clast to 125 cm below the core top. With the exception of the bioturbation features already mentioned, Unit C displayed few structural features from below the clast to 115 cm below the core top. However, below 115 cm from core-top, several microfaults were apparent. These were especially evident at 115 cm and 207 cm below the core-top, where an offset of about 1 cm was seen in both cases. Continuing to the base of the core, Unit C was interbedded with 5 darker grey mud/clay bands that ranged in width from 10 cm to 1 cm (average approximately 5 cm). Both the lighter and darker grey bands within Unit C (from 115 cm below core-top to the core base) displayed disturbed and wavy laminae, with indistinct and patchy dark material (organic?) throughout.

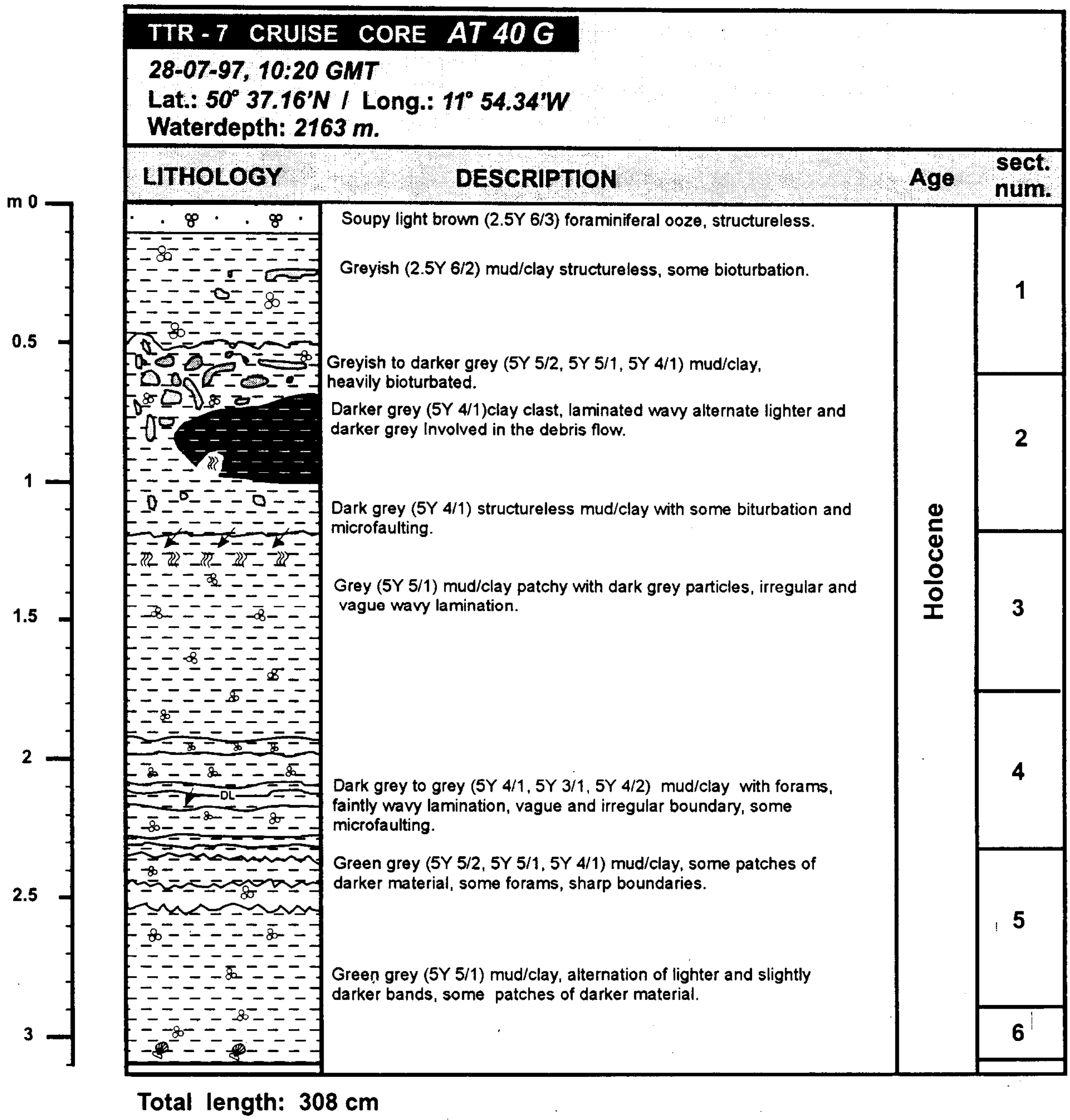

Fig. 68. Core log AT-40G

INTERPRETATION OF CORES FROM MIDDLE GOLLUM CHANNEL

A. Wheeler, S. Zaragosi, and A. Sautkin

A series of gravity cores (AT27G to AT31G) where retrieved from the Gollum Channel and levees in order to infer turbidite activity in the Gollum Channel and elucidate the magnitude and style of the preserved turbidites. The cores were taken in two transects, which were coincident with lines ORAT-6 and ORAT-7. Core AT27G was taken from the levee of the Gollum terrace in an attempt to sample overbank turbidite activity. The ORAT6 profiler record, terminating about 3 km east of this side, reveals an about 5 m thick cover of layered sediment covering more chaotic reflectors. The gravity core sampled the upper layered unit and showed it to be composed of a hemipelagic mud sequence with the absence of turbidites. Core AT28G was located on the northwestern terrace of the Gollum Channel, adjacent to the main channel. It was hoped that this core would display overbank turbidite activity, but, again, it sampled a hemipelagic sequence devoid of turbidites. Two attempts were made to sample the thalweg of the channel (AT29G and AT30G) but, due to problems in positioning, the gravity core retrieved sedimentary sequences from the flanks of the channel. These cores, however, did record a sequence of turbidites interspersed with hemipelagic sediments. The two remaining cores (AT31G and AT32G) were also targeted for the thalweg of the Gollum Channel, but further north and basing on ORAT7 data, in order to determine any spatial variability in channel activity and in an attempt to improve the probability of sampling the channel thalweg. Due to a wrong positioning, Site AT31G missed the thalweg, and the core was taken from a high on the flank of the channel. This recorded a hemipelagic sequence devoid of turbidites. Site AT32G made a direct hit on the thalweg, although the core recovery was poor, with only 22 cm of hemipelagic sediment retained in the core. Observations of material in the core catcher and of water issuing from the core as it was taken on the deck, indicated that the corer penetration and the suspected loss of the material may be caused by an underlying sand unit. This is in accordance with the interpretation for the OREtech sidescan sonar data.

Sedimentary features

The upper sections of all cores revealed a foraminiferal marl whose micropalaeontological characteristic testifies to a Holocene age. This upper section was often highly bioturbated and light brown in colour, suggesting oxidation. A "geochemical front" was often evident between oxidized and reduced sediments which frequently had a dark colour with an occasional greenish hue. Green horizons were observed in numerous levels in the cores and were interpreted as former oxic/reduction "fronts" where mineralization had occurred. At depth, it appeared that this mineralization had the ability to partially lithify the sediment. The mineralization was sometimes associated with the upper, or more usually, lower contact of a thin lithological unit, although normally there was no determinable lithological variation across the zone of mineralization. Layers of mineralization were characteristically around 1 cm thick.

Apart from the turbidites which are described below, lithological variations also occurred due to the incorporation of ice-rafted debris. In some cores, isolated dropstones were present, although often a bed of coarse sands and silts with dropstones was preserved. Turbidites rarely contain sand-sized material and are composed of reworked hemipelagic mud. Sorting within the turbidite flows results in the concentration of foraminiferal tests at the base of the flows which occasionally preserved an erosive base. The concentration and size of foraminiferal tests decrease upwards as the flow velocity of the turbidity current decreases, with the result that the turbidite grades upwards into silty clays and structureless clays. The top of the turbidite unit is often bioturbated. The turbidites can all be ascribed to Bouma's Td and Te sub-divisions (Bouma, 1962), with modification made for the absence of silt and the presence of foraminiferal lagged bases. Turbidites typically reach a thickness of 10 cm.

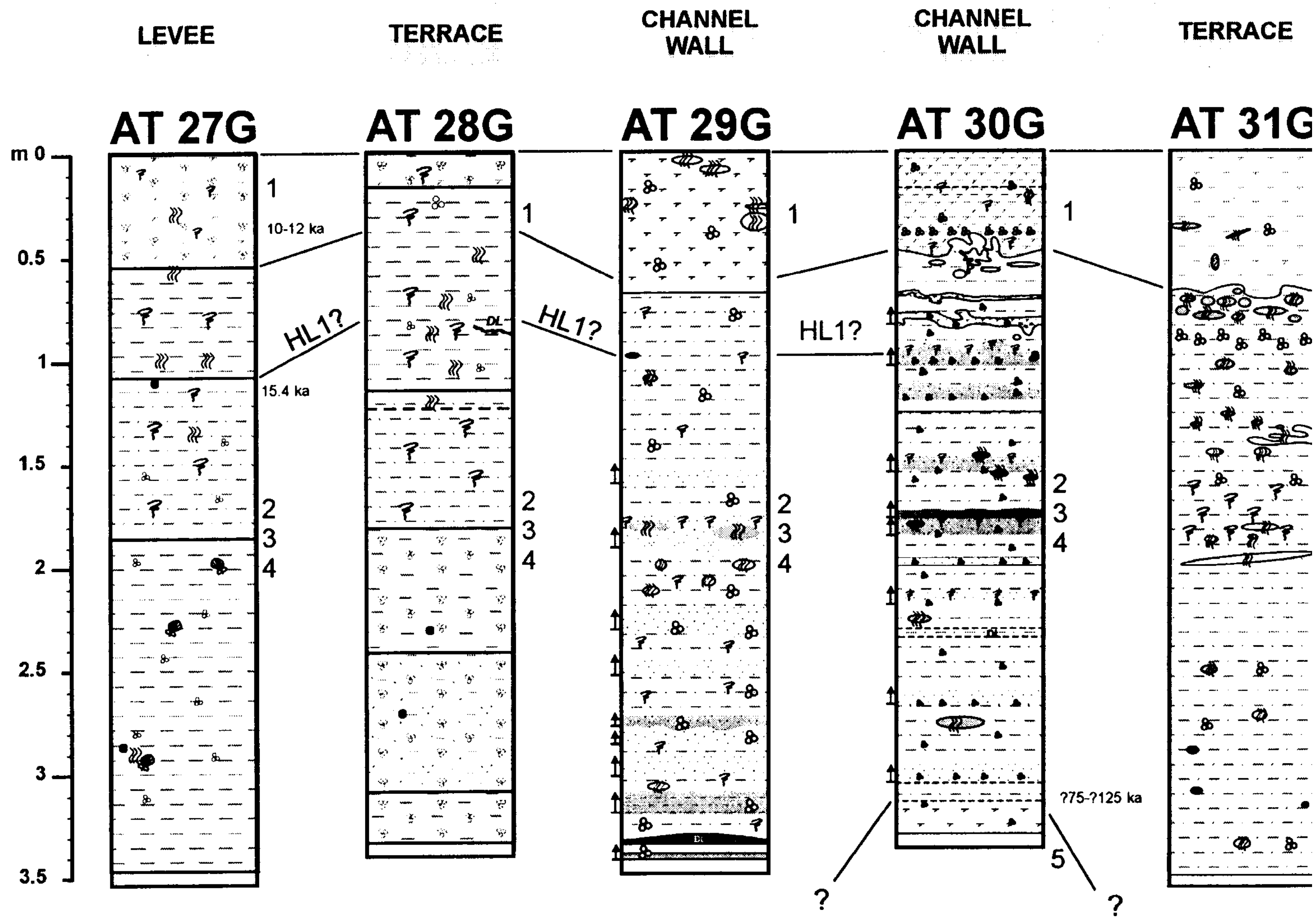

Fig. 69. Correlation of Gollum channel cores

Chronostratigraphy and turbidite frequency

Chronostratigraphic interpretations have been made on the cores in order to infer the age of turbidite activity. A diagram showing the correlation between cores is presented in Figure 69. The top of each core was marked by a foraminiferal marl of which the upper section was characteristically oxidized. The base of the foraminiferal marl may be inferred as the transition between Oxygen Isotope Stages 2 and 1 (Termination 1A is at 12 ka and Termination 1B is at 10 ka). Micropalaeontological assays revealed the presence of coccoliths, silicoflagellates, and diatoms supportive of a Holocene age. This inference was also supported by a consistent depth of this contact in the cores. Given the proximity of the location of the cores, it is reasonable to correlate by approximate depth in the core. All of core AT32G is inferred as Holocene. A second stratigraphic marker horizon is also inferred by the presence of layers of ice-rafted debris and dropstones which occurred in the majority of cores. This horizon could be an Heinrich Event (maybe the last Heinrich Event at 15.4 ka). Again, a similar depth of horizon is used to support this correlation, although in some cores this layer is marked by a single dropstone. It must be stressed that this correlation is tentative. Despite the presence of numerous layers of mineralization, these show no depth correlation and are envisaged as being time transgressive and specific to each core. Correlation between turbidite units is also problematic with an unequal number of turbidites preserved in adjacent cores. Further dropstones and layers of ice-rafted debris are recorded in the cores, although it is seen as too tenuous to allow correlation. Despite these problems, on the basis of micropalaeontological and lithological data, it is possible to correlate these deposits with Oxygen Isotope Stages 2, 3 and 4. The base of core AT30G contains a unit of foraminiferal marl which has been correlated with Oxygen Isotope Stage 5 (between 128 and 72 ka) based on micropalaeontological assays. It is not suspected that this is an artefact of coring and represents a re-sampling of the Holocene sequence due to the distinctive nature of the coccolith assemblage. This core was taken from the channel wall, and thus presumably sampled older exposed sediments. This implies that in core AT30G, only 259 cm of sediment were deposited in a minimum of 65 ka, giving a significantly low sedimentation rate less than 4 cm/ka. This is despite the inclusion of turbidite units which usually thicken sedimentary sequences. It may be that major hiatuses and/or erosion events exist in this core, and the inferred sedimentation rate is not representative of the area as a whole. Based on these dates, we can infer that 10 turbidites were recorded between 13 ka and 78 ka, giving a frequency of 1 turbidite/6.5 ka (assuming the absence of hiatuses and/or erosion). In conclusion, it can be inferred that the turbidite channel was active during the last glaciation, although turbidites were not of a large enough magnitude to deposit sediment onto the terraces of the channel or the levees. This implies that the system was active before Oxygen Isotope Stage 5 when most of the channel was emplaced. There is no indication of activity during the Holocene in this part of the channel system.

INTERPRETATION OF CORES FROM GOLLUM CHANNEL SYSTEM HEAD

B. Cronin, N. Kenyon, A. Wheeler, N. Satur, and S. Zaragosi

A series of three cores were taken from the head of the Gollum Channel system, on the basis of GLORIA bathymetry (Fig. 70). The purpose was to retrieve material from three locations which have different characteristics on the GLORIA interpretation.

Core AT37G was taken on the northern side of one of the main channels (waterdeph 740 m), where a series of slope-parallel linear features were seen on the GLORIA sidescan mosaic. Here we had no recovery the first time, though the corer hit the seafloor solidly. We were not sure whether the corer had hit fine sand or some other obstacle, so we dropped it again on the same site, this time with a sand trap made out of folded plastic sheet inside the core catcher. This time there was a small amount of fine and medium sand recovered. A quick smear slide revealed the material to be reworked from the shelf. This result was confusing because if the material had been contour current material, it would have to have been transported from the south, over the dense network of Gollum Channel System heads.

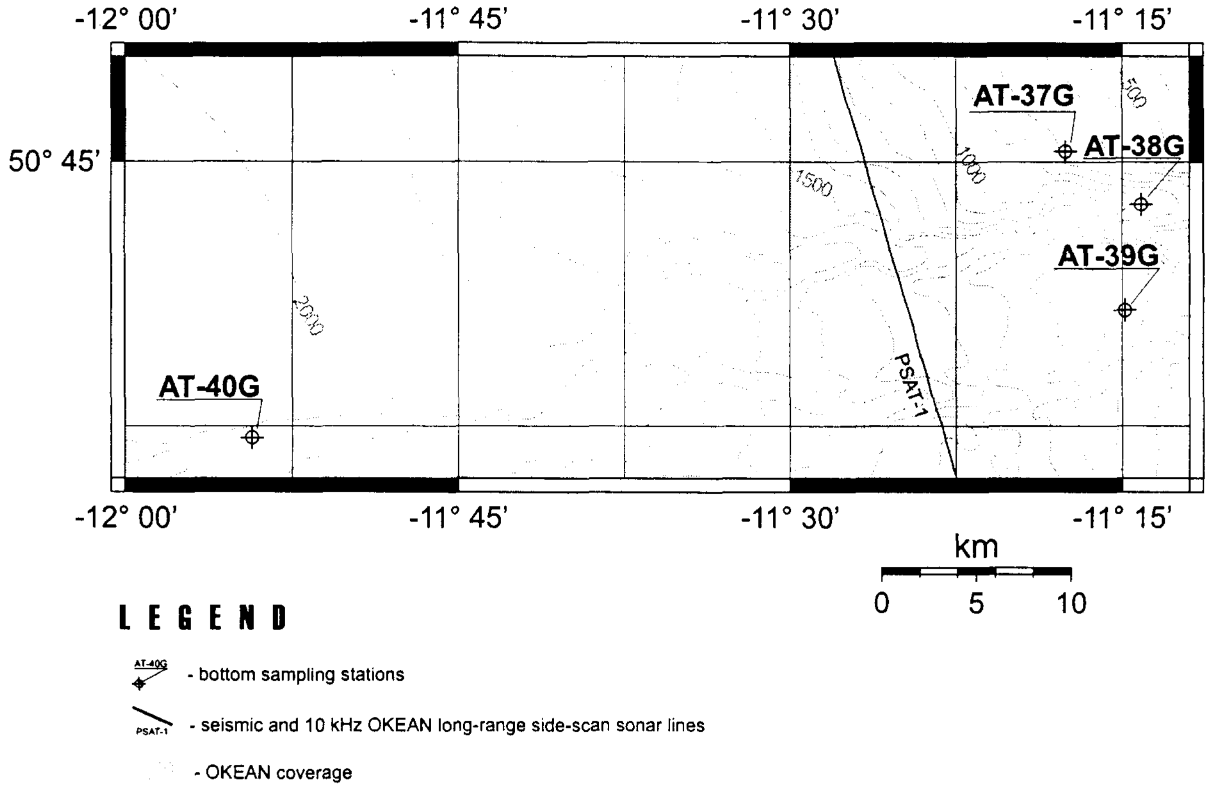

Fig. 70. Bottom sampling stations in the area of Gollum channel system upper reaches

Core AT38G was targeted at the thalweg of the channel (983 m waterdepth), where the channel floor was flatter (on seismic line) and wider (OKEAN/GLORIA sonographs), and thus less likely to miss. We recovered a small amount of medium-coarse sand on the seafloor.

Core AT39G was targeted on the southern side of the channel, where we hoped to encounter levees. The corer returned a pelagic sequence with sandy gravel, containing numerous dropstones, on the seafloor surface. Though a little disappointing overall, the exercise showed that there was a substantial amount of sand on the slope, and that much of this had to have been reworked from the shelf. The sand is resting directly on the seafloor, suggesting vigorous recent current. The sand is possibly being introduced to the slope from the shelf by an unknown process.

Core AT-40G from the channel floor at 2163 m, below the supposed current reworked sand, has 6 cm of hemipelagic ooze over a debris flow unit. It proves that the Gollum Channel system inactive in the Holocene. The slumpimg may have been from a neighbouring channel wall.

I.6. Biological data

P. Sumida and R. Kennedy

Table 3 shows the occurrence of the 101 taxa identified from the sampling sites. The bulk of the taxa identified are suspension feeders, few taxa are deposit feeding, carnivorous or omnivorous. The two main calcareous corals found were *Lophelia pertusa* and *Madrepora oculata*. Line drawings of the more common taxa are shown in Figure 71.

Scleractinian corals have a calcareous exoskeleton around which grows a layer of tissue which prevents the settlement of other biota on the living corals. However the coral near the bottom of the thicket tends to die off as an effect of bacterial attack (Henrich et al., 1996). This results in a branching structure of dead coral underlying the living coral, which provides a large surface area of microniches for other fauna to settle on. The dead coral material was extensively colonised by Porifera (sponges), bryozoans, hydroids, octocorals (soft corals), ascidians, serpulids (calcareous tube dwelling polychaetes), zoanthids, crinoids and bivalves. These suspension feeders appear to be using the coral as a substrate from which to exploit a probably increase in current speed owing to the elevation of the bottom. Also noteworthy was the presence of many large eunicid worms and sipunculids burrowing inside the coral material. These animals appear to be commensal with the coral, using the coral as a refuge, but probably not benefiting the coral in any way. Large eunicid burrow linings termed "parchments" were often observed. It is possible that the worms induce the corals to lay down a calcareous lining to the inner skeleton which is smoothed by the burrowing of the worm before calcification is complete (see Henrich et al., 1996). This would provide the worm with the ideal conditions in which to forage and shelter. The suspension feeding ophiuroid *Ophiactis balli* (Fig. 71) was also abundant sheltering in the dead coral material. The common suspension feeding bivalve *Astarte* sp.1 was abundant in the sediment underlying the thickets at stations AT4D, AT8D and AT15GR, but absent at AT24GR.

Polychaete sp. 1 is apparently a wandering deposit feeder from its general morphology. It was abundant in the sediment at all sites, but was also observed to be burrowing in the corals. Other deposit feeders recovered included sipunculid spp. 1 and 3, three species of capitellids, holothurian spp. 1 and 2 and Spatangoidea sp.1. As can be seen from Table B1, far more suspension feeding taxa were found than deposit feeders.

OREtech Stereo Photosystem footage showed that the areas around the mounds are extensively bioturbated, apparently by echiuran worms, cerianthid anemones and caridean shrimps. Both echiurans and carideans appeared in the grab samples. This may be because they are less common on the crest of the mounds than in the surrounding areas.

OREtech Underwater TV Survey

An underwater TV survey of the bottom from 52° 11.140'N, 12° 45.029' W to 52° 06.945' N, 12° 47.295' W was made on 12.07.97. The survey began on the flat and progressed up the slope to the crowns of LM4 and LM2.

The area approaching the mounds were extensively bioturbated, apparently by echiurans, cerianthids and caridean or thalassinidian shrimps. Numerous burrows were visible, and cerianthids could be observed feeding. This phenomenon is common in deep sea soft bottom communities. Sea pens were abundant on the sediment surface. Other visible epifauna included echinoids (sea urchins) and holothurians (sea cucumbers). Shoals of small fish swarmed to the camera lights, and larger solitary species were common.

Approaching the mounds it was noteworthy that cobbles and boulders began to appear on the sediment surface, possibly exposed by an increase in bottom shear as the currents pass the mounds. These may provide an exposed hard substrate on which juvenile corals can settle. Juvenile corals were observed to have settled on a cobble in sample AT8D.

Observation of the coloration of live coral material in the dredge and grab samples seems to suggest that *Madrepora* is an orange-red colour while *Lophelia* is a pale rose colour. The observed live coral in the TV footage was differentiated on this basis. There appeared to be no vertical zonation of species as the camera progressed up the slope, but there was a tendency for the amount of coral to

TAXA	*STATION NUMBER*				*FEEDING MODE*
	AT 4D	AT 8D	AT 15GR	AT 24GR	
Porifera					
Porifera sp.1	•	•	•	•	s
Porifera sp.2	•		•	•	s
Porifera sp.3		•	•		s
Porifera sp.4		•			s
Porifera sp.5			•	•	s
Porifera sp.6			•	•	s
Porifera sp.7			•		s
Porifera sp.8			•	•	s
Porifera sp.9				•	s
Porifera sp.10				•	s
Porifera sp.11				•	s
Porifera sp.12				•	s
Porifera sp.13				•	s
Cnidaria					
Hydrozoa sp. 1	•		•	•	s
Hydrozoa sp.2			•		s
Actiniaria sp.1	•		•		s
Actiniaria sp.2			•		s
Actiniaria sp.3				•	s
Lophelia pertusa	•		•	•	s
Madrepora oculata	•	•	•	•	s
Flabellidae? sp.1	•				s
Caryophyllidae? sp.1			•		s
Scleractinia 1 Juvenile		•			s
Scleractinia 2 Juvenile		•			s
Octocorallia sp.1	•				s
Octocorallia sp.2	•	•	•	•	s
Octocorallia sp.3			•	•	s
Octocorallia sp.4	•		•		s
Octocorallia sp.5				•	s
Zoanthidea sp.1	•	•	•		s
Zoanthidea sp.2				•	s
Mollusca					
Chlamys sp.1	•	•	•	•	s
Chlamys sp.2			•		s
Astarte sp.1		•	•		s
Arcidae sp.1	•	•	•	•	s
Ostreidae sp.1		•	•	•	s
Bivalvia sp.1	•				?
Bivalvia sp.2		•			?
Gastropoda sp.1				•	?
Gastropoda sp.2				•	?
Gastropoda sp.3				•	?
Trochidae sp.1			•		?
Nassariidae? sp.1			•	•	?

TAXA	*STATION NUMBER*				*FEEDING MODE*
	AT 4D	AT 8D	AT 15GR	AT 24GR	
Polychaeta					
Eunicidae sp.1	•		•	•	o
Juvenile Eunicidae			•		o
Capitellidae sp.1	•				d
Capitellidae sp.2	•				d
Capitellidae sp.3			•		d
Terebellidae sp.1		•			s
Terebellidae sp.2			•		s
Aphroditidae sp.1	•				?
Phyllodocidae sp.1	•		•	•	d
Gonadiidae sp.1	•			•	c
Serpulidae sp.1	•	•	•	•	s
Nereiidae sp.1			•		d
Polychaeta sp.1	•	•	•	•	d
Polychaeta sp.2				•	?
Crustacea					
Cirripedia sp.1	•	•	•	•	s
Asellota (Janiridae?) sp.1	•		•	•	o
Amphipoda sp.1			•		?
Amphipoda sp.2			•		?
Amphipoda sp.3			•		?
Caridea sp.1			•	•	o
Caridea sp.2			•	•	o
Penaeidea sp.1				•	o
Brachyura sp.1			•	•	o
Xanthidae sp.1		•	•		o
Majidae sp.1		•			o
Majidae sp.2		•		•	o
Majidae sp.3			•		o
Munidae sp.1	•	•	•		?
Galatheidea sp.1	•		•		?
Galatheidea sp.2	•				?
Paguridea sp.1			•		o
Sipuncula					
Sipuncula sp.1	•	•		•	d
Sipuncula sp.2	•		•	•	s
Sipuncula sp.3				•	d
Ectoprocta					
Bryozoa sp.1	•	•	•	•	s
Bryozoa sp.2	•	•	•		s
Bryozoa sp.3		•	•		s
Bryozoa sp.4			•		s

TAXA
Echinodermata
Ophiactis balli
Ophiactis abyssicola
Ophiacantha sp.1
Amphiura sp.1
Amphiuridae sp.1
Echinus sp.1
Echinus sp.2
Juvenile Echinus
Cidaroidea sp.1
Juvenile Cidaroidea
Spatangoidea sp.1
Crinoidea sp.1
Holothurioidea sp.1
Holothurioidea sp.2
Tunicata
Tunicata sp.1
Tunicata sp. in this area
Indeterminate 2
Indeterminate 3
Indeterminate 4

s= suspension feed

Table 3. Taxa recorded at the stations sampled and possible feeding mode

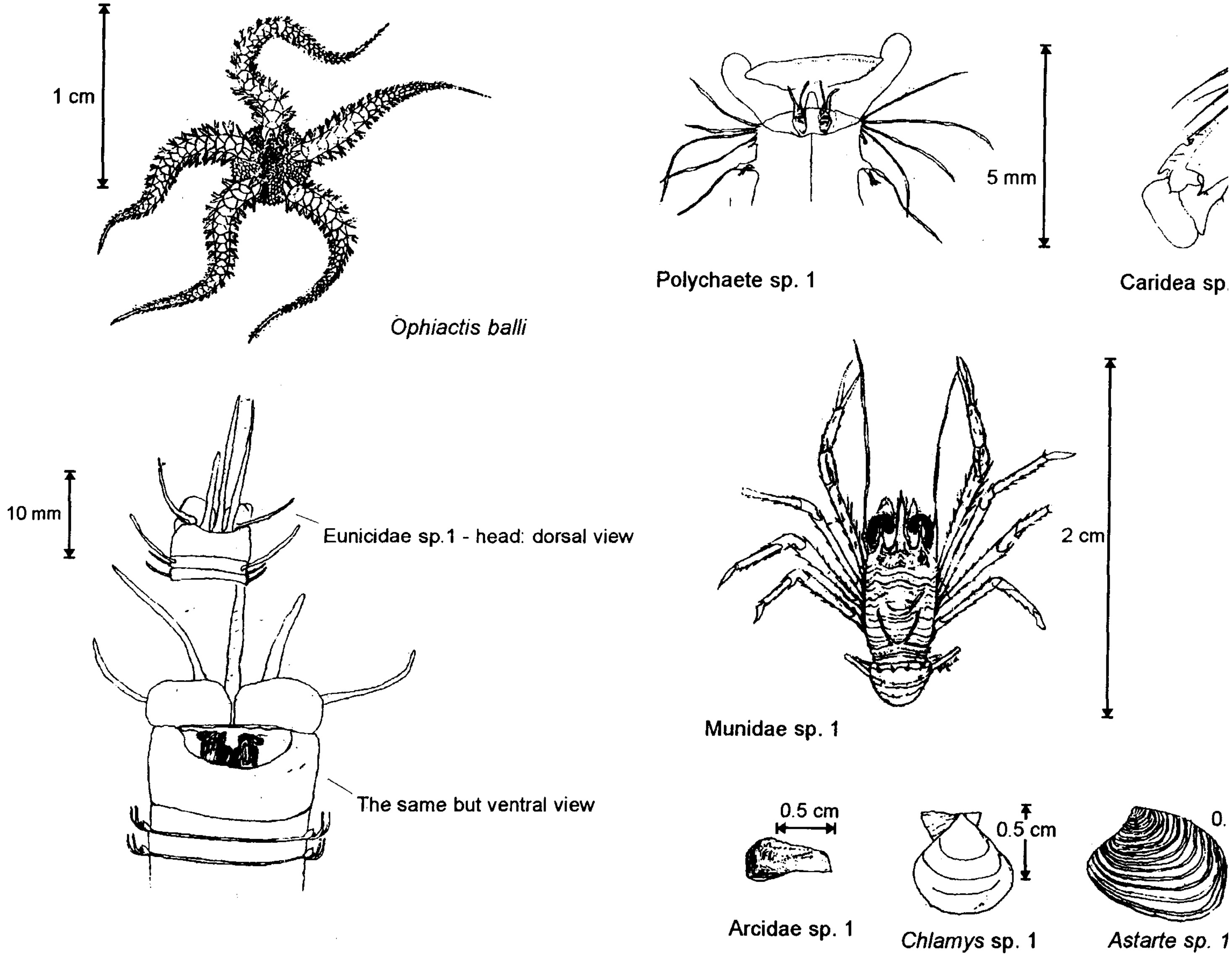

Fig. 71. Hand drawings of some specimens collected from Porcupine Seabight bottom sampling stations

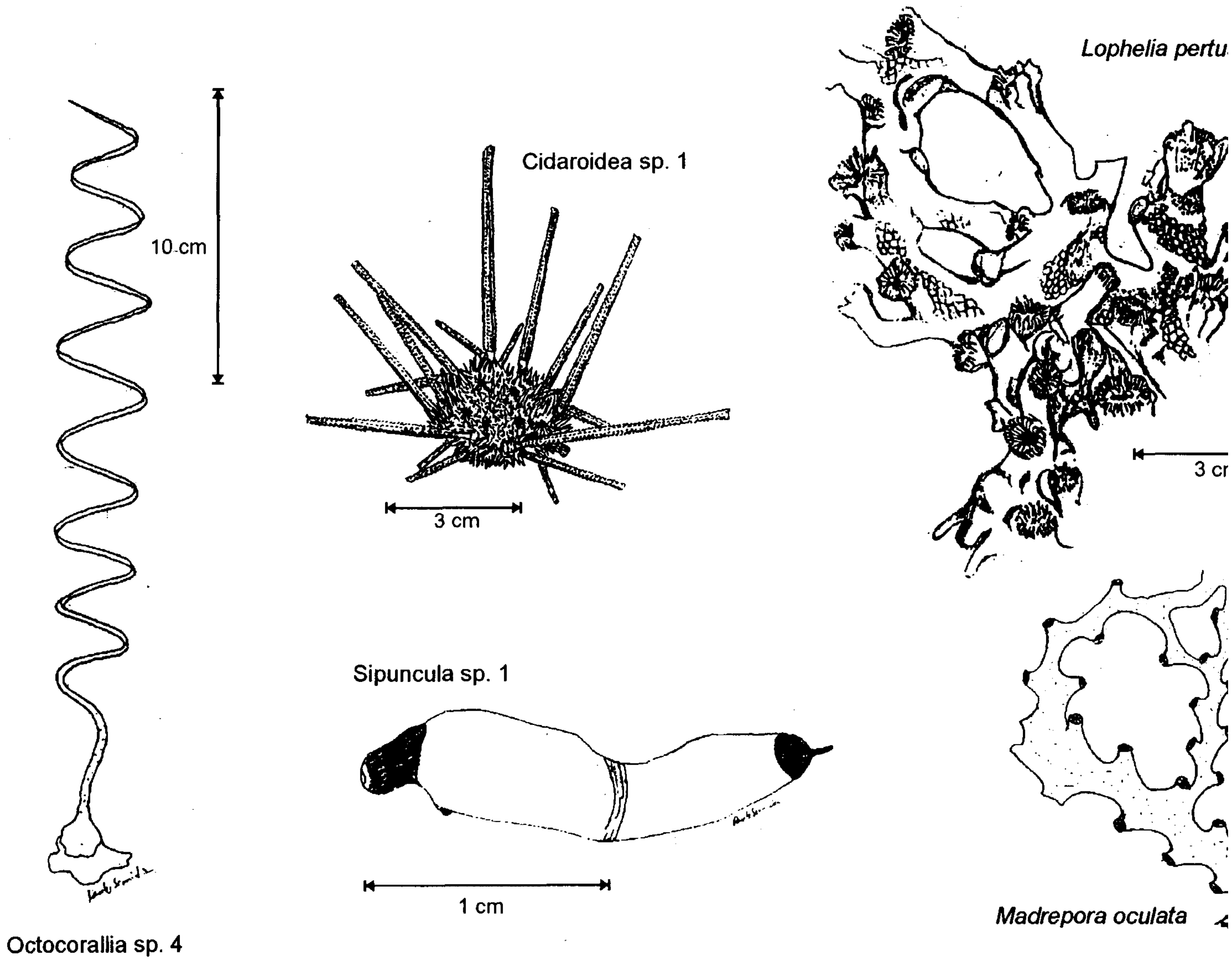

Fig. 71. Hand drâwings of some specimens collected from Porcupine Seabight bottom sampling stations (*continuation*)

increase further up the slope. The coral was growing in discrete clumps termed "thickets", and was patchy in its distribution. The absence of coral material in cores from the mounds may reflect this patchy distribution.

There appeared to be far more live *Madrepora* than *Lophelia*, which is verified by the grab and dredge samples. This is also true of the dead coral material in the grab and dredge samples, and there is no *a priori* reason to suggest that the ratio of dead *Madrepora* to *Lophelia* is different in the TV footage. The vast bulk of coral material appeared to be dead on all parts of the mounds, which is also verified by the grabs and dredges.

The ahermatypic corals *Lophelia pertusa* and *Madrepora oculata* are widely distributed in the northeast Atlantic (Wilson, 1979). There is no irrefutable evidence to date to show these animals are related to hydrocarbon gases, although Hovland (1990) suggests the corals could be growing on a mixed diet of chemoauthotrophic bacteria and other particulate food, based on stable carbon isotope values (see also Hovland and Thomsen, 1997). The fauna found associated with these thickets of coral do not appear to be specialised to exploit such resources. It is interesting that live *Madrepora oculata* appears to be far more common than live *Lophelia pertusa*. These thickets were expected to be dominated by *Lophelia*, but this does not appear to be the case. Coral communities of this kind typically grow at upper slope depths (Wilson, 1979). It would appear that the corals have settled on these mounds to take advantage of the increased currents present off bottom, and the associated increased supply of suspended material (and availability of hard substratum for settlement?). The apparent absence of authigenic carbonate material and sediment hydrocarbon gases (no present day evidence was found) corroborates the hypothesis that the distribution of these corals is not correlated with these materials.

I.7. Conclusions

N. Kenyon, M. Ivanov

The main results of the first leg of the TTR-7 cruise, that was basically undertaken in the Porcupine Seabight can be summarised as follows:

1. We undertook the first reported sampling of the mounds, which proved, at the surface, to consist almost entirely of pure carbonate mud with a patchy but extensive covering of cold water corals. The mounds can have very step sides and can be very large, up to 350 m high and 2 km long. There is a great variation in size and in shape, from simple conical shapes to complex, composite ridges. They seem to occur in clusters.
2. The mounds are associated with vigorous bottom currents. A strong northward flowing contour current was discovered from observations of sandy bedforms between 500 and 1000 m in the eastern Porcupine Seabight. The mounds here are elongate and have streamlined shapes, parallel or near parallel to the peak current direction. The moats and contourite drifts seen on profiles from the northern mound province show that there are vigorous bottom currents here also. However the absence of sandy bedforms, and the irregular and rounded shapes of the mounds, point to lower current speed.
3. We were not able to detect traces of gas escape or any other manifestations of fluid migration in the study area by geophysical methods nor was there any evidence of gas presence in bottom samples which were taken from different parts of carbonate mounds. We did observe a few areas which could be interpreted as pockmark fields on the sonographs although there were no signs of gas presence on subbottom profiler data.
4. Sidescan sonar survey and subsequent sampling within different parts of Gollum Channel system showed that there was no turbidite activity in Holocene times. However some coarse sand was recovered from the channel bottom at the head of the system, indicating that there maybe a recent supply of such material to the slope areas from the shelf.

II. ROCKALL TROUGH (Leg II)

II.1. Geological setting and objectives

N. Kenyon

SOUTHEASTERN ROCKALL TROUGH

The eastern margin of the southern Rockall Trough, the slope west and north of Porcupine Bank, is poorly explored apart from a large amount of unavailable commercial seismic data. The effort of the TTR-7 cruise in this area was chosen from among a number of outstanding problems that were identified from initial appraisal of a GLORIA survey carried out in 1996 from the R/V *Siren* and from seismic data made available to us by Dr. Tjeerd van Weering (R/V *Pelagia* cruise, 1997). They are problems that fall within the MAST-III supported ENAM 2 programme. ENAM 2 aims to study the processes and pathways of sedimentation on the northwest European margin. A portion of the direct financial support for the cruise came from six ENAM partner organisations and data for planning was provided by these organisations and others. The investigations are also of interest to Irish organisations and to the offshore hydrocarbons industry. Phillips Petroleum made available some helpful information, as did British Petroleum. Topics addressed were:

- nature and origin of mounds near top of slope.
- nature and origin of mounds near bottom of slope
- nature of potential slope failure near base of slope
- reasons for backscatter variation on GLORIA sidescan sonar

Bathymetry from the latest GEBCO maps incorporates a narrow strip of swath mapping for the southern part of the slope but the northern part is mapped from relatively sparse echo sounder lines (GEBCO, 1997). The margin tends to be exceptionally steep, especially in the south, and is typically convex in profile, being steepest at the base. The base of the slope is at about 3000m and is flanked by a rise in the south that extends down to the Porcupine Abyssal Plain at 4300m but in the north it abuts directly onto a flat floor at 3000m depth and the rise is absent. The shelf break is relatively deep at about 450-500m. The main interruption to the slope is a prominent northeast trending deep, steep sided valley, near an underlying structure called the Galway Graben, that coincides to some extent with a filled basin, the Bean Basin. Canyons were known north of the Bank (Kenyon, 1987) from a single long-range GLORIA swath. This has now been supplemented by a GLORIA survey of most of the southern Rockall Trough deeper than 600m which shows that there are at least 13 canyons between 53°N and 54°20'N. The canyons are in part guided by tectonic trends, as some cross the contours at very oblique angles. Some of the canyons start well down the slope and are thus presumed to be largely due to infrequent slumping rather than to frequent failures fed by transport of material across the shelf to the shelf edge. It is clear that they do not drain large areas of the shelf yet they are quite deep and have some development of tributaries. There are undissected areas of slope between the canyons. The top of Porcupine Bank has been studied by sampling and photography (Scoffin et al., 1988). There is a predominance of clastic carbonate sediments with lithic gravels and boulders. Some sand transport is reported. Iceberg ploughmarks are found down to 550m (Belderson et al., 1973). Published seismic lines include those of Bailey et al. (1974) from north of the Bank and Dingle et al. (1982) from the west. The most useful profiles are those from the recent R/V *Pelagia* cruise. The profiles show that there is a major, late Eocene angular unconformity, a thin development of sediment sequences above acoustic basement and possible outcrop of basement near the base of slope. The margin is relatively starved in the Plio-Pleistocene and bears more resemblance to the margin west of the Outer Hebrides in this respect, in contrast to the thick glacial fan sequences seen off the cross shelf troughs cut by ice, The nearest of the latter is the Barra Fan (Stoker et al., 1994). There is slope instability along much of the margin, shown by Dingle et al. (1982), by the GLORIA sidescan survey and by the R/V *Pelagia* seismics. The significance of slope parallel currents on this margin is shown by a number of studies. Thorpe and White (1988) has measured currents of

15-20 cm/sec near the southern slope of the Bank. Dickson and McCave (1986) have attributed nepheloid layers to winnowing of sediment on the Bank at depths of 700-800 m. Lonsdale and Hollister (1981) have shown from a photographic traverse of the whole slope along a line east of our survey area that there are strong currents at various depths, presumably contour currents. The R/V *Pelagia* profile ENAM 97-01 shows a contourite drift bounded by reduced or no sedimentation near the top and near the base of the slope. Dredging in canyons has produced some rather unconvincing age data (Bailey and Haynes, 1974) and sampling from a submersible has produced rather more reliable age dating (Masson et al., 1989). The sequences and reflectors mapped from seismic across the Rockall Trough have been correlated and dated from ODP borehole data (Masson and Kidd, 1986).

SOUTHWESTERN ROCKALL TROUGH

Like the Porcupine Bank slope the eastern slopes of Rockall Bank are little studied. The GEBCO bathymetry is not based on swath bathymetric mapping but on echo sounder profiles. It shows that there is a fairly constant slope gradient, not as steep as the Porcupine Bank slope, although there is a tendency to become steeper towards the north. The edge of the shelf is shallower in the north, being about 550m deep in the area that we are working in but about 300m deep further north. The foot of the slope is at about 2200m in the north and 2500m in the south. There are east-west oriented sections of the slope at approximately 54°30'N and 55°30'N. There are no known canyons. In this respect it differs from the Porcupine Bank slope which has canyons in its northern part. Profiles from the northern slope, north of 56°40', have shown that there is a major slide with its headwall in water depths of about 310-440m (Roberts, 1972). The erosion and deposition from this slide has been surveyed by deep towed sidescan sonar on the floor of the Rockall Trough and the failure dated at 15000-16000 B.P. (Flood et al., 1979). A deep-tow line using sidescan and bottom photography was run from the base of the slope and up to not far below our working area (Lonsdale and Hollister, 1979). It showed that there were strong currents near the base of the slope. It also showed that there were small sand waves with crests oriented along the contours and lee slopes on the upslope side. These were attributed to internal wave action. The GLORIA survey from the R/V *Siren* in 1996 showed that there were two very extensive areas of strong backscatter that extended from the top edge of the survey, in about 1000m of water, to the foot of the slope. The reason for this unusual feature, not seen on other slopes surveyed by GLORIA was not known. Mounds had been seen on commercial seismic profiles from an area part way down the slope. They were also found on profiles taken with a higher resolution profiler by NIOZ in 1987. The depth of the mounds (approximately 700-1100m) was similar to the depth of the possible "carbonate mounds" in the northern Porcupine Seabight (Hovland et al., 1994). The main aim of the investigation in this area was to study the origin of these mounds.

II. 2. Seismic data

II.2.a. SOUTHEASTERN ROCKALL TROUGH

A. Limonov, T. Nielsen, M. Ivanov, J. Taylor, J. Foeken, N. Kenyon

Introduction

Seismic profiling was carried out on the northern margin of the Porcupine Bank as part of an investigation of several groups of unknown mound features shown on both GLORIA sidescan sonar and hydrocarbon industry seismic data. Survey speed was approximately 4 knots (the minimum speed for the weather conditions), and the shot interval was 10 seconds. Six channels of data were recorded. Two profiles were taken: one along-slope at the top of the continental slope and oriented SW-NE, and a second, downslope, trending SE-NW (Fig. 72). The first line (PSAT-13) examined a field of mounds which appear to be confined to the upper slope region, at about 700 metres water depth, and extend southwards around the western margin of the Porcupine Bank. The second line (PSAT-14) extends from a group of mound features at the top of the slope to a second, but morphologically different group, mapped by GLORIA at the base of the continental slope.

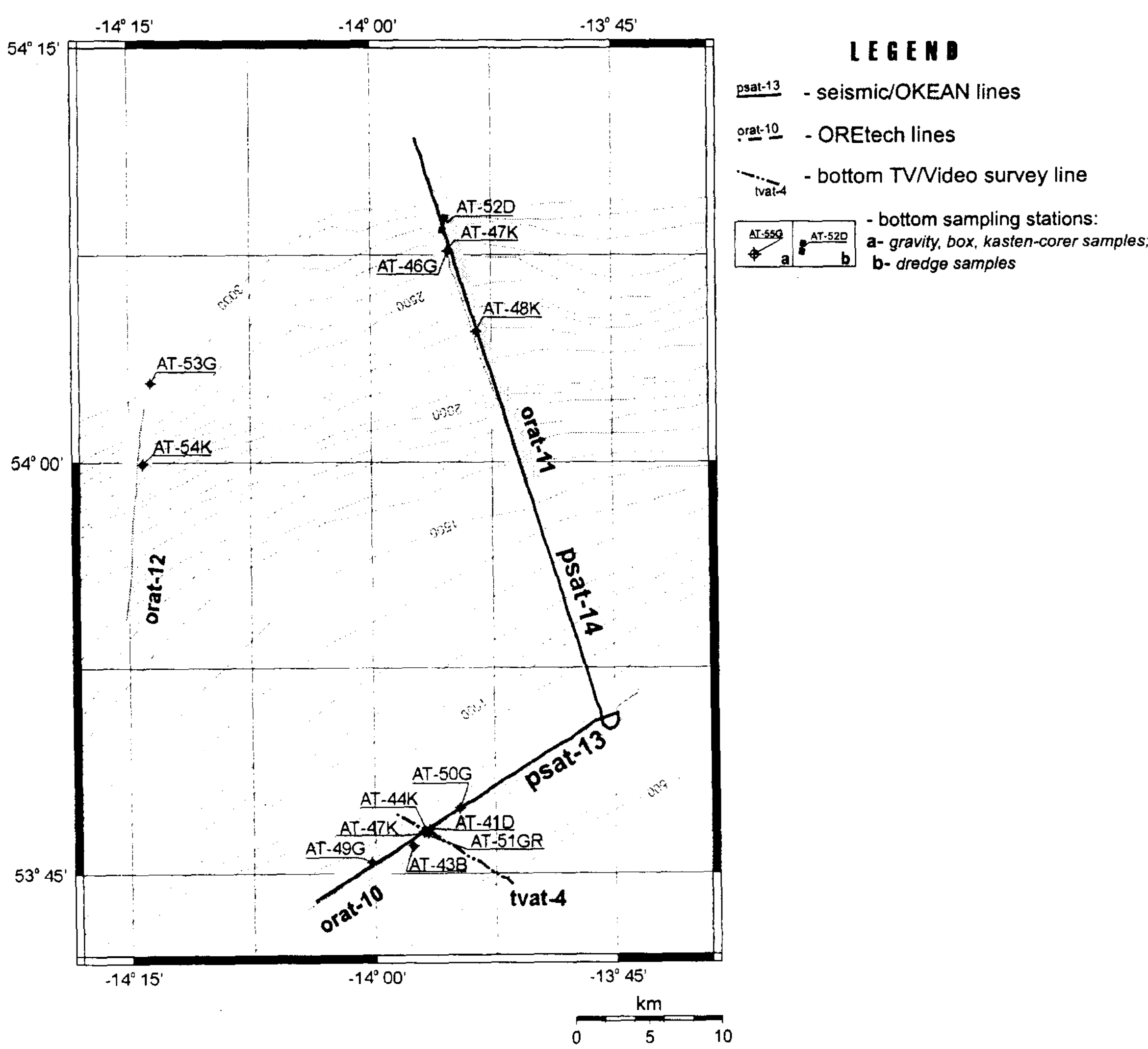

Fig. 72. Location map for southeastern Rockall Trough study area

Seismic line PSAT-13

4 seismic units were identified on this line. Surface morphology is a generally smooth, very gently dipping towards the south-west, from 1100 to 1130 ms TWT. The surface reflector is generally a high amplitude, strong return, but is broken by parabolic reflectors which are topographic highs (mounds) at frequent intervals. Only one mound is passed over directly (at approximately 1:15). In addition to this direct pass, there are 2 sideswipes and 5 near-misses (Fig. 73). Surface morphology is asymmetrical either side of the mounds, built up to the south-west, and lower on the north-eastern side. The build-up is only a few 10's of milliseconds, and most apparent in the south-western section of the profile.

The first unit (A1) is roughly 100 ms TWT thick, and thins slightly towards the south-west. It has a straight lower boundary which dips slightly towards the north-east, from 1200 to 1250 ms TWT, and is clear, continuous and prominent in the south-western region. The internal reflector pattern is of several types; below the parabolic mounds, signal is chaotic and indistinct. The signal appears to be greatly attenuated. Between the mounds, reflectors are visible, but discontinuous. They are clearly seen, of medium strength returns, and between timemarks 0:40 and 1:00 pinching out of reflectors is visible. Between 2:20 and 2:40, where there are no mounds, the internal reflectors show downlap.

The second unit (A2) varies between 30 and 150 ms TWT thick, thinning towards the north-east. The lower boundary is a clear, continuous and, in the south-western area, prominent subhorizontal reflector of medium strength and amplitude. The dip is from 1280 to 1350 ms TWT towards the south-west. It is principally defined by truncating reflectors beneath. Internal reflectors are very indistinct and appear in only small sections, subparallel to the lower boundary.

The third unit (A3) is confined to the most north-eastern area (Fig. 73) and is approximately 250 ms TWT thick. The lower boundary is curved, from 2:30, thickening NE, being a continuous, clear, strong reflector. Internal reflectors are reasonably continuous and show onlap towards the SW. It is the termination of internal reflectors which defines the south-western limit of the unit, rather than a distinct, single reflector.

The fourth unit (A4) extends beyond the penetration of the record, and shows occasional internal reflectors most clearly between 2:00 and 2:30. These reflectors are parallel, medium amplitude, dipping towards the northeast. Reflectors are otherwise unclear and chaotic.

Seismic line PSAT-14

5 or 6 seismic units are identified on this line, on the basis of examination of single and multichannel migrated and unmigrated data. The seabottom reflector is strong and high amplitude between 3:40 and 9:00. It is smooth and gently dipping downslope (south-east to north-west), from 1050 to 4000 ms TWT. At about 3:40 there are 2 minor escarpments, 50 and 40 ms TWT in height respectively; they are separated by a level surface (Fig. 74). Between 6:00 and 7:10, the topography becomes very slightly undulating, with an otherwise similar acoustic character. 7:10 to 8:50 shows a region of massive parabolic reflectors, demonstrating a very irregular surface. Migration also shows that the topography here is very rough. Within this region, between 7:30 and 8:00 there is the intercession of a curved, strong, continuous, high amplitude reflector with small undulations. From 8:50 to the 9:20, the seabottom reflector is extremely flat, level, with a strong character. Due to the complexity of the profile, it is described in three sections.

<u>Crest to midslope</u>

First unit (U1) is only present at the crest of the slope (Fig. 74), between 3:10 and 3:40, seeming to terminate at the first escarpment. The unit is 125 ms TWT thick; at the centre of the crest it is slightly thinner, giving the unit in this area the look of two sets of infill either side of the crest. The basal reflector of this unit is medium strength, being less distinct at the margins. Internal reflectors indicate general infill, being curved, medium strength and onlapping very slightly.

The second unit (U2) thickens downslope from approximately 60 to 100 ms TWT. On the upper part of the slope, the lower reflector is undulating and generally strong. Further downslope undulation increases and the reflector becomes more and more disrupted and discontinuous, less

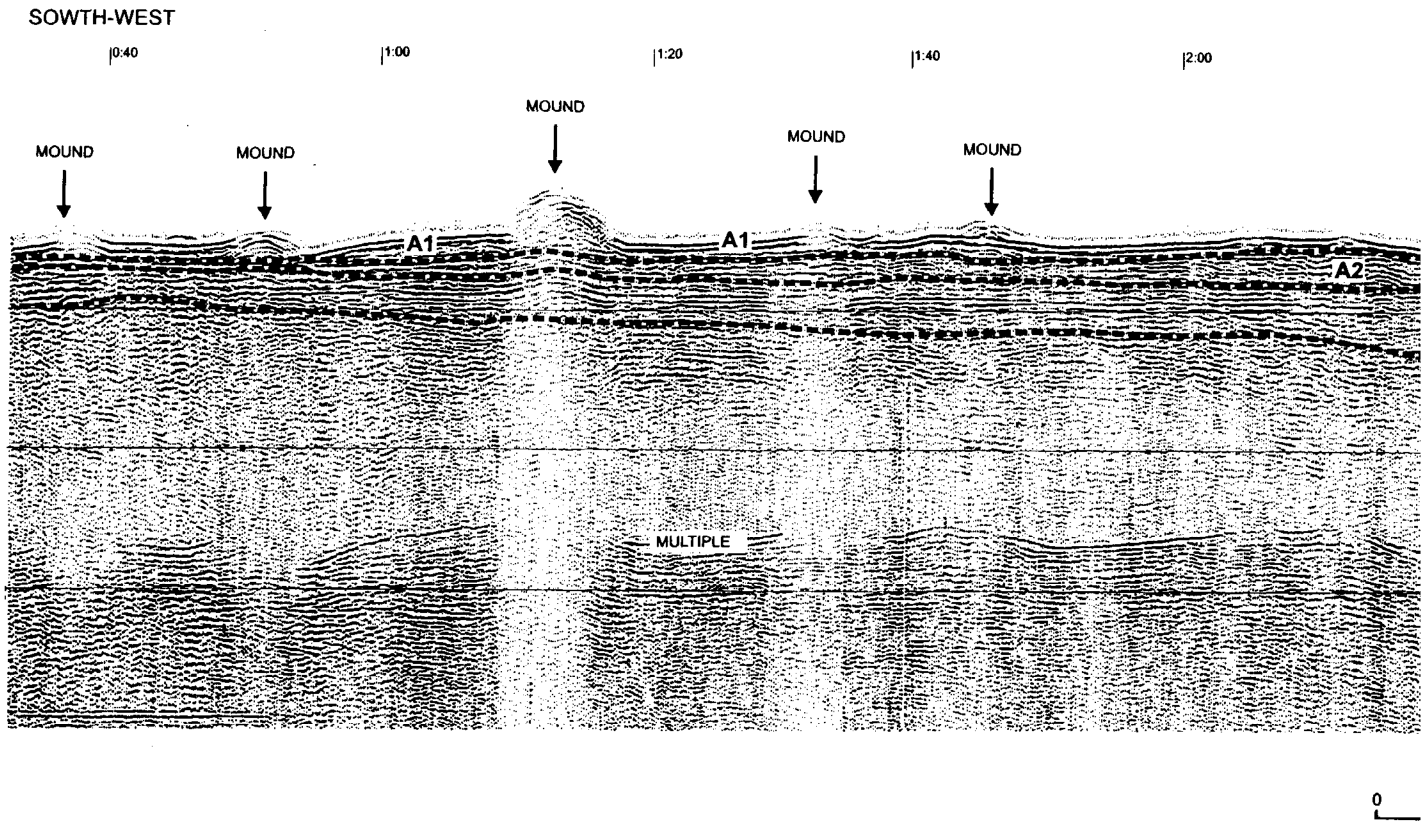

Fig. 73. Fragment of seismic line PSAT-13 showing mounds and downlapping reflectors within unit A1. Onlapping of A3 pa
seen at the north-eastern part of the line

distinct, and medium strength. Internal reflectors are noisy, discontinuous, subparallel, and weaken downslope, where they also become discontinuous. There is evidence for occasional infilling reflectors, especially in the lower section, for example 5:45 and 6:45 to 6:50 (Fig. 75). At the top of the slope, below the surface escarpments, there appears to be a faulting structure extending down only 10-20 ms TWT, beyond which there is much distortion.

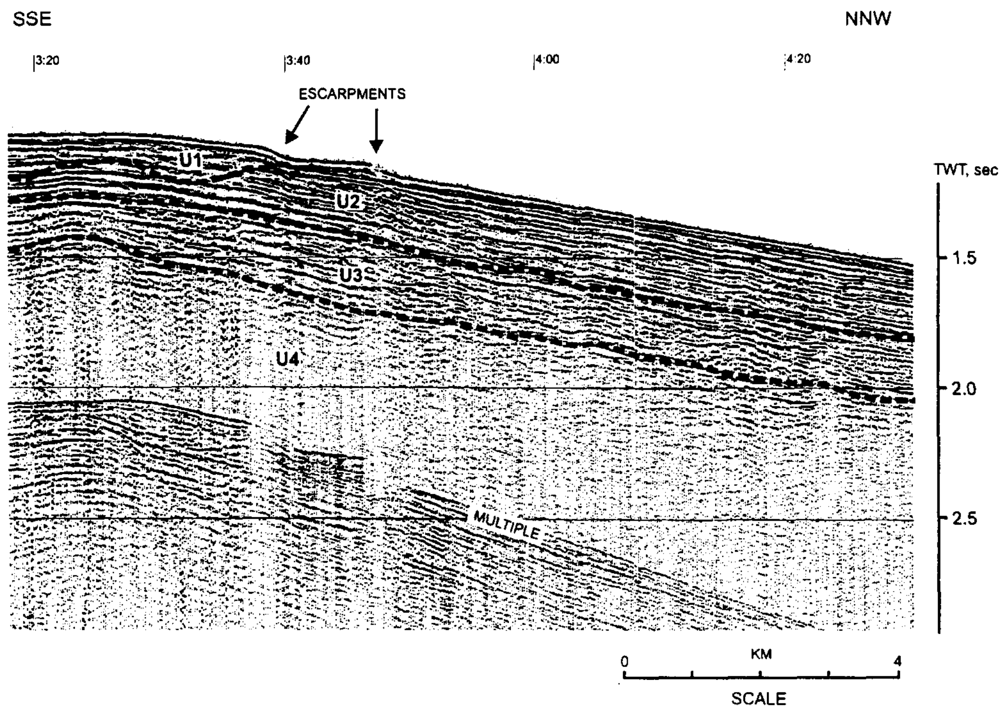

Fig. 74. Fragment of PSAT-14 showing the crest and the upper slope of the Porcupine Bank with units U1 to U4. Note the escarpments in unit U2 with small offset

The third unit (U3) is a constant 200 ms TWT thick, except at the crest, where it is 100 to 200 ms TWT thick. At the crest, the lower reflector is undulating and disrupted. Downslope it is a strong, high amplitude and almost totally continuous reflector. Midslope, the reflector becomes interrupted, at 6:10, 6:25, and 6:55, but not in-between these points; interruptions become smaller downslope (Fig. 75). Internal reflectors are parallel and strong at the top of the slope, but downslope become gradually weakened and then chaotic. Beneath the crest reflectors appear to be enhanced through merging and interference. At 6:10, 6:25, and 6:55 acoustic voids can be seen, with slight push up of visible internal reflectors at the edges.

The fourth unit (U4) seems to extend beyond the penetration of the data, but occasionally the base of the unit may be resolved (U5?). Internal structure is extremely unclear. On the unmigrated multichannel data there appear to be internal reflectors of medium amplitude, which dip alternately SE/NW. These are only apparent around midslope, with a minor occurrence in the area just off the crest.

Lower slope

The lower slope is bounded by two regions which are topographically rough and upstanding; within this is a gently curved surface between 7:35 and 8:10, which has a small depression near the base of the area, and beyond which the topography is relatively level (Fig. 75).

The flat intermediate area consists of three clearly discernible seismic units (L1, L2, L3). The first unit (L1) is 150 ms TWT thick. The lower boundary is a strong continuous reflector upslope, becoming medium strength for the lower two-thirds. Internal reflectors are weak, undulating, and discontinuous and onlap at the upslope end.

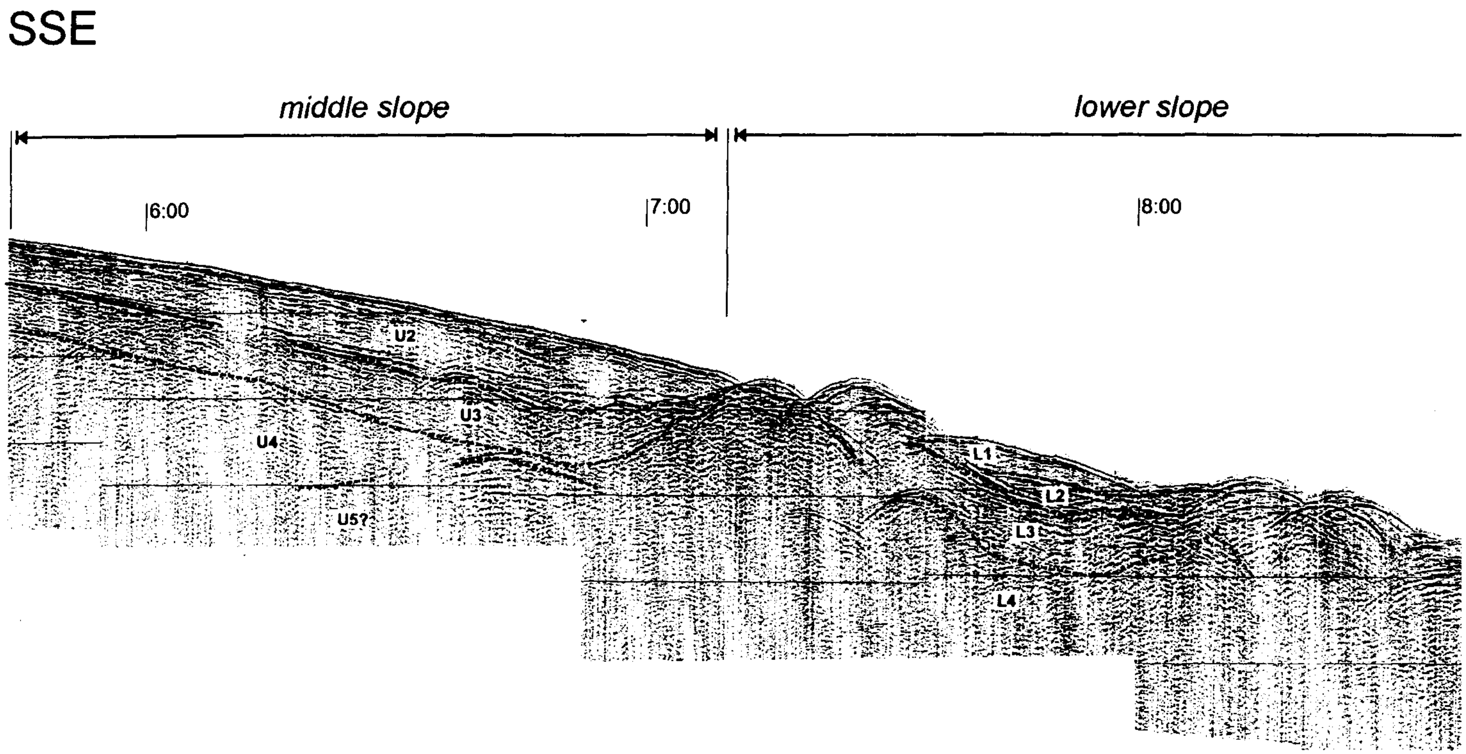

Fig. 75. PSAT-14 seismic line running from middle slope down to basin floor

The lower reflector of L2 is high strength and concave and appears to be pushed up between 7:55 and 8:00. Internal reflectors are relatively weak and also appear to be pushed up in the region of thinning. The unit is 80-90 ms TWT at it thickest, to ~40 ms TWT above the 'push' form.

The third unit (L3) extends beyond the penetration of the data. Internal reflectors are medium amplitude and rather discontinuous.

In the rough areas, migrated data show that the surface morphology is extremely rough with individual peaks (~200 ms TWT high). Only one seismic unit (L4) can clearly be identified. On unmigrated data this is represented by massive parabolic reflectors with a chaotic and weak, if present at all, series of internal reflectors. A further unit (L5?) may exist below this, indicated by very sporadic and discontinuous portions of strong reflectors.

Basin plain

There is a sharp transition at the base of the slope (Fig. 75), as shown by the surface reflector morphology described above. Four units are described (P1-4) on the plain.

The thickness of the first unit (P1) is roughly 10-20 ms TWT. The lower boundary is undulating, but hidden and smeared by the bottom reflector. Internal structure is hidden due to the thickness of the layer. There are signs of minor disruption between 9:05 and 9:10, when surface topography also becomes slightly rougher and internal reflectors appear undulating.

The lower boundary of the second unit (P2) is described more by onlapping and truncation than by a single reflector surface. It thickens to a maximum of 300 ms TWT in the NW. Internal reflectors show onlap and are medium amplitude, continuous and parallel.

The lower reflector of the third unit (P3) is undulating (perhaps faulted?), and shows high amplitude and strength. Internal reflectors are weak, discontinuous, medium strength returns.

The fourth unit (P4) extends beyond the penetration of the data and displays only weak internal structure at depth. At the top of the unit, internal reflectors are very strong high amplitude returns and all display an undulating or perhaps faulted form (suggested by parabolic reflectors).

II. 2.b. SOUTHWESTERN ROCKALL TROUGH

T. Nielsen, J. Taylor, M. Ivanov, J. Foeken, M. Horstink, T. Mikkelsen, A. van der Molen, N. Kenyon

Seismic description

Seven lines of multichannel reflection seismic, labelled PSAT-15 to 21, and contemporaneously acquired OKEAN long-range sidescan sonar data were collected over the period 5th to the 6th August 1997 (Fig. 76). Average speed for collection of these data was about 6 knots, and shot interval for the seismic data was 10 seconds. Total length of data collected approaches 250 km.

PSAT-15 is a single line in the south and west of the northern eastern part of the survey area (eastern Rockall Bank). PSAT-16 to 21 form a grid with associated OKEAN mosaic consisting of 4 alongslope lines in three rows and two downslope connecting lines at either end.

Description and analysis of the seismic lines was performed on stacked six channel, deconvoluted, band pass filtered data. Because of the grid form of the data, it is possible to tie lines so that a three-dimensional description and interpretation can be performed.

The overall dip of the area is to the south, the area being highest in the NE (600 ms TWT end line 19) and lowest in the southern-most area of the grid (1600 ms TWT beginning line 18). Downslope is from NNE to SSW, and alongslope orientation is WSW to ENE. The most obvious feature of the area is the central section of rough topography, formed by mounds up to 250 ms TWT in height. They are seen in the bathymetric range 800 to 1450 ms TWT. They are best expressed on PSAT-15 between 12:25 and 18:40 and continuation of the zone can be found on PSAT-16 between 20:00 and 22:20. Between the mounds, the surface is relatively flat. Eastwards the mounds disappear after 22:40 on PSAT-16. There is one isolated mound at 7:00, PSAT-20. Upslope of the mound region, the surface character becomes more wavy and contains no mounds. Downslope, surface topography is level, with escarpments at PSAT-17, 21:20, 21:50, 22:10 and 22:30. There is associated

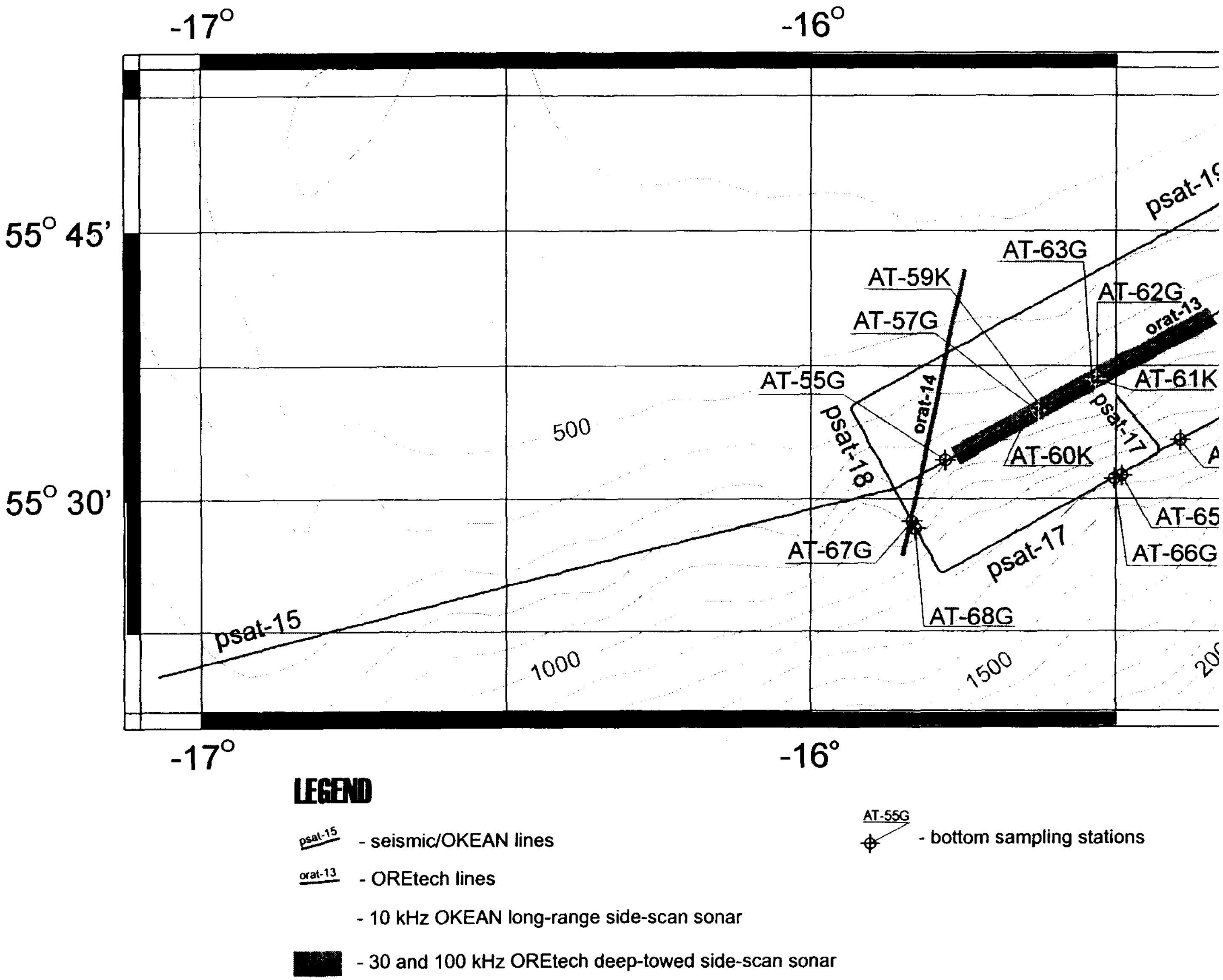

Fig. 76. Location map for the southwestern Rockall Trough study area

offset of up to 200 ms TWT. The far east of the survey area appears to be bounded by a 300 ms TWT high escarpment at 7:00, PSAT-20 (Fig. 77), and by a slightly hummocky and depressed zone in the middle of PSAT-21.

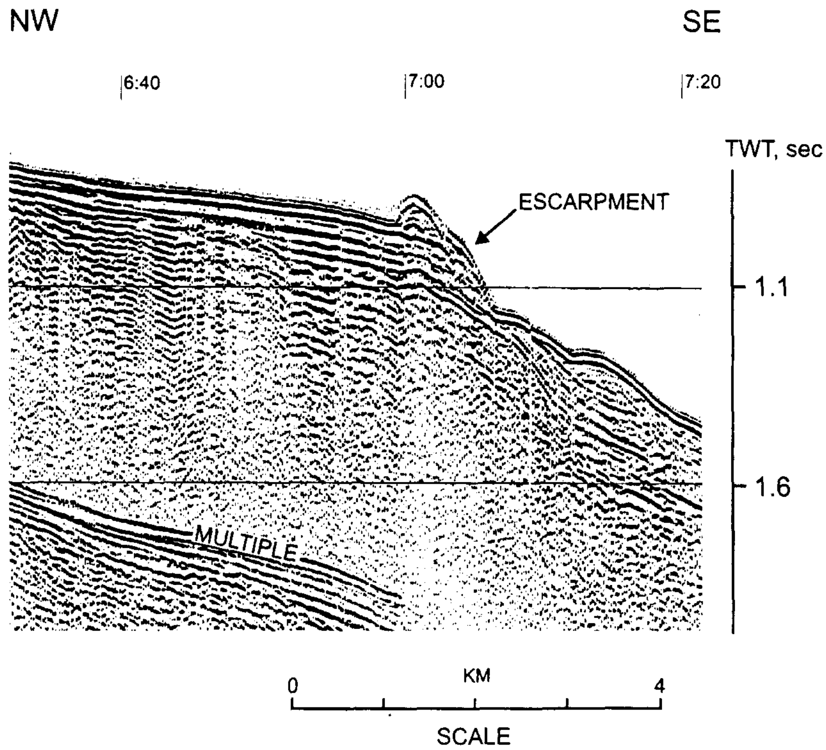

Fig. 77. Southeastern end of PSAT-20 showing fault-related escarpment separating regions one (upslope) and two. Note mound located at the escarpment edge

On this basis, it is possible to divide the area into two distinct geological regions.

Region one

Six seismic units are identified within this region and these are labelled (upwards) the acoustic basement, lower, middle, upper, surface and mound units.

The **acoustic basement** is defined by a reflector which is discontinuous across most of the area, but very distinct when closest to the surface. It is smooth and undulates at a large scale, forming several basins. There are few to no internal reflectors. The unit is nearest the surface in the north-eastern most part of the survey area (50 ms TWT below the surface), and dips gently towards the south and west.

The overall expression of the **lower unit** is one of filling the basins formed by the acoustic basement. The top reflector is level and clear where the unit is thick due to basins and irregular and discontinuous at the margins. The unit is absent where the basement is most upraised. Again, the unit dips towards the south and west. The thickness varies according to the basement topography. However, the unit generally thins in the far NE and is more uniform in thickness in the downslope area of the grid. Internal reflectors are generally subparallel, medium strength, but some areas have a chaotic pattern. Onlaps are visible against the highs of the acoustic basement.

The top reflector of the **middle unit** is very strong and continuous, although less distinct towards the south-western end. The unit forms an elongate, thin lens, with an average thickness of ~100 ms TWT. It is completely absent downslope (PSAT-17), disappearing at roughly 1700 ms TWT depth (0:00, PSAT-18). The unit becomes very thin in the NE (~20 ms TWT thick). Internal reflectors are medium amplitude, subparallel and mostly continuous. They show onlap and infill of depressions in the lower unit.

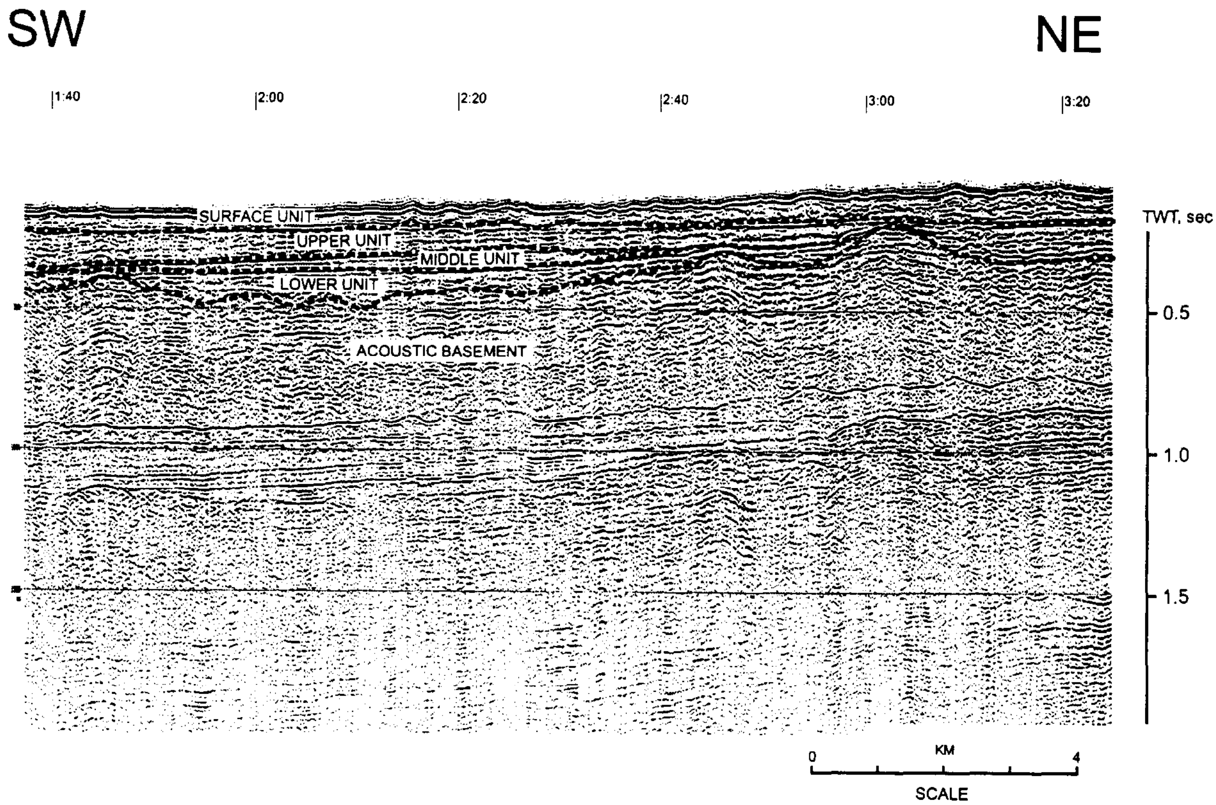

Fig. 78. Fragment of seismic line PSAT-19 with a number of seismic units recognised in sedimentary succession at the northernmost part of the study area

The **upper unit** forms a smooth sheet over the units below. The unit thins NE, SW and downslope, with a maximum thickness of 190 ms TWT on PSAT-19 (Fig. 78). This unit is extremely close to the surface in the NE and downslope zones. The upper reflector is flat, almost totally continuous and strong. The top reflector is extremely flat beneath the mounds in contrast to the signs of pull-up seen in connection with mounds studied in other areas examined during the TTR 7 cruise, on southeastern margin for example. Further investigation by the geophysics team demonstrate that the reflector here shows negative polarity. Internal reflectors are strong, continuous, subhorizontal and subparallel. Onlaps are seen against highs in the lower units. Truncation is clearly seen in the western upslope area (PSAT-19 around 3:00), and there is further evidence suggestive of truncation in the northern and eastern zone, i.e. at the most upslope section of the area (eastern ends of PSAT-16 and 19).

The **surface unit** is an approximately 100 ms TWT thick sheet-like unit in the north (PSAT-19). Further downslope the unit is present between mounds as a fill (Fig. 79). The unit thins and is no longer visible downslope and to the NE. Internal reflectors are medium amplitude, discontinuous in parts and undulating in the upslope area. They are hidden by the surface reflector where the unit is very thin. There are weak indications of downlap in the intermound area of the central section.

The **mound unit** is distinguished on the basis of multi-peaked, rough topography, below which the internal reflectors are chaotic. Mounds are similar in seismic structure to those described in the crest region of the southeastern Rockall Trough. The geophysics team calculated the velocity within the mounds to be very high, >2000 m/s. Two of the mound areas differ from the majority, being clearly bounded at the base by a doming strong reflector, beneath which is an acoustic void (PSAT-16, 22:00 and PSAT-18, 0:20) (Fig. 79 and 80).

SW

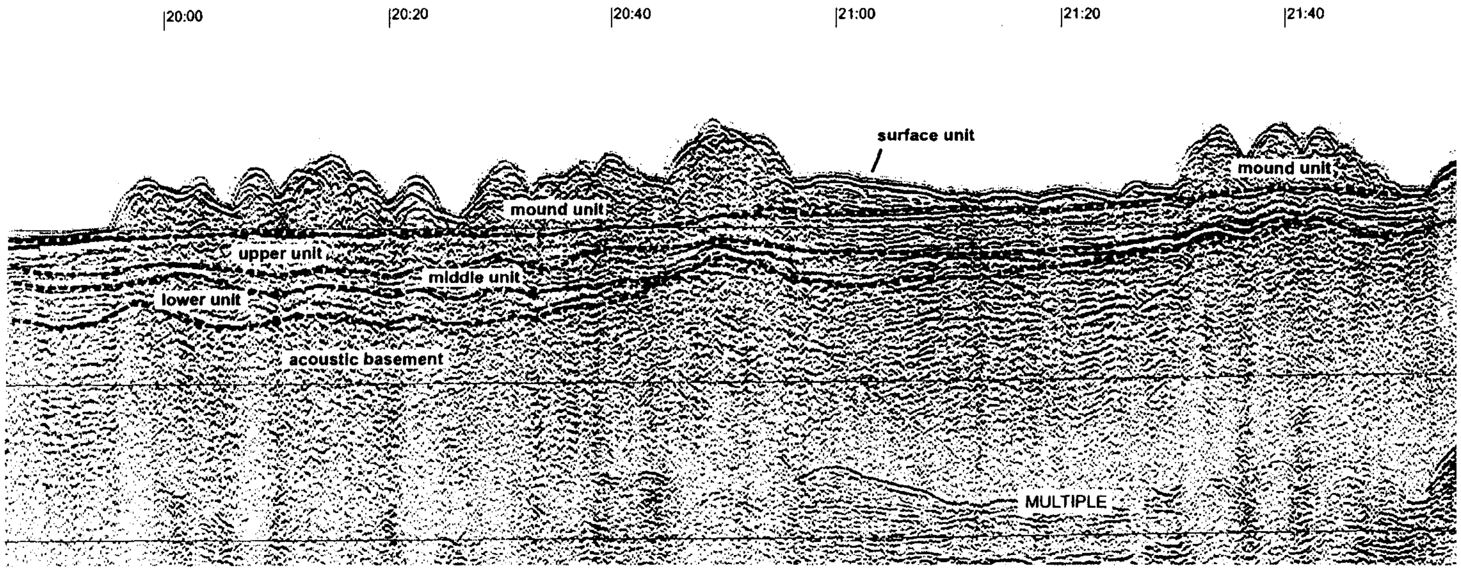

Fig.79. Line PSAT-16 showing carbonate mounds. Note the extremely flat upper reflector of the upper unit below the mounds, pull-up. Also note the build-up of the surface unit against the mounds at the middle of the section, indicating sediment transpo feature, with mounds upon it, is seen at the northeastern end of the section

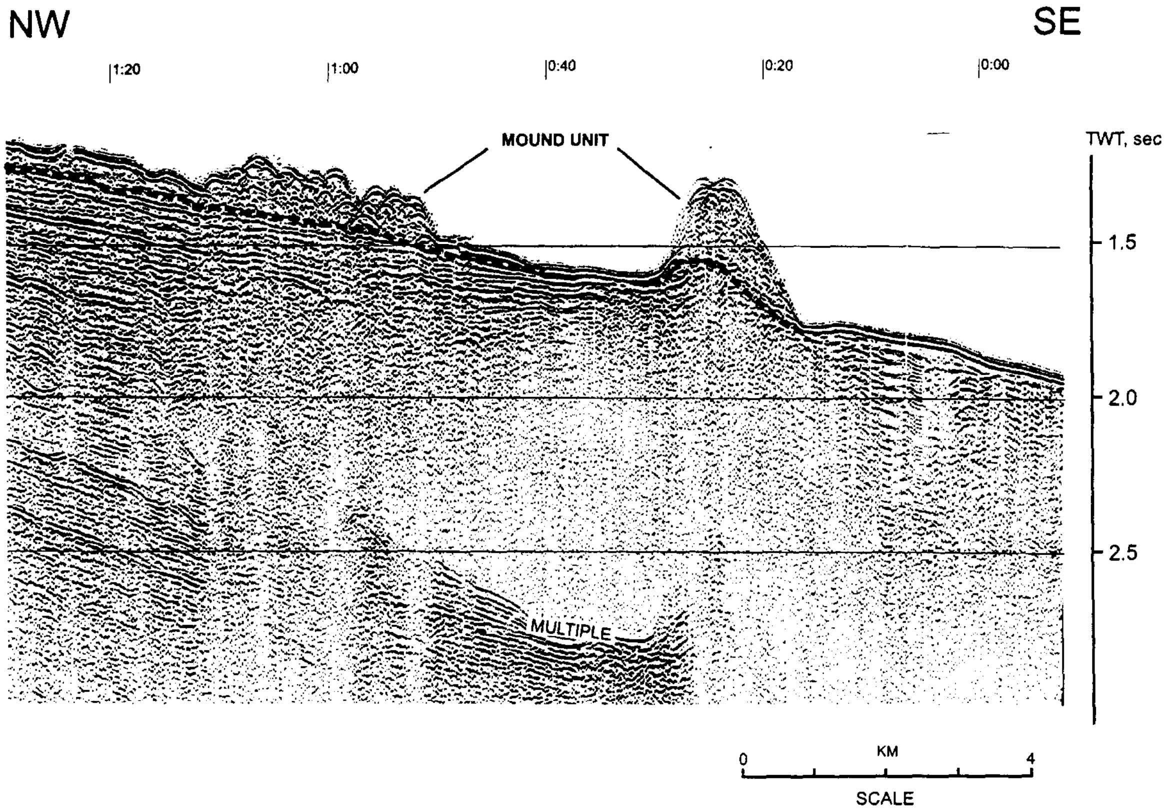

Fig. 80. Fragment of PSAT-18 displaying giant carbonate mound above pre-existing elevation

Region two

Region two is small and confined to the easternmost part of the area. It consists of only three seismic units, the acoustic basement, and lower and upper unit.

The top reflector of the basement is strong but discontinuous, describing the form of a large, deep basin. There are no internal reflectors.

The top reflector of the lower unit is strong and continuous. It also describes the shape of a basin, the unit forming a fill about 300 ms TWT thick. Internal reflections are faint and subparallel at the margins of the unit, where they also show onlap. In the centre, the internal reflectors are chaotic.

The upper unit is approximately 300 ms TWT thick and also displays a basin fill morphology. Its upper surface is a strong continuous reflector. Internal reflectors are medium amplitude, subparallel and subhorizontal. Towards the escarpment on PSAT-20, they show a sigmoidal form.

II.3. OKEAN and OREtech data

II.3.a. SOUTHEASTERN ROCKALL TROUGH

A. Limonov, T. Nielsen, J. Taylor, J. Foeken, M. Ivanov, and N. Kenyon

Introduction

OREtech lines (Fig. 72) were run over several regions within the southeastern margin of the Rockall Trough in order to investigate further the series of mounds and apparently rough topography identifiable primarily on GLORIA sidescan sonar, but also on hydrocarbon industry seismic lines. The three different lines examine three different types of backscatter and reflecting area within relatively close proximity to one another.

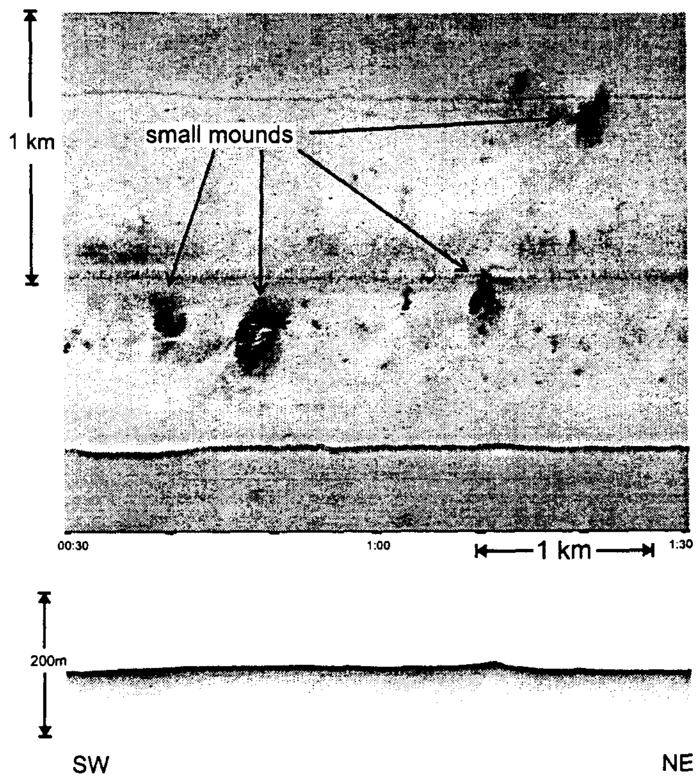

Fig. 81. Low backscattering area at the southwestern end of ORAT-10 with several patches of high backscatter interpreted as small carbonate build-ups. Subbotom profiler record is also shown

Line ORAT 10

ORAT 10 trends SW-NE and runs approximately along the 700 meter contour. It was collected overnight of the 1st/2nd August, 23:40 to 07:30 GMT. It covers a distance of 21 km, and complements the seismic line collected for the same area, PSAT-13; travel direction is reversed however.

The initial 7.5 km is a surface with relatively featureless low backscatter (Fig. 81). Over this surface there are very small (20 metres and lower) spots of high backscatter, with an apparently random distribution. There are also approximately 15 larger areas, of various sizes, of very high backscatter, several of which cast shadows, indicating a significant topography and a rough surface. The profiler record shows that this area is relatively smooth, with a very gently sloping surface. These highest backscatter features are up to 200 metres across and subcircular, and the backscatter decreases slightly in intensity from base to top. At the base of these mounds are tails of low backscatter, extending hundreds of metres, and trending due north. These are believed to be sand shadows.

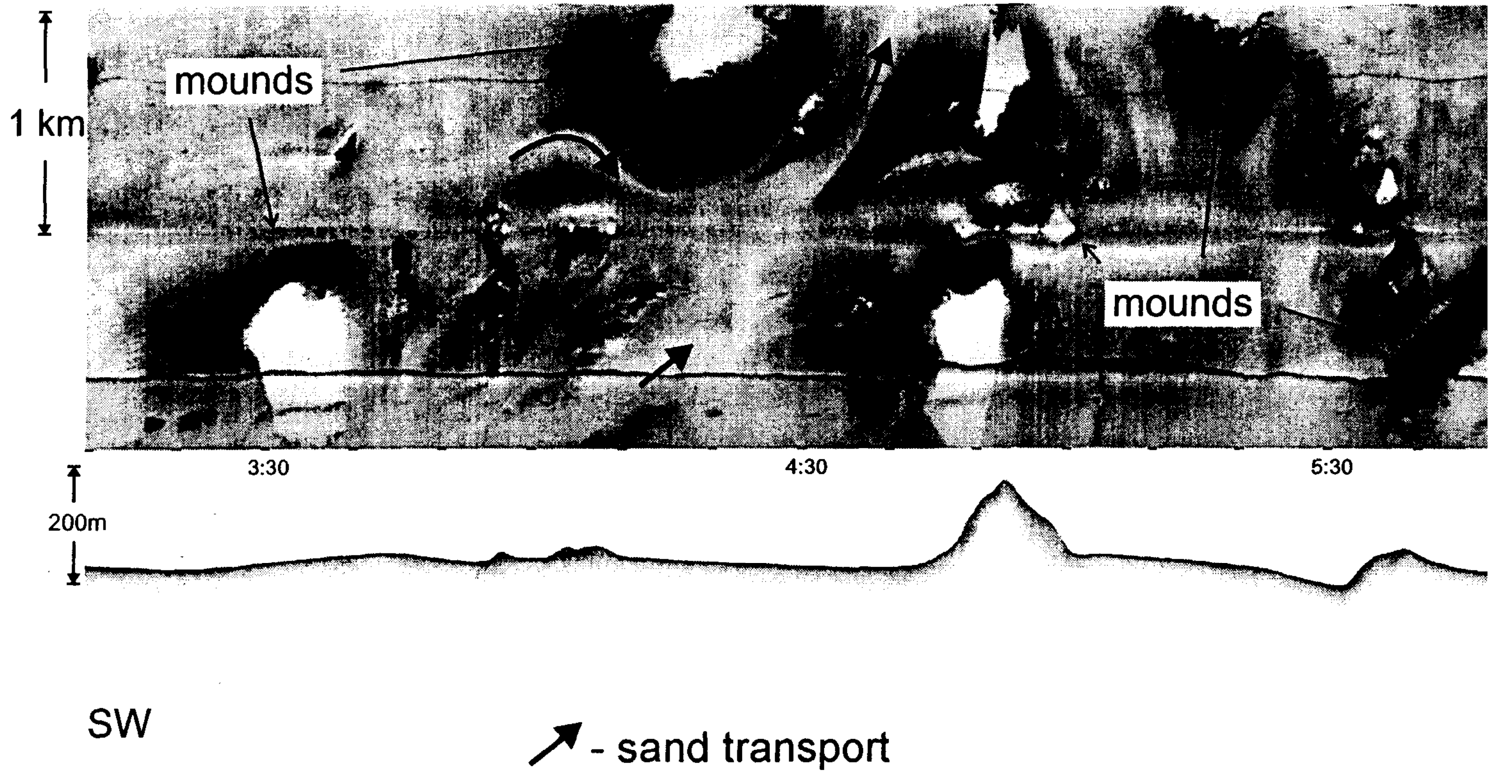

Fig. 82. Carbonate mounds seen on the ORAT-10 sonograph and subbotom profile record. Low backscattering bands swe
to be sand sheets

The next 8 km of sidescan record display a complex morphology and set of reflectors and backscattering surfaces. There are more than 30 patches and areas of very high backscatter in this region, with a variety of sizes, up to 1 km in length and typically 5-700 metres in width. They present a distinctly linear morphology, oriented SSW/NNE, with a clear crest. Shadow shape suggests that they have very steep sides and a relatively flat, multi-peaked top, demonstrated also by hyperbolic reflectors from the profiler record when it crosses these features. Smaller features are more conical, and up to 30 metres high. Large mounds are 150-200 metres high. The mounds show rings of high backscatter at their base, most prominent to their north and east sides; the profiler demonstrates that these are deeps, the 'moats' described elsewhere, but not completely surrounding the mounds. The sediment surface is higher by 20-30 metres on the SW side. Inter-mound areas are of generally medium backscatter, with areas of pronounced low backscatter that indicate a flow pattern. These low backscatter areas wind between mounds, and are also sourced from the western and eastern margins of mounds, curving and streaming in a northerly direction (Fig. 82).

The final 3.5 km represents a return to the mottled medium backscatter seafloor at the beginning of the profile, with the associated very small spots of high backscatter. The bottom profile in this region is flat and offers zero penetration. There is one small circular mound feature to be found at the end of the line, with associated shadow. The final feature to mention is a potential iceberg ploughmark, to be seen between 06:20 and 06:40 on the downslope side of the line at the depth of about 700 m. It is an irregular linear feature with a wavy plan shape. It is an area of low backscatter and shows high backscatter edges.

Line ORAT 11

ORAT 11 covers the lower half of the slope and was run to complement a part of the seismic line which had been collected previously (PSAT-14). Orientation of ORAT 11 is roughly SE-NW, and the length is approximately 27 km. The line was collected on the 3rd August 1997, between 05:09 and 14:05 GMT. The profiler shows that the slope has an overall convex form, steepening at 2000 metres depth and then terminating sharply at the transition from slope to basin plain.

The first 9.8 km from 05:09 to 09:15, depth 1500 to 2000 metres, is a uniform, low backscatter surface, with extremely small (<20m), randomly placed specks of higher backscatter. The specks are more common on the upper part of the line. There is also a faintly seen, curving, relatively high backscatter region between 05:38 and 06:30; it is approximately 1 kilometre in width, and 3.5 kilometres in length and strikes N-S, seeming to correlate with a low (~20 m high) bulge on the seabottom, seen on the profiler record at approximately 1650 metres depth.

The next 15.6 km is an area of generally medium to high surface backscatter, with large (500 metres to 1.5 kilometres) regions of high backscatter. These regions are concentrated between 08:48 to 10:12 and 11:22 and 13:32. Between 10:12 and 11:22, there is an area of medium to high backscatter with no features within it, other than a broad (1 km^2) patch of high backscatter on the south-western side, at roughly 10:40. The character of the profiler record differs significantly between these high backscatter areas and the rest of the surface, being parabolic (hence topographically rough), and giving a more prolonged return where it crosses these regions. This suggests a solid (rocky?) seabed. In both sections, areas of high backscatter appear to be surrounded on either side by sections of relatively low topography (moats), and in the downslope area, the mounds are of conical cross-section (Fig. 83). The upslope regions of very high backscatter demonstrate no obvious plan-view shape, but display indications of shadowed lineations (ridges) trending SW-NE on their surface. A ridge of high backscatter at the upslope margin of the area, extending for some 2 km and trending W-E is also apparent.

The downslope region of high backscatter (11:22 to 13:32) shows three concentrations of high backscatter, at 11:28, 12:05 and 12:50. The first two are approximately circular and conical, and are 500 metres and 1.5 kilometres in diameter and 100 and 200 metres high respectively. Their surface texture is again rough, although there are no signs of lineation in this lower region in the sonar data.

The final 1.4 km, from 13:32 is an area of uniform medium backscatter, with no apparent surficial features. The profiler shows a completely level and slightly undulating surface, and offers some penetration into the sediment below. Internal reflectors show basinfill. Depth is almost exactly 2900 metres.

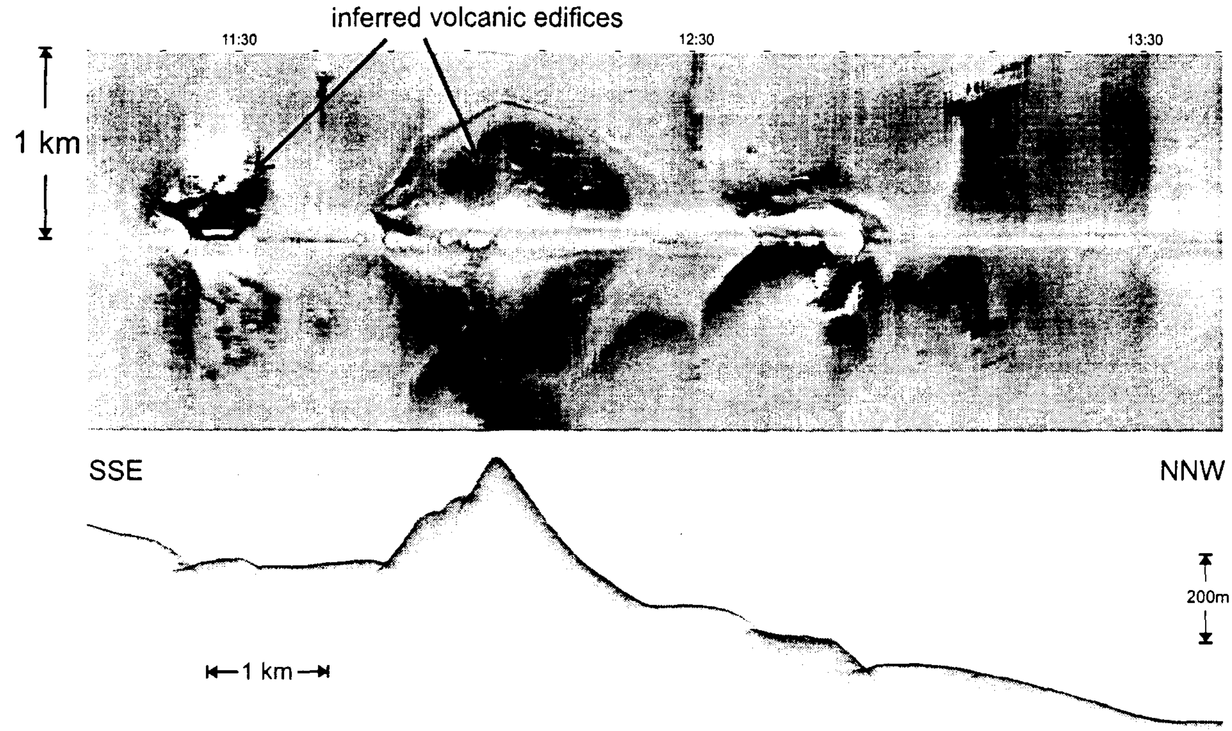

Fig. 83. Highly backscattering conical mounds crossed by line ORAT-11 which are likely to be volcanic in nature

Line ORAT 12

This line was collected on 4th August 1997, between 05:34 and 11:57 GMT, and runs at about 45° to the downslope direction. The profile is on the lower part of the slope, west of ORAT 11. It crosses an area which, on GLORIA data, is characterised by arcuate features resembling slump escarpments. This area is different in character again from the mound structures seen at the base of the slope further north and east and from those upslope. Overall slope morphology steepens downprofile, being steepest at the mid-section, before the slope gently descends to the flat plain at its foot. Once again, therefore, overall slope morphology is convex for the most part.

The uppermost part of the line shows a featureless region of medium backscatter with some very occasional, very small specks of higher backscatter. The profiler record shows some penetration of apparently stratified material here.

Further downslope there three regions of high backscatter which cross-cut the profile along the slope (Fig. 84). They are narrow (3-400 metres), linear features, 2.0 km or more long with a rough texture. These have a narrow (~1-200 metres) region of medium-to-high backscatter downslope. Three negative topographic features with a steep downslope and gentler, concave upslope shape are seen. The downslope drops 150, 100 and 50 metres respectively, and the base of the depressions appears to contain a sediment package. It is this latter, which is apparently imaged as the band of medium-to-high backscatter on the sonar.

The lowermost part of the profile from 09:00 is an area of very variable backscatter. It shows a 1 km^2 region of low backscatter on the northern side of the profile, with a neck feature upslope. The profile here is relatively level and smooth and there is some penetration into the sediments. This feature appears to be a downslope flow, possibly of sand because of the very low backscatter. At the base of the slope are two subcircular high backscatter features of rough surface texture. One is crossed directly and shows a hummocky, peaked profile.

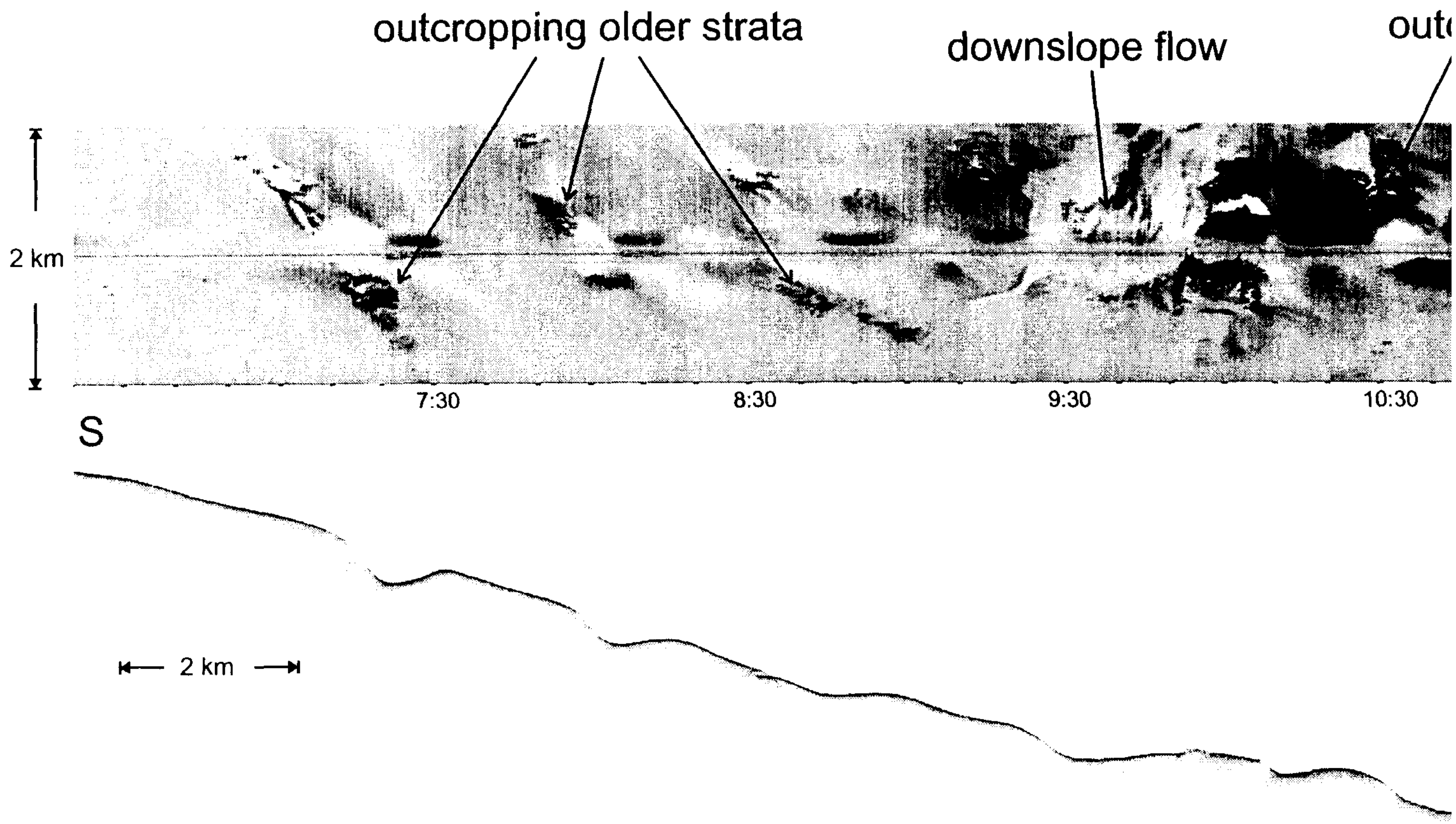

Fig. 84. Linear, slope parallel, highly backscattering features on the ORAT-12 sonograph and subbotom profiler record in the headwall of slumps

Otherwise the region is a mosaic of medium to high backscattering surfaces. The base of the slope is clearly demarcated by a linear high backscatter feature, after which the plain, is a structureless low backscatter area. The subbottom profiler offers good penetration and shows stratified material.

II.3.b. SOUTHWESTERN ROCKALL TROUGH

J. Taylor and N. Kenyon

Introduction

Nine lines of sidescan sonar data were collected, the seven OKEAN long-range lines mentioned above (PSAT-15 to 21), and two higher resolution OREtech lines, ORAT-13 and 14 (Fig. 76). The OKEAN data form a mosaic across the study area, extending approximately 120 km alongslope, with an overall downslope width of 30 km in the northern half of the survey region.

OKEAN mosaic

Five acoustic zones are identified within the OKEAN mosaic, labelled one to five, on the basis of features and morphology and the overall levels of backscatter (Fig. 85).

Zone 1 is seen across the majority of the survey area. It consists of an extremely variable backscatter regime with complex plan morphology. Areas of high backscatter appear to be approximately linear alongslope and extremely undulating in plan view and contain areas of low backscatter between them. There are areas where other features are visible. Towards the centre of the PSAT-16 OKEAN data there is an area of low backscatter trending roughly N-S. There is also an apparently channel-shaped feature near the top of PSAT-18 and another across the NE end of PSAT-15.

Zone 2 is an area of low backscatter in the most upslope part of the study area (port side, PSAT-19 OKEAN record). It is gradational, with the undulating features of zone 1.

Zone 3 is found immediately downslope of Zone 1 and is an area of mainly uniform high backscatter. In places it shows wave-like structures, but otherwise displays little else by way of surface morphology other than a few rough features.

Zone 4 is the most downslope zone imaged. It is separated from Zone 3 by a linear high backscatter area with a rough morphology and surface texture. Below this boundary, the general level of backscatter grades from medium to high westwards, and there are only a few backscatter features within this.

Zone 5 is found only in the extreme SW of the survey area. Like Zone 2, it is a zone of generally low backscatter and shows only a few short, undulating, linear features of higher backscatter.

OREtech 30 kHz sidescan and 5 kHz subbottom profiler

ORAT 13 was collected along the central region of PSAT-16 and falls almost entirely within Zone 1. It therefore provides a clarification of the OKEAN data from PSAT-16.

The section to 03.24 is similar to zone 2 in being low backscatter and clearly shows narrow, parallel curved lineations, some of which extend in a SW direction from obstacles. The profiler gives prolonged penetration.

Beyond this, there is a sharp transition to the area associated with zone 1 (Fig. 86). The 30 kHz data also show a complex backscatter pattern and surface morphology. Some of the extremely high backscatter areas (mounds) are subcircular in shape and conical, while others appear to be ridge-like. These topographic features give no penetration on the profiler record and are between 75-200 metres high. The tops of mounds are rough and invariably show regular 20-30 metre wavelength lineated features resembling waves. These are oriented alongslope. There is one massive mound recorded on both sidescan and profiler at 03:50 to 04:50. The edges are quite steep, and the surface is flat, with smaller mounds upon it. The intermound area west of this large mound and other intermounds areas further west have a very low backscatter and show indications of bedforms. There

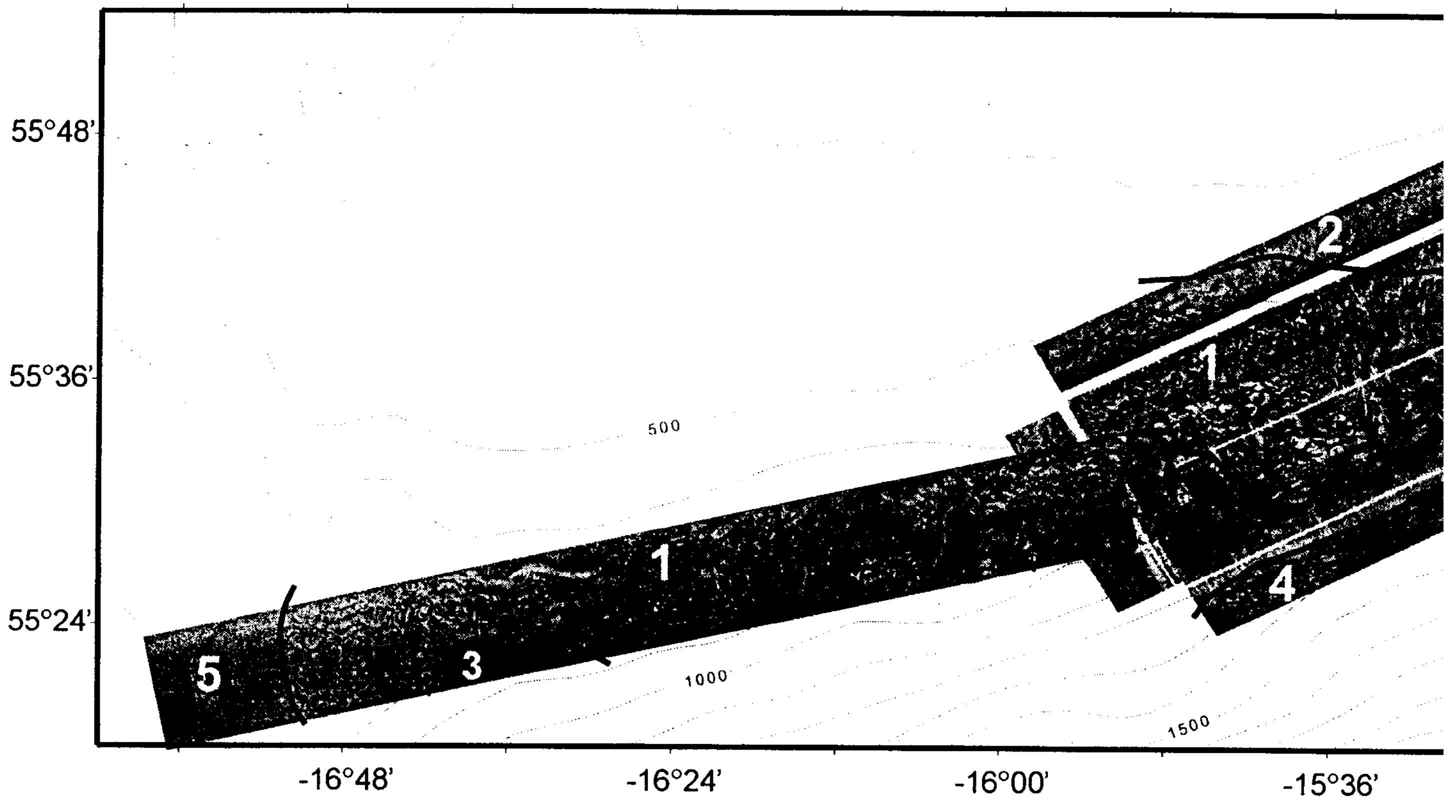

Fig. 85. OKEAN imagery of the study area. Numbers correspond to zones described in the text

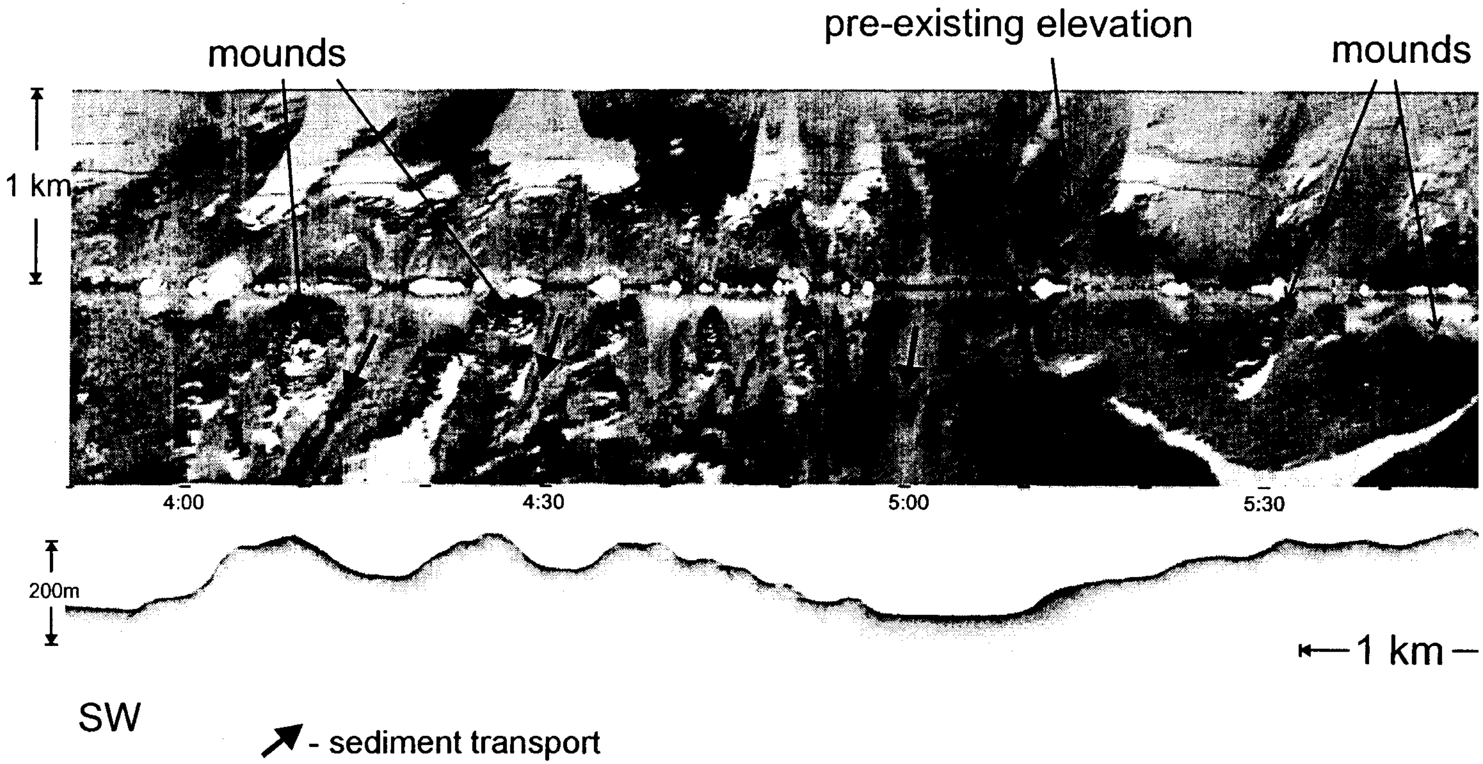

Fig. 86. Fragment of ORAT-13 line running across the carbonate mounds area. Sediment transport pathways can also be d
may be an igneous feature

appears to be westward transport of sand along slope (Fig. 87).

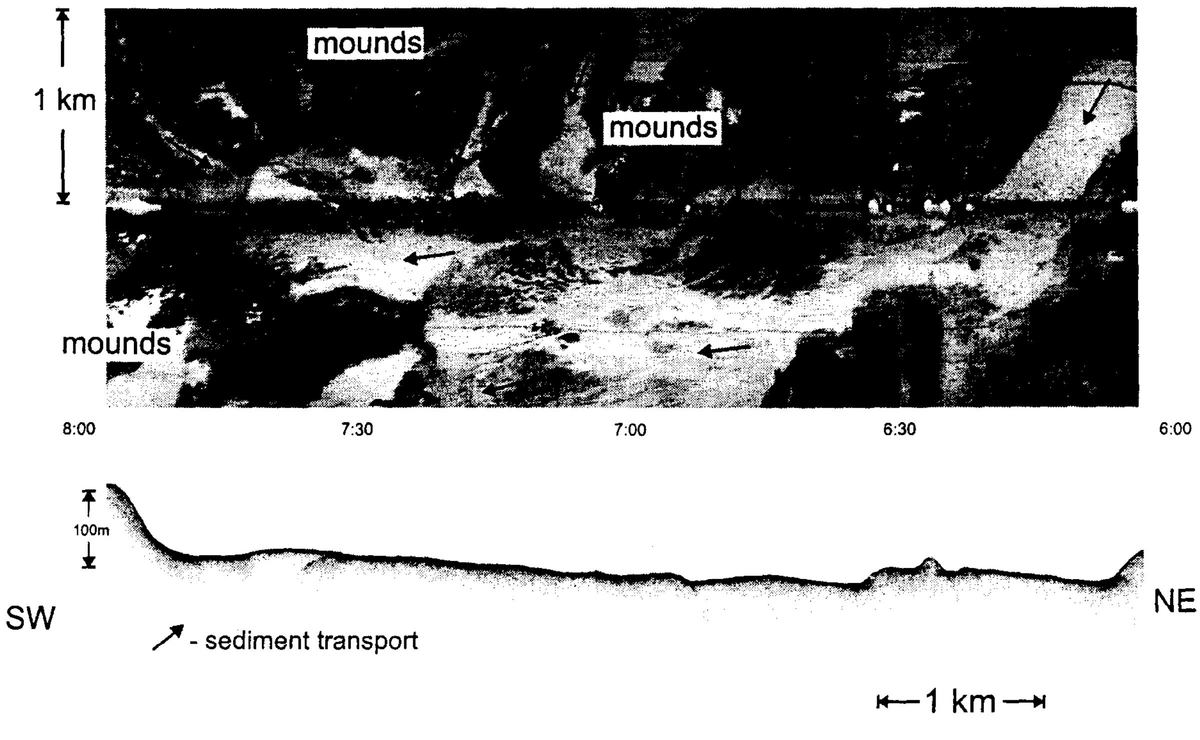

Fig. 87. ORAT-13 (fragment) sonograph and subbotom profiler record showing inter-mound area with low backscatter cover with indications of sediment transport southwestwards, alongslope

OREtech 100 kHz sidescan and 5 kHz subbottom profiler

ORAT-14 gives a higher resolution view of the seafloor across a number of different zones at the western end of the OKEAN mosaic. For the first hour and a half of the run the deep towed fish was clearly unstable and the sidescan sonar record has a regular distortion. However the remainder of the run produced a high quality record which greatly helps in interpreting features otherwise viewed only at lower resolutions.

The line begins upslope in OKEAN zone 2, which is a zone of very low acoustic backscatter that is presumed to be a sand cover, as it is ornamented by regular small waves. The cover is interrupted by a number of high backscattering elongate scours that are presumed to be formed by enhanced flow downstream of boulders. The flow is directed to the southwest. Many relatively small mounds with rounded profiles are crossed (OKEAN Zone 1). These are the carbonate mounds and they appear as high backscattering with a very high backscatter speckled pattern (Fig. 88). This speckling is fairly regular and may be coral thickets. Between the mounds there are fields of small sand waves. Some of the sand is swept across the mounds themselves. One well imaged field of sand waves is shown in Figure 89.

The 350 m tall, isolated mound that is seen in profile on Figure 80, has an ornamentation of fairly straight crested waves, moulded in some high backscattering material. The cores from the mounds all contained muds with coral debris. Thus the waves may be mud waves. There are more waves in high backscattering sediments at the lower end of the line. These latter are not sand waves but may be gravel waves, possibly formed by internal waves, or some type of current other than contour following currents, as the dominant direction of the crests is along slope.

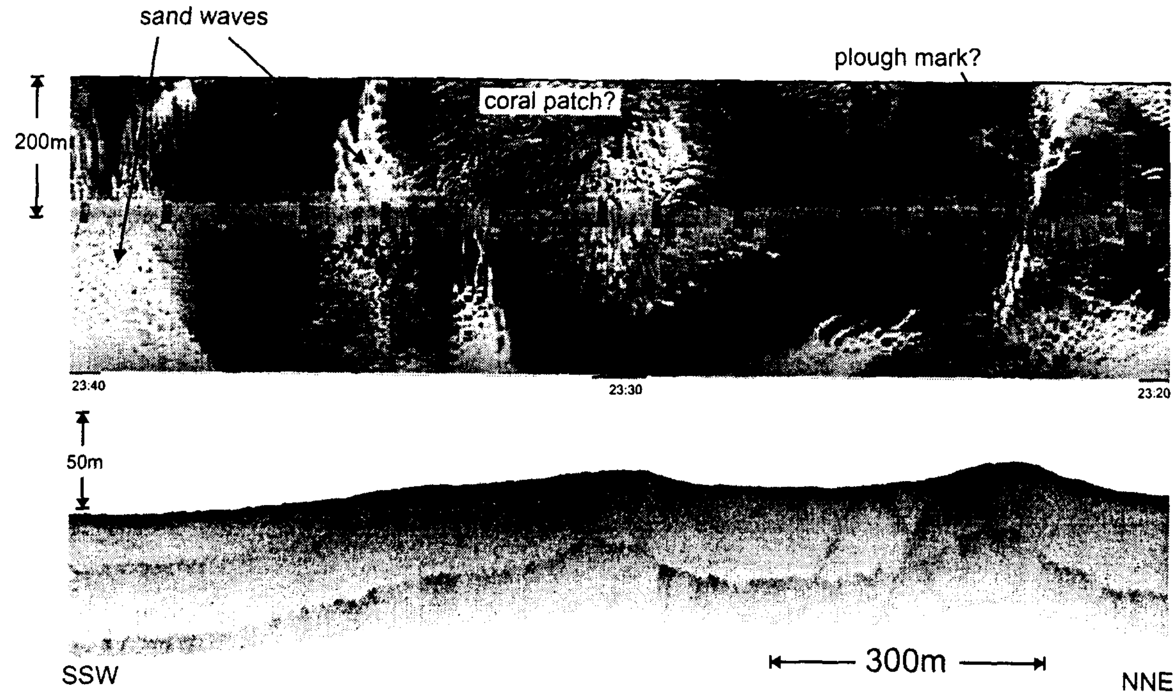

Fig. 88. ORAT-14 sonograph with resolution of 100 kHz. Areas of speckled acoustic backscatter are interpreted as possible coral patches or carbonate mounds

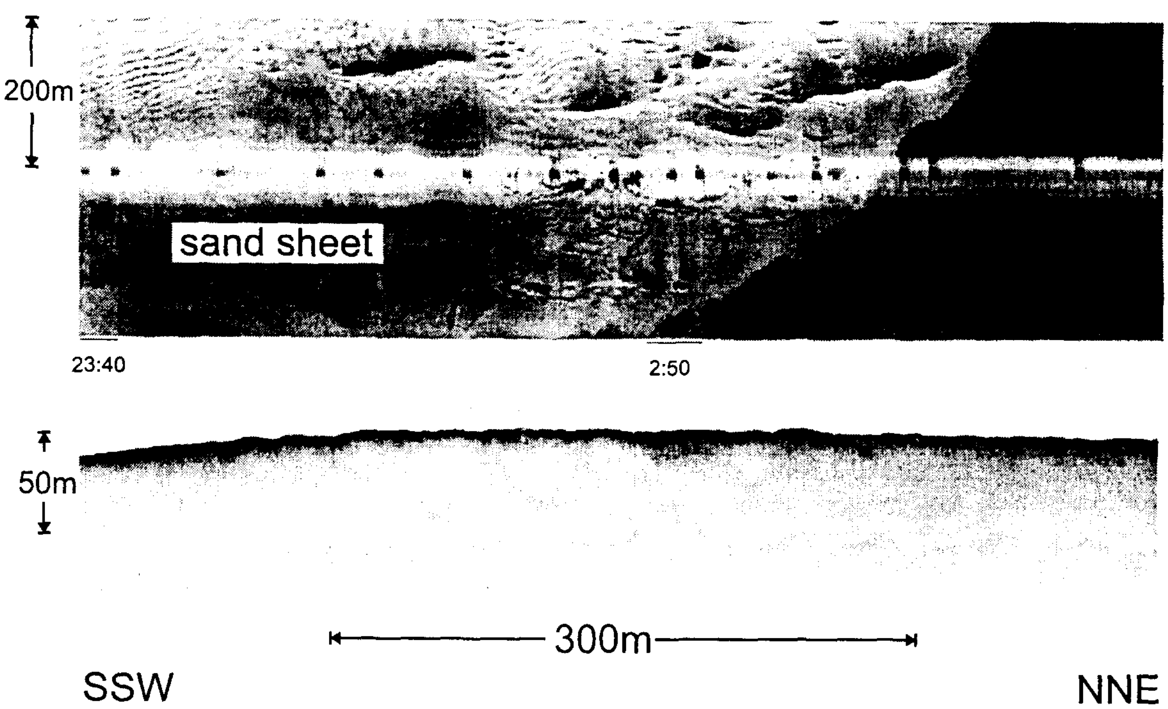

Fig. 89. Two contrasting zones of acoustic backscatter observed on the ORAT-14 sonograph which are most likely caused by presence of a rippled sand moving over gravel

II.3.c. SEISMIC AND OREtech LINE TIES AND INTERPRETATION: SE ROCKALL TROUGH

T. Nielsen, J. Taylor, J. Foeken, N. Kenyon, M. Ivanov, and A. Limonov

The interpretation presented here is made only on the basis of data collected during the TTR-7 cruise and the GLORIA sidescan sonar data from the R/V *Siren* cruise (1996). The data are of good quality, despite bad weather, and show a range of interesting and intriguing features. Interpretation is based on various versions of the (seismic) data, processed to different stages and representing both single and multichannel plots.

Labelling of seismic units is on the basis of divisions of the data made due to the complexity of the record. Therefore units pre-fixed 'A' are alongslope, from PSAT-13, and units labelled 'U', 'L', and 'P' are upper slope, lower slope and abyssal plain units from PSAT-14. These units are described above. Backscatter areas from the sonar data are not labelled as acoustic facies.

All the sections of the two seismic lines suggest the existence of a basal unit, identified on the basis of weak boundary reflectors. This unit is identified as A5, U5, and L5. The surface dips very gently to the NW and the set of overlying units thicken upslope. This is interpreted as the **base unit**.

Above the base unit is another unit (A4, U4, L3, L4? and P4) which seems to be constructed of dipping and possibly faulted bedrock, which forms escarpment shoulders on PSAT-14. Reflectors in this area on PSAT-13 are therefore the bedding of the rock in this area. Correlation of units L3 together with L4 with P3 and U3 would indicate that the high backscatter linear and conical features imaged on ORAT-11 are outcrops of this material, and that the rough surface texture is due to the bedding and internal structures exposed. This is interpreted as the **faulted unit**, and is topped by an erosive unconformity. It is the upslope thickening of this unit which significantly contributes to the whole succession lying above the base unit.

Above the erosional unconformity, the interval consisting of A3, U3, and L2 is apparent. This onlaps the faulted unit to the SW and thickens north-eastward, alongslope. It is imaged in cross-section in PSAT-14 and appears uniform downslope and then thins at the slope's lower end (end of U3, and L2). It is not believed to be present on the abyssal plain. Due to the outer shape and the internal reflectors, we believe this to be a sedimentary unit, labelled **lower unit**, topped by another erosive unconformity.

The downslope third of the lower unit is repeatedly disrupted by what appear to be intrusive, upwarping structures (**intrusion features**). Their origin may be related to volcanic or evaporite diapiric activity, associated with faults and weakness within the faulted unit below. Analysis of the phase and amplitude of the seismic signal rules out the possibility that these features are gas-related.

The next unit (A2, U2, and L1) forms the sea bottom for the majority of the downslope profile. The unit describes a sheet of material which covers the entire slope, from crest to plain, but not the outcrops of the faulted unit. Internal reflectors are subparallel for the most part, becoming increasingly undulating downslope. This may be an indication of a depositional environment dominated by a current regime concentrated at the base of the slope. This sedimentary unit is labelled **upper unit**. The small escarpments and associated minor faulting in this unit at the top of the slope, just below the crest, together with a small tilting of the internal reflectors, are suggestive of a rotational failure of the sediments. This failure may be due to the loading of the crest unit found only on the upper-most section of slope (see below). The degradation of internal reflectors, most apparent just above the first outcrop, may be attributed to disturbance from the intrusion features beneath. The sonar record shows no indication of current transport on the upper and mid-slope. In the outcrop area, there is some indication of northward alongslope transport, mainly evidenced by backscatter patterns (principally asymmetric moats).

The final unit, A1 and U1, is to be found only on the crest of the slope, and thickens progressively NE, alongslope. This is identified as the **crest unit**. It is banked up against the mounds seen at the top of the slope. Internal reflectors between mounds are downlapping, indicating a depositional environment. The mounds are partly buried by this unit in the SW. The mounds become smaller to the NE, possibly indicating that they become completely buried. The seismic data indicate that mounds have developed as the upper sediment of the crest unit has been deposited. The sonar record shows evidence for strong current transport northeastwards on this crest unit. The seismic data offer no indication of the internal structure of the mounds. However, samples indicate that the upper region of the mounds is constructed almost totally of carbonate, apparently built up in association with the coral found on top of them.

Basin plain geology is different from that associated with the slope. The units are apparently separated from those upslope by a large steep normal fault at the base of the slope, trending almost E/W and dipping NNW. Unit P4 is interpreted to correlate with the faulted unit, demonstrating a displacement of 400 ms TWT. It is not possible to correlate units P3 and P2 with the upslope units. It is possible to see that unit P2 is onlapping, indicating basinfill. Unit P1 is very thin on the multichannel seismic data, but the profiler offers some penetration here, indicating an unconsolidated unit. Sonar shows no features and medium backscatter, and sampling recovered only a little sandy material.

Extrapolation of this interpretation to ORAT-12 is difficult due to its isolated nature, both in distance and lack of other data. However, we believe that the similarity between the sonar and profiler data of ORAT-12 and the interpretation from further east make some conjecture possible.

The downslope area of highly variable backscatter is thought to be outcrop of the faulted unit, and that the rough surface texture is due to the bedding and internal structures exposed. The lineations upslope could be where this faulted unit has become partially buried. The negative topography is caused by northwest dipping normal faults within the outcrop unit. There is some evidence suggestive of northward alongslope transport in the form of tails of high backscatter behind outcrops. There is also strong evidence of downslope transport of low backscattering material. The profiler record offers some penetration for most of the length of the data, which suggests that the sedimentary environment here differs slightly from that east, where much less penetration was seen, concentrated at mid-slope. The only firm correlation possible is between the basin plain environments, which are similar both in backscatter and profiler data in ORAT-12 and 11.

II.3.d. INTERPRETATION OF SEISMIC AND SIDESCAN SONAR DATA: SW ROCKALL TROUGH

T. Nielsen, J. Taylor, J. Foeken, N. Kenyon, M. Horstink, T. Mikkelsen, A. van der Molen

It is evident from seismic data that the study area is divided into two separate regions. Region one forms the majority of the study area, region two only the eastern-most corner. Region two is separated from region one by an escarpment and a depressed hummocky zone. It is not possible to correlate between regions on the basis of the data collected.

There is no evidence for large-scale mass movement within region one, although at the most downslope part of the area there is some suggestion of failure.

In region one, the acoustic basement forms an undulating surface with several basins across the area. The units above appear to be infill deposits, gradually levelling the area over the deposition of the lower, middle and upper units. The surface of the upper unit is interpreted to be an erosive unconformity, above which are found the surface and mound units. Mounds occur only within 600-1000 metres water depth and get smaller and finally disappear to the SW.

The distribution of mounds obtained from seismic data matches well with that obtained from sidescan sonar. Here, the complex patterning in zone one is attributed to the mass of mounds found in this area, with their complex morphology and associated shadows. In between mounds are areas of lower backscatter, thought to be sandy sediment from upslope (see below). Inference of the existence of the surface unit across the whole area, at a thickness below the resolution of the seismic data, can be made from both sampling and sidescan data.

Below some mounds the top reflector of the upper unit is unusually flat and shows polarity reversal, indicating that the acoustic impedance of the units above is greater than the upper unit. Not all mounds display the unusual lack of velocity pull-up, however. These differences may be attributable to the mounds themselves being constructed of differing materials. It may also be that mounds which do not show the expected pull-up contain something additional within them or there is something different about the top layers of the upper unit in these areas. Work in the North Sea, for example, shows the existence of a carbonate consolidated layer associated with CH_4 or CO_2 charged porewater seeps at the base of carbonate reefs (Hovland, 1990). The results from sampling of the mounds indicated the possible existence of rather consolidated layers near the surface of the mound, which may explain the high velocity (>2000 m/s) if this material is present throughout. In contrast, it does not explain the flat nature of the underlying reflector. Since we are unable to see the relation between the surface and mound units clearly in the seismic data, it is not possible to say which explanation is the more likely, and there are many possible hypotheses.

The sonar data offer no help in explaining the relation between the surface and mound units. However, the sonar data do indicate that in the instance where there is a doming reflector beneath the mound, this is a generally flat area with steep sides, upon which the mounds seem to form. This suggests that the seafloor morphology is not constructed of solely the surface and mound units. The acoustic void beneath this doming structure makes it impossible to infer which unit forms this feature.

Surface processes in the survey area are inferred mainly from the sidescan data. Generally high backscatter can be attributed to the generally coarse nature of material found at the sea floor. The build-up of the surface unit against some of the bigger mounds suggests presence of an alongslope transport environment. This is confirmed by the presence of what are interpreted to be sand and gravel waves seen on both high and low backscatter areas in zones one and three. Waves appear on the top of mounds also. The direction of transport seems to be from NE to SW, from trails of coarse material seen extending from obstructions on the sea floor. The widespread occurrence of the features indicates that the current is active across the whole area. It may be partly responsible for moving sandy material found in zone two along and downslope into zone one.

There is evidence for a more direct downslope movement in the form of flows of material between mounds (Fig. 86). A thin, almost channelised, transport feature is seen at the western end of the main mosaic.

Upslope, the pairs of dark reflectors seen in zone two are interpreted as iceberg ploughmarks. This is because of their random orientation, and the dark reflectors are probably the ridges formed by the ploughing action of the iceberg.

II.4. Bottom sampling results

II.4.a. SOUTHEASTERN ROCKALL TROUGH

A. Mazzini, M. Ivanov, G. Akhmanov, A. Akhmetjanov, P. Friend, E. Kozlova, E. Ivanova, L. Mazurenko, Yu. Naumov, I. Belen'kaya, A. Saprykina, A. Stadnitskaya, A. Balashova, and R. Cave

Introduction

The area of investigation was the northeast margin of the Rockall Trough. A total of 14 stations were sampled using 5 different methods. The samples consisted of 2 dredges, 1 grab, 4 kasten cores, 2 box cores, and 5 gravity cores. Recovery of sample material throughout the area was poor, especially in the areas of sandy substrate and outcropping rocks. Maximum gravity core length retrieved was 135 cm (TTR7-AT-49G). The main sampling site parameters and sedimentological, acoustic and geological characteristics are summarised in Tables 4 and 5.

Core No	Date	Time (GMT)	Latitude	Longitude	Cable length, m	Depth, m	Recovery
TTR7-AT-41D	31.07.97	11.27 11.48	53°46.60'N 53°46.49'N	13°56,61'W 13°56,98'W	805 800	680 730	several corals and fauna trapped in the tangles
TTR7-AT-42B	31.07.97	14.17	53°46.55'N	13°56,83'W	670	668	a few corals and foramineferal ooze
TTR7-AT-43B	31.07.97	16.29	53°45.99'N	13°57,64'W	778	783	27 cm
TTR7-AT-44K	31.07.97	20.32	53°46.54'N	13°56,83'W	673	689	10 cm
TTR7-AT-45G	01.08.97	11.24	53°13,03'N	14°00,26'W	2991	2983	Core Catcher (CC)
TTR7-AT-46G	01.08.97	15.24	54°07,61'N	13°55,20'W	2470	2380	CC
TTR7-AT-47K	01.08.97	17.16	54°07,64'N	13°55,21'W	2510	2370	some clasts
TTR7-AT-48K	01.08.97	20.14	54°04,73'N	13°53,45'W	2185	2165	some clasts
TTR7-AT-49G	02.08.97	10.58	53°45,39'N	14°00,22'W	755	743	135 cm
TTR7-AT-50G	02.08.97	21.32	53°47,38'N	13°54,72'W	751	746	CC
TTR7-AT-51Gr	03.08.97	00.06	53°46,48'N	13°56,71'W	711	685	1 tonne
TTR7-AT-52D	03.08.97	22.17 22.48	54°08.82'N 54°08,41'N	13°55,37'W 13°55,48'W	2855 2655	2851 2750	a few corals and sponges
TTR7-AT-53G	04.08.97	15.58	54°02,85'N	14°13,64'W	2986	2991	CC
TTR7-AT-54K	04.08.97	17.59	53°59.93'N	14°14,15'W	2840	2823	CC

Table 4. General information on the cores sampled on the southeastern Rockall Trough margin

The study area can be subdivided into three main sectors:

1. Carbonate mounds on the upper slope
2. Outcropping rocks on the lower slope (east)
3. Outcropping rocks on the lower slope (west)

On the upper slope due to bad weather, the first carbonate mound core-sampling stations were chosen using data obtained previously (during a GLORIA profile of the area in 1996), and echo-sounder data obtained during this leg and the rest of the stations were selected on the basis of OREtech line ORAT-10. Sampling sites on the lower slope were chosen after analysis of OREtech 30 kHz sidescan sonar lines ORAT-11 and 12 and echosounder data.

The following descriptions are not necessarily in chronological order, but are classified according to sector.

Core No.	Geographical Setting	Sedimentary Summary	Instrumentation	Acoustic characteristics
TTR7-AT-41D	Upper slope: top of the carbonate mound (at 4:50 on ORAT 10) in the northwestern part of Porcupine bank	Corals and allochthonous fauna	OREtech sidescan sonar, single channel high resolution seismics	Moderate backscatter on the OREtech line 10
TTR7-AT-42B	Upper slope: flank of the carbonate mound. Close to AT-41D	Living corals, foraminiferal ooze, shells and coral fragments	OREtech sidescan sonar, single channel high resolution seismics	Same at AT- 41D on the OREtech line 10
TTR7-AT-43B	Upper slope: Flat area close to the carbonate mound (at 5:15 on the OREtech line 10. Close to AT-41D	Sequence of sands, becoming finer towards the bottom and muddy silts; layers rich in shells	OREtech sidescan sonar, single channel high resolution seismics	Flat area with current bedforms and low backscatter on the OREtech line 10
TTR7-AT-44K	Upper slope: second attempt to sample the top of the carbonate mound.	Mixture of foramiferal ooze, living corals and associated fauna	OREtech sidescan sonar, single channel high resolution seismics	Same location as AT-41D
TTR7-AT-45G	Lower slope, to the east: Flat area at the base of the Porcupine slope	Almost no recovery, small portion of foraminiferal ooze	Echo sounder and GLORIA profile	Flat area with very low backscatter on GLORIA profile
TTR7-AT-46G	Lower slope, to the east: close to the top of a large mound (at 12:00 on the OREtech line 11)	Small portion of medium sized sand very rich in forams, drop stones up to 6 cm in diameter	OREtech sidescan sonar, single channel high resolution seismics	Mound with conical structure with high backscatter on the OREtech profile 11
TTR7-AT-47K	Lower slope, to the east: Second attempt to sample the top of the mound. Same position as AT-46G	Small amount of sediment: foraminiferal ooze, drop stones, corals, sponges	OREtech sidescan sonar, single channel high resolution seismics	Same characteristics as previous core
TTR7-AT-48K	Lower slope, to the east: top of a large mound (at 9:45 on the OREtech line 11)	Some drop stones recovered	OREtech sidescan sonar, single channel high resolution seismics	Large mound with high backscatter on the OREtech profile 11
TTR7-AT-49G	Upper slope: Top of a small elongated carbonate mound at 6:05 on the OREtech line 10	Corals in the upper part overlying foraminiferal ooze that becomes more consistent towards the bottom and contains rotten corals	OREtech sidescan sonar, single channel high resolution seismics	Very low backscatter probably due to the acoustic shadow of the mound
TTR7-AT-50G	Upper slope: Top of a small carbonate mound at 4:05 on the OREtech line 10	Small amount of fine grained foraminiferal sand with clasts of non-lithified foraminiferal ooze, one clast covered by bryozoans	OREtech sidescan sonar, single channel high resolution seismics	Mound with very high backscatter in moderate backscatter area on the OREtech profile 10
TTR7-AT -51Gr	Upper slope: top of carbonate mound (at 4:50 on ORAT-10) sampled at AT-42B and AT-44K	1 tonne of foram ooze, drop stones, lithic fragments, shells, corals	OREtech sidescan sonar, single channel high resolution seismics	Moderate backscatter on the OREtech line 10 in a patchy area
TTR7-AT-52D	Foot of slope, to the east: a flank of seabed mounds at the foot of the northwestern Porcupine Bank margin	Few just broken corals covered by manganese (?) crust and sponges. Some of them were found alive	OREtech line 12	Low backscatter within an area of high backscatter
TTR7-AT-53G	Lower slope, to the east: to the northeast of the OREtech line 12	Relatively small amount of poorly sorted medium sandy sized sediment composed of forams with significant admixture of dark gravel	Echo sounder profile	
TTR7-AT-54K	Lower slope, to the east: top of the inferred slump body	Few cm^3 of brown marl, foram rich	Close to the OREtech sidescan sonar line 12, further echo sounder lines had to be done to localise the sampling station	

Table 5. Sedimentological, acoustic and geological characteristic of sampling stations on the southeastern Rockall Trough margin

Carbonate mounds on the upper slope

Dredge TTR7-AT-41D

The recovery consisted of corals and associated fauna trapped in tangles on the dredge. Most of the corals and other fauna found were alive. Main fauna identified: *Lophelia pertusa, Madrepora oculata* (corals), *Eunicid* sp. (polychaetes), sponges, brachiopods (for more detail refer to Chapter II.5. Biological data)

Core TTR7-AT-42B

Box corer almost empty. Recovered some assemblages of dead corals and associated fauna, plus some living coral and a small portion of foram ooze.

Core TTR7-AT-43B (Fig. 90)

There were three different intervals within the box-corer, with a total recovery of 27 cm. The first interval (0-8 cm) consisted of poorly sorted medium/coarse sand, structureless, rich in forams and shell fragments. On the upper surface, there were centimetre size drop stones (of different lithologies) and live bivalves. The second interval (8-12 cm) showed finer-grained sand with a higher content of clay fraction. The third interval (12-27 cm) contained two horizons (at 14 and 18 cm) rich in brachiopod shells. These were very well preserved in silty/muddy structureless sediment, rich in forams and organic detritus. The orientation of the shells could indicate bottom reworking by currents. Coral fragment found at 22 cm.

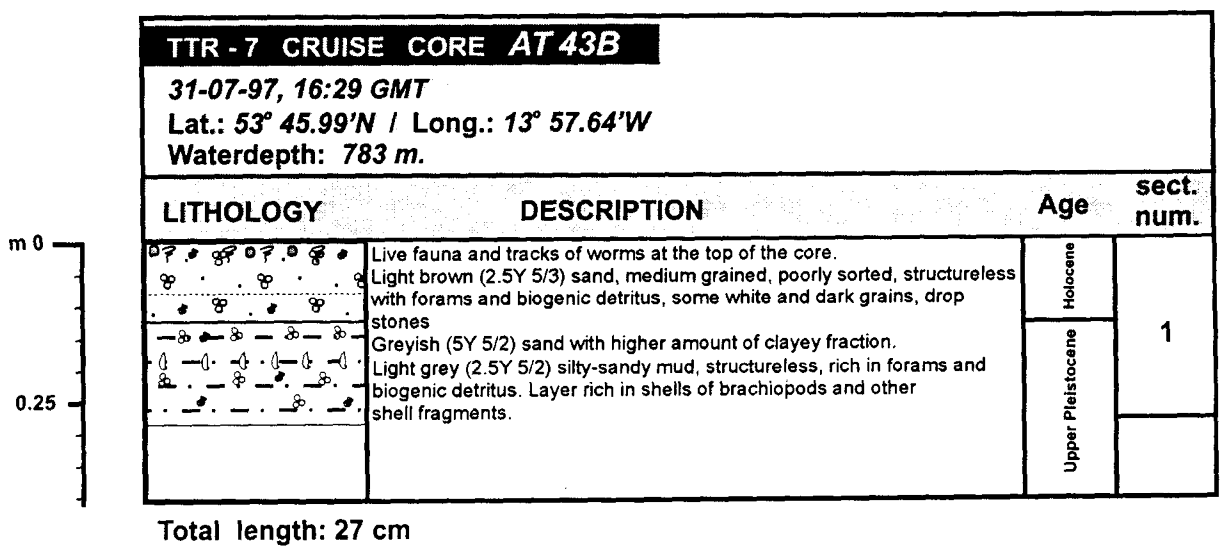

Fig. 90. Core log AT-43B

Core TTR7-AT-44K

Chaotic mixture of foram ooze, with living/dead corals and associated fauna (brachiopods, echinoderms, worms and sponges) in the upper part.

Core TTR7-AT-49G (Fig. 91)

The core can be subdivided into four main units:

1. The upper 5 cm consisted of corals and shell fragments in a light-brown foram ooze, becoming more consolidated (carbonate crust) towards the bottom.
2. Sharp boundary above 5 to 17 cm, of very light foram ooze, more consolidated in the upper part.
3. From 17 to 108 cm the sediment became a light-grey, soupy, water-saturated, foram ooze, containing well-preserved bivalve shells (at 39, 63, 81,87, 97 cm) and fragments of echinoderm spines (49 cm). At 79 cm there was a distinct oxidised layer, tilted in oblique orientation.
4. The lowest unit (108-135 cm) consisted of grey foram ooze containing a higher clay fraction and scattered rotten corals (some structural preservation of septum visible) and bivalve fragments. The sediment in this unit was a more consistent texture than that of previous units.

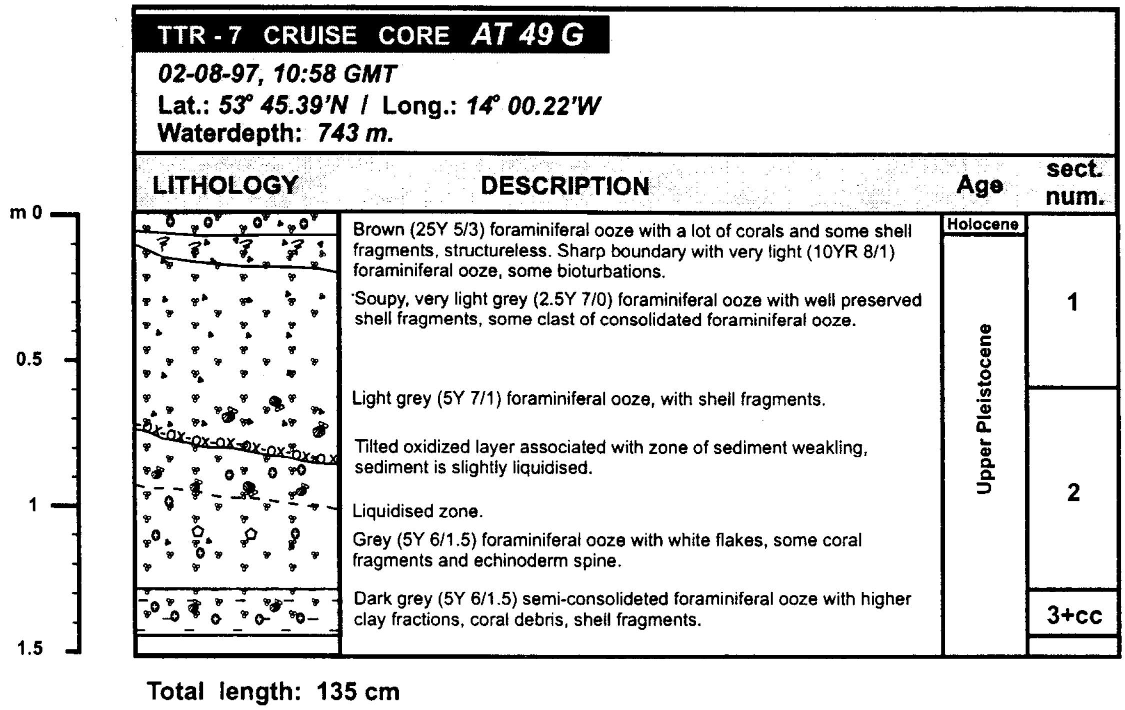

Fig. 91. Core log AT-49G

Core TTR7-AT 50G

Only a small amount of fine-grained foraminiferal sand with clasts of non-lithified foram ooze, and one clast covered by bryozoans.

Grab TTR7-AT-51GR

Generally, the sample comprised a grey hemipelagite containing lithic fragments, coral debris and shell fragments. The apparently undisturbed surface consisted mainly of shell debris and a 1-2 cm layer of patchy coral debris (*Lophelia pertusa* and *Madrepora oculata*), one living colony of *M. oculata* (approximately 20 cm in height), one living colony *L. pertusa* (approximately 20 cm in height), a cidaroid, a hydrozoa, and several bivalves. Sediment colour ranged from grey-green to yellowish-brown, with one white chalky interval. Lithic fragments were found throughout the sample. No internal structure could be determined, due to the disturbance caused by grab sampling.

In order to establish different sediment types, smear slides were produced and analysed by optical microscope. Due to the availability of only one sieve with 1.25 mm mesh size, the samples

were limited to the > 1.25 mm fraction. Following this analysis, six sediment types were described, as follows:
(1) Top layer, greyish-brown, fine gravel of shell and coral debris, with some sponge spicules (Si02).
(2) Brownish-grey sand, 50% foram and shell debris, 50% quartz grains, with some echinoderm debris and small black lithic fragments (< 1cm diameter).
(3) Muddy yellow foram ooze, containing a carbonate clast and some coral fragments with yellow oxidised coating.
(4) Pale brown foram ooze, with small siliciclastic component (approx. 10% quartz grains).
(5) Pale yellow-green foram ooze (80%), almost no shell debris, some quartz grains.
(6) Chalky white interval, contained within (5).

Lithic fragments: A total of 175 lithic fragments with lengths ranging from 23 cm to 1cm (average overall length of approximately 5 cm), and a total weight of about 60 kg were recovered from the grab. The lithic fragments appeared to be randomly spaced throughout the sample. Generally, they consisted of subangular to rounded sedimentary rocks, and angular to subangular metamorphic and igneous rocks. Of all rock types, the sandstones were the most rounded. Striation marks occurred on 5 of the lithic fragments (1 basalt, 1 chert and 3 schists), each with one surface that had been abraded flat. Of particular note, were 2 large, rounded light-brown sandstone dropstones, each with a length of approximately 23 cm, and a width of 16 cm. Most of the lithic fragments had some form of epifaunal covering (solitary corals, calcareous worm-tubes, and some inarticulate brachiopods) from which the coral colony is supposed to start its growth. For the purposes of this description, lithic fragments are classified according to type: igneous, metamorphic and sedimentary. Of the 175 lithic fragments recovered, it was not possible to classify 14 of them without further analysis. The unclassified fragments were of differing lithologies, grey/black in colour, subrounded, and had an average length of 6 cm.
Igneous: There were 39 igneous fragments within the sample. The majority were a grey to black, sub-rounded basalt. The black basalt clasts averaged 6 cm in diameter, and were wholly or partially covered by a brown iron oxide coating, itself covered by semi-consolidated hemipelagite matrix. The grey basalt clasts were slightly smaller, several displaying vesicles of approximately 1 mm diameter. There were 2 angular red granite clasts. The larger clast was 9 cm in length, and had a feldspar/quartz crystal size of 3-4 mm, with occasional 1 mm biotite. There were 2 angular granodiorites, each with lengths of about 6 cm, and 3 angular acid-igneous rocks (rhyolite?) with an average diameter of 5 cm.
Metamorphic: The sample contained 54 metamorphic fragments, comprising schists (total of 33), gneisses (14), quartzite (6) and amphibolite (1). Generally, the schists were larger (average 11 cm diameter) and more angular than the gneisses (average 7 cm diameter). The schists were mainly grey/black mica schists, with the exception of one garnet-mica schist (15 cm length) and 4 reddish quartzose schists (average diameter 7 cm). The 6 quartzite fragments were angular, and a light grey/brown colour. In two of the quartzite fragments, primary lamination was visible.
Sedimentary: There were a total of 68 sedimentary fragments in the sample, the majority of which were sandstones (total 49). The sandstones were fine to coarse, and light-brown, grey and red in colour. The clasts ranged in length from 23 cm to 2 cm, with an average diameter of approximately 5 cm. Of particular interest were several sandstone clasts that appeared to be halves of what originally been well-rounded, complete clasts. Included in the sandstones were the 2 large dropstones described earlier. In addition, there were 6 subangular light-grey to brown limestones. Of these, 3 had been heavily bioturbated, while the others displayed lenticular voids left by the dissolution of small (3-4 mm) bivalve shells. Of major interest was the discovery of several barely-consolidated light grey limestones, within which were incorporated coral debris, foraminifera tests, shell fragments, and worm casts. There were 7 subangular to rounded grey mudtone fragments (of 2 cm -8 cm in length), and one grey/black angular shale fragment approximately 3 cm length. Finally, there were 5 subangular to rounded brown cherty clasts, 2 of which had one surface that was 'polished' flat, and striated.
Interpretation: As the origin of the lithic fragments is not known, care has been taken not to refer to them *en masse* as 'dropstones'. While several of them clearly have an ice-rafted origin (indicated by the striation marks), some of the clasts (particularly the iron-oxide coated basalts) may have been derived from higher up the slope. Indeed, iron-stained conglomerates have been found at 500 m below

sea level on the western margin of the Porcupine Bank (Scoffin and Bowes, 1988). Other, more angular clasts may have been scoured locally by icebergs ploughing exposed bedrock on the continental shelf. Scoffin and Bowes (1988) identify metamorphic bedrock outcrops on the western margin of the Porcupine Bank, at the shelf edge and bank crest. Although it is suspected that not all of the semi-consolidated limestone clasts were recovered from the grab sample, the existence of a few indurated concretions may indicate alteration due to the presence of hydrocarbons or carbon dioxide-charged pore waters (Hovland and Judd, 1988). Geochemical analysis is required to further investigate the reasons for consolidation. There may be several mechanisms acting to accumulate material on the 'carbonate mound'. A biogenic input is evident from coral and shell debris. Evidence for an ice-rafted input is provided by the presence of dropstones and siliclastic sediments in the hemipelagic matrix.

Outcropping rocks on the lower slope (east)

Core TTR7-AT-45G

Almost no recovery. Only a small portion of foraminiferal sand and light-grey mud/clay found inside the core-liner.

Core TTR7-AT-46G

Small portion of medium-sized, poorly-sorted sand, very rich in forams and containing some dropstones of undetermined lithology (some basaltic?) up to 6 cm diameter .

Core TTR7-AT-47K

Only a small amount of core was recovered, consisting of: a) about ten clasts (some well-rounded) of different size and lithologies (dropstones?), including quartzite, fine brown sandstone, laminated siltstone, and arkosic sandstone, all covered by a thin black (Mn?) coating; b) foram ooze, rich in dark grains, c) one piece of siliceous sponge, several octocorals, live polyps and pteropod fragments described elsewhere in the report.

Core TTR7-AT-48K

Only 12 clasts (drop stones?) with black encrustation of different lithologies were recovered, 11 of small size (0,5-1 cm). The biggest, very well rounded, showed three worm tubes on the surface.

Dredge TTR7-AT-52D

Very little recovered in dredge. Several fragments of black-coated coral (*Desmophyllum cristigalli*) and some black sponges were found. Where the coral had fractured, the internal structure was white. On top of one coral fragment, was a white, living sponge. These observations indicate that the conditions under which the black coating is acquired may occur only periodically or take a long time to take effect.

Outcropping rocks on the lower slope (west)

Core TTR7-AT-53G

Less than 50 cm^3 poorly sorted, light-brown medium-sized foram sand. Approximately one third consisted of coarse, black subrounded grains of undetermined lithology. There were occasional larger (4 -8 mm diameter) subangular quartz clasts, plus several pteropods and other shell fragments, and some well-rounded sandstones. Also, an unusual 2 cm rusty-brown cylindrical clast (worm cast?).

Core TTR7-AT54K
Only a small volume (a few cm^3) of marl rich in forams was found on the external surface of the corer.

Discussion

It is possible to distinguish two different types of environment in the study area: i) a coral-colonization environment and ii) a bottom current influenced depositional system.

The first is mainly characterised by the presence of carbonate mounds at a water depth ranging from 690 m to 746 m for the tops, and about 790 m for the bases of mounds. Colonisation by corals is evident from the samples retrieved. In the longest core recovered in this area (TTR7-AT-49G), it is possible to recognise two different lithologies. The first consists of a mixture of foraminiferal ooze and predominant broken corals. The second shows a perceptible predominance of foraminiferal ooze over broken corals. The evident alternation of these two lithologies in the core could be related to two different external mechanisms:

1) The growth of the entire carbonate mound is associated with environmental fluctuations: during unfavourable conditions (e.g. climatic fluctuation, colder current appearance, increase in terrigenous input, etc.), the coral colonies may exhibit decreased production, with the deposition of a foraminiferal ooze-supported lithology. With the onset of propitious conditions, there is the formation of a coral-supported lithology.

2) The relocation of the coral colonies within the same mound in response to a change in the local hydrodynamic regime/ambient water characteristics and hence nutrient conditions around the carbonate mound. The coral-supported lithology, therefore, could represent optimal periods for coral-growth at a particular site, while foraminiferal ooze-dominated lithology may well indicate the relocation of the coral colonies to, for instance, the opposite side of the mound.

Only one box-core (TTR7-AT-43B) was taken in the flat zone adjacent to the carbonate mounds, where the OREtech sidescan sonar profile showed evidence of bottom-current activity. Also, the seismic profile indicated the presence of downlapping layering, suggesting the transportation and deposition of material by currents. The sediment recovered here consisted of different and alternating sandy layers, implying deposition from strong bottom-currents. Some layers have abundant, well-preserved shells. The sandy fraction becomes coarser towards the top, probably reflecting a recent increase in current strength.

It is presumed, therefore, that the growth of the carbonate mounds is closely related to bottom-currents. However, it is still hard to explain the co-existence of both strong bottom-currents, which are able to wash out even coarse sediments and foraminiferal ooze in the same environment. A periodicity in current activity is proposed as an explanation of this phenomenon. The colony grows upwards, supported by a strong current flux, which washes out all the pelagic foraminiferal ooze. A period of reduced current activity could permit the deposition of foraminiferal ooze which covers the colony, forming the mixtures of corals and ooze mentioned above. A new period of current activity could wash out the majority of foraminiferal ooze deposited. Only ooze incorporated in the colony, and protected by its framework, would be involved in a further diagenetic process. A new cycle of coral productivity can start from the uppermost branches of the colony.

Bottom-current activity is also evident in the eastern part of the lower slope. The small amount of material obtained limited a complete interpretation of the sedimentary environment. Only a small portion of poorly sorted fine to coarse-grained sand containing lithic fragments was recovered from the lower slope. Eight different lithologies were identified. This diversity of lithologies, the striations on their surface and their rounded shape are evidence that most of them can be classified as ice-rafted material. Some of the rock fragments found might originate from the outcropping rocks, which were clearly recognised on seismic line 14 and on the sidescan profile 11 (Fig. 92). All the drop stones exhibit a dark manganese crust on their exterior.

The microscopic analyses of the sandy fraction show polymictic composition, suggesting different source areas. Abundant fragments of basalt, fragments of igneous rocks, carbonate rocks, siliceous rocks, fresh mafic volcanic glasses, quartz grains, rounded garnet grains, manganese oxides, grains of olivine, limonite, pyroxene, and manganese nodules were described in smear slides. Probably a small amount of material belongs to the outcropping rocks, but the compositional variety is best explained by ice-rafted deposition.

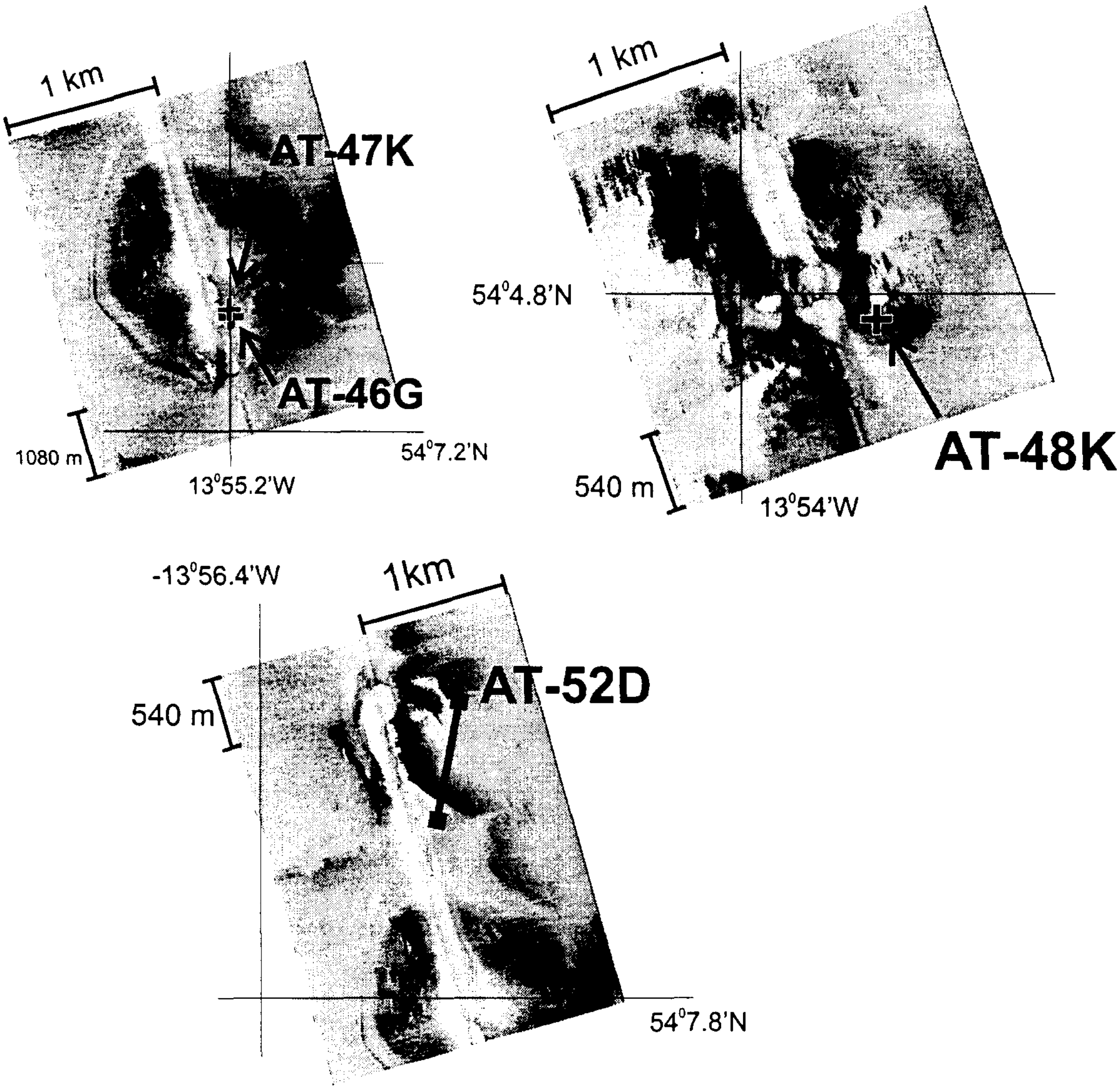

Fig. 92. Sampling sites projected onto OREtech sonographs (line ORAT-11)

The relatively well-sorted sandy material recovered from the flat area at the foot of the slope (core TTR7-AT-45G) indicates sorting of the sediment during transport.

It is difficult to draw conclusions for the western part of the lower slope. Only two sampling stations were visited, without exciting results. Only one station provided a sufficient amount of sediment for analysis. This showed the presence of poorly sorted, medium-grained sand, confirming the current activity indicated by the sidescan sonar profile ORAT-12.

It is likely that the outcropping rocks and the sandy layers (with scattered dropstones of different sizes) did not allow sufficient penetration of the gravity corer on the lower slope.

II.4.b. SOUTHWESTERN ROCKALL TROUGH

A. Mazzini, G. Akhmanov, A. Akhmetzhanov, P. Friend, E. Kozlova, E. Ivanova, L. Mazurenko, Yu. Naumov, I.Belenkaya, A. Saprykina, A. Stadnitskaya, A. Balashova, R. Cave

Introduction

A total of 14 stations were sampled, 11 by gravity corer and 3 by kasten corer. Recovery was relatively poor, especially when bottom-current deposits were the targets. Maximum core length recovered was 241 cm (AT-68G). The main sampling site parameters and sedimentological, acoustic and geological characteristics are summarised in Tables 6 and 7.

Core No	Date	Time, GMT	Latitude	Longitude	Cable length, m	Depth, M	Recovery, cm
TTR7-AT-55G	06.08.97	12.24	55°32.22'N	15°46.82'W	817	825	CC
TTR7-AT-56G	06.08.97	13.57	55°34.64'N	15°38.67'W	588	598	143
TTR7-AT-57G	06.08.97	14.35	55°34.95'N	15°37.67'W	710	714	CC
TTR7-AT-58G	06.08.97	15.08	55°35.00'N	15°37.23'W	694	698	CC
TTR7-AT-59K	06.08.97	15.56	55°35.10'N	15°37.23'W	700	700	CC
TTR7-AT-60K	06.08.97	16.59	55°34.65'N	15°38.67'W	590	590	50
TTR7-AT-61K	06.08.97	18.39	55°36.75'N	15°31.88'W	595	594	20
TTR7-AT-62G	06.08.97	19.26	55°36.79'N	15°31.91'W	605	604	61
TTR7-AT-63G	06.08.97	20.02	55°36.61'N	15°32.25'W	660	657	174
TTR7-AT-64G	07.08.97	11.59	55°33.34'N	15°23.70'W	1125	1135	CC
TTR7-AT-65G	07.08.97	13.35	55°'31.39N	15°29.43'W	1133	1140	CC
TTR7-AT-66G	07.08.97	14.11	55°31.17'N	15°30.20'W	1200	1210	CC
TTR7-AT-67G	07.08.97	16.32	55°28.78'N	15°50.07'W	666	684	61
TTR7-AT-68G	07.08.97	17.26	55°28.34'N	15°49.73'W	900	870	241

Table 6. General information on the cores sampled on the southwestern Rockall Trough margin

The investigated area can be subdivided into two main parts according to the recovery and the geological setting:
1. The upper slope
2. The middle slope, to the south

Sampling was undertaken on the basis of the data provided by sidescan sonars and echosounder.

The upper slope

<u>Core TTR7-AT55G</u>

Small quantity (<50 cm^3) of poorly sorted polymictic sand, some corals and abundant shell fragments. Also, reddish to black/brown subangular rock fragments (from a few millimetres to 2 cm in diameter) of unidentified lithologies, some with epifauna attached.

<u>Core TTR7-AT56G (Fig. 93)</u>

The surface (0-7 cm) comprised some living coral, plus coral debris. There were 3 main units in the core. Unit A (from 17 cm to 53 cm) consisted of semi-consolidated, grey, foram ooze that was rich in shell-fragments and coral debris. From 53 cm to 61 cm, the foram ooze became more consolidated, and richer in shell fragments with less coral debris. From 61 cm to 88 cm, the grey foram ooze was rich (up to 45%) in biogenic debris, and the water content increased. Unit B comprised 4 sub-sections. From 88 cm to 118 cm, poorly sorted, brown carbonaceous gravelly sand with a significant siliclastic content. From 118 cm to 129 cm, a brown foram ooze containing pebbles and shells. From 129 cm to 134 cm, a fairly well-sorted brown layer represented by gravel-sized coral fragments. From 134 cm to 138 cm, a dark brown foram ooze with branching and solitary coral fragments of differing sizes. Unit

Core No.	Geographical Setting	Sedimentary Summary	Instrumentation	Acoustic characteristics
TTR7-AT-55G	Upper slope: flank of a supposed carbonate mound (at 19:50 on PSAT-16),	Small amount of poorly sorted sand, lithic fragments, shell fragments, and some corals	OKEAN sidescan sonar; single channel high resolution seismics	
TTR7-AT-56G	Upper slope: top of the carbonate mound (at 8:02 on ORAT-13)	60 cm of sediment with alternation of foraminiferal ooze rich in corals and without corals. Sandy layer with dropstones	OREtech sidescan sonar; OKEAN sidescan sonar; single channel high resolution seismics	High backscatter on the ORAT-13
TTR7-AT-57G	Upper slope: moat of the carbonate mound sampled at station AT-56G	2 cm^3 of poorly sorted medium grained sand, shell fragments, and some small clasts	OREtech sidescan sonar; OKEAN sidescan sonar; single channel high resolution seismics	Low backscatter area on ORAT-13; evidence of sediment transport by current
TTR7-AT-58G	Upper slope: flat area at the foot of the carbonate mound sampled at AT-56G (at 7:35 on ORAT-13)	10 cm^3 of poorly sorted medium grained sand rich in shell fragment, coral fragments, and few small clasts	OREtech sidescan sonar; OKEAN sidescan sonar; single channel high resolution seismics	Low backscatter area on ORAT-13
TTR7-AT-59K	Upper slope: same position as the station AT-58G	small amount of the same material as at the station AT-58G recovered	OREtech sidescan sonar; OKEAN sidescan sonar; single channel high resolution seismics	Low backscatter area on ORAT-13
TTR7-AT-60K	Upper slope: second attempt to sample at the same place as the station AT-56G	Large amount of corals, some of them alive, and foraminiferal ooze	OREtech sidescan sonar; OKEAN sidescan sonar; single channel high resolution seismics	High backscatter on ORAT-13
TTR7-AT-61K	Upper slope: top of the carbonate mound (at 5:50 on ORAT-13)	Broken corals, foraminiferal ooze, and shell fragments	OREtech sidescan sonar; OKEAN sidescan sonar; single channel high resolution seismics	High mound with a conical shape in a large area with high backscatter on ORAT-13
TTR7-AT-62G	Upper slope: top of the carbonate mound (at 5:50 on ORAT-13)	Living corals at the top, foraminiferal ooze, and coral debris	OREtech sidescan sonar; OKEAN sidescan sonar; single channel high resolution seismics	High mound with a conical shape in a large area with high backscatter on ORAT-13
TTR7-AT-63G	Upper slope: flank of carbonate mound previously sampled at the station AT-61G (at 5:58 on ORAT-13)	Alternation of foraminiferal ooze rich in coral debris and homogeneous layers with smaller amount of corals	OREtech sidescan sonar; OKEAN sidescan sonar; single channel high resolution seismics	Medium backscatter area on the steep flank of the carbonate mound on ORAT-13
TTR7-AT-64G	Rough area on the middle slope of the south-eastern Rockall Bank margin	Very small portion of fine grained sand, and some small clasts	OKEAN sidescan sonar; single channel high resolution seismics	
TTR7-AT-65G	Middle slope of the south-eastern Rockall Bank margin	Small amount of medium grained sand with pebbles and shell fragments and live sponges	OKEAN sidescan sonar; single channel high resolution seismics	
TTR7-AT-66G	Middle slope of the south-eastern Rockall Bank margin	0.5 cm^3 of poorly sorted sand	OKEAN sidescan sonar; single channel high resolution seismics	
TTR7-AT-67G	Upper slope: large carbonate mound	Corals dead and alive, foraminiferal ooze	OREtech sidescan sonar; OKEAN sidescan sonar; single channel high resolution seismics	
TTR7-AT-68G	Upper slope: steep flank of the carbonate mound previously sampled at AT-67G	Corals and foraminiferal ooze mixture; some layers with lesser amount of coral debris	OKEAN sidescan sonar; single channel high resolution seismics	

Table 7. Sedimentological, acoustic and geological characteristics of sampling stations on the southwestern Rockall Trough margin

C consisted of light-brown, fairly well consolidated foram matrix with a very high (up to 70%) coral and shell debris content.
Interpretation: It seems likely that the three units represent three different stages in the activity of the carbonate mound. The high coral debris content of Unit C appears to be similar in structure to the top of active carbonate mounds. It may, therefore, represent the top of a once-active mound. The gravelly sand layer in Unit B suggests a change in the activity of the mound due to high input of coarse material. Possible ice-rafted debris could explain also the presence of centimetric rounded clasts. In Unit A, the mound has again become active, indicated by similar greyish foram ooze and live coral growth seen on the top of carbonate mounds investigated on the southeastern margin of the trough.

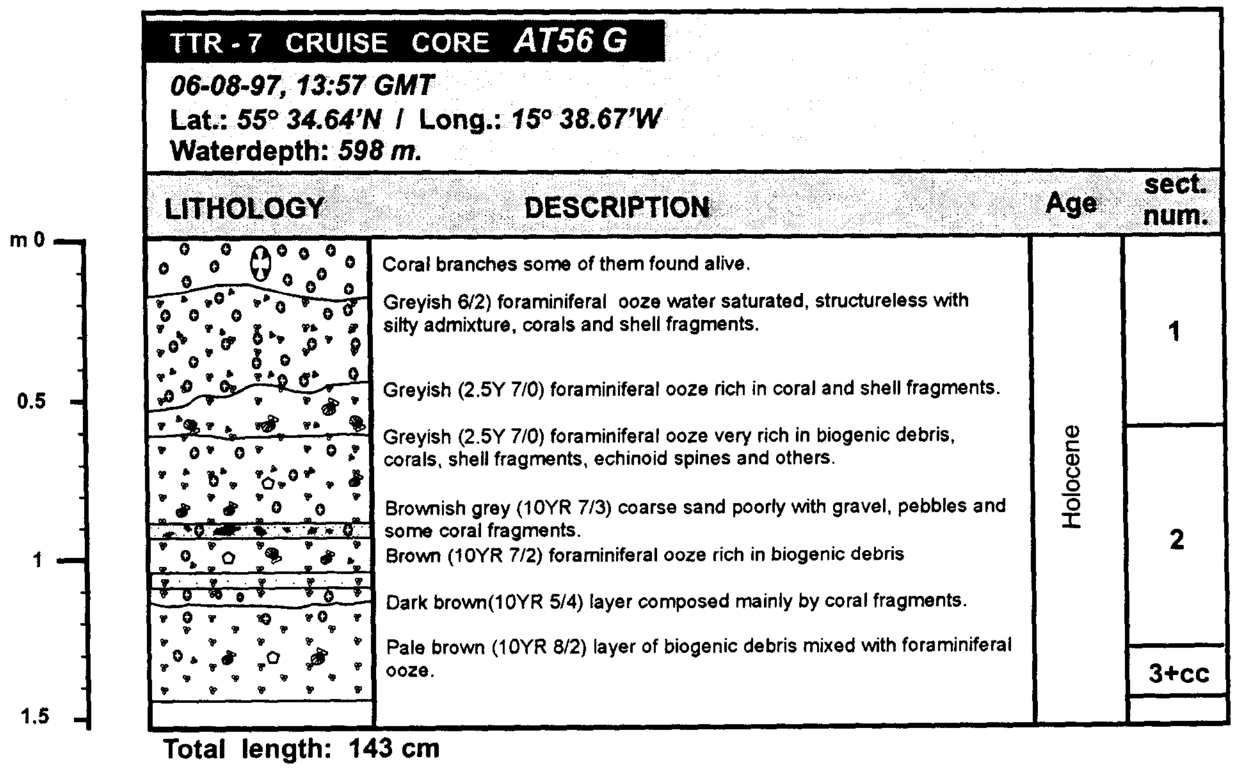

Fig. 93. Core log AT-56G

Core TTR7-AT57G

A small volume (<2 cm^3) of poorly sorted medium-sized shelly sand was recovered. Included were several small, brown/black, tabular, gravel-sized clasts of differing lithologies, and one cidaroid spine (6 cm in length).

Core TTR7-AT58G

A slightly larger volume (<10 cm^3) of material was recovered than in the previous core. The sediment was poorly sorted, medium-sized shelly sand, with less small gravel-sized clasts, but contained more coral fragments.

Core TTR7-AT59K

Small sample of poorly sorted, medium-sized, shelly sand recovered, of similar type as previous 2 cores. The sediment contained several small granite clasts (<1.5 cm in diameter) and one piece of degrading coral.

Core TTR7-AT-60K

The top of the carbonate mound, previously sampled by AT56G, was cored for the second time primarily in order to recover biological specimens. The top surface of the core comprised a thick layer (up to 20 cm) of both living and dead coral (*L. pertusa* and *M.oculata*), as well as a number of other biological specimens. Below the surface coral layer, there was light grey foraminiferal ooze.

Core TTR7-AT-61K

Only a small recovery comprising light grey foram ooze, rich in broken corals, pteropod fragments, and other shell fragments. Several cidaroid spines and some degraded coral fragments were also found.

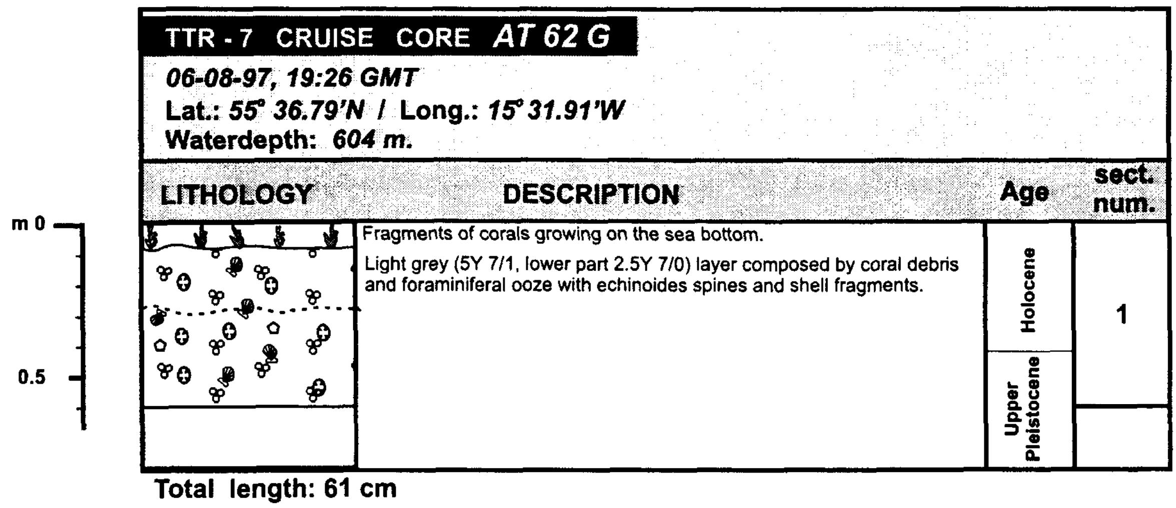

Fig. 94. Core log AT-62G

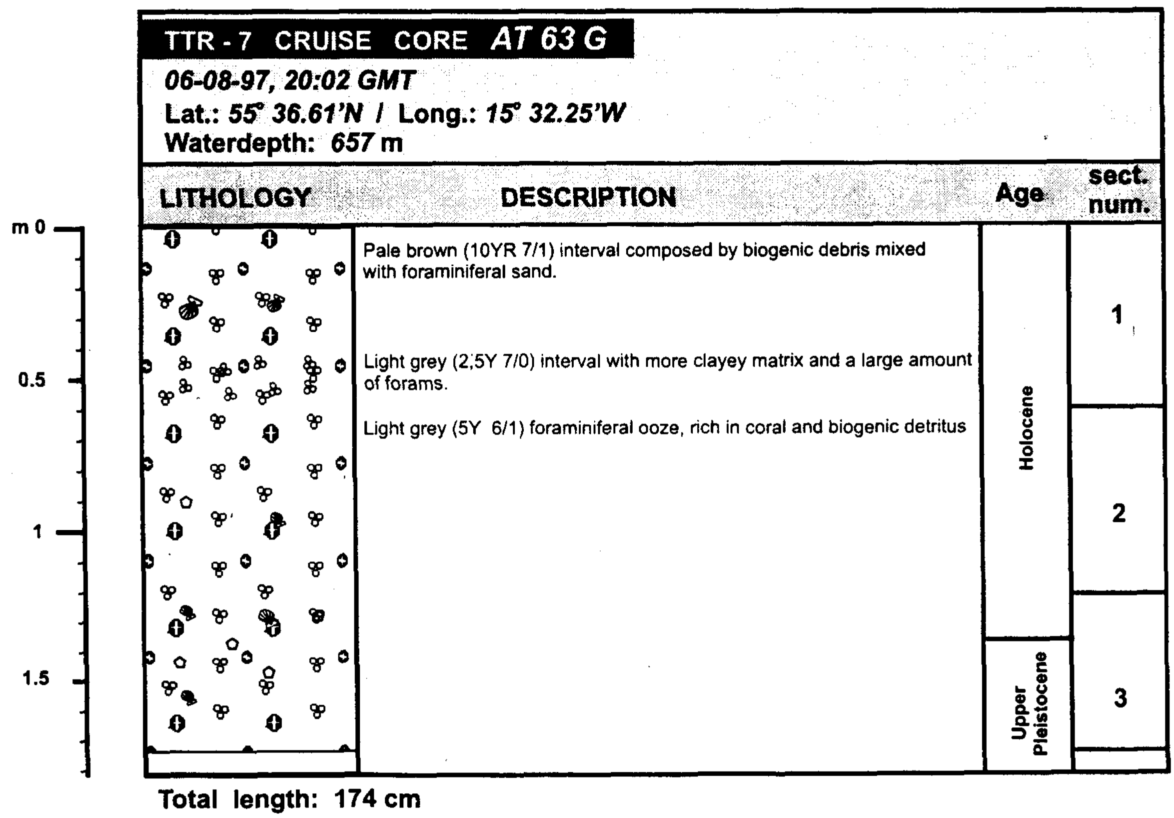

Fig. 95. Core log AT-63G

Core TTR7-AT-62G (Fig. 94)

The general core composition was grey, foraminiferal ooze containing broken coral fragments. The surface layer (0 cm to 7 cm) consisted of broken coral fragments. Below this (7 cm to 11 cm) there was a soupy, grey foram ooze, and from 11 cm to the base of the core, light grey foram ooze (containing abundant coral debris, occasional cidaroid spines and shells), changing gradually through brownish grey to dark grey.

Core TTR7-AT-63G (Fig. 95)

A broadly homogenous core composed of biogenic debris in light grey to grey foram ooze matrix. The matrix in interval 0-39 cm was light grey sandy foram ooze, while that in the interval 39 cm to 59 cm was darker, with a higher clay and water content, and a reduced foram content. From 60 cm to the base of the core, composition was structureless, light-grey foram ooze, with coral debris, diffused shell fragments and echinoderm fragments.

Core TTR7-AT-67G (Fig. 96)

Generally, the core composition was light grey, structureless foram ooze, containing coral debris and, at 54 cm, shell fragments. Several living and dead corals were found at the top of the core.

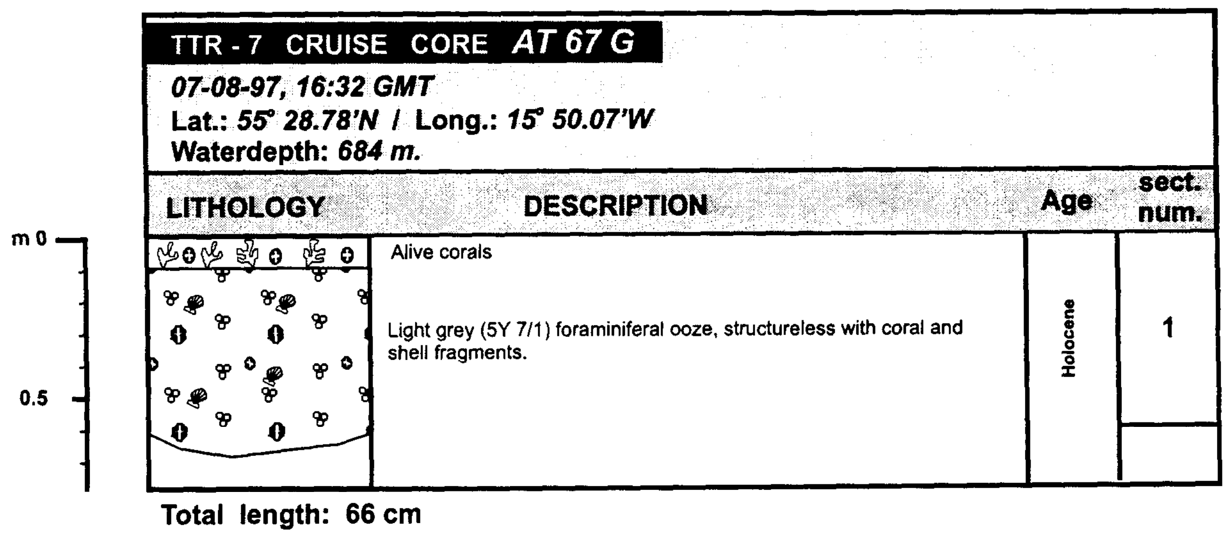

Fig. 96. Core log AT-67G

Core TTR7-AT-68G (Fig. 97)

The surface was comprised mostly of dead coral fragments with some small live colonies. Generally, the core was fairly homogenous foram ooze matrix containing coral debris and shell fragments as before. Certain subtle colour and textural differences, however, were apparent. From 10 cm -22 cm there was brownish, slightly soupy foram ooze, and from 22 cm to 60 cm, more consolidated, structureless, greenish foram ooze with similar fragments as above. From 61cm to the base of the core, there was little variation in colour. Here, the composition was rather dry light grey ooze, with coral debris. Between 119 cm and 178 cm there were occasional sand-sized black grains of unknown origin. From the core top to base, a small, but noticeable, decrease in the amount of coral fragments was observed.

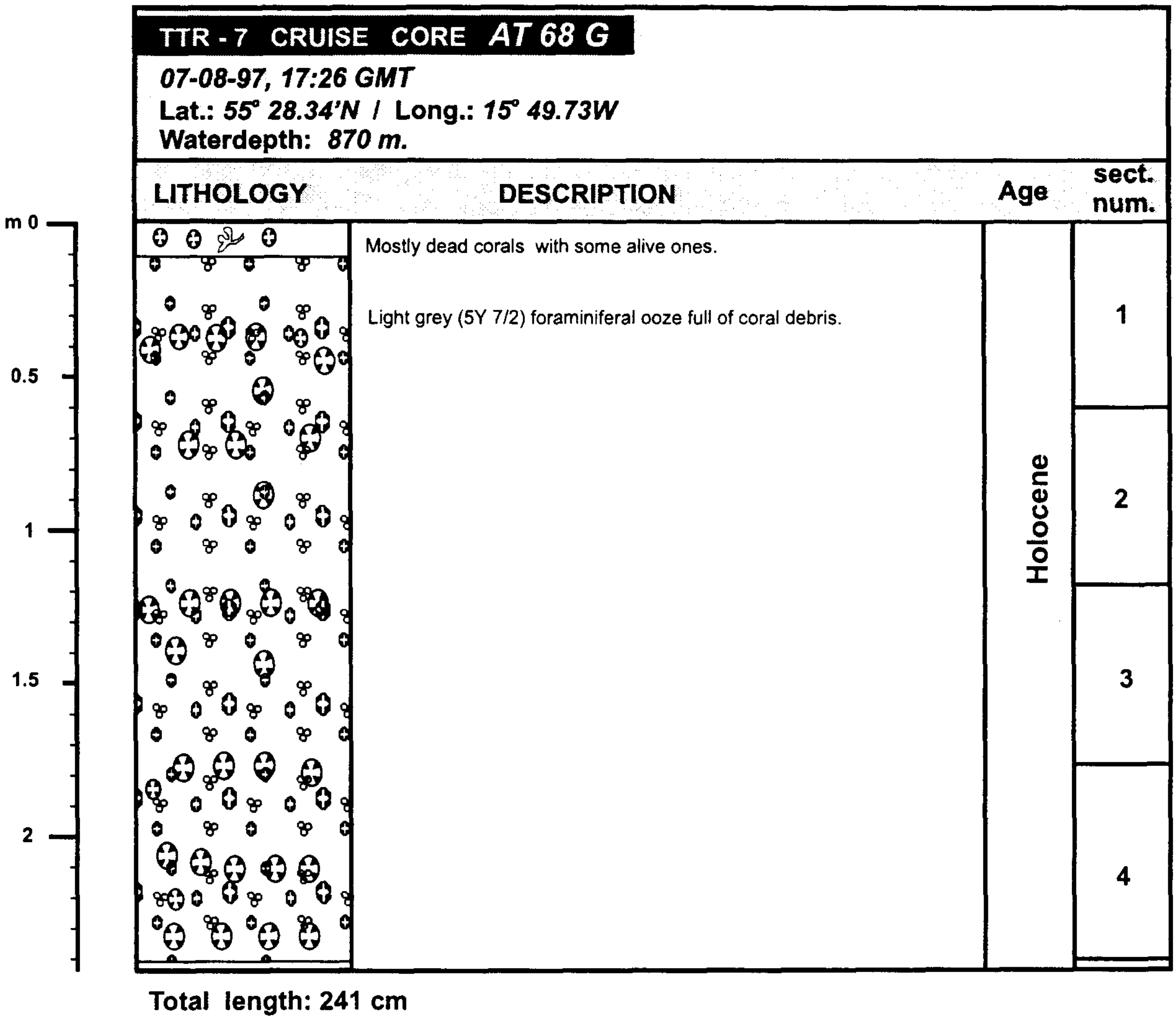

Fig. 97. Core log AT-68G

The middle slope, to the south

Core TTR7-AT-64G

Very small recovery. A trace of fine sand, including one cidaroid spine and 5 gravel-sized lithic clasts. These comprised 3 dark grains (3 mm in diameter) of unidentified lithology, and 2 larger (sandstone?) clasts approximately 1 cm in diameter.

Core TTR7-AT-65G

Only a small recovery of poorly sorted, coarse sand, including 3 fairly well-rounded pebbles (2 cm to 4 cm) of unidentified lithologies (dropstones). Some yellowish, horny shell fragments, small live sponges and barnacle plates.

Core TTR7-AT-66G

A very small volume (0.5 cm^3) of poorly sorted, biodetritic and siliciclastic sand. The siliciclastic content comprised grains of differing colours (from dark brown, red and yellowish) and unidentified lithologies.

Discussion

The same environments and lithologies described in the previous chapter can also be recognised on the southwestern Rockall Trough margin.

On the upper slope, characterised by the presence of carbonate mounds, the alternation of the two different lithologies, coral-supported and foraminiferal ooze-supported, is predominant on the topographic highs. Sampling was also performed at the base of these mounds where the sediment recovered consisted of medium-grained poorly sorted sand, containing clasts, shell fragments, some corals and biogenic detritus. The size class of the sand, and the large biogenic component, suggest a combination of current-transported sand with supply of biogenic material from the nearby carbonate mounds.

As can be observed from sidescan data and coring results, the carbonate mound area is affected by bottom-currents. It is likely that, once again, the growth of the coral colony is closely related to current activity, as observed on the southeastern margin of the trough. Through mineralogical analyses of the composition of the coarser sediment fraction, a wide variety of different fragments is observed. They range from quartz, feldspar, limonite, sulfides, and hornblende, to magmatic rock fragments, hematite, and glauconite. Such a large diversity could be explained by ice-rafted deposits reworked by bottom-currents.

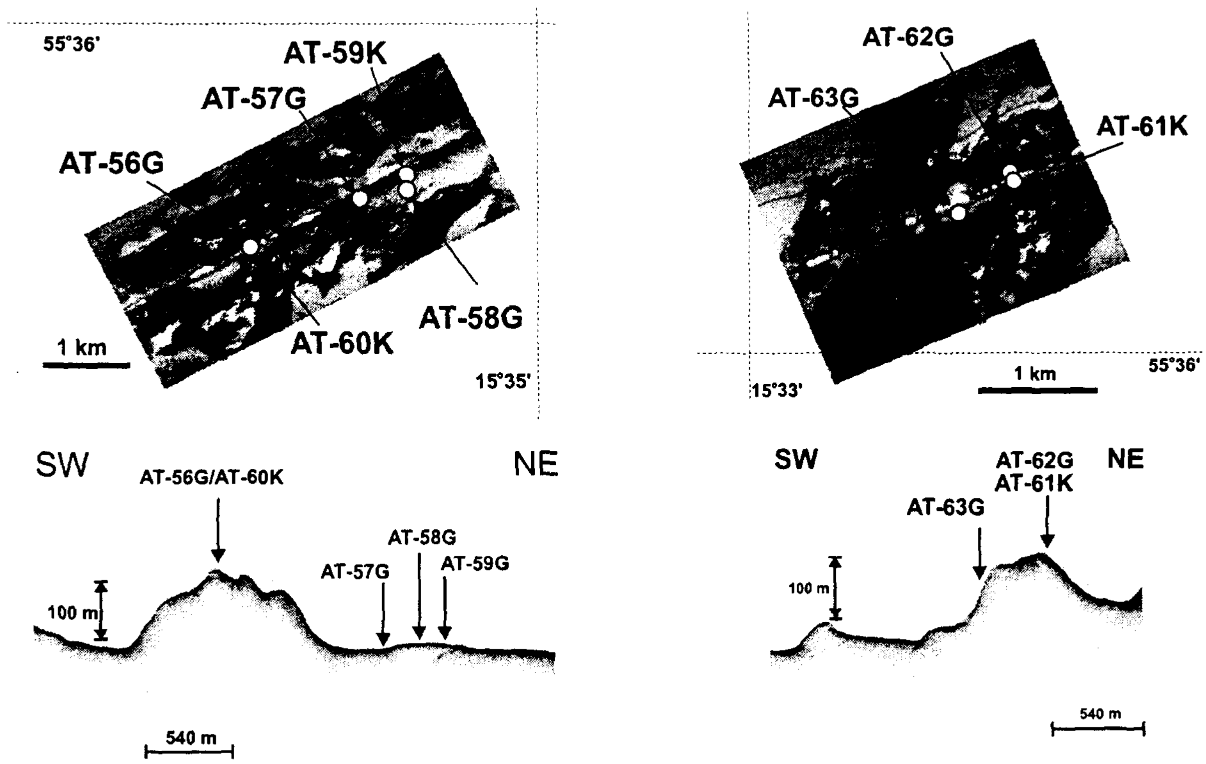

Fig. 98. Sampling stations projected on the ORAT-13 sonographs

It is also worth noticing that the tops of carbonate mounds are located in this area at a water depth ranging from 590 m to 870 m, whereas their bases are situated between 700 m and 900 m (Fig. 98). The comparable results with area 5 could suggest that coral colonies grow preferentially at the same depth.

In the southernmost part of the area recovery from the sampling stations was basically the same as for the samples taken from the base of the carbonate mounds, but with a lower amount of biogenic material. This material is presumably transported by the strong currents whose effect can also be recognised on an OKEAN profile.

II.5. Biological data:
MACROFAUNAS AND BIOGENIC CARBONATES FROM THE NORTH SLOPE OF PORCUPINE BANK, SOUTH EAST SLOPE OF ROCKALL BANK AND WEST OF FAEROE BANK CHANNEL

J. Wilson and C. Vina Herbon

Introduction and methods

Samples were obtained from north slope of Porcupine Bank and the south-east slope of Rockall Bank in order to investigate the carbonate producing macrofaunas and the nature and composition of the sediments forming the distinctive mounds and knolls observed on sonographs (both long-range and medium range) and seismic profiles obtained both prior to and during the cruise.

Samples were collected using a gravity corer, Kasten corer (with box area of 40 cm by 40 cm), box corer (with box area of 50 cm by 50 cm) and a Preussag TV grab capable of taking a sample of over one tonne of sediment. Where possible a traverse was undertaken with the underwater TV and camera system.

Faunal data was obtained by initial examination of the samples immediately following collection and afterwards in the laboratory. Where possible, identification of species present was undertaken and tables prepared (Tables 1 and 2) showing the occurrence of macrofaunal species - particularly corals and molluscs -within each sample. Molluscs were identified using Tebble (1976) and Graham (1988).

Occurrence of deep-water coral on the carbonate mounds

Deep-water corals especially *Lophelia pertusa* are widely distributed in the north-east Atlantic (Wilson 1979a). The distribution on Porcupine Bank and in the Porcupine Seabight was described initially by Duncan (1873) and referred to by Wyville Thomson (1874). Joubin (1922a,b) published a distribution based on data supplied by French fishermen who recorded the presence of *L. pertusa* and *Madrepora oculata* ('corail blanc') and *Dendrophyllia cornigera* ('corail Jaune') and further observations were given by Le Danois (1948).

Observations from samples and TV video records obtained during the TTR-7 to the Porcupine Bank and Rockall Bank suggest that the summits and upper slopes of the majority (if not all) of the many carbonate mounds and knolls identified on sidescan sonar and other records of the northern flank of Porcupine Bank and on the south-eastern slope of Rockall Bank are covered by a carpet of coral debris which supports a living coral fauna consisting principally of the two colonial species *Lophelia pertusa* and *Madrepora oculata.* The solitary coral *Desmophyllum cristagalli* and the octocoral *Stylaster* sp are also ocasionally present. It seems probable that, amongst the living coral fauna, the relative proportions of *L. pertusa* and *M. oculata* colonies collected or observed were either similar or there was a preponderance of *Lophelia. L. pertusa* dominated the dead coral debris however. Most of the live colonies collected in the samples are up to 15 cm in height. Underwater TV observations suggest that many colonies are up to 30 cm in height. Perhaps two or three colonies more that 30 cm high were observed during the TV tow down the northern flank of Porcupine Bank. This contrasts with the submersible observations made in the Porcupine Seabight (Tudhope and Scoffin, 1995) and on Rockall Bank (Wilson, 1979b) where colonies 1.5 to 2m in height and occurring in patches were observed.

Specimens showing the attachment of the coral to the substrate are rare (Wilson, 1979b,c). They are hard to collect from the surface by dredging or trawling as that tends to break off the specimens above the point of attachment during the process of collection. Several specimens were collected using the gravity core, Kasten core and TV Grab which included the point of attachment and which showed in some detail the relationship between the eunicid worm *Eunice* sp and both *M. oculata* and *L. pertusa* where the early growth of the colonies was determined by the direction of growth of the worm tube (Wilson and Freiwald, in preparation). Evidence from these specimens and from the video record showed that in these instances the colonies developed from planular settlement.

Observations from the TV video record suggests that asexual budding and the development of rings of colonies as proposed by Wilson (1979b) appears to be the method of growth on the upper part of the mounds where coral debris forms a carpet over the surface. Groups of cobbles and small boulders were observed adjacent to the coral debris towards the top of the mound. Planular settlement appears to have taken place on many of these cobbles, giving rise to individual coral colonies.

Southeastern Rockall Trough

SAMPLE	41	42	43	44	49	51
MOLLUSCS:						
Gastropods						
Scissurella crispata		X				
Emarginula conica				X		
Margarites sp.			X	X		
Jujubinus clelandi				X		
Calliostoma granulatum				X		
Calliostoma occidentale						X
Alvania cimicoides		X				
Manzonia zetlandica		X				
Lunatia montagui				X		X
Lunatia sp.			X			X
Boretrophon truncatus		X		X		
B. clathratus		X		XX		X
Volutopsius norwegicus						X
Colus gracilis						X
C. howsei						X
Turrisipho fenestratus			X			
Turrisipho sp.	X					
Neptunea antiqua						X
Troschelia berniciensis				X		X
Spirotropis monterosatoi			X			X
Oenopota trevelliana						X
Oenopota rufa			X	X		XX
Eumetula costulata			X			X
Cerithiella metula			X			
Triphora adversa				X		
Triphora sp.		X	X			
Bivalves						
Nucula sulcata			X			
Nucula turgida				X		
Nuculana minuta		X				X
Arca sp.	XX	XX	X	XX	X	XX
Arca pectunculoides		X	X	X		X
Limopsis aurita	X					XX
Monia patelliformis	X	X				
Heteronomia squamula	XX	XX	X	X		XX
Pecten maximus						X
Chlamys sulcata	X	X		X	X	XX
C.varia		XX		X		XX
C.nivea				X		X
C. vitrea	X	X		X		
Chlamys sp.		X	X		X	
Astarte elliptica	X		XX	XX		XX
Spisula sp.				X		
Hiatella arctica	XX	X		XX	X	
Cuspidaria cuspidata			X			

Southwestern Rockall Trough

SAMPLE	55	56	60	61	62	63	65	67	68
MOLLUSCS:									
Gastropods									
Scissurella crispata	X		X	X			X	X	X
Emarginula conica			X						
Collisella tessulata			X						
Margarites sp.			X						
Skenea basistriata							X		
Setia sp.					X				
Capulus ungaricus				X					
Lunatia montagui							X		
B. clathratus			X						
Trophonopsis barvicensis			X						
Oenopota rufa			XX	XX		X	XX	XX	XX
Eumetula costulata									X
Cerithiella metula				X					
Epitonium clathratulum			X						
Pyramidelids					X				
Bivalves									
Arca sp.	XX	XX	XX	X	XX	XX	X	X	X
Arca pectunculoides		X				X			
Limopsis aurita		XX							
Monia patelliformis		X							
Heteronomia squamula		XX	XX	XX	X	XX		XX	X
Chlamys sulcata			X	X					
C.varia			X	X	X	X			
C.nivea			X						
C. vitrea			XX	XX	X		X		X
Chlamys sp.			XX						
Acesta excavata			XX						X
Hiatella arctica		X	X	XX					

Table 8. Taxa recorded at the stations sampled

Detailed observations on faunas in cores and samples -northern slope of Porcupine Bank

TTR7-AT-41D

Live coral community –*L. pertusa* and *M. oculata* -ecosystem on a base of coral debris. The associated fauna appears to be well developed with 48 species represented. There is a high species diversity -mostly sponges and polychaetes. Suspension feeders are the dominant feeding type in this ecosystem.

The most important mollusc species are *Arca* sp and *Heteronomia squamula*, followed by *Hiatella arctica* and *Chlamys* sps (Table 8). *Arca* sp and *Hiatella arctica* nest on the branches of the coral and within the calcified eunicid tubes. *H. artica* is also found in dead calices. *Heteronomia squamula* is found on the branches with the attached valve cemented to the coral. Some molluscs such as *Limopsis aurita* and some *H. artica* were found with bioeroded and grey, discoloured shells. *Astarte elliptica* is abundant in the sediment with both fresh and old valves. The *Chlamys* species found here (*C. sulcata* and *C. vitrea*) are typical of deep water and appear to be associated with *C. varia* and *C. nivea* on the coral banks.

TTR7-AT-42B

Dead assemblage of coral debris of *L. pertusa* and *M. oculata*. The sediment is sand composed of foraminiferas, bivalve debris, echinoid spines and small fragments of coral. The coral debris and some of the bivalves show heavily bioeroded surfaces with extensive evidence of attack by microborers -particularly fungi. Others borers such as sponges and gastropods are also present. No living specimens were found.

Arca sp and *Chlamys varia*. are again the most abundant bivalve species. These species exhibit more bioerosional characteristics but attack by microborers is also seen in specimens with fresh looking ornament such as *Hiatella arctica*, *C. vitrea* and *Heteronomia squamula*. The bivalves *Nuculana minuta*, *C. sulcata* and the gastropod *Boreotrophon clathratus* had shells which were not attacked by microborings and had unaltered ornamentation. *Nuculana minuta* is a species typical of mud and fine sand bottoms. *B. clathratus* is a subfossil, Arctic species.

The foraminifera indicate a Holocene age. The benthic forams have a high diversity suggesting well-ventilated conditions with sufficient nutrients to sustain the population.

TTR7-AT-43B

Dead assemblage of coral debris with brachiopod and bivalve debris. The brachiopod species is very abundant and differs from that found alive on the corals.

Astarte triangularis was the most abundant bivalve and it is common in the sediment. Some specimens were live. Species such as *Arca* sp. and *Triphora* sp. were heavily bioeroded. The molluscs in this sample appear to have fewer bioeroded features than the previous sample. *Nucula sulcata* and *Eumetula costulata* had unaltered shells. *N. sulcata* lives in muddy sea floor while *E. costulata* is a subfossil, Arctic species.

TTR7-AT-44K

The sediment surface consists of dead and bioeroded *L. pertusa* and *M. oculata* fragments, mostly approximately 2-4 cm in length. Many of the fragments are lying more or less horizontally on the surface. Occasional branches stick out almost vertically for up to 2 cm above the sediment surface.

The sediment is coarse sand composed of mainly coral debris and fragments. Other contributers are bivalves, echinoid spines (*Cidaris* sp) and serpulids. Gastropods are present but in a lesser extent. The fauna is mostly dead and includes *Chlamys* sps, ophiuroids, octocorals and brachiopods. A *Sertularia* sp.colony was growing on a coral branch together with *Hydroides norvegicus*. The fauna present is primarily composed of detritivores and secondarily of suspension feeders.

Some shells are heavily bioeroded and are also microbored. These include *Chlamys nivea, C. varia, Astarte elliptica, Arca sp., A. pectunculoides, Hiatella arctica, Heteronomia squamula* and *Troschelia berniciensis. Nucula turgida, Oenopota rufa, Lunatia montagui, C. sulcata, Boreotrophon truncatus* and *B. clathratus* are also present but with less altered shells. The last two are Arctic species and have a limited distribution, *B. clathratus* was abundant. It is subfossil in the area. *Jujubinus clelandi* and *Margarites* sp. were unaltered.

TTR7-AT-46G

Small sample obtained. Only hydroids present.

TTR7-AT-47K

Small sample of pebbles and mud obtained. Fauna included live sponges and hydroids with some delicate octocorals and dead pteropod shells.

TTR7-AT-49G

No live *Lophelia* was present. Coral debris was present on the top of the core together with remains of bivalves and brachiopods. All are very bioeroded. The inarticulate brachiopod *Crania anomala* was found alive on the coral branches. Below the sediment surface there was evidence of burrowing activity, problably by worms, together with coral and bivalve debris. One small cirripede fragment (*Balanus* sp.) was found. Coral debris disappears below the top few centimetres of the sediment. The only coral debris found lower in the core was approximately 140 cm below the surface where two pieces of about 1 to 1.5 cm were located. These fragments were very fragile and bioeroded. Between 60 and 120 cm below the surface there were occasional *Chlamys sulcata* and *Chlamys* sp. valves with a few echinoid spines and other bivalve debris.

The complete absence of coral debris over much of the length of the core may be due either to the removal of the coral by iceberg action when the bergs grounded on the top of the knoll or to the effects of a strong current acting on the coral bank which removed the remains of coral. This was followed by a period where conditions may have been unfavourable for the establishment of new colonies. These could be due to either to the absence of recruitment of planulae, to changes in the current direction or maybe to a period of unsuitable temperature conditions for the growth of the coral (too warm or too cold). Nannoplankton and microfaunal data suggest that the sediment was deposited during the interglacial Riss-Wurm period (Isotopic Stage 5). This could be an effect of temperature throughout the water column at this stage.

TTR7-AT-50G

One dropstone and some foraminiferal ooze of Lower Pleistocene age were recovered. The pebble supported an extensive cover of encrusting epifauna especially bryozoans and some hydroids with erect branches of less than 1 mm in height. All the fauna was of small size. Attached valves of inarticulate brachiopods which are bioeroded to a greater or lesser degree and the remains of the cemented portion of a serpulid polychaete tube 7 mm in width traversing the dropstone were also clearly visible.

The absence of any erect epifauna on the dropstone may suggest the periodic passage of sand in transit over the pebble which would prevent the development of such a fauna.

TTR7-AT-51GR

The sediment surface consists of coarse sand and grit with occasional branches of *M. oculata* and *L. pertusa*. Occasional branches stick out from the surface. Some are more or less vertical. Other biogenic carbonate includes otoliths, bivalves and brachiopod valves. The sediments consist of coarse sand composed of coral debris with a high proportion of bivalves, brachiopods, serpulids and echinoid spine debris.

Live colonies of *M. oculata* and *L. pertusa* were present on the surface. They were both attached to dead *Lophelia* fragments. The associated living fauna was similar to that in previous samples. Two large calcareous fragments of octacoral attachments were found within the sediment. The dropstones support abundant individuals of the serpulid *Placostegus tridentatus,* with its characteristic tubes, which are initially cemented to the surface and later stand erect from the substrate. *Serpula vermicularis* was also very important. Other dropstone fauna included solitary corals similar to *Balanophyllia* sp. Again articulate brachiopods were abundant in the death assemblage as in sample AT-43B.

Large gastropod shells such as *Neptunea antiqua* (12 cm in height), supporting live polychaetes within the aperture were obtained. Other large gastropods included *Voluptosis norwegicus* (9.5 cm in height). Some of the molluscs had bioeroded surfaces with borings (probably sponge) and microborings. Other shells such as *Colus howsei* (rare) and *Spirotropis monterosatoi* appear to be largely unaltered. *Arca sp, Astarte elliptica, Chlamys sulcata, Oenopota rufa, Heteronomia squamula* and *Limopsis aurita* are the common mollusc species. Again Arctic and cold water species were found. Some of the species present have not been recorded previously at this depth.

TTR7-AT-52D

Sample consisted solely of dead epifauna removed from a rock surface by the dredge. This included the solitary coral *Desmophyllum cristagalli* and a distinctive siliceous sponge, both encrusted with manganese. The coral showed perfect septal structure and is heavly stained deep black. Small living sponges were attached within the calices of the dead coral. Living foraminifera were also present. The dead sponges were heavily stained with manganese and some presumed solution of the silica forming the spicules had taken place, but the spicular structure could still be detected. A siliceous sponge spicular skeleton, half of which was encrusted with manganese, was recovered. This suggests that during the slow process of encrustation by manganese, some of the spicules appear to be have been destroyed perhaps by partial solution of the silica.

Observations on faunas in cores and samples -south east slope of Rockall Bank

TTR7-AT-55

A small quantity of sand with dropstones was recovered. The coarse sand was composed of coral and bivalve debris with cirripede plates. Other components included serpulids (*Serpula* sp.) and irregular echinoids. Sabellarids (arenaceous polychaetes) and small hydroids were present on the dropstones. Cirripede plates were abundant. Some were large (2 cm), with very corroded and dark surfaces while others had a fresh appearance. The mollusc debris was mostly *Arca* sp. *Scissurella crispata* was also found (Table 8).

The size and characteristics of the cirripede plates suggest that some transport of these sediments has taken place. Barnacles live attached to cobbles, rock outcrops and large shells. They are suspension feeders. The dark staining on the surface of some of the cirripedes suggests anoxic conditions. The presence of fresh, unstained carbonate fragments associated with these bioeroded plates may indicate that the cirrepede plates have been reworked. The dark cirripedes were perhaps within an anoxic sediment.

Black stained barnacle plates which gave a radiocarbon date of ca. 11000 years BP were found on the continental shelf west of Scotland (Wilson, 1982). In this case the plates came from barnacles growing in much shallower water during low sealevel conditions.

TTR7-AT-56G

Gravity core with living colonies of *Lophelia* and *Madrepora* attached to coral debris. This coral was very bioeroded with a high content of microboring and boring (probably sponges). The fauna present was similar to that seen in previous cores and included sponges, hydroids, bryozoans and ascidians attached to the dead parts of the coral. Living fauna included the polychaete *Aphrodita* sp. and the inarticulate brachiopod *Crania anomala*. Live specimens of *Arca* sp. were growing on the corals. Some dead shells - mostly *Heteronomia* and *Arca* sp. - were found on the bottom of the living coral colonies (Table 8).

Coral debris and fragments -some large, up to several centimetres in length -were present throughout the length of the core. This differs from the cores obtained on the west side of Porcupine Bank (AT49) in that coral fragments are not present throughout the core.

Large cirripede plates were recorded 75 cm from the top of the core. They have very bioeroded surfaces. Some of them are white while others are yellow stained (probably limonite) suggesting oxidising conditions. Both have encrustations of bryozoans, serpulids and corals. Some remains of bryozoans which are unstained were growing on top of this limonite layer, suggesting that the plates were exposed at the sediment surface some time after the staining had taken place.

A small layer of bivalves consisting of *Arca* sp, *Limopsis aurita, Hiatella arctica* and *Arca pectunculoides* -all with the black patches on the shells -was located 120 cm below the surface. The black staining was also lining or filling the microborings. *Heteronomia squamula* was another abundant bivalve but the black staining on these shells was less well developed and some of the microborings were not lined with the black colouration.

Below 120 cm, coral debris was again abundant even at this depth within the core. This is in marked contrast to previous gravity cores where no coral debris was found in the deeper sections of the core. The fragments have a yellow (limonite?) stained layer with very bioeroded and microbored surfaces. Bivalve debris and cidaroid spines were also present in the core.

As already stated, cirripedes grow on hard subtrates. They need a solid base. A possible explanation of the presence of cirripedes here is that they were growing either on the coral or on top of a cobble or other solid base -possibly a bivalve -that would allow these cirripedes to survive. The possibility of transport of the cirripede plates in this instance is difficult because the sample was collected from the top of a large knoll. If the cirripedes were growing on the coral, this would have to have been on a large diameter calcified eunicid tube associated with large branches because of the size of the cirripede plates.

The black colour on the shells and corals may be produced by anoxic conditions at the bottom of the coral colony due to the accumulation of organic material.

TTR7-AT-60K

One small living colony of *L. pertusa* (7 cm in height) and a smaller single branch of *M. oculata* were growing on an accumulation of dead coral branches on carbonate mud and bivalve debris. The fauna present on the coral was the same as that on the Porcupine Bank with the exception of the presence of the bivalve *Acesta excavata*. This bivalve was common. It is 4.5 cm across. They were attached to the coral branches in the same way that *Chlamys* sps are attached. Other abundant bivalves growing on the coral were *Arca* sp and *Heteronomia squamula*. In the dead assemblage *Oenopota rufa* and *Chlamys vitrea,* together with the cold water species *Trophonopsis barvicensis* and *Boreotrophon clathratus,* were the most abundant molluscs. Other fauna present included a live nemertine worm. Nemerteans had not been found at previous sampling sites. A cirripede plate fragment (5 cm) and a smaller plate both white in colour and unaltered, were found among the coral fragments. A specimen of the solitary coral *Desmoplyllum cristigalli* was recovered alive. The southern species *Epitonium clathratulum* was also found.

The coral debris present was of three distinct colours, buff yellow and non bored, pale brown or yellow brown with extensive borings and microborings and a dull white colour which also shows evidencc of extensive microboring and bioerosion. Generally the intensive sponge and microboring was commoner on one side of the branch than the other. This suggests that that side was probably in close proximity to the sediment surface while the upper surface was exposed to grazers. The debris was 90 -95% *Lophelia,* 5 -10% *Madrepora* and less than1% *Stylaster*. Some of the *Lophelia* branches displayed massive calcification while others were relatively thin.

This sample was situated on top of the same knoll as the previous sample. The presence again of cirripede plates, in this case unaltered, suggest the growth of barnacles either within the coral or on a nearby rocky area.

TTR7-AT-61

Dead assemblage of coral debris -mostly *Lophelia* -with some *Madrepora* and *Stylaster* sp. present. The general colour of the coral and bivalve debris is less black, as was seen in earlier samples such as AT56. The living fauna included ophiuroids, some hydroids and sponges. The more abundant molluscs were *Oenopota rufa, Heteronomia squamula, Chlamys vitrea* and *Hiatella arctica*. With the exception of a few specimens, almost all the molluscs have white shells which are not bioeroded. The gastropods *Capulus ungaricus* and *Cerithiella metula* were also present.

TTR7-AT-62G

Gravity core of less than 60 cm in length. The top consisted of dead *Lophelia* branches and debris again with live ophiuroids, small hydroids and sponges. Some of the coral had a darker colouration while other fragments were much whiter in appearance. Specimens of *Arca* sp. were growing on the coral branches. Below the dead coral, at the sediment surface, remains of *Arca* sp., *Heteronomia squamula* and *Chlamys vitrea* were present. Within the core the sediment was composed of coral debris, brachiopods, cidaroid spines and bivalve debris. A few specimens of *C. vitrea, C. varia* and *Chlamys* sp. were present.

TTR7-AT-63

Living sponges and hydrozoans were attached to the branches of the dead coral colonies. Large pieces of coral were found within the core as in previous cores from the area. The most abundant molluscs are *Oenopota rufa, Heteronomia squamula* and *Arca* sp. They have white surfaces and are not very bioeroded.

TTR7-AT-65

A few small pebbles with some sand were recovered. Two living sponge species were present with ophiuroids living inside them. Pteropod shells and very distinctive cirripede plates were present in the sand. Some of these cirripede plates were a distinctive yellow-brown colour and were stained with limonite while others were black in colour and were heavily bioeroded. The small, attached, calcareous serpulid *Spirorbis* sp (also black in colouration) was present together with remains bryozoan remains. Cemented sand was adhering to the inside of the possibly limonite stained cirripede plates. Many foraminiferans were attached to the surfaces.

The presence again of these yellow and black cirripede plates in this sand suggests some sediment transport. The colour differentation can possibly represent differences in the chemical conditions within the sediments in which they were buried before they were reworked and transported to this location. Chemical analysis will be required to determine the exact nature of the staining. The presence of an encrusting fauna on the cirripede plates indicates exposure on the sediment surface that would permit the colonisation of the plates by these organisms.

The molluscs found here were *Oenopota rufa* (abundant), *Sissurella crispata, Lunatia montagui, Skenea basistriata, Arca sp* and *C. vitrea.* The presence of species characteristic of soft bottoms indicates probable transport from a muddy or sandy area. The presence of cirripedes suggests transport from an area of rock outcrop or cobbles.

TTR7-AT-67

Living colonies of *Lophelia* and *Madrepora* on coral debris. The associated fauna was the same as on other living colonies. Some small, white fresh-looking unbioeroded fragments of cirripede plates were present. The coral and bivalve debris was very black in colour and the surfaces were bioeroded. Some specimens of *O. rufa* have microborings filled with this black colouration. This may be caused by anoxic conditions developed among the debris below the living coral related to the presence of organic matter. Coral debris was present throughout the core as in previous samples, but the fragments appear to be smaller.

TTR7-AT-68

Dead coral assemblage with *Stylaster* sp growing on some of the coral branches. Living sponges, hydroids and ophiuroids are also present. Coral debris is present thoughout the core, but as in the sample AT-67, the size appears to be smaller and more dispersed than in previous cores from the area. *O. rufa* and *Arca* sp are the most common molluscs. The shell surfaces are white and not very bioeroded. *C. vitrea* found below the top with *Scissurella crispata.* A few large coral fragments are present. A complete valve of *Acesta excavata* was found below 120 cm in the core. In the lower part of the core (180-240 cm) more coral debris was present.

The differences in the cores in this area may be explained by differences in current strengths. The presence of cirripede plates (*Balanus* sp) suggests rock or cobble surfaces.

Observations on faunas in cores - west of Faeroe Bank Channel

TTR7-AT-69G

Gravity core consisting of fine sand and mud. No living fauna was observed on the surface. Sponge spicules are the principal biogenic contributor to the sediments. Irregular aggregations of debris were observed at irregular intervals down the core. These do not form an extensive layer. They appear to be subrounded or posssibly elliptical in cross section and are probably faecal pellets. Burrowing activity is present throughout the core.

TTR7-AT-70G

This core was taken on the floor of a northwest -southeast trending channel where strong currents were presumed to be operating. Only a short core was recovered. Some sponges were growing on small pebbles at the surface. A noteworthy feature was observed in these sponges namely the presence of very small pebbles and lithic fragments which were incorporated into the structure of the sponges. In some cases these lithic fragments covered most of the sponge. Some bioeroded and abraded cirripede plates were present. The surface has lost most of the surficial growth lines and were also heavily microbored by sponges. The bivalve *Yoldiella lucida* -also attacked by microborers -was present. In this area, situated on a channel floor, there is some evidence of sediment transport. The cirripedes were probably transported from an appropriate substrate -possibly a rock outcrop - elsewhere.

TTR-AT-71G

This core was collected part way up the slope on the northeast slope of the channel. The sediment is mostly composed of mud. Two live ophiuroids and delicate, erect sponges 5 cm in height were present on the top surface of the core. The living fauna therefore includes both detritivores and filter feeders. The delicate nature of the sponges suggests only weak current activity. Burrowing activity was observed throughout the core.

Fragments and a complete specimen of the bivalve *Yoldiella lucida* were located 377 cm below the top of the core.

TTR7-AT-72G

The core was collected on the floor of a second channel to the north of the first channel. Only a short core was recovered. Several rolled brachiopod shells filled with fine sediment were present both on the top of the core and also within it. *Yoldiella lucida* was also again present. It was white in colour and was not extensively bioerodedroded by microborers (sponges). A single solitary coral *Caryophyllia* sp was located 17 cm from the top of the core.

It is possible that the currents through this channel are less strong than in the channel to the southwest. The brachiopods were almost certainly derived either from the slopes to either side of the channel or were transported by currents travelling along the channel.

TTR7-AT-73G

Gravity core consisting mostly of mud. No living fauna was found on the top of the core. The very fragile and extensively bioeroded remains of an articulate brachipod were located some 370 cm below the top of the core. The shell was extensively bored and excavated by clionid sponges.

Discussion

Some faunal differences between the Rockall Bank area and the Porcupine area can be detected. The Rockall area has a lower diversity of mollusc species, with fewer cold water species. Some species found in the Porcupine area such as *Oenopota rufa* are very abundant on Rockall Bank. The presence of *Achesta* sp in the living colonies on Rockall Bank and its absence on Porcupine Bank may be related either to differences in the water quality or simply to the sampling scheme used. The presence of *Acesta excavata* within the cores indicates that it was also present before in the area. The high proportion of coral debris throughout the gravity cores suggests that a coral bank at a particular location could develop over a considerable period of time.

The perceived differences between Rockall Bank and the Porcupine Bank area may be due either to the relatively few samples on which this study is based or to differences in the water movements between the two areas following the last glaciation.

The differences between the two locations sampled on Rockall Bank indicate two different depositional conditions. One (AT-56) was suitable for the accumulation of coral while the other (AT-

67\68) had less abundant coral remains. This could suggest that either the growing conditions were less than ideal or that the material was partially transported.

The small size of the living coral colonies in an area associated with a well developed carpet of dead coral suggests that the conditions were suitable for the growth and development of the coral banks at an earlier stage but now either the current, the temperature or the food supply are not so appropriate for their sustained development. Another possible explanation of this is that fishing activity in the area is very intensive and repeated trawling does not allow time for the continual growth of the coral colonies.

II. 6. Conclusions

N. Kenyon, M. Ivanov, A. Akhmetzhanov

The presence of carbonate mounds suspected from scarce seismic data and GLORIA imagery was confirmed on both margins of Rockall Trough. On both margins the mounds again were found to be associated with strong bottom currents whose effects were clearly seen on the sidescan sonar data. The mounds reassemble those studied during the first leg in Porcupine Seabight except that they are more abundant. Numerous samples taken from the mounds proved that they are densely populated by the deep-water corals *Lophelia pertusa* and *Madrepora oculata*, and associated fauna. An OKEAN survey on the southeastern Rockall Bank margin discovered a vast number of closely spaced mounds localized within a narrow band at a depth between 500-1000m. This area extended along the margin for over 150 km. Some of the mounds reached considerable heights (up to 350 m). Their preference for a preexisting raised platform from which to develop was clearly demonstrated. Bedforms due to current on the southeastern Rockall Bank show evidence for both alongslope currents, stronger to the southwest, and for up and/or downslope currents. Bottom sampling data show that there is significant accumulation of coarse sandy material between mounds, transported and deposited by the strong bottom currents.

Detailed study of several seabed mounds located at the foot of the southeastern Rockall Trough margin shows that according to seismic and high-resolution sidescan sonar data they are most likely to be volcanic rocks outcropping at the seafloor. Age dating is required to see whether this is another of the Tertiary igneous centres found around the continental margin in this part of the northeast Atlantic

III. FAEROE MARGIN (Leg II)

III.1. Objectives and geological setting

N. Kenyon, M. Ivanov, A. Akhmetzhanov

It is becoming increasingly clear that there are some places where currents in the deep sea are strong enough to move sands and there are even hydrocarbon reservoir rocks that have been interpreted as sandy contourites. However, modern examples have been little studied apart from the region west of the Straits of Gibraltar, where the Mediterranean Undercurrent flows out into the Atlantic Ocean (Kenyon and Belderson, 1973). Another potential area of sandy contourites is west of the Faeroe Bank Channel where the Norwegian Sea overflow water (NSOW) emerges into the North Atlantic. This area had been little studied and we expected that a sidescan sonar survey and sampling programme would provide useful data on the geometry of sand deposits as well as mapping pathways of one of the most important links in the global ocean circulation.

The Faeroe-Shetland Channel and Faeroe Bank Channel carry the NSOW across the Greenland-Iceland-Faeroe Ridge. The channels run between, the continental shelf west of the Shetland Islands and the Wyville-Thomson Ridge, and the Faeroe Platform. In the most of the Faeroe-Rockall Plateau area a succession of early Tertiary volcanic rocks are present (Roberts et al., 1984; Rasmussen and Noe-Nygard, 1970). The basaltic succession, related to rifting and the formation of a passive volcanic continental margin, constitutes the substratum of the Eocene to Recent sediments at the same time as it covers the pre-Paleocene geological succession. The deep-water current passing the Faeroe-Shetland Channel and the Faeroe Bank Channel had an important role in transporting sediments in the Neogene. As a result of these processes a cover of variable thickness of Eocene to Recent sediment has been deposited above the basalt (Boldreel and Andersen, 1995).

III.2. Seismic data

T. Nielsen, J. Taylor, J. Foeken, M. Horstink, T. Mikkelsen, A. van der Molen, and N. Kenyon

Ten lines of seismic and contemporaneous OKEAN sidescan data were collected over the period 10th to 13th August 1997 (Fig. 99). Average speed during collection was approximately 6 knots and shot interval was 10 seconds. The lines are labelled PSAT-22 to 31. The seismic and OKEAN data form a grid oriented SW-NE, although no tie lines were collected.

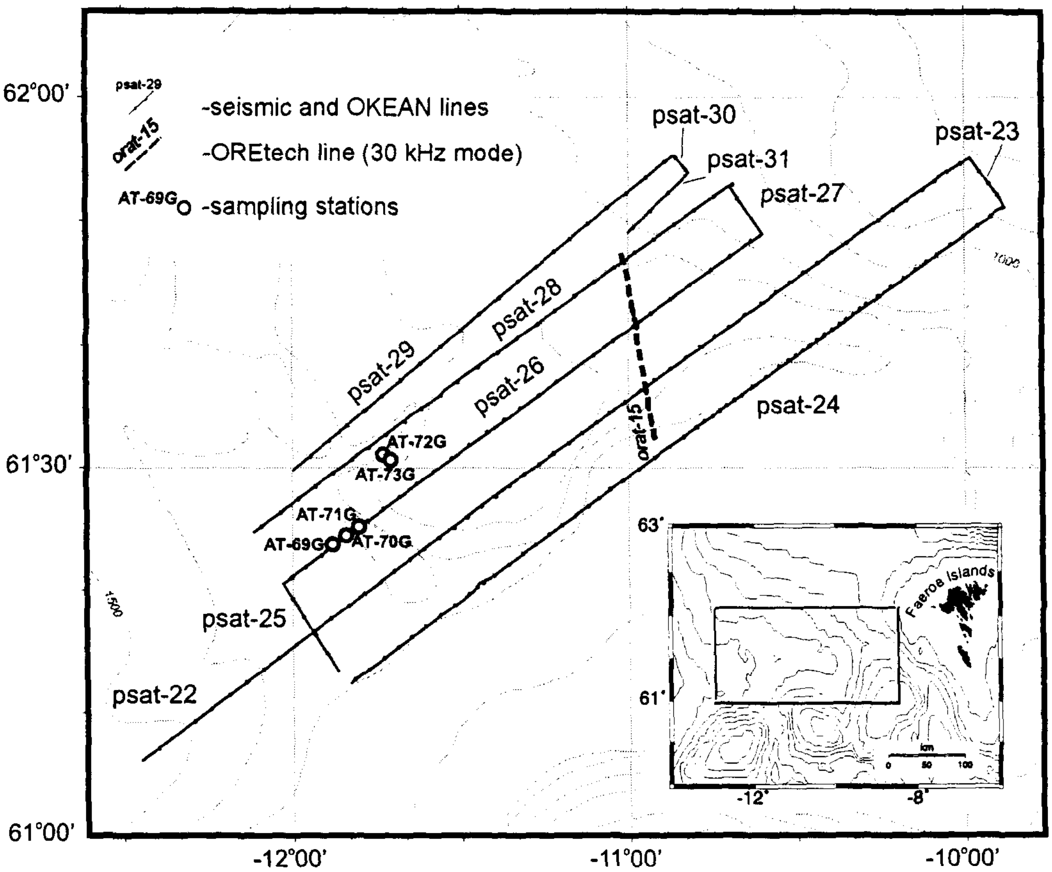

Fig. 99. Location map of the study area

Description and analysis of the seismic data are here performed on only the fourth channel of the data, which has been deconvoluted and band pass filtered. Because of the grid form of the data, it is possible to perform a three-dimensional description, although due to the complexity of the area, a 3D interpretation is not possible without more data. Two units are identified.

The top reflector of the **acoustic basement** is strong and continuous for the most part, with a series of escarpments and/or faults. There is an overall dip of the unit from NE to SW, from 1175 ms TWT to 2500 ms TWT. In the central survey area the acoustic basement forms a high, which is bounded on the northwest and southeast by two basins. In the northeast part of the area the high is no longer present, whilst it continues beyond the study area towards southeast. In this part a low in the top of the high is seen, elsewhere the top is flat and level, and is at 1525 ms TWT at its highest.

The acoustic basement is seen to outcrop in the NE at 17:40 on PSAT-22 and 03:50 on PSAT-24. Other, smaller outcrops are to be found on PSAT-24, SE of the survey area, at 12:30 and 09:50. All outcrops are very flat and level. Internal reflectors in the basement unit are very vague and occasional.

The **surface unit** generally infills the basins and lows found in the acoustic basement. The top reflector is strong and continuous throughout the survey area, but differs in shape. In the SW the surface reflector is flat and gently dipping (SW flat section), whilst in the NE it is flat and level (NE

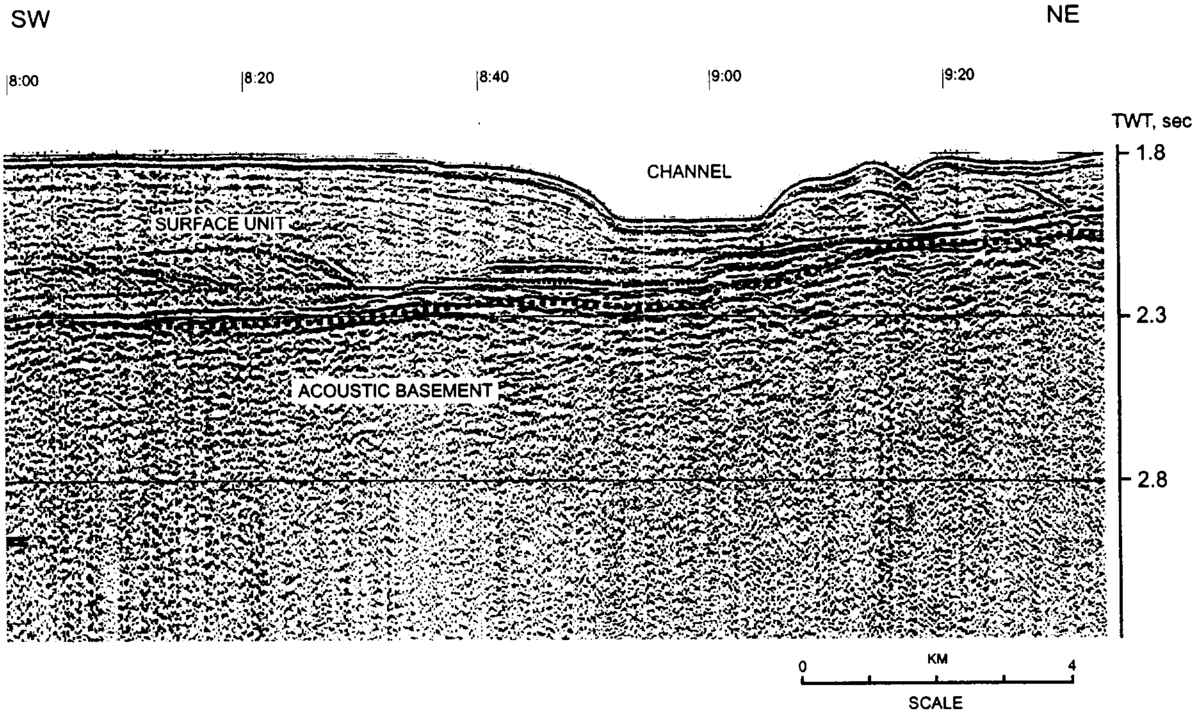

Fig. 100. Fragment of PSAT-22 showing a flat U-shaped channel. The internal reflector patterns of the surface unit show a north-eastward progradation of the channel

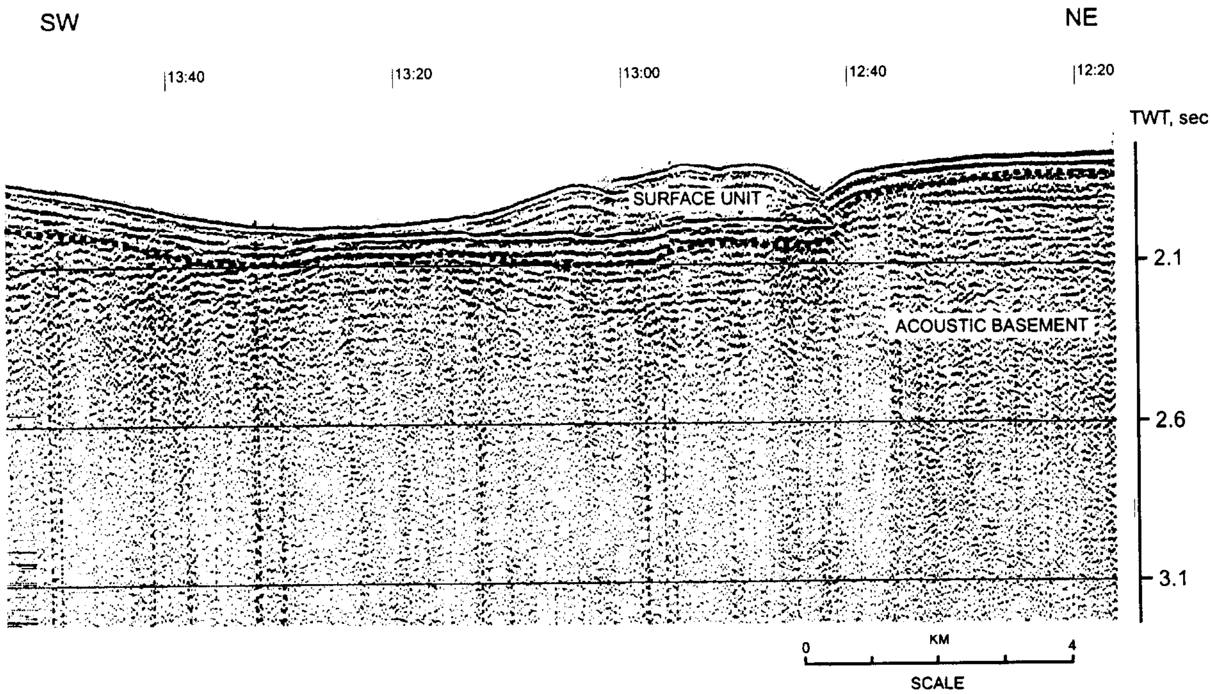

Fig. 101. PSAT-24 showing a wide U-shaped channel formed in the surface unit. Towards the NE, the acoustic basement outcrops

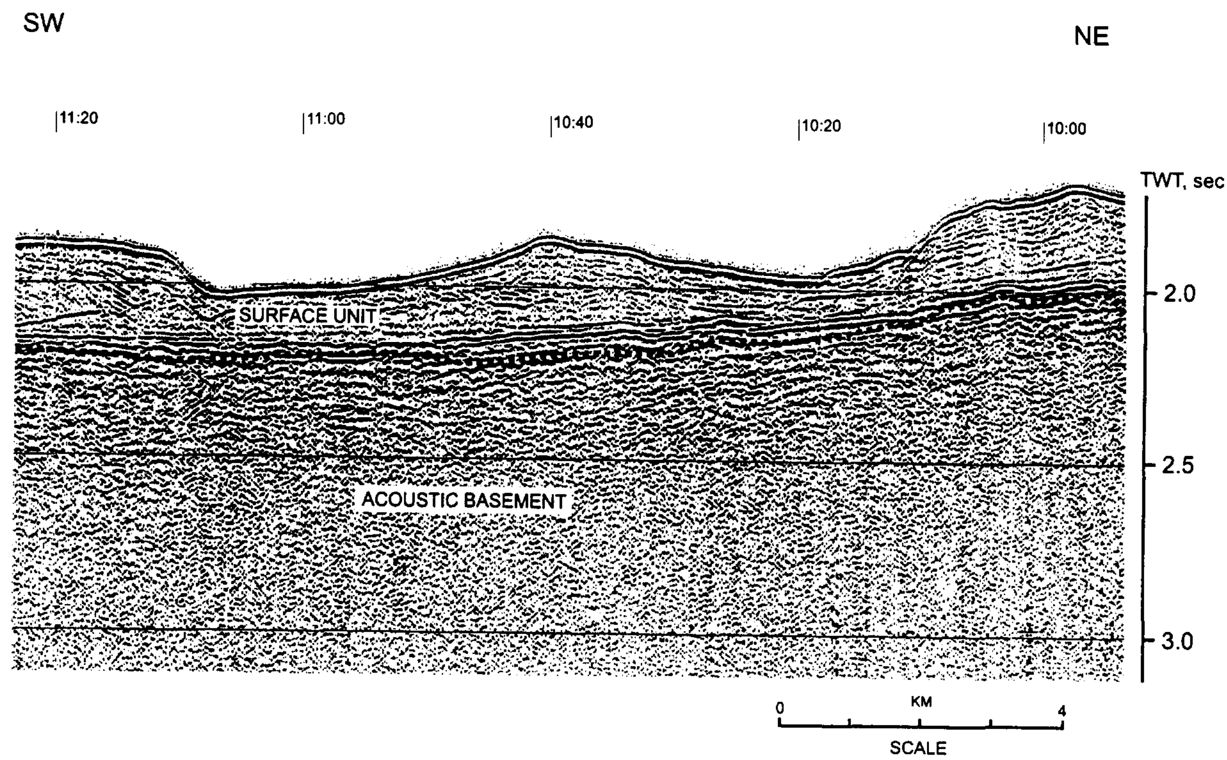

Fig. 102. Asymmetrical channels cutting through the surface unit seen on the PSAT-28 seismic line

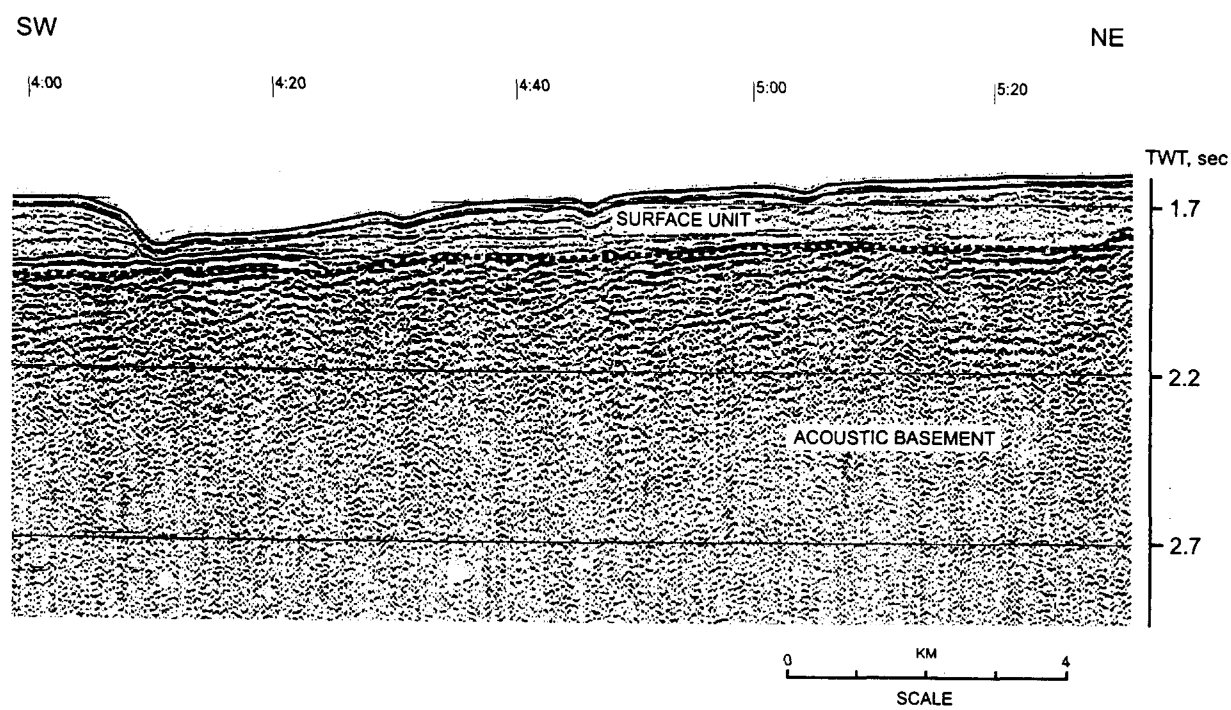

Fig. 103. Small notch like channel profiles at the NW of the survey area observed on the seismic line PSAT-29

level section). In between, over the central high formed by the acoustic basement, it is very hummocky (hummocky section). The surface unit is cut several times by channels of varying morphology around the central high. Channels tend to be either U-shaped (with a flat bottom and gently sloping sides) (Fig. 100 and 101), asymmetrical (no flat bottom at all) (Fig. 102), or small notches cut into the surface (Fig. 103). They have a distinct distribution, with U-shaped channels concentrated in the E and S, asymmetrical channels in the W and NW, and notches on the NE side of the basement high. They also display different depth ranges, U-shaped being approximately 200 ms TWT deep, asymmetrical channels 120-180 ms TWT deep and notches 100-120 ms TWT deep. Channels are therefore smallest and shallowest in the NE.

Internal reflectors within the hummocky section of the surface unit are few, but offer some suggestion of layering in the NW. The hummocky section thickens NW from roughly 170 ms TWT to about 300 ms TWT. Internal reflectors in the NE level section are generally absent apart from a single strong, continuous, flat and level reflector seen in several lines (although this does not mean they are the same reflector given the wide-spread nature of channels in this region). This reflector is strongest in the NE and weakens westwards. The SW flat section of the surface unit consists of several subunits. They all display downlaps onto a strong, flat reflector with the uppermost subunit downlapping to the flat floor of a U-shaped channel (Fig. 100). On the opposite flank of the channel internal reflectors are weak, but appear to downlap away from the channel. In the eastern part of the survey area this overall reflection pattern of the surface unit around the U-shaped channels displays an south-westward progradation of the channel, while it displays a northward progradation of the channel in the southern part of the area. The thickness of the complete surface unit in the SW flat section varies from approximately 400 ms TWT in the NE to 650 ms TWT at its greatest in the SW.

III.3. OKEAN and OREtech sidescan sonar data

T. Nielsen, J. Foeken, J. Taylor, A. van der Molen, N. Kenyon, M. Horstink, T. Mikkelsen

Introduction

Ten lines of OKEAN sidescan sonar data were collected (PSAT-22 to 31), together with a single OREtech line (ORAT 15) which cross-cuts the OKEAN mosaic approximately N-S (Fig. 99). The OKEAN data form a mosaic, extending SW-NE. The mosaic is approximately 50 km in width and 350 km in length.

OKEAN mosaic

Five acoustic zones are tentatively identified on the OKEAN mosaic (Fig. 104) on the basis of backscatter levels and features.

Zone 1 occurs in the far NE and is high backscattering and featureless, except for vague lineations which are oriented N-S. The second zone occurs to NW of this and is of medium backscatter. This is also generally featureless. There is a faint band of lineations associated with a channel approximately 5 km wide in the central region of this zone (01:00 PSAT-26 and 05:45 PSAT-28). The third zone forms the majority of the study area and is an area of medium backscatter, grading to high to the NW. The area is subcircular and bounded by narrow high backscattering surfaces associated with a channel (zone 5).

The fourth zone is SW of a channel seen as a band of low backscatter, approximately 1-2 km wide. The zone has a train of low backscatter features extending NW. These latter are wave-forms with their crests oriented SW-NE. The belt of features bends to the west as it progresses NW. Beyond this distinct area, there are several low backscatter features without regular shape of orientation.

OREtech data

In the north of the line (12:45 to 13:30), a channel is clearly imaged. The bed is high backscattering and has parallel longitudinal bedforms within it, oriented SE-NW. The SE bank of the channel is low backscattering, and the profiler data show stratification in this location (Fig. 105).

From 13:30 to 17:00 there is a southward dipping surface which is dissected by a 50 metre deep channel. The north side of the channel is a small level plain, which appears as a low backscatter area on the sonar data. The southern boundary of the channel is steep-sided, and the surface beyond is flat and level. There is stratified sequence from 16:00.

From 17:00 to 17:30, on the starboard side of the data, there is an area of high backscatter and rough surface texture that corresponds to a subcircular high backscatter feature on the OKEAN. Ramped against this is a smooth high backscatter surface. South of this area, the surface becomes low alternating to medium backscatter. Some sections (e.g. 18:00 to 18:30) show waveforms with crests trending N-S, which pass across the profile at the edge of a low backscatter zone. The northern-most low backscatter area shows some penetration on the profiler record.

Interpretation of seismic and sidescan sonar data

The data collected in this area are intended to look at and map sediment pathways associated with the spreading of Norwegian Sea Overflow Water (NSOW) once it leaves the fast-flowing confinement of the Faeroe Bank Channel.

The seismic data allow the identification of two units, the acoustic basement and the surface unit. The acoustic basement outcrops in the NE of the survey region and appears as a region of high

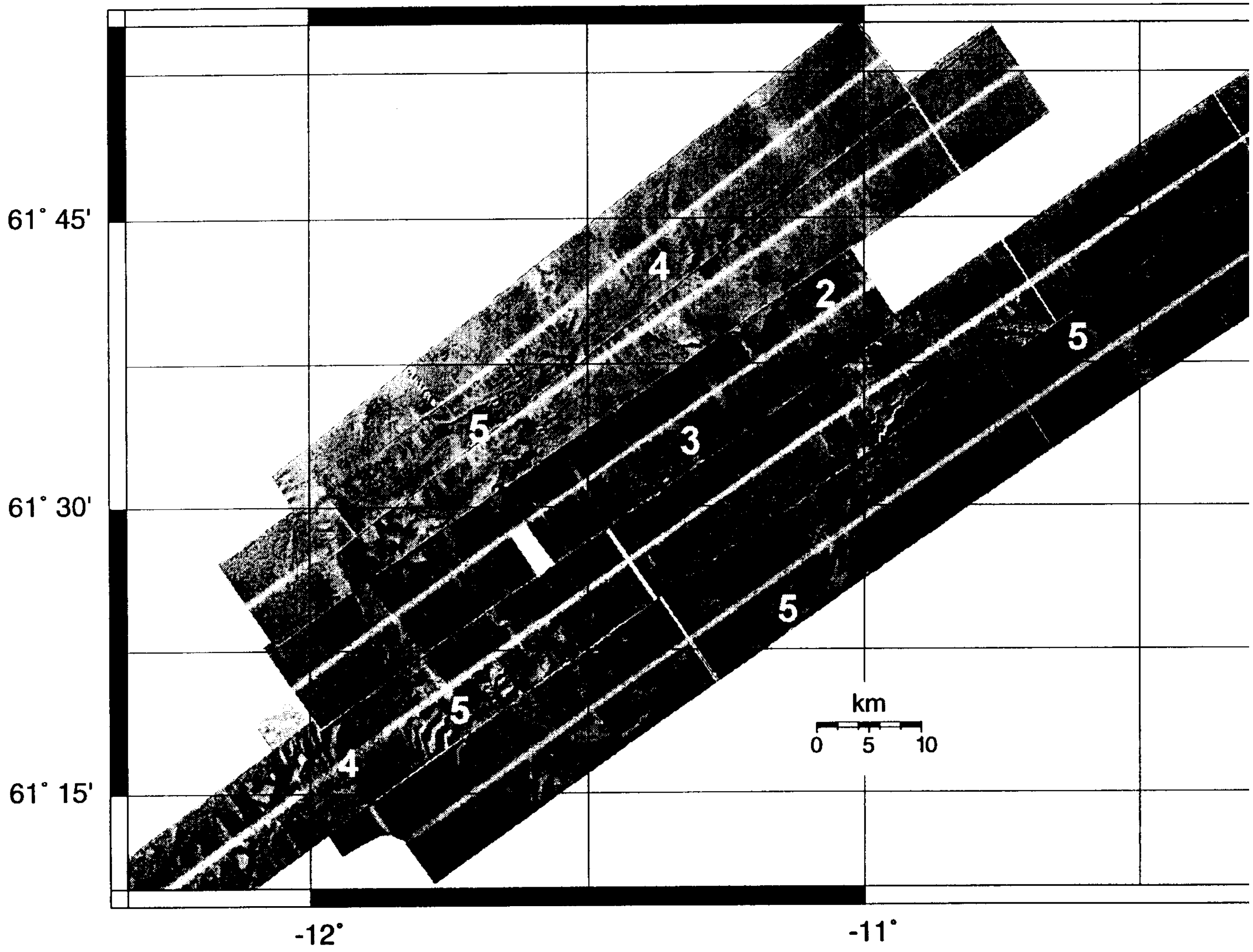

Fig. 104. OKEAN mosaic of the study area. Numbers indicate zones with different backscatter patterns described i

backscatter on the OKEAN mosaic. Elsewhere the acoustic basement forms a gently dipping surface, with a central high. Occasionally the unit also outcrops within the high and at its margins. The high is bound to the NE and SW by two basins, it is seen from the OKEAN mosaic that the high forms a subcircular feature. The acoustic basement is thought to be basalt formed subaerially during the opening of the North Atlantic. This is because of the generally basaltic nature of the surrounding region and the strong reflector. By analogy with the nearby banks, it is suggested that the central high is a result of compression (Boldreel and Andersen, 1993).

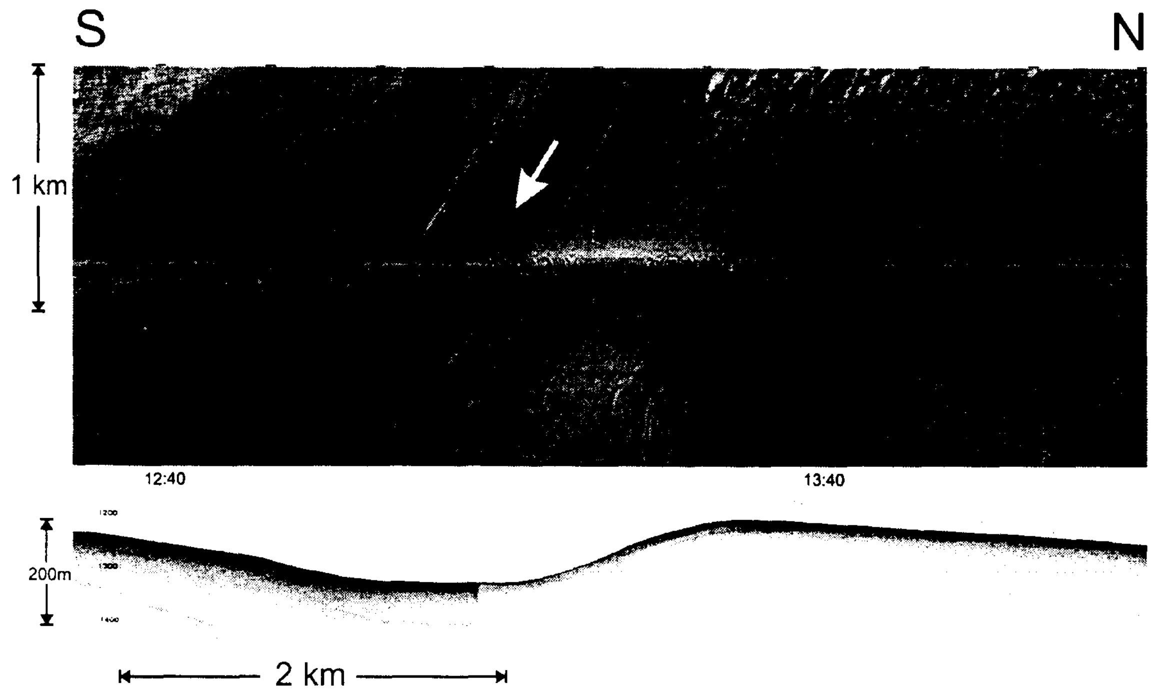

Fig. 105. Fragment of ORAT-15 sonograph and profile showing channel in the NE of the survey area with linear longitudinal bedforms. Note the northern bank is of low backscatter and stratified on the profiler record. Arrow indicates sediment transport.

The surface unit infills and smooths the acoustic basement topography. It is present both around and on top of the central high. On top of the latter the surface unit is hummocky, whilst around the high the topography is smooth. The smooth surfaces are cut by several channels of a variety of forms and depths (75 - 150 m). The channels to the south and west are U-shaped or asymmetrical, whilst those to the far north are shallow V-shaped notches. Some of the channels in the S and E show progradation, indicating a flow direction.

The sonar data shows the complete pathways of the channels through the survey area. Channels enter the region from the SE, flow around the basement high and exit to the NW. There are several other sections of channel in the NE, which do not appear directly connected to the principal channel around the high. These also flow SE-NW (from the OREtech data) but are more linear in plan. The banks of most of the channels are often low backscattering, indicating the accumulation of sand material. The channel to the SW of the central high also has a set of waves to the left of it. These are interpreted to be overbank mud waves.

III.4. Bottom sampling results

A.. Akhmetjanov, M. Ivanov, A. Mazzini, G. Akhmanov, P. Friend, E. Kozlova, E. Ivanova, L. Mazurenko, Yu. Naumov, I. Belenkaya, A. Saprykina, A. Stadnitskaya, A. Balashova, R. Cave

Introduction

An area lying to the west of the Faeroe Bank Channel was one the principal targets. It was considered as a potential area of sandy contourites. After the seismic and long-range sidescan surveys 5 coring sites were defined and successfully sampled (Fig. 99). Five gravity cores were retrieved and in total they contained about 13 m of sediments. Maximum recovery was 419.5 cm which is the longest core obtained during the whole cruise. The main sampling site parameters, sedimentological and other relevant information are shown in Tables 9 and 10.

Core No	Date	Time, GMT	Latitude	Longitude	Cable length, m	Depth, m	Recovery, cm
TTR7-AT-69G	12.08.97	15.02	61°23.71'N	11°52.88'W	1380	1380	419,5
TTR7-AT-70G	12.08.97	16.05	61°24.47'N	11°50.52'W	1508	1504	53
TTR7-AT-71G	12.08.97	17.09	61°25.16'N	11°48.28'W	1375	1375	377
TTR7-AT-72G	12.08.97	20.22	61°31.06'N	11°43.97'W	1450	1440	80
TTR7-AT-73G	12.08.97	21.22	61°30.65'N	11°42.68'W	1378	1382	382

Table 9. General information on the cores sampled on the Faeroe margin

Core No.	Geographical Setting	Sedimentary Summary	Instrumentation	Acoustic characteristics
TTR7-AT-69G	Western Faeroe margin, overbank from the southern channel (at 8:34 on PSAT-26)	Sequence fining toward the bottom (sandy sized sediments at the top, clay at the bottom), intensive bioturbation	OKEAN sidescan sonar; single channel high resolution seismics	Gently dipping on the seismic profile
TTR7-AT-70G	Lowermost part of the southermost channel (at 18:54 on PSAT-26)	Pebbles on the upper layer and sandy sequence which is fining toward the bottom	OKEAN sidescan sonar; single channel high resolution seismics	Flat area on the seismic profile with subparallel layering
TTR7-AT-71G	Opposite flank of the southern channel sampled at (at 19:00 on PSAT-26)	Sandy layer on the top and silt/clay alternation in the rest of the core, intensively bioturbated	OKEAN sidescan sonar; single channel high resolution seismics	Gently dipping on the seismic profile
TTR7-AT-72G	Thalweg of the northern channel	Coarse to fine grained sand with silt interlayering	Echosounder	Flat area on the echo-sounder profile
TTR7-AT-73G	Flank of the northern channel	Sandy layer at the top and clayey sequence interbedded with a few sandy layers.	Echosounder	Steep flank on the echo-sounder profile

Table 10. Sedimentological, acoustic and geological characteristics of sampling stations on the Faeroe margin

Two channels observed on seismic and echosounder lines were chosen for sampling. One of them (described here as southern channel) is located to the southwest of a basaltic plateau described elsewhere in this cruise report and another one (described here as northern channel) passes around the plateau from the northeast. Three cores were taken along a seismic line crossing the southern channel (Fig. 106) and two cores were planned along an echosounder line running across the northern one (Fig. 107).

<u>Core TTR7-AT-69G (Fig. 108)</u>

Generally, the core composition was grey-brown silty sand in the top 118 cm of the core with little evidence of bioturbation, changing gradationally through a bioturbated, grey, silty clay to a

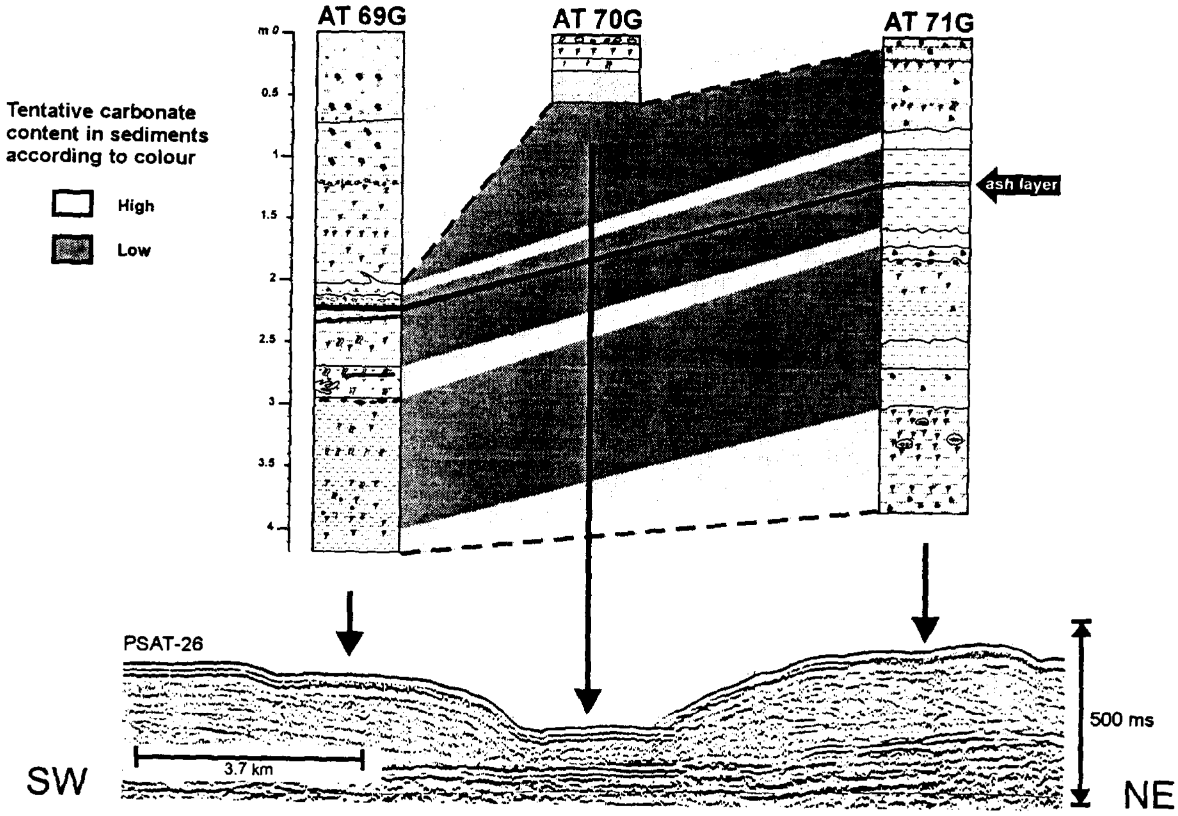

Fig. 106. Location of sampling stations and tentative correlation of cores taken along seismic line PSAT-26

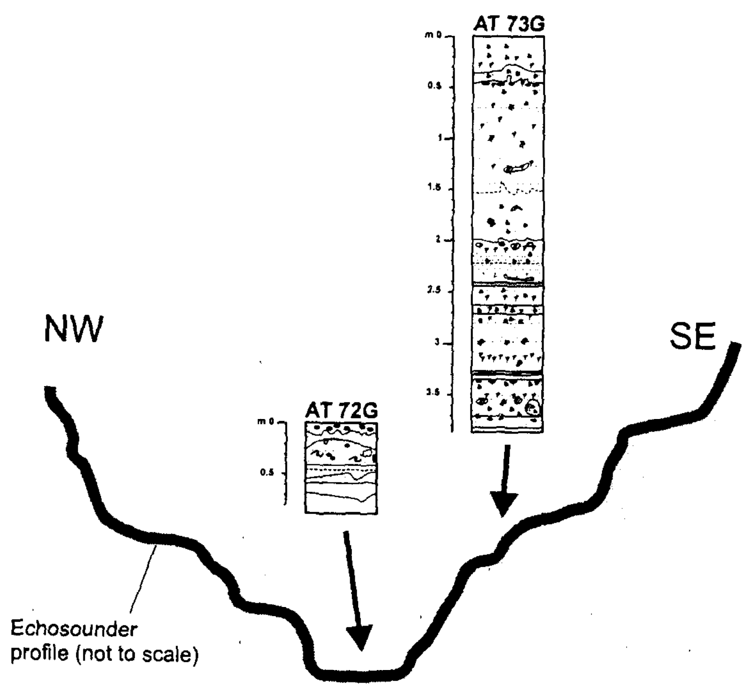

Fig. 107. Location of sampling stations along echosounder line PRAT-01

bioturbated, grey clay/mud. There was a varying foraminiferal content throughout the core. A patchy, but nevertheless distinct, dark layer was seen at ca. 220 cm from the top of the core.

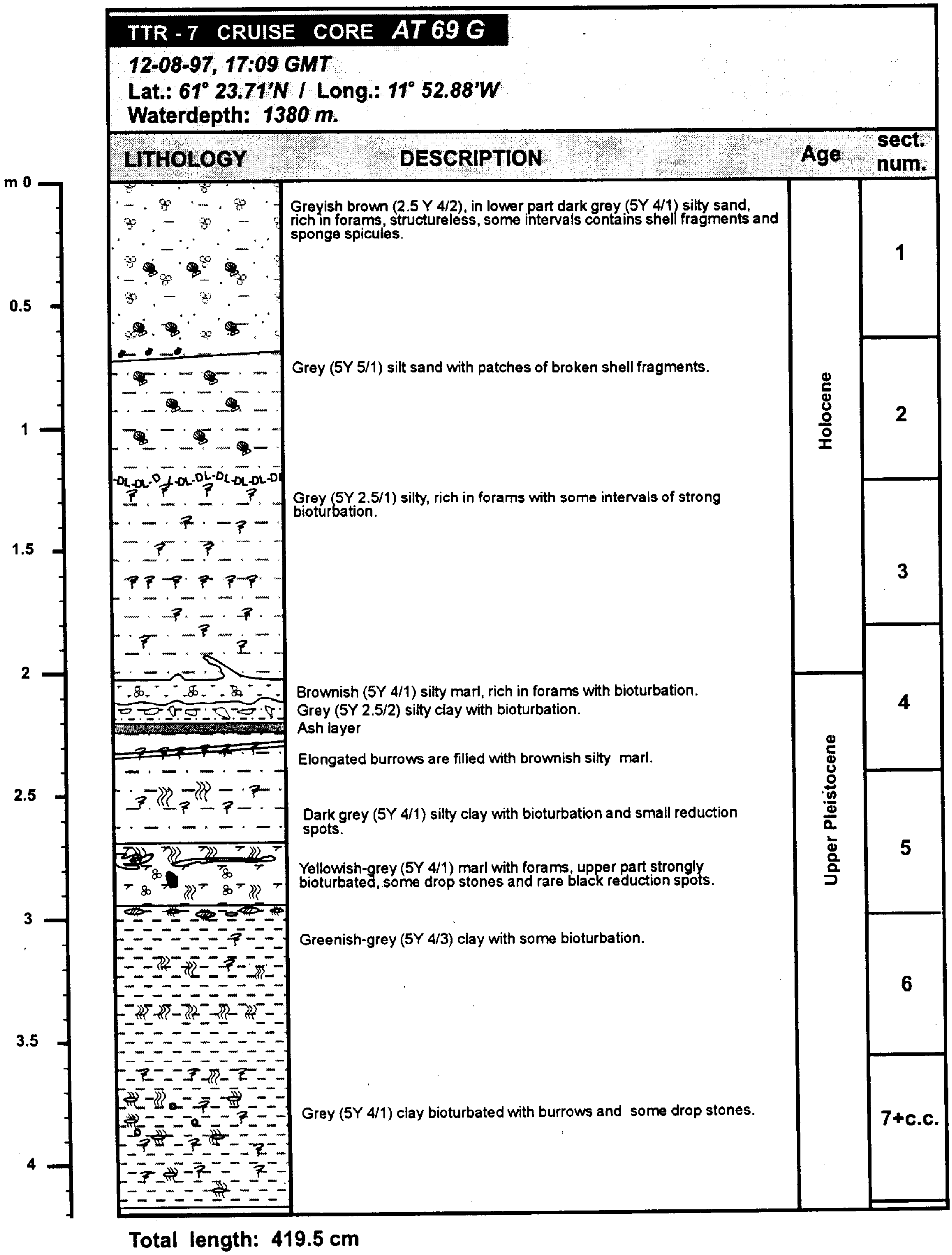

Fig. 108. Core log AT-69G

Core TTR7-AT-70G (Fig. 109)

A poorly-to well-sorted sandy core with gravel and small pebbles in the top section (to 18 cm) and shell fragments throughout. Some bioturbation evident and a generally low foram content.

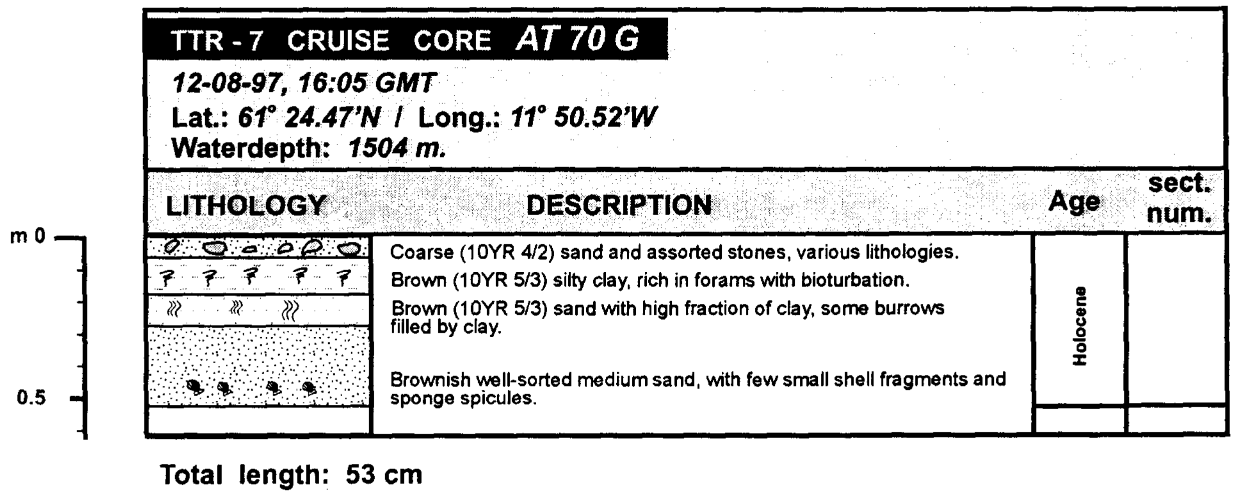

Fig. 109. Core log AT-70G

Core TTR7-AT-71G (Fig. 110)

A high degree of detail is evident in the core. Broadly similar in lithology to core AT-69G, but generally the sediment was more clay-rich. It was possible to distinguish some 26 different intervals, some of which alternated between a reddish brown and grey clay. Well-preserved bioturbation throughout the core. The same dark layer that appeared in core AT69G was easily discernible at 51 cm.

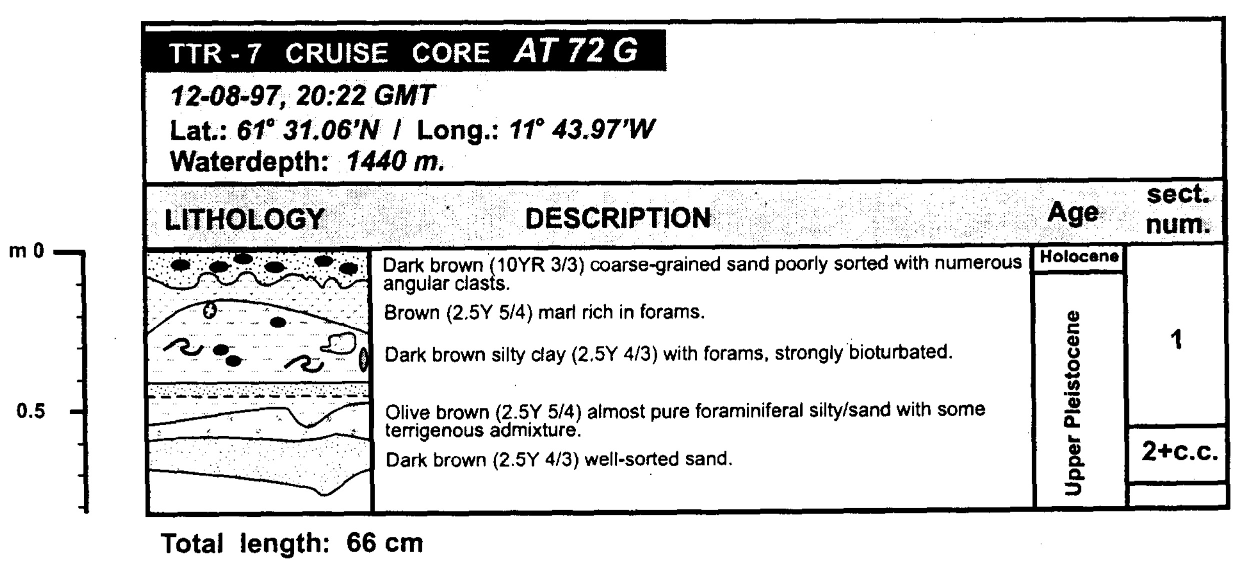

Fig. 111. Core log AT-72G

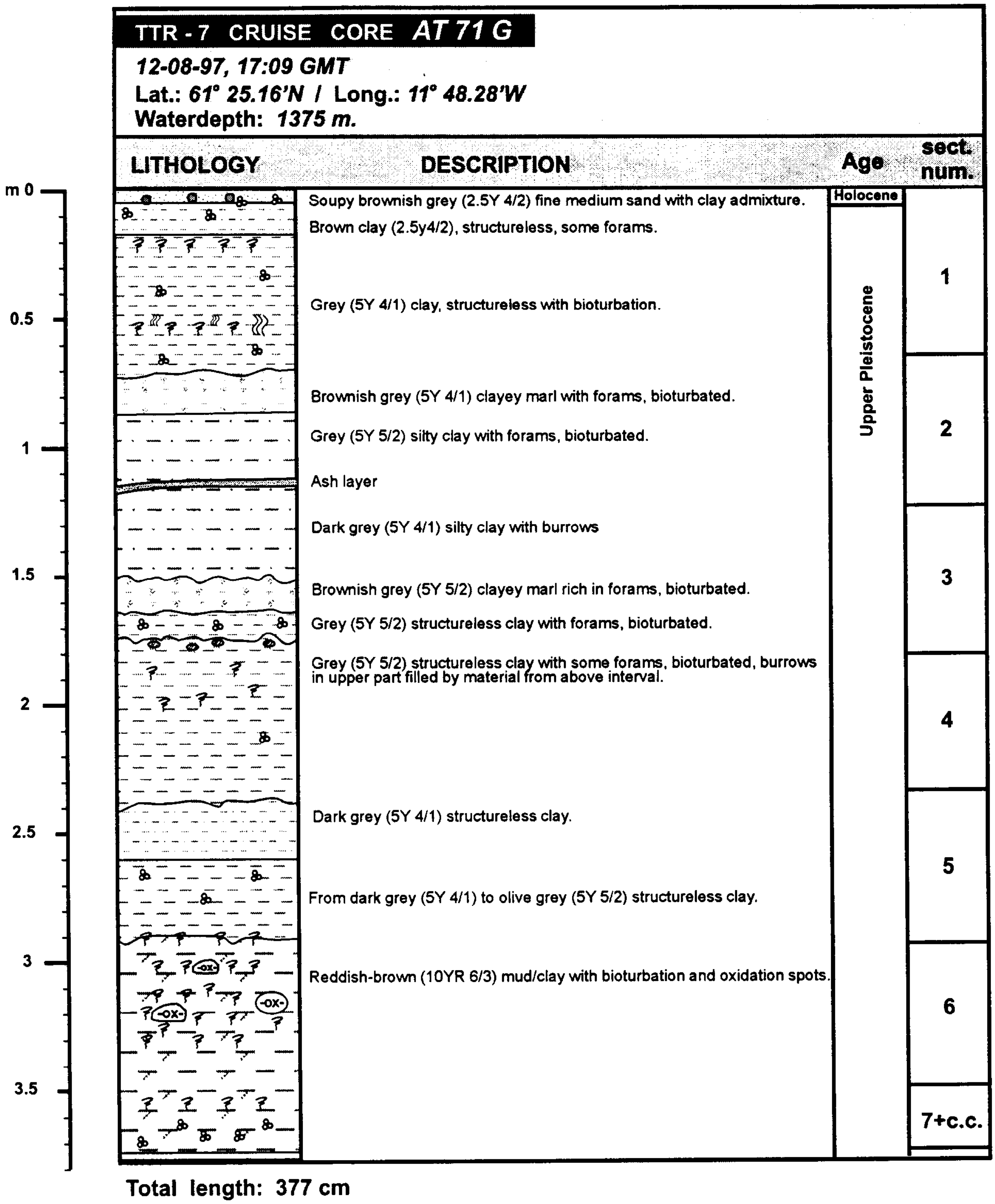

Fig. 110. Core log AT-71G

Core TTR7-AT-72G (Fig. 111)

A coarse to fine-grained sandy core with pebbles at the surface and two clay intervals, plus one coarsening-upwards sequence.

From 0 cm to 10 cm, a dark-brown, poorly-sorted coarse sand containing numerous angular clasts of differing lithologies, plus some biogenic debris. Between 10 cm to 25 cm, brown foram-rich marl, then dark-brown, strongly-bioturbated, foram-rich silty clay, the burrows infilled with an almost pure foram-sand. A coarsening-up sequence (from silty clay to fine sand) was apparent from 41 cm to 53 cm, with an irregular lower boundary. A fine to medium sand with a very high foram content (plus a small terrigenous content) from 53 cm to 56 cm, then, to the core base, a fine well-sorted foram sand containing many semi-consolidated sandstone clasts (up to 3 cm diameter), with a different lithology to the surrounding sediment.

Core TTR7-AT73G (Fig. 112)

Another core with good recovery showing broadly similar lithologies to cores AT69G and AT71G. A sandy top section to 43 cm, gradually fining to a brown/grey bioturbated clay with common silty/sandy patches. A very prominent 3 cm dark layer at 242 cm, of a similar lithology to the dark layers observed in cores AT69G and AT71G. 19 different intervals were recognised in this core.

Interpretation

All the cores obtained from the area virtually fall into two groups: cores taken from the bottom of the channels and cores taking from the banks of the channels.

The first group is characterised by poor penetration and these cores contained mainly sand and gravel whose age was micropaleontologically dated as Holocene. Core AT-70G obtained from the southern channel was mainly sandy with gravel testifying to the presence of rather strong current. Core AT-72G from northern channel also contained silty-sandy layers with gravel interbedding with clayey layers. The presence of these clayey layers together with coarsening upward silty layers is evidence that the current along this channel is rather unstable and its core possibly can migrate within the channel.

Another group represents cores taken from banks of the channels (AT-69G, AT-71G and AT-73G). These cores are mainly composed of interlayering clayey, silty, and marl interval. Some sandy layers were also observed, mainly at the uppermost part of the cores. According to micropaleontological study all sediments recovered belong to *Emiliania Huxley Acme* zone that suggests Upper Pleistocene and Holocene for the sediments. Analysis of foraminiferal assemblages reveals two main intervals which had been formed in different climatic conditions. The uppermost one is characterised by *Neogloboquadrina pachyderma dex, Globoquinita glutinata, Globorotalia scitula* and also some subpolar species like *Turborotalia quinqueloba*. Such fauna is characteristic of relatively warm periods and indicates a Holocene age. Below this interval faunal diversity becomes low and the foraminiferal assemblage is represented almost entirely by the polar species *Neogloboquadrina pachyderma sin.*

All the cores contained a distinguishing layer of black fine sand, which after microscopic study was found to be an ash layer. This layer was found at a depth of 2.2 m in Core AT-69G, at a depth of 1.2 m in Core AT-71G and at the depth of 2.55 m in Core AT-73G. Comparison with published data allows to suggest that this layer might be Ash layer I described by Rasmussen et al. (1996). The age of this layer had been established to be 10.6 ka (Rasmussen et al., 1996).

Presence of this layer allows conducting a correlation between these cores (Fig. 106 and Fig 113). Also marl layers and carbonate clay with relatively high carbonate content were used for the same purpose. As a result the sedimentary succession can be divided into two parts: pre-ash and post-ash ones. The pre-ash succession can be dated as Upper Pleistocene in age. Correlation of some layers within this succession can be easily done because of presence of brownish and relatively light olive grey foram-rich marl and carbonate clay layers interbedded with predominant terrigeneous grey clay and silty clay layers. Individual layers do not reveal significant variations in thickness, being traced

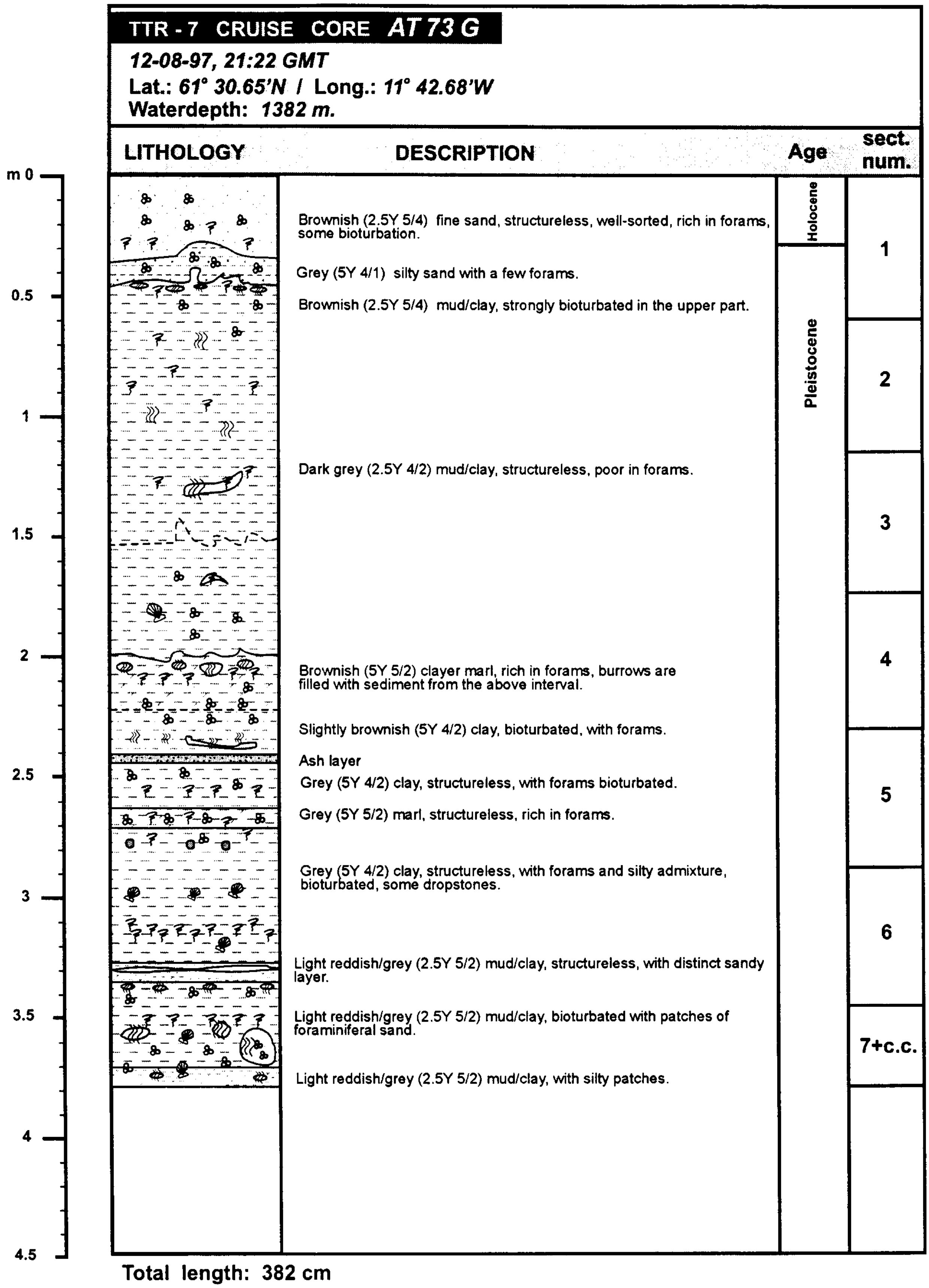

Fig. 112. Core log AT-73G

from core to core. Also this succesion is relatively enriched with benthic foraminifera species *Cassidulina laevigata* and *Cassidulina crassa* that is probably due to absence or weak activity of bottom current during formation of this succession.

The post-ash succession shows rather variable thickness of internal layers. If our ash is Ash I of Rasmussen et al. (1996) then this part of the core should contain the Upper Pleistocene/Holocene boundary but it cannot be precisely defined due to absence of stable isotope data and also because of uniform foraminiferal assemblage. The only thing we can conclude is that in Core AT-69G the 2.1 m thick warm interval was found lying almost above the ash layer while in Cores AT-71G and AT-73G it is underlain by a grey clay interval with cold water fauna with thickness of 1 m and 2.3 m in AT-69G and AT-73G, respectively. Warm intervals in last two cores are characterised by significantly less thickness: 15 cm in Core AT-71G and 35 cm in Core AT-73G. In the case of Core AT-69G it is worth noticing that the warm interval is represented mainly by foraminiferal ooze which in the sense of grain size can be characterised as well-sorted medium to coarse sand with clay fraction content increasing near the bottom. Sedimentation rate for this succession is about 22 cm/ka which is rather high. These facts may infer a bottom current activity which was responsible for the formation of this interval. This conclusion is also supported by seismic data which show a sediment drift at the coring site. In the case of Cores AT-71G and AT-73G for the post-ash succession one can clearly notice the dominance of a cold water interval, which is particularly thick in Core AT-73G. A warm water interval again is represented by probably current-derived foraminiferal ooze. The origin of the cold water interval remains unclear since it could be either a result of deposition of ice-rafted material, or deposited by weak current bearing mainly clay and silty material or, finally, it can be a result of a slumping event. The last reason seems to be most unrealistic as no relevant sediment structures have been observed.

To conclude it must be said that the coring data show that the southern channel is currently rather active as a depositional system and sediment drift is being developed. Current activity in the northern channel seems to be weaker at the end of Upper Pleistocene and especially during the Holocene.

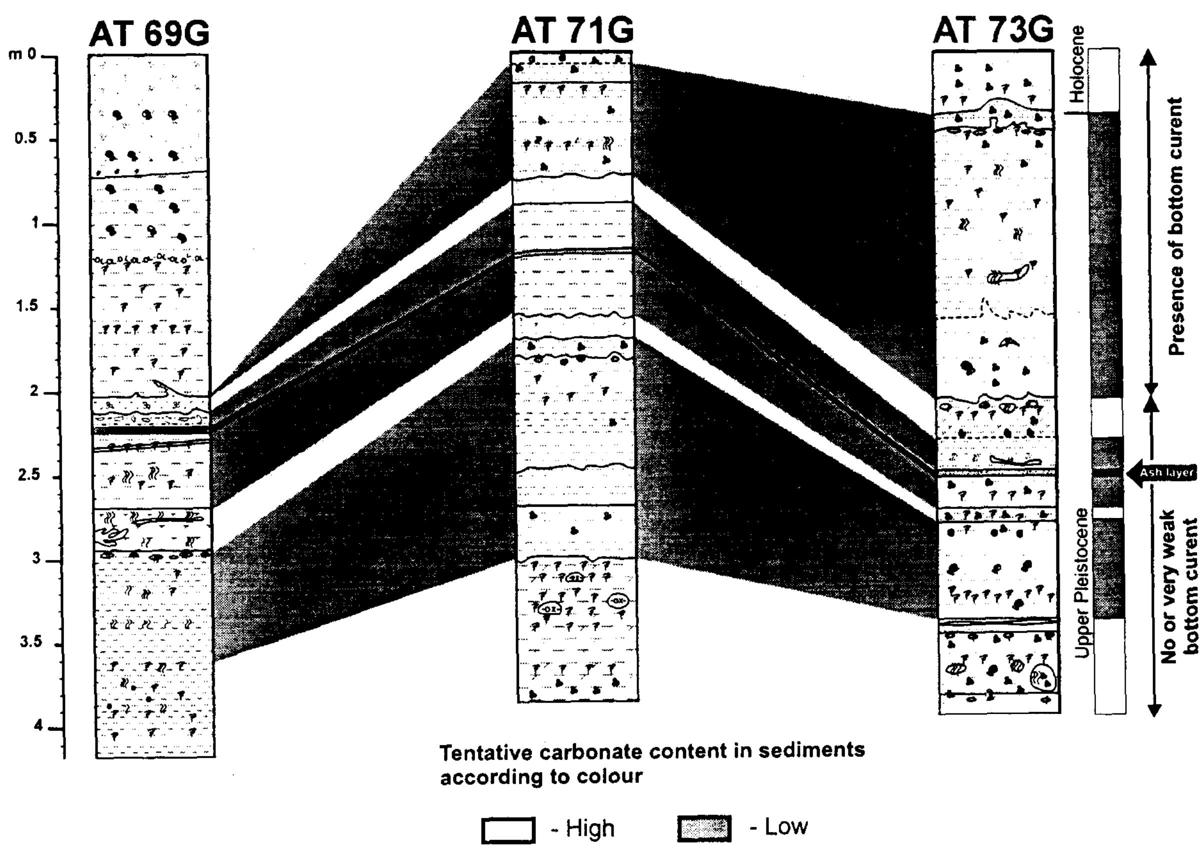

Fig. 113. Tentative correlation of the cores taken from the channel banks

III.5. Conclusions

N. Kenyon, M. Ivanov, A. Akhmetzhanov

Sidescan sonar and seismic surveys conducted on the southwestern Faeroe margin allowed us to trace and map pathways of Norwegian Overflow water spreading out from the Faeroe Bank Channel into the Iceland Basin.

The main channel flows south and west of an upstanding area, presumed to be a basalt plateau. Other channels flow north of the high and yet others flow along the contours to the north. The evidence for aggradation, seen on several channel crossings (Fig. 100), implied that contourite channels could form thick bodies of coarse sediment.

Large mud waves up to 1 km wavelength were observed beyond the bank of the southern channel and a channel in the east of the mapped area. As was expected, coring showed that the channel bottom is covered with coarse sand, sand waves and sand ribbons which implies considerable speed of flowing water masses. Outside the channel there are thick deposits of presumed contourite silt and mud.

REFERENCES

Bailey, R.J., and Haynes, J.R., 1974. **New dredge samples from the continental margin bordering Rockall Trough.** *Marine Geology,* 16: 57-62.

Barrett, T.J., Jarvis, I., Longstaffe, F.J., and Farquhar, R., 1988. **Geochemical aspects of hydrothermal sediments in the eastern Pacific Ocean: an update.** *Canadian Mineralogist,* 26: 841-858.

Belderson, R.H., Kenyon, N.H., and Wilson, J.B., 1973. **Iceberg plough marks in the northeast Atlantic.** *Palaeogeography, Palaeoclimatology, Palaeoecology,* 13: 215-224.

Boldreel, L.O. and Andersen, M.S., 1993. **Late Paleocene to Miocene compression in the Faeroe-Rockall area.** *In:* Parker, J. (Ed.), *Petroleum Geology of Northwest Europe: Proceedings of the 4th Conference.* The Geological Society, London, 1025-1034.

Boldreel, L.O., and Andersen, M.S., 1995. **The relationship between the distribution of tertiary sediments, tectonic processes and deep-water circulation around the Faeroe Islands.** *In:* Scrutton M.S., Stoker M.S., Shimmield G.B., and Tudhope A.W. (Eds.), *The Tectonics, Sedimentation and Palaeoceanography of the North Atlantic Region.* Geological Society Special Publication, 90: 145-158.

Bol'shakov, A.M., and Egorov, A.V., 1987. **On the use of the phase-equilibrium degassing method in gasometric study.** *Okeanologiya,* 35, 5: 861-862 (in Russian).

Bouma, A. H., 1962. **Sedimentology of some flysch deposits: a graphic approach to facies analysis.** Elsevier, Amsterdam, 168 pp.

Brenot, R., and Berthois, L., 1962. **Bathymetrie du secteur Atlantique du bans Porcipine (ouest de l'Irlande) au Cap Finisterre (Espagne).** *Rev. Trav., Inst. Pech. Marit.,* 26: 219-246

Croker, P.F., and Shannon, P.M., 1987. **The evolution and hydrocarbon prospectivity of the Porcupine Basin, Offshore Ireland.** *In:* Brooks, J., and Glennie, K., (Eds.), *Petroleum Geology of North West Europe.* Graham and Trotman, 633-642.

Dickson, R.R., and McCave, I.N., 1986. **Nepheloid layers on the continental slope west of Porcupine Bank.** *Deep-Sea Research,* 33A: 791-818.

Dingle, R. V., Megson, J.B., and Scrutton, R.A., 1982. **Acoustic stratigraphy of the sedimentary succession west of Porcupine Bank, NE Atlantic Ocean: a preliminary account.** *Marine Geology,* 47: 17-35.

Duncan, P.M., 1873. **A description of the Madreporaria dredged up during the expeditions of H.M.S. 'Porcupine" in 1869 and 1870.** *Transactions of the Zoological Society of London,* 8: 303-344.

Flood, R.D., Hollister, C.D., and Lonsdale, P., 1979. **Disruption of the Feni sediment drift by debris flows from Rockall Bank.** *Marine Geology,* 32: 311-334.

Graham, A., 1988. **Molluscs: Prosobranch and Pyramellid Gastropods. Synopsis of the British Fauna (New Series) No 2,** Second Edition. Linnean Society of London and Estuarine and Brackish Water Association, E. J. Brill/Dr W.Backhuys, Leiden, New York, 662 pp.

Henrich, R., Freiwald, A., Wehrmann, A., Schäfer, P., Samtleben, C., and Zankl, H., 1996. **Nordic cold-water carbonates: occurrences and controls.** *In:* Reitner, J., Neuweiler, F. and Gunkel, F. (Eds.). *Global and regionäl controls on biogenic sedimentation. I. Reef evolution.* Research Reports - Göttinger Arb. Geol. Paläont., Sb 2: 35-52.

Hovland, M., 1990. **Do carbonate reefs form due to fluid seepage?** *Terra Nova,* 2: 8-18.

Hovland, M., and Judd, A.G., 1988. **Seabed pockmarks and seepages.** Graham and Trotman, London, 293 pp.

Hovland, M., and Thomsen, E., 1997. **Cold water corals-are they hydrocarbon seep related?** *Marine Geology,* 137: 159-164.

Hovland, M., Croker, P.F., and Martin, M., 1994. **Fault associated seabed mounds (carbonate knolls?) off western Ireland and North-west Australia.** *Marine and Petroleum Geology,* 11: 232-246.

Hunter, P.M, and Kenyon, N.H., 1984. **Bathymetry of the Porcupine Seabight and the Porcupine Bank. Charts at 1:274.000.** *Institute of Oceanographic Sciences, Internal Document.*

Ivanov, M.K., Limonov, A.F., and Cronin B.T. (Eds.), 1996. **Mud volcanism and fluid venting in the Eastern part of the Mediterranean Ridge. Initial results of geological, geophysical and geochemical investigations during the 5th Training-through-Research Cruise of R/V Professor Logachev (July-September 1995).** *UNESCO Reports in Marine Science,* 68, 126 pp.

Joubin, L., 1922a. **Distribution geographique de quelques coraux abyssaux dans les mers occidentales europeennes.** *Compte Rendu hebdomadaire des seances de l'Academie des sciences,* 175: 930-933.

Joubin, L., 1922b. **Les coraux de mer profonde nuisibles aux chalutiers.** *Notes et memoires. Office scientific et technique des peches maritimes,* 18: 16.

Kenyon, N.H., 1987. **Mass-wasting features on the continental slope of North-West Europe.** *Marine Geology,* 74: 57-77.

Kenyon, N.H., Belderson, R.H., 1973. **Bed forms of the Mediterranean undercurrent observed with side-scan sonar.** *Sedimentary Geology,* 9: 77-99.

Kenyon, N.H., Belderson, R.H., and Stride, A.H., 1978. **Channels, canyons and slump folds on the continental slope between South-West Ireland and Spain.** *Oceanologica Acta,* 1: 369-379.

Laughton, A.S., 1986. **The best way to exploit GLORIA ...** *Ocean Science News,* 27(48): 1-2.

Le Danois, E., 1948. **Les Profondeurs de la Mer.** Payot, Paris, 303 pp.

Lonsdale, P., and Hollister, C.D., 1979. **A near-bottom traverse of Rockall Trough: hydrographic and geological inferences.** *Oceanologica Acta,* 2: 91-105.

Mangerud, L., Lie, S.E., Furnes, H., Kristiansen, I.L., and Lomo, L., 1984. **A Younger Dryas ash bed in Western Norway, and its possible correlation with tephra in cores from the Norwegian Sea and the North Atlantic.** *Quat. Res.,* 21: 85-104.

Masson, D.G., and Kidd, R.B., 1994. **Revised Tertiary seismic stratigraphy of the southern Rockall Trough.** *In:* Ruddiman, W.F., Kidd R.B., Thomas, et al., *Init. Repts. DSDP,* 94: 1117-1126.

Masson, D.G., Auzende, J-M., Cousin, M., Coutelle, A., Dobson, M.R., Rolet J., and Vaillant, P., 1989. **Geology of Porcupine Bank and Goban Spur, northeastern Atlantic - preliminary results of the "Cyaporc" submersible cruise.** *Marine Geology,* 87: 105-119.

McGrane, K., Readman, P.W., Jacob, A.W.B., Unnithan, V., Shannon, P.M., Keary, R., and Kenyon, N.H., 1997. **Long-range sidescan sonar survey of the Rockall Trough.** *Abstract, AGU, 1997 Fall Meeting,* F350-F351.

New, A.L., Herrmann, P., and Molines, J.M., 1996. **Dynamics of North Atlantic models (DYNAMO): circulation and structure of the northeast Atlantic Ocean.** *In:* UK Oceanography '96. University of Wales, Bangor, 2-6 September 1996. Programme and abstracts. Bangor: University of Wales for Challenger Society for Marine Science, 40.

Rasmussen, J. and Noe-Nygaard, A., 1970. **Geology of the Faeroe Islands.** *Danmarks Geologiske Undersogelse,* 1, serie 25.

Rasmussen, T.L., van Weering Tj.C.E., and Labeyrie L., 1996. **High Resolution Stratigraphy of the Faeroe-Shetland Channel and Its Relation to North Atlantic Paleooceanography: The Last 87 kyr.** *Marine Geology,* 131: 75-88.

Rice, A.L., Billett, D.S.M., Lampitt, R.S., and Thurston, M.H., 1991. **The Institute of Oceanographic Sciences Biology Programme in the Porcupine Seabight: background and general introduction.** *J. Mar. Biol. Assoc. U.K.,* 71: 281-310.

Roberts, D.G., 1972. **Slumping on the eastern margin of the Rockall Bank, North Atlantic ocean.** *Marine Geology*, 13: 225-237.

Roberts, D.G., 1974. **Marine geology of the Rockall Plateau and Trough**. *Phil. Trans. Roy. Soc.*, 278: 447-509.

Roberts, D.G., Hunter, P.M., and Laughton, A.S., 1979. **Bathymetry of the northeast Atlantic : continental margin around the British Isles**. *Deep-Sea Research*, 26A, 417-428 and *Admiralty chart* No.C6567.

Roberts, D.G., Schnitker, D., et al., 1984. *Deep Sea Drilling Program, Initial Reports*, 81, 923 pp.

Rowell, P., 1995. **Tectono-stratigraphy of the North Celtic Sea Basin**. *In:* Croker, P.F., and Shannon, P.M. (Eds.), *The Petroleum geology of Irelands Offshore Basins,* Geological Society Special Publication, 93:101-137.

Scoffin, T. P., and Bowes, G. E., 1988. **The facies distribution of carbonate sediments on the Porcupine Bank, northeast Atlantic**. *Sedimentary Geology*, 60: 125-134.

Shannon, P.M., 1991. **The development of Irish offshore sedimentary basins**. *Journal of the Geological Society, London,* 148: 181-189.

Sibuet, J.C., Hunter, P.M., and Mathis, B., 1984. **La ride Pastouret (plaine abyssale de Porcupine; une structure eocene (1))**. *C.R. Acad. Sc. Paris,* Serie II. 299 (20): 1391-1396.

Stoker, M.S., Leslie, A.B., Scott, W.D., Briden, J.C., Hine, N.M., Harland, R., Wilkinson, I.P., Evans, D., and Ardus, D.A., 1994. **A record of Late Cenozoic stratigraphy, sedimentation and climate change from the Hebrides Slope, NE Atlantic Ocean**. *Journal of the Geological Society, London,* 151: 235-249.

Stow, D. A. V., 1994. **Deep sea processes of sediment transport and deposition**. *In:* Pye, K. (Ed.), *Sediment transport and depositional processes*, Blackwell Scientific Publications, 257-291.

Tebble, N., 1976. **British Bivalve Seashells.** Second Edition. Royal Scottish Museum, Her Majesty's Stationery Office, Edinburgh. 212 pp.

The GEBCO Digital Atlas, 1997. The British Oceanographic Data Centre on behalf of IOC and IHO.

Thomson, C. W., 1874. **The depths of the sea**. Macmillan, London, 527 pp.

Thorpe, S.A., and White, M., 1988. **A deep intermediate nepheloid layer**. *Deep-Sea Research*, 35(9A): 1665-1671.

Tudhope, A.W., and Scoffin, T.P., 1995. **Processes of sedimentation in Gollum Channel, Porcupine Seabight: submersible observations and sediment analysis**. *Transactions of the Royal Society of Edinburgh: Earth Sciences,* 86: 49-55.

Wilson, J.B., 1979a. **The distribution of the coral Lophelia pertusa (L.) [L Prolifera (Pallas)] in the north-east Atlantic.** *J. Mar. Biol. Assoc. U.K.*, 59: 149-164.

Wilson, J.B., 1979b. **'Patch' development of the deep-water coral *Lophelia pertusa* (L.) on Rockall Bank.** *J. Mar. Biol. Assoc. U.K.*, 59: 165-177.

Wilson, J.B., 1979c. **The first recorded specimens of the deep-water coral *Lophelia pertusa* (Linnaeus, 1758) from British waters.** *Bulletin of the British Museum Natural History (Zoology)*, 36: 209-215.

Wilson, J.B., 1982. **Shelly faunas associated with temperate offshore tidal deposits**. *In:* Stride, A.H. (Ed.). *Offshore Tidal Sands: Processes and Deposits*. Chapman and Hall, 126-171.

Wilson, T.R.S., Thomson, J., Hydes, D.J., Colley, S., Culkin, F., and Sorensen, J., 1986. **Oxidation fronts in pelagic sediments: diagenetic formation of metal-rich layers.** *Science*, 232: 972-975.

Woodside, J.M., Ivanov, M.K., and Limonov, A.F., (Eds.), 1997. **Neotectonics and fluid flow through seafloor sediments in the Eastern Mediterranean and Black Seas – Parts I and II.** *IOC Technical Series 48*, UNESCO. 266 pp.